Modelling and Optimisation Based Drug Delivery systems for the treatment of Acute Myeloid Leukemia (AML)

A thesis submitted to Imperial College London for the degree of Doctor of Philosophy

by

Eleni Pefani

Centre for Process Systems Engineering, Department of Chemical Engineering,

Imperial College London, United Kingdom.

September 2013

In the memory of my mother,

Rita

Declaration of Originality

I hereby declare that this is my own work and any published and unpublished work used here has been cited in the text, and the list of references in the bibliography section at the end of thesis.

Copyright Declaration

Eleni Pefani

Abstract

Leukemia is a malignant disease of the bone marrow and blood where immature white blood cells which are not able to develop into normal functioning blood cells are overproduced and build up in the bone marrow and blood. The most common treatment for most types of leukemia is intensive chemotherapy. This therapy can itself be life-threatening since only relatively few patient-specific and leukemia-specific factors are considered in current protocols; choice of chemotherapy, intensity and duration often depends on the treating physician's experience with significant international protocol variability. With the advent of novel treatments and large amounts of patient- and leukemia-specific genomic data, there is a clear need for a systematic approach to the design and execution of chemotherapy regimens.

We have developed a model for the simulation of patients with Acute Myeloid Leukemia (AML) undergoing treatment with two standard chemotherapy protocols, one intensive and the other non-intensive. The proposed model combines critical targets of drug actions on the cell cycle, together with pharmacokinetic (PK) and pharmacodynamic (PD) aspects providing a complete description of drug diffusion and action after administration. Tumour-specific and patient-specific characteristics are incorporated into the model in order to gain insights into the personalised cell dynamics during treatment.

Sensitivity analysis of the developed model identifies cell cycle times as the critical parameters that control treatment outcome. For model analysis, clinical data of 6 patients who underwent chemotherapy are used for the estimation of cell cycle time distribution.

The chemotherapy process is formulated as an optimisation scheduling algorithm aiming to obtain the chemotherapeutic schedule which would maximise leukemic cell kill (therapeutic efficacy) whilst minimising death of the normal cell population, thereby reducing toxicities. This optimisation algorithm is solved for all the patient case studies and the results clearly demonstrate the potential improvement of treatment design through optimisation.

Acknowledgments

Completing my PhD degree is probably the most challenging activity of my first 29 years in life. Thankfully along the way I had the pleasure and the luck to share the best and worst moments with great people who helped me reach the end of this wonderful experience. First and foremost, I would like to thank my supervisors Professor Stratos Pistikopoulos and Dr. Nicki Panoskaltsis for encouraging me to work in an interesting and challenging field of drug delivery systems. Prof. Pistikopoulos' enthusiasm, passion for work, innovative ideas, great leadership qualities have always inspired me to strive for extra and try to make my own mark. This PhD would have been impossible without his and Dr. Panoskaltsis' support, consistent feedback and guidance. I am really grateful for the discussions I had with Dr. Panoskaltsis on the scientific and ethic principles of the medicine field (completely unknown to me) that have been instrumental not only for the successful completion of the project but had a key role in shaping me as a researcher. I would also like to thank prof. Sakis Mantalaris and the BSEL laboratory for their help on the cell cycle part of my model and for their consistent support throughout the project.

I would like to thank the European Research Council (MOBILE, ERC Advanced Grant, No: 226462) for the financial support of the project.

Starting from the early days of my PhD I would like to thank the senior Greek committee of the office consisting of Dr. Kouramas, Dr. Koutinas, Dr. Kiparissides, Dr. Panos and Matina Zavitsanou. Our meetings in the LG, G or even the Queens Lawn grass the one sunny day of the year made me feel like back home and made the first years of my PhD the most enjoyable. I would also like to thank Romain Lambert for our daily coffees in the common room and Maria, Nick and Eirini for making the days of my last year in Imperial less grey!

Although away from home the last 5 years I would like to specially thank my close friends Maro, Eirinaios, Maria, Manolis, Vasilis, Fani for always being there for me and for making my holidays really special. A special thanks to Yannis for his patience and support during all this transition period from completing my PhD – to making job applications and finally start working. Thank you as this was a stressful period and you have made it a lot easier for me!

Lastly, I would like to express my deepest gratitude to my father Dimitris, my sisters and advisors Efi and Artemis and my brother-in-law Panagiotis who have always been in my side supporting me with all their possible means. Of course I would have to thank the two most adorable and younger members of my family, my nephew Stavros and our new baby girl who I patiently wait to meet this Christmas! However, special thanks go to the most important person in my life, my late mother Rita. She brought us up with love, she armed us with morals in life and she taught us to always be ambitious and try for the best. This thesis is too little to thank her for all her sacrifices and for the nights she spent being stressed for mine and my sisters' future. I will always love her with all my heart and although her loss is the hardest and the most painful event in my life I am grateful to God for giving me this mother even for only 25 years.

Contents

List of tables

List of figures

List of abbreviations

ALL	-	Acute Lymphoid Leukemia
AML	-	Acute Myeloid Leukemia
Ara-C	-	Cytosine Arabinoside anti-leukemic agent
BM	-	Bone Marrow
CLL	-	Chronic Lymphoid Leukemia
CML	-	Chronic Myeloid Leukemia
DA Protocol	-	Protocol with mixed DNR and Ara-C anti-leukemic agents
DNR	-	Daunorubicin anti-leukemic agent
G_o-phase	-	Cells in the quiescent phase
G_1-phase	-	Cells in the RNA synthesis phase (non-proliferation state)
G_2-phase	-	Cells in the pre-mitotic phase (proliferation state)
HSC	-	Hematopoietic Stem Cells
iv	-	Intravenous
LDAC Protocol	-	Protocol with low doses of Ara-C sc administered
M-phase	-	Cells in the mitosis phase (proliferation state)
PD	-	Pharmacodynamics
PK	-	Pharmacokinetics
S-phase	-	Cells in the DNA synthesis phase (proliferation state)
sc	-	Subcutaneous
Tc	-	Duration of the full length cell cycle process
T_{G1}	-	Duration of the G_o / G_1-phase
T_{G2M}	-	Duration of the G_2 / M-phase
Ts	-	Duration of the S-phase
SPC	-	Summary of product characteristics

Chapter 1

Introduction

1.1Project Objective

In the UK (Cancer Research UK data, 2008), it is estimated that more than 1 in 3 people will be afflicted with cancer in their lifetime. For one such cancer, leukemia - a neoplasm of the blood and bone marrow (BM) - 1 in 71 men and 1 in 105 women will be affected, with incidence sharply rising in adults over the age of 50. Approximately 40% of those affected with leukemia will have Acute Myeloid Leukemia (AML).

Leukemia is a cancer of the BM and blood wherein blood cells are unable to develop or function normally, are overproduced at an immature stage of development and overtake any normal elements remaining in the BM and blood. This uncontrolled growth compounds the morbidity and mortality due to the disease by inhibiting development of healthy blood and immune cells through multiple mechanisms (Panoskaltsis et al., 2003; Panoskaltsis et al., 2005).

The most effective treatment for most types of leukemia is intensive chemotherapy administered through the vein (intravenous). This therapy can be life-threatening since only relatively few patient-specific and leukemia-specific factors are considered in current protocols; choice of chemotherapy, intensity and duration often depends on either the availability of a clinical trial, the treating physician's experience or the collective experience of the treating centre, with significant international protocol variability. Inter-patient and intra-leukemia variability add complexity to these treatment decisions and are not yet adequately addressed, possibly accounting for the 30-45% long-term survival rates in young people with one type of BM cancer, AML. For those whom are cured, there is a lifetime of increased risks of secondary cancers, cardiovascular disease and diabetes due to the adverse effects of treatment.

In order to overcome these limitations, there is a need for personalised treatments that incorporate both the individual patient characteristics and features specific to the patient's leukemia (different for every patient).

Personalised healthcare is expected to deliver a "step change" in a) quality and value of care, with more precise/personalised diagnostics and cost-effective/targeted therapies and will also benefit the pharmaceutical industry via efficient drug development processes based on modelling of patient- specific and disease-specific biomarker endpoints. Towards this end systematic work is required from clinicians, experimentalists and engineers in order to (i) derive experimental *in vivo* and *in vitro* methods that will give the ability to gain further insight to the disease dynamics (ii) identify the factors that are highly correlated to the treatment outcome (ii) design and validate automated systems that can *a priori* capture patient and treatment outcome and (iv) suggest the most efficient treatment protocol as defined by specific measurement of patient and disease characteristics.

Mathematical modelling is undoubtedly a useful tool that can be used for the automation of chemotherapy treatment due to its advantages in systematically exploring extensive datasets in order to capture a system's dynamics and subsequently provide better insight for process enhancement. Towards this direction various mathematical models have been developed for different biomedical systems (Dua et al., 2008; Ledzewicz, Schattler, 2007; Harrold, Parker, 2009; Sherer et al., 2006; Parker, Doyle, 2001; Krieger et al., 2013) with aim to describe the disease under chemotherapy and afterwards propose the optimal treatment design. The aim of the optimisation algorithms is to minimise the number of cancer cells at treatment completion subject to dynamic constraints that include the drug PD, PK and toxicokinetic effects. A powerful methodology is developed and presented in the work of (Harrold, Parker, 2009) on the conversion of a dynamic model to a mixed-integer algorithm for the scheduling of chemotherapy treatment with inclusion of clinical relevant constraints. Moreover, in the work of (Dua et al., 2008) a dynamic optimisation problem is presented for the control of breast tumour progression while constraining the toxicity of the bone marrow. Lastly, optimisation works exist that consider the optimisation problem of cancer disease as a stochastic system. Such an algorithm is presented in the work of (Coldman, Murray, 2000) where the tumour population is described by a set of various cell mutation probabilities and the optimal treatment is based on the probability of drug effect on each cell type i.e. mutant cell type, resistant cell type and sensitive to the treatment cell type.

In their majority, these systems aim to describe the disease dynamics of a hypothetical average patient case study. Under this assumption, these models do not include patient- and disease-specific characteristics as parameters in the model but rather they use mean values derived from a number of patient/volunteers studied. To our knowledge, there is a lack of

models that include personalised patient and disease information and use optimisation methods in order to design optimal personalised chemotherapy protocols.

The representation of human cancers with mathematical models that involve individualised patient-specific parameters can be used for detailed simulation and optimisation studies. This ***valid mathematical representation of disease behaviour may then be used by physicians as an assistive device in decision making of more effective and less toxic chemotherapeutic strategies***.

The desired mathematical model for the simulation of patient behaviour and tumour response during chemotherapy should consist of three parts: (i) the cell cycle model, which is the target of drug action, (ii) PK and (iii) PD aspects that provide the complete description of drug diffusion and action after administration. Cell cycle is the process under which the cell replicates its genetic material, divides into two daughter cells and is separated into four phases: the growth phase (G_1-phase), the DNA synthesis phase (S-phase), the pre-mitotic phase (G_2-phase) and the mitosis phase (M-phase). The most interesting branches of pharmacology essential for both drug development and modelling of chemotherapy treatment are PK and PD. PK generally gives time-concentration history of the drug throughout the body while PD describes drug effects on the body. The two descriptors are intimately connected as the effect of a drug on the body depends on drug concentration at the target site of action. A PK-PD model combines the two elements and gives the time-profile of drug action on cell populations and is used to improve and direct management of individual patients.

The objective of the current project is to combine the available cell cycle and pharmacologic information (PK and PD aspects) to develop a mathematical model able to capture AML disease dynamics during chemotherapy treatment for different patient and disease characteristics. Moreover, this model will serve as a basis for the ***formulation of an optimal control problem with aim to obtain the chemotherapeutic schedule which would maximise leukemic cell kill (therapeutic efficacy) whilst minimising death of the normal cell population, thereby reducing toxicities***.

1.2 Project deliverables and thesis structure

In this project a mathematical model is presented that captures the AML disease dynamics during treatment with two anti-leukemic agents; cytarabine (Ara-C) and daunorubicin (DNR). The chemotherapy protocols followed are consistent with standard clinical practice (Milligan et al, 2006) and include one intensive and one non-intensive protocol: (a) DNR and Ara-C used in standard intravenous (iv) doses (DA 3+10) and (b) low dose Ara-C (LDAC) administered subcutaneously (sc). Both DNR and Ara-C are cell-cycle specific agents. Specifically, Ara-C acts on the proliferation phase of the cell cycle (S-phase) (Kufe et al, 2006) and DNR acts on the S-phase and the growth phase of the cell cycle (G1-phase) (Huffman, Bachur, 1972). The specificity of the drugs indicates that cell cycle undoubtedly is an important factor that needs to be included in the mathematical model together with the pharmacology aspects of PK and PD that provide the complete description of drug diffusion and action after administration.

Sensitivity analysis of the developed model identifies cell cycle times as the critical parameters that control treatment outcome. In order to improve effectiveness of AML therapy and reduction of toxicity, treatment with chemotherapy is presented as an optimal control problem with the main aim of obtaining a treatment schedule which could maximise leukemic cell kill, yet minimise death of the normal cell population in the BM. The aim of remission induction therapy described by the current presented model is to achieve the rapid restoration of normal BM function. By treatment completion, the leukemic population should be reduced to a level of approximately 10^9 cells, defined as a complete morphologic remission and at which point BM hypoplasia is achieved. Moreover, the normal population should be higher than that of the leukemic and a 3-log reduction is the maximum permissible level of population reduction.

For model analysis, historical clinical data of 6 patients who underwent chemotherapy are used for the estimation of cell cycle time distribution. The patient data is comprised of disease characteristics (tumour burden, cell cycle times, normal cell population) as well as patient-specific characteristics (gender, age, weight and height). The optimisation algorithm is formulated and solved for all patients for both intensive and non-intensive treatment protocols with maximal and minimal thresholds set for efficacy and toxicity, respectively. For iv Ara-C, total drug administration is set between 50mg and 4000mg, with infusion duration

between 1 min to 24 hours. The time window for DNR dose optimisation is stricter due to potential toxic effects and the only independent variable is dose with 30mg – 90mg per infusion. For sc Ara-C, the maximum dose per day is 40mg and doses are permitted up to four times daily for a maximum period of 20 days. Optimisation treatment protocols are obtained for all the analysed patient case studies and clearly reveal the usefulness of optimisation methods for treatment improvement.

The rest of the thesis is organised as follows. **Chapter 2** presents a literature review of the modelling and optimisation of AML. This chapter concentrates on the description of AML as a disease system and discusses the sources of patient and disease variability to treatment outcome. Moreover, mechanisms of action of anti-cancer agents are analysed in this chapter together with the chemotherapy treatment protocols in use in standard current clinical practise. **Part I** focuses on chemotherapy treatment as a process systems application. **Chapter 3** presents the framework for the design of personal optimised chemotherapy protocols by combining drug information together with patient and disease characteristics in order to develop the proper optimal dosing schedule for each individual. The developed mathematical model for the two chemotherapy protocols, the non-intensive (LDAC) and the intensive (DA) protocols is presented in this chapter and simulation results are presented for two hypothetical patient case studies with data found in the literature. Furthermore, **Chapter 4** presents the chemotherapy process as an optimisation problem and the derived algorithm is solved for the two hypothetical patient case studies analysed in the previous chapter. In **Appendix A** the model simulation and optimisation results of the two hypothetical patients are listed in detail. For the clinical data the project is submitted and approved by the North West London Hospitals Trust for the provision of anonymised health records of patients diagnosed with AML and treated within Northwick Park Hospital, London UK, using DNR and Ara-C anti-leukemic agents in the DA or LDAC regimens. The obtained data are presented in **Part II - Chapter 5** and are listed in detail in **Appendix B** of the current thesis. The already presented modelling and optimisation methods are used for the simulation of the different treatment outcome dynamics for the studied patients using primary data and also for the optimisation of treatment protocols taking account of individual characteristics (physiological and disease) for each case study. The simulation and optimisation results for these patients are listed in detail in **Appendix C**. Last but not least, some concluding remarks are presented in **Chapter 6** together with the future potential extensions of the current work.

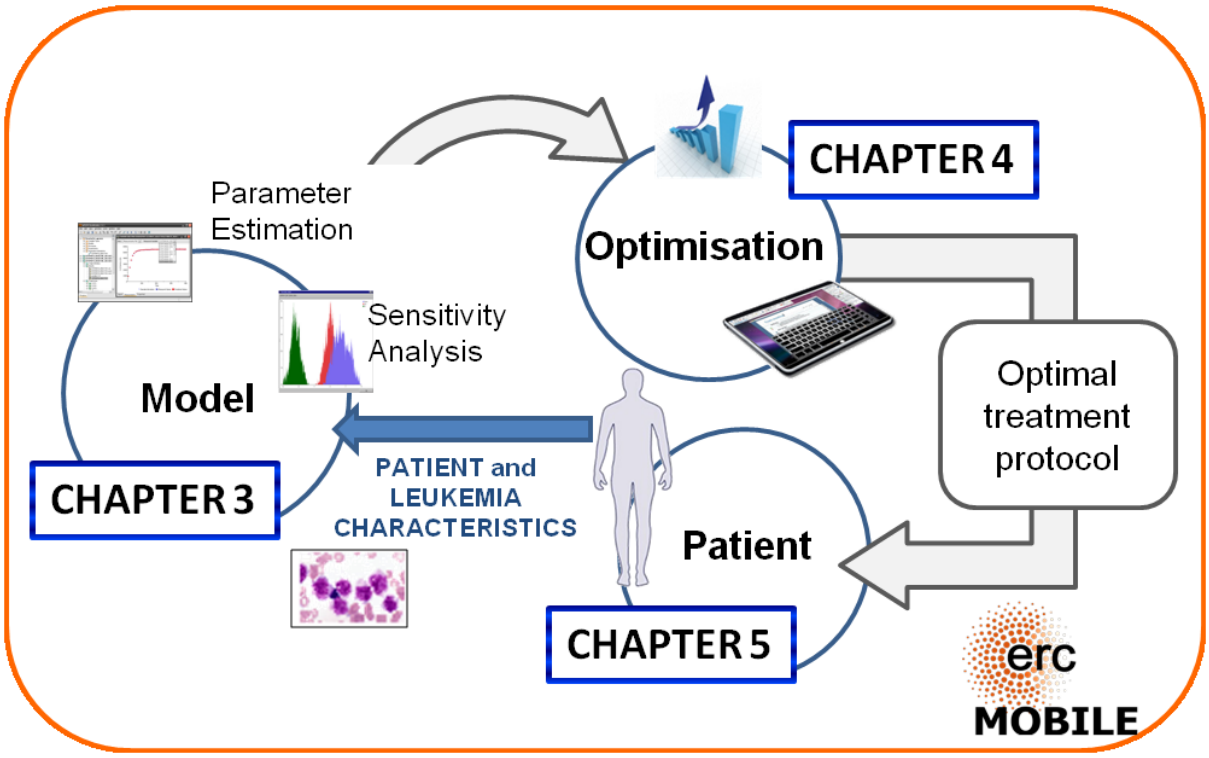

Figure 1.1: Schematic representation of project objectives and thesis structure

Chapter 2

Literature Review

2.1 Introduction

This chapter presents a literature review of the modelling and optimisation of AML. Section 2.2 presents an overview of leukemia as a cancer and the probable sources of patient variability are analysed. Moreover, section 2.3 presents the concept of chemotherapy as the means of treatment for AML, wherein section 2.3.1 presents the available drugs for AML treatment and section 2.3.2 presents the stages of chemotherapy treatment and the chemotherapy protocols as clinically applied. Section 2.4 proposes a mathematical model for AML disease dynamics under the influence of chemotherapy. This section is separated into four subsections; section 2.4.1 presents an overview of the literature regarding modelling of cell cycle, section 2.4.2 presents the principles of pharmacology of the existing anti-leukemic agents and sections 2.4.3 and 2.4.4 present the PK and PD aspects, respectively.

2.2 Leukemia – disease principles and patient variability

Blood is unquestionably one of the most vital factors for human life due to its ability to transport the necessary ingredients between the different organs of the human body. The 55% of human blood volume consists of the blood plasma that serves as the reservoir for the ingredients of the blood fluid where important proteins such as serum, albumin, hormones, clotting factors, enzymes and other nutritive materials exist. The remaining 45% consists of the erythrocytes, leukocytes and platelets which are the most important blood cells and indicators of the health state of an individual. Erythrocytes or red blood cells are the oxygen carrier-cells that transport the oxygen from the lungs to the body's capillaries. Leukocytes or white blood cells are the immune system's cells with primary function in the human defence against infectious diseases. Lastly, platelets or thrombocytes have a primary role in the formation of blood clots to prevent bleeding (Williams et al., 1983).

The daily demand of an adult human for blood cells amounts to 2.5 billion red blood cells, 2.5 billion platelets and 1 billion granulocytes per kg of body weight (Panoskaltsis et al.,

2005). This demand is covered by the proliferation of hematopoietic stem cells (HSCs) and haematopoietic progenitor cells which are cells with extensive proliferation capacity and ability to self-renew into three different cell lineages: leukocytes, platelets and erythrocytes (figure 2.1).

Blood production has to be robust to cover the daily individual needs and durable i.e. to be maintained throughout adult life. HSCs replicate to produce two daughter cells with the same capabilities as the parent cell and also differentiate into different blood cells. These two abilities make HSCs capable of both maintaining and restoring blood production. After the proliferation state, HSCs differentiate into lymphoid and myeloid progenitor lineages that form blood cells through the maturation process (Williams et al., 1983). Haematopoiesis occurs on BM stroma that is organised into niches which provide the supportive microenvironment for HSC function and also regulate the balance between cell proliferation and differentiation.

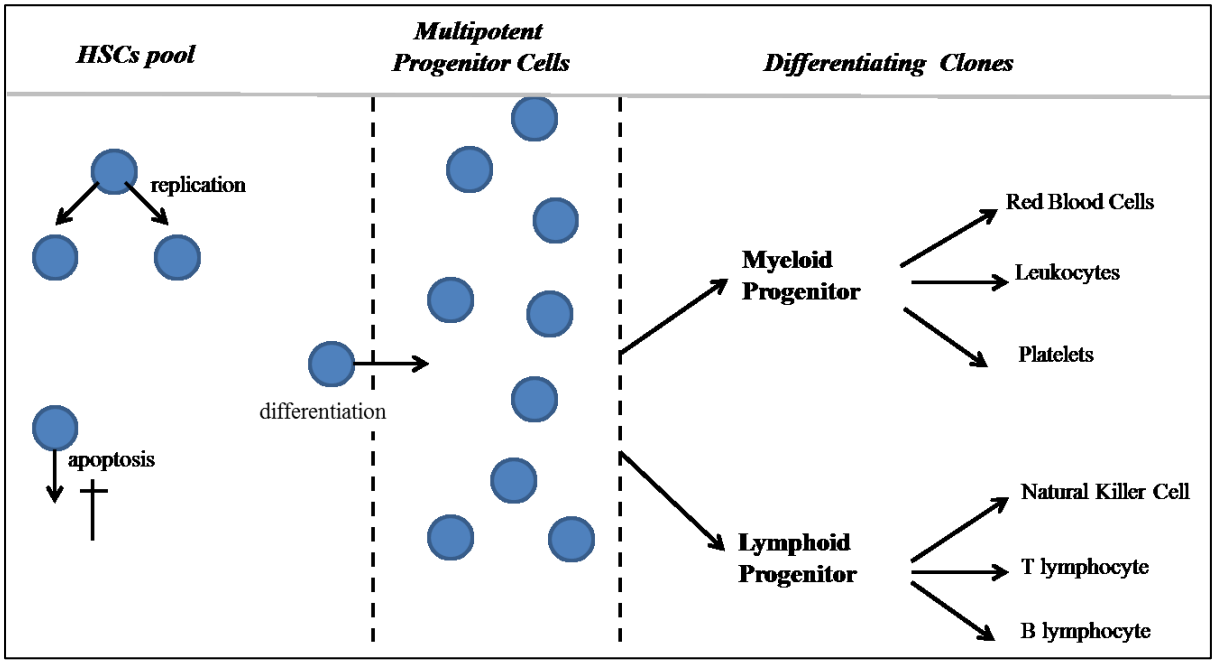

Figure 2.1: The Hematopoietic System: The HSC has the capability to replicate into two new-born cells, proceed to natural death (apoptosis) or differentiate towards progenitor cells. Progenitor cells afterwards differentiate into lineage-specific cells (myeloid and lymphoid) which mature to form the blood cells (Williams et al., 1983).

Leukemia subtypes are divided into myeloid and lymphoid depending on the stem cell pathway leading to myeloid or lymphoid cells, respectively (Bain, 2003). Moreover, blood cancers are divided into chronic and acute leukemias (Bain, 2003). In the case of acute

leukemia, the BM extensively produces and provides the body with malfunctioning blood cells. Acute leukemia is an aggressive and fast growing cancer for which immediate treatment is required for survival of the host. In contrast, chronic leukemia has slower growth and usually requires prolonged treatment or periods of active monitoring without the need for specific therapy. In that way leukemia cancer types are broadly divided into chronic or acute, and further subdivided into lymphoid or myeloid leukemias. The four categories are: Chronic Myeloid Leukemia (CML), Chronic Lymphoid Leukemia (CLL), Acute Myeloid Leukemia (AML) and Acute Lymphoid Leukemia (ALL).

AML is a biologically and clinically heterogeneous disease with diverse morphologic, immunophenotyping and cytogenetic characteristics. The main characteristic of AML is the excessive number of abnormal cells unable to differentiate into functional mature cells, such as granulocytes or monocytes. These cells reveal a high proliferating capacity that has driven researchers during the last decade to the conclusion that leukemic population expansion is due to their enhanced capability to self-renew. Based on this cell characteristic, similarities between leukemic and hematopoietic stem cells (HSC) have been investigated leading to current theories which mark the origins of leukemia in a stem cell with an initial chromosomal mutation and which requires further mutational (either genetic or epigenetic) change for the full leukemic phenotype and heterogeneous clonal progression (Bonnet, Dick, 1997; Horton, Huntly, 2012).

The excessive numbers of malfunctioning white cells replace normal cells in BM and/or disrupt the production of normal cells. This abnormal behaviour of the BM causes haematopoietic and immune system insufficiency since there is a loss of red cells, white cells and platelets. Depending on the decrease in these cell populations, AML symptoms can consist of fatigue, haemorrhage, infections and fever. Moreover, dyspnoea or other symptoms may occur due to the severe anemia and as leukemic cells circulate in the body and infiltrate tissues. The health condition of the patient depends on the amount of normal blood cells compared with those that are cancerous or leukemic. Thus, in the BM of patients with AML, cancer cells can be described as the highly proliferative fraction and mal-functioning cells whereas normal cells are the normally functioning and normally proliferating cells.

Numerous chromosomal abnormalities have been detected that lead to AML and are correlated to treatment outcome. For this reason, attempts have been made to classify the disease into certain subtypes using these recurrently identified chromosomal and genetic

mutations (WHO defined classification) (Nakase et al., 2000; Marcussi et al., 2005; Weinberg et al., 2009) towards the promotion of more specialised treatment design.

There are three mutation subgroups related to treatment success: favourable, unfavourable, and standard/intermediate prognostic subgroup (Hoffbrand et al., 2006,). The favourable subgroup consists of patients with chromosomal translocations t(15; 17), t(8; 21), or inv(16) having a high probability of cure (~80%) and lower probability of relapse (30-40%). The unfavourable subgroup is comprised of patients with AML with cytogenetic abnormalities in more than two chromosomes where the probability of cure is less than 20%. Such cytogenic abnormalities are either monosomies in chromosomes 5 or 7 or deletion of the long arm of chromosome 5 or of chromosome 3. The third subgroup is the standard subgroup that consists of patients with various types of translocations, different from those of the other groups and whose probability of being cured is unpredictable.

Although the above described classification is based on sophisticated methodologies used for patient diagnosis incorporating morphologic features and molecular genetics, a thorough BM genetics examination still remains essential for disease evaluation. These three subgroups, i.e., favourable, unfavourable and standard/intermediate prognosis, are too sparse and fail to include the appropriate level of disease heterogeneity. Recently, intra-patient disease heterogeneity has been acknowledged due to the multiple clones of leukemic stem cells within the same patient (Kennedy, Barabe, 2008; Horton, Huntly, 2012).

This inconsistency and heterogeneity of molecular genetic abnormalities in AML make the development of targeted individual therapies extremely challenging. Several works have shown a high correlation between the level of disease heterogeneity, treatment outcome and the existence of residual disease after treatment (Hoffman et al., 2012; Vo et al., 2012). This is due to the fact that even a small subpopulation of cells with diverse molecular properties may be of importance for relapse of disease and should be considered in treatment design.

Moreover, in addition to the stochastic behaviour of the leukemic cells, the disease is also controlled by the pathologic connection of the cells' behaviour with the microenvironment that surrounds them, partly defined by the BM stroma. Under normal conditions hematopoietic cells are produced in the BM within a complex microenvironment, organised in "niches" regulating survival, self-renewal, proliferation and differentiation (Panoskaltsis et al., 2005). Deregulated growth of normal cell development within this functional space generates neoplastic clones which contribute to leukemogenesis (Olsen et al., 2008). Genetic

and epigenetic alterations in the leukemic blast cells are the biological basis of pathological disease (Kennedy, Barabe, 2008), but recently it has been shown that the BM microenvironment has a fundamental role in hematopoietic cell fate regulation (Doan, Chute, 2012). In particular studies, it has been revealed that myelodysplastic (pre-leukemic) stromas can initiate malignant cell differentiation of normal cord blood cells (Borojevic et al., 2004). This abnormal microenvironment, through the production of specific signalling molecules, growth factors and cytokines supports the malignant phenotype and suppresses normal haematopoiesis (Colmone et al., 2008). Alterations of the hematopoietic environmental pathways can further affect drug responses in AML; in fact stromal cells sustain proliferation and delay terminal differentiation which leads to disease expansion and can confer multi-drug resistance phenotype (Nair et al., 2010).

This disease heterogeneity and effects of stroma on cancer cells make the disease uncontrollable in terms of chemotherapy efficiency, resistance to the treatment and residual disease. All these three clinical states are linked to the number of cancer cells in dormancy before and during the treatment process.

All cells can broadly be grouped into two states: the proliferating and the dormant state. After the completion of the proliferative state, the cell has the possibility of either entering the proliferation cycle again and follow another cycle of duplication of genetic material, or to become inactive and, therefore, enter the dormant state (Eisen, 1979). When extracellular conditions are such that there is no necessity for further cell division, metazoan cells enter this state (Lewin et al., 2007). During this dormancy (or quiescence), the cell can be described as inactive and the process of proliferation is ceased. When a cell is in dormancy, it may differentiate or it may stay unchanged until it undergoes apoptosis. Moreover, when there is an inadequate number of cells due to abnormal conditions, nutrients and signals are supplied that activate cells in dormancy and they re-enter cell cycle through transition to the growth phase. Generally these cells stay in reserve in case of lack of cells, e.g. in the case of BM depletion. However, conditions that activate dormant cells are still under investigation.

When cells are in dormancy they cannot be affected by chemotherapeutic agents and thus are not susceptible to these drugs. The leukemic population contain a proportion of slow proliferating cells that are largely in the dormant state (Komarova, Wodarz, 2005; Michor, 2008). These experimental works also indicate that the success of chemotherapy treatment depends on the initial proportion of cells in the quiescent state and the transition rate into

proliferation. Specifically, patients whose BM samples presented a higher proliferating population at the point of biopsy or even during the early chemotherapy cycles were the ones most likely to be cured of AML after chemotherapy, whereas the remainder of patients relapsed after treatment (Stryckmans et al., 1970; Cheung et al., 1972; Hayes et al., 1977).

2.3 Chemotherapy for the treatment of AML

2.3.1 Introduction to clinically used anticancer agents for chemotherapy treatment

A sequence of research led to the design and use of chemotherapy treatment as cure for cancer. The first chemotherapy drug was synthesised in 1940, by Goodman and Gilman in the USA department of defence as a chemical weapon during World War I and it was found to be effective for cancer treatment (DeVita, Chu, 2008). This was an important breakthrough especially for leukemic patients who received treatment with that drug as at that time leukemia was considered to be incurable. In the subsequent decade, anticancer agents were evaluated based solely on empirical applications on diseased animals.

The cell cycle as an important factor of clinical medicine was first introduced in 1855 when Rudolph Carl Virschow presented the *"omnis cellula e cellula*" (every cell stems from a cell) theory, stating that all diseases stem from changes in normal cells (Nurse et al., 1998). This theory launched the field of cellular pathology, the first stage of which was to assess disease as a product of changes in normal cells. During this decade, research was focused on the observation of cell function and the identification of model organisms on the premise that simple organisms could be studied to gain knowledge on more complex organisms. In 1953, an important breakthrough was achieved with the description of the DNA double helix by Watson and Crick. This discovery gave rise to the full description of the mitotic cycle that formed the basis for expanded research of the cell cycle and, by extension, the burgeoning sector on anticancer drug discovery.

The description of cell cycle mitosis upgraded the level of knowledge and insight into cancer biology leading to the synthesis of cell-cycle specific agents applied even today in clinical practice (DeVita, Chu, 2008). Further advances in the *in vitro* study of cancer cellular dynamics developed from the successful isolation and growth of cancer cell lines in laboratory conditions. Various cultures and pre-clinical methods have been established that provide the infrastructure for the study of a drug on cellular culture and the development of the PK model of drug action on tumour populations (figure 2.2).

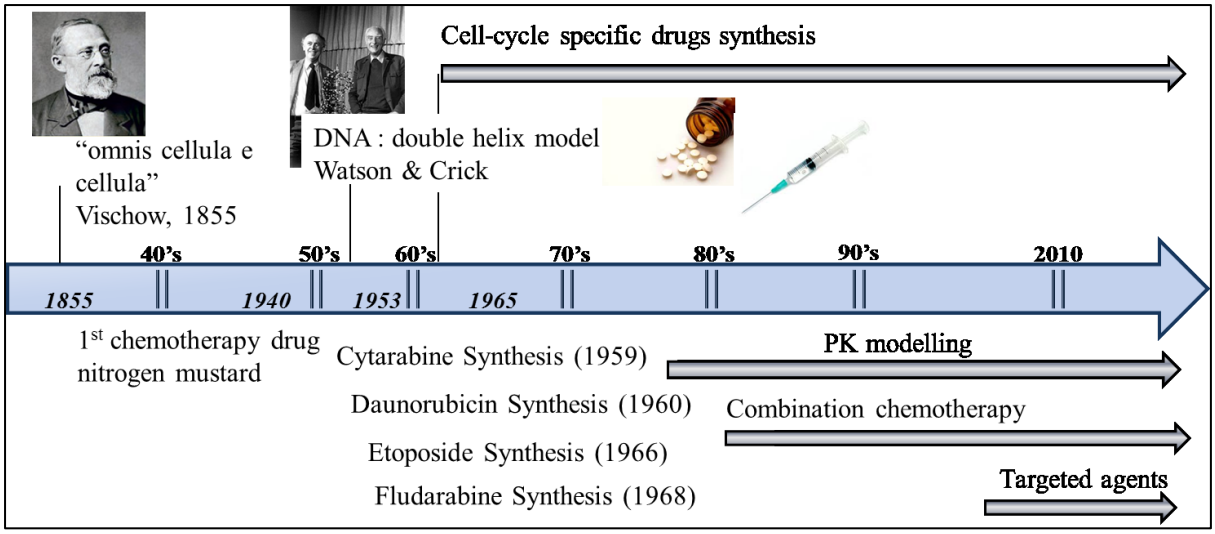

Figure 2.2: Key advances in the development of chemotherapy treatment. Cell-cycle specific drugs used in current clinical practice were synthesised in the 1960's. PK models simulating drug concentration and action profiles were thereafter developed in the 1970's. This change in drug development is undoubtedly connected to advances in cell cycle research with the most important being the delineation of DNA structure by Watson & Crick.

Chemotherapy cell-cycle specific agents discovered in the 1970's are still used in current clinical practice for the treatment of cancer. For AML, the most commonly used agents consist of Ara-C, DNR, mitoxantrone, etoposide, idarubicin, fludarabine and amsacrine. The analysis of all these agents is out of the scope of the current work. However, the profile of Ara-C and DNR is presented in this section as these are the agents used for analysis in the current thesis. Section 2.3.2 gives a general presentation of the chemotherapy treatment stages for AML and presents the induction treatment that is modelled and optimised in the current study.

2.3.2 Studied chemotherapy treatment protocols

As described above, AML is the cancer of the BM and blood wherein blood cells are unable to develop or function normally, are overproduced at an immature stage of development and overtake any normal elements remaining in the BM and blood. This uncontrolled growth compounds the morbidity and mortality due to the disease by inhibiting development of healthy blood and immune cells through multiple mechanisms (Panoskaltsis et al., 2003; Panoskaltsis et al., 2005).

Treatment for AML aims at the cure of the disease i.e. the complete eradication of the abnormal cells from the BM. The first stage of treatment is induction chemotherapy treatment

which aims to achieve the rapid restoration of normal BM function. Induction therapy in the acute leukemias aims to reduce the total body leukemic cell population by a 3-log level during which BM hypoplasia will be achieved (10^9 leukemic cells). The desired hypoplastic marrow will be characterised by a reduced and weakened leukemic population and a higher proportion of normal BM cells normally functioning to support blood production and the immune system. It is generally assumed, however, that after completion of induction treatment a substantial burden of leukemia cells will remain undetected (minimal residual disease). Postremission therapy is therefore directed towards further reduction in the residual leukemic cell number, which may be as high as 10^8 to 10^9 cells at initial Complete Morphologic Remission (CR). The elimination of these residual leukemic cells may be accomplished by either cytotoxic chemotherapy, causing significant myelosuppression or by replacement of a patient's stem cells through allogeneic transplantation, a procedure combining myeloablation and immunotherapy (Williams et al., 1983).

For more than 20 years, standard remission induction chemotherapy has included an anthracycline (e.g. DNR) and Ara-C. The most common regimen combines 3 days of DNR with 10 days of Ara-C. This is known as the DA 3+10 regimen (Milligan et al., 2006), and is presented in Table 2.1.

Table 2.1: Schedule of standard DA treatment protocol

Protocol	Dose	Application duration	Route	Application Schedule
DA 3 + 10				
DNR	60 mg/m^2	1 hr	IV	1 daily application for days 1,3,5 of treatment
Ara-C	100 mg/m^2	Short-duration (push)	IV	Two daily applications, every 12 hours, for days 1-10

However, the DA protocol is suitable only for patients with adequate performance status (i.e., who are fit) and for those who choose to have intensive chemotherapy treatment. For elder patients or those less fit with a high probability of not being able to withstand the toxicity of chemotherapy, a lower intensity induction treatment is used, such as low doses of Ara-C subcutaneously administered. The low dose Ara-C (LDAC) protocol is presented in Table 2.2.

Table 2.2: Schedule of LDAC treatment protocol

Protocol	Dose	Application duration	Route	Application Schedule
Ara-C	20 mg	Short-duration (push)	SC	Two daily applications, every 12 hours, for days 1-10

2.4 Mathematical modelling of chemotherapy treatment for AML

Motivated by the challenge to define the most appropriate anticancer drug combination, dosing regimen and chemotherapy schedule in order to minimise drug toxicity and maximise efficacy of treatment, cure rate and the patient's life expectancy, engineers have tried to represent cancer using mathematical models. These mathematical models should describe the disease dynamics as they evolve for individuals by including patient-specific and disease-specific parameters. These models can be used afterwards for detailed simulation and optimisation studies that will provide a better insight of disease progression as a first step and will set the basis for the derivation of automated tools for the design of optimised treatment protocols.

To this end, mathematical models have been developed as early as the 1970's (Eisen, 1979). However, none of these models have found use in clinical applications. One of the main reasons for this failure in application is the lack of knowledge of the actual values of crucial parameters, making the developed models empirical in most cases. These models include algorithms which are based on poor information of the system and they succeed only to simulate the behaviour of a standard patient case study. However, both the complexity of cancer as a disease and the intricacy of the human body indicate that such a gross response of a treated patient would be quite different than that of the majority of individuals.

Three types of information are required for the derivation of these models: (i) information of the distribution of proliferating cells at the time of drug action (ii) the drug concentration profile of the drug in the tumour location and (iii) the active drug efficiency when reacting with cancer cells. These three aspects comprise the cell cycle model, the PK and the PD, respectively. In the case of AML the existing models, to our knowledge, fail to include this information in detail and usually cover either the pharmacology or the cell cycle part in detail combined with empirical equations for the other components (Afenya, 2001; Andersen, Mackey, 2001; Ledzewicz Schattler, 2007; Sherer et al., 2006; Coldman, Murrary, 2006).

Optimisation applications in this area are expectedly limited as well since, for an optimisation algorithm to be accurate, a valid model is necessary (Harrold, Parker, 2009; Gardner, Fernades, 2003; Swierniak et al., 2009; Parker, Doyle, 2001).

The following sections review the current state of mathematical models for the cell cycle of leukemic cells and the pharmacology aspects (PK, PD) of anti-leukemic drugs.

2.4.1 Cell Cycle modelling

Cell cycle is a set of cell mechanisms that results in duplication of cellular material and the division into two daughter cells with the main purpose to either preserve or expand the cell population. Cancer is unavoidably connected to the cell cycle as the origin of the disease is unregulated cell growth due to an abnormality in the process of cell proliferation. The macro-effect of this abnormal cell proliferation is the uncontrollable regulation of tissue growth leading to the creation of tumours, i.e. masses of malfunctioning cells that are harmful to the body. Hence, better insight into the cell cycle will provide more information on cancer cell dynamics which would inform chemotherapy treatment design. In section 2.4.1.1, a description of the cell cycle and modelling principles are presented, whereas section 2.4.1.2 presents a literature review of mathematical models for the characterisation of the cell cycle.

2.4.1.1 Cell Cycle principles in normal and abnormal BM cells

The cell cycle is separated into four phases: the growth phase (G_1-phase), the DNA synthesis phase (S-phase), the pre-mitotic gap phase (G_2-phase) and the mitosis phase (M-phase). Each phase is governed by the timed expression of phase-specific cyclins, which are degraded upon completion of their task. G_1-phase is the interval phase between the newborn cell and the duplication of its genetic material where RNA and proteins (e.g. cell enzymes) are produced. The next phase is S-phase where the DNA material is duplicated. This phase is the most common target of cell-cycle specific chemotherapeutic drugs - if DNA synthesis is blocked then the cell is forced to undergo apoptosis. Afterwards, G_2-phase occurs which is a gap phase between DNA-synthesis and M-phase wherein cell division takes part and two daughter cells are formed (Figure 2.3).

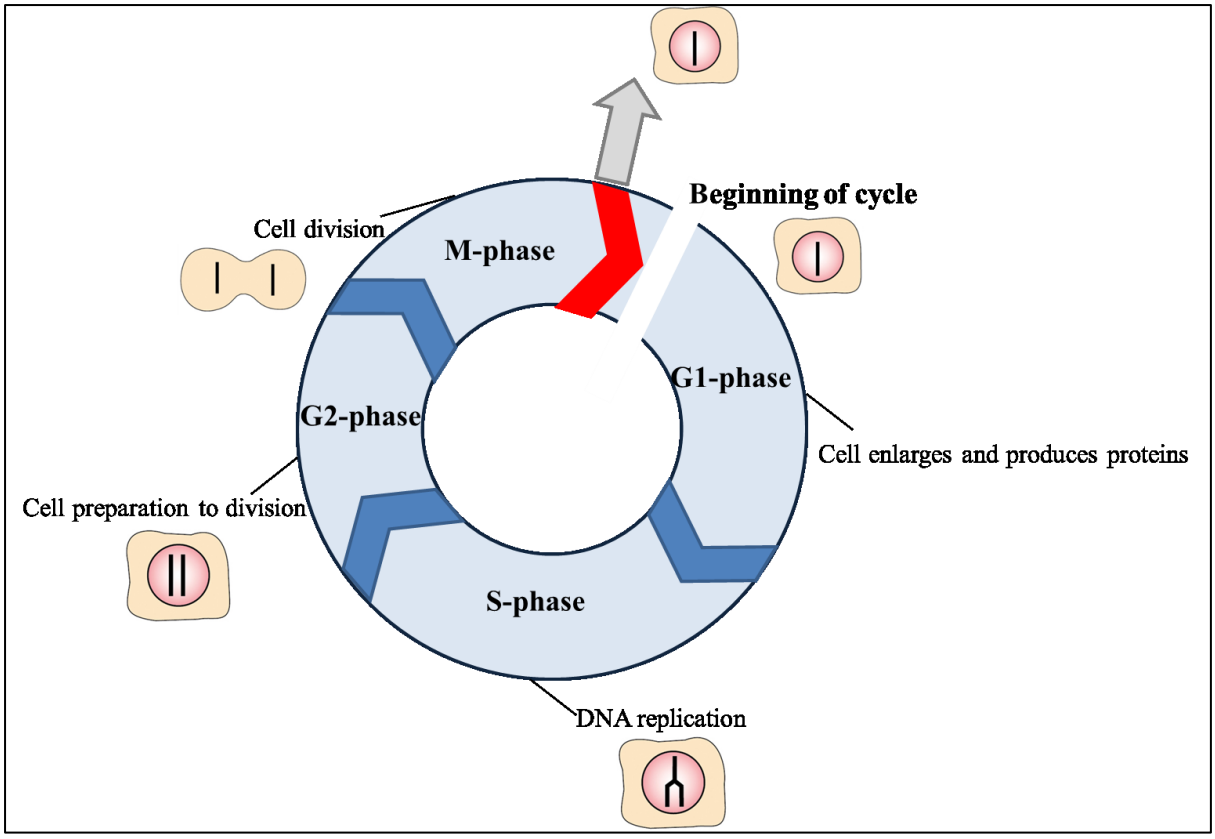

Figure 2.3: Description of the Cell cycle. Cell cycle populations have the capability to preserve the number of the population or re-populate through the proliferation process. This process includes the replication of the genetic material and the division of the cell into two new-born cells. The cell cycle is separated into four phases the G_1-, S-, G_2- and M- phases which serve as standpoints for the description of the cell cycle proliferation process. After the mitosis phase (M-) the new-born cells either immediately proceed to a new proliferation cycle or they are transferred to the quiescent phase where they remain in dormancy.

Another important state of the cell is the quiescent state, a phase wherein the cell is dormant and the procedure of proliferation is temporarily or permanently prevented. When extracellular conditions are such that there is no necessity for further cell division, metazoan cells enter the G_o phase, a state between mitosis and growth phase (Lewin et al., 2007). During the Go phase, the cell can be described as inactive and the process of proliferation stops. When a cell is in dormancy, it may differentiate or it may stay unchanged until it undergoes apoptosis. Moreover, when there is an inadequate number of cells due to abnormal conditions, nutrients and signals are supplied that activate G_o cells and they re-enter cell cycle through transition from G_o to G_1 phase. Conditions that activate cells in G_o are still under investigation - generally these cells are likely in reserve in case of depletion of cells, e.g. in the case of BM failure states. In order to both maintain a supply of mature blood cells and not

to exhaust HSCs throughout the lifespan of the organism, most HSCs remain quiescent and only limited numbers enter the cell cycle (Ezoe et al., 2004).

Extensive literature exists on the modelling of the HSC replication process, the majority of which represent the HSC pool as containing cells which can replicate, differentiate or die (Ezoe et al., 2004; Andersen, Mackey, 2001; Colijn, Mackey, 2005; Adimy et al., 2009; Catlin et al., 2011). These cells are grouped into two compartments, proliferating (P) and non-proliferating (Q) cells (figure 2.4). Non-proliferating cells are the quiescent HSCs which differentiate in progenitor cells with a differentiation rate (v), to generate into granulocytes. These cells are activated and transmitted to the proliferating compartment in a rate (β(Q)) that is reciprocal to the number of the quiescent cells i.e. when the number of cells is low, more cells will be activated in order to preserve the stem cell population. Both proliferating and quiescent cells have a death rate (γ and δ respectively). However, proliferating cells are affected by chemotherapeutic drugs and are forced into apoptosis.

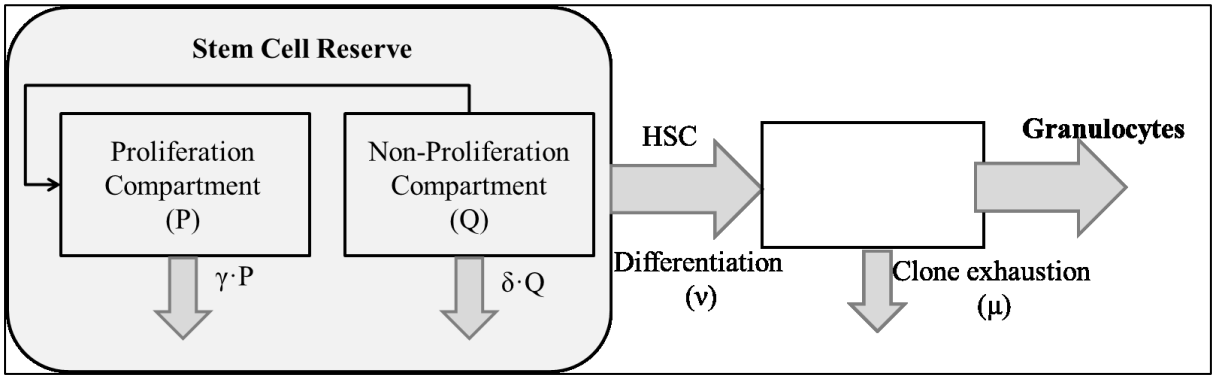

Figure 2.4: Representation of the full model of the HSC behaviour. The HSC has the capability to replicate into two newborn cells (proliferation compartment), proceed to natural death (γ) or differentiate into progenitor cells (ν). Progenitor cells afterwards differentiate into granulocytes i.e. white blood cells, erythrocytes, lymphocytes and platelets.

In principle, leukemic cells are malfunctioning HSCs (Bonnet, Dick, 1997; Horton,Huntly, 2012), thus the same modelling principles can be used for the description of leukemic function. However, the set of parameters characterising leukemic cells will differ in the abnormal percentage of cells in quiescence and also in proliferation capacity. The kinetics of leukemic cells have been evaluated experimentally and a great inter-patient and intra-patient variability has been reported (Preisler et al., 1993; Chiorino, Lupi, 2002; Raza et al., 1987). This variability concerns the percentage of cells in the quiescent and proliferating phases, as well as on the distribution of the cell population in the cell-cycle phases and on the duration

of each cell cycle phase. As a consequence, the derivation of a set of values for parameters that would adequately describe the cell cycle of all patients is not feasible. To make matters even more complex, these reports also prove the existence of intra-patient variability of cell cycle characteristics i.e. two cells of the same leukemic population will have different cell cycle distribution, proliferation potential and transition rates.

This variability in the kinetics of the tumour population is also correlated to treatment outcome and in particular disease resistance. For example, BM samples of 21 children with leukemia were analysed before and after chemotherapy treatment with vincristine, Ara-C and corticosteroids (Lampkin et al., 1969). The experimental aim was to observe the effect of these drugs, alone and in combination, on the cell cycle of leukemic cells of the patients. The results revealed that drugs used successively is preferable to the simultaneous use of two drugs acting on different cell cycle phases (Lampkin et al., 1969). Hence, drugs acting on a particular cycle phase will affect the entire cell cycle making it more efficient to "attack" the cell population in two different phases successively than at the same time. This is one of the first works in the open literature to suggest that the knowledge of the time course of the mitotic cycle could give rise to the improvement of treatment design. Work dating back to the 1960's and 1970's correlate characteristics of the cell cycle with treatment outcome (Hayes et al., 1977; Stryckmans et al., 1970; Cheung et al., 1972; Lampkin et al., 1969; Raza et al., 1990). Thus, the patient-specific characterisation of leukemic cell kinetics is of utmost importance for the treatment effectiveness and the design of personalised treatment protocols**.**

2.4.1.2 Cell Cycle mathematical models

Chemotherapy drugs aim to stop the uncontrollable cell proliferation by interfering within the cell cycle and killing the cells in replication. Chemotherapeutic drugs are classified according to the cell cycle phase in which they are active. Some drugs act selectively with cells on a particular cell-cycle phase (cell-cycle specific drugs), whereas others act with cells in all phases (cell-cycle nonspecific drugs). Some examples of commonly used cell-cycle-specific drugs are the anthracyclines, such as DNR, doxorubicin and idarubicin that inhibit DNA and RNA synthesis i.e. S- and G_1-phases; antimetabolites such as methotrexate and Ara-C that are S-phase specific drugs, whereas cell-cycle non-specific drugs are drugs such as platinum drugs (ex. carboplatin) that react with all phases of the cell cycle. The drug specificity makes the role of cell cycle a critical factor for the efficacy of the treatment.

The advance of new experimental tools and protocols gave rise to more sophisticated experiments and research in the 1980's and 1990's focused mainly on the characterisation of patient variability on cell cycle kinetics.

Mathematical models that describe the cell cycle have been developed from when the very first experimental data were obtained. The most common type of modelling approach is the compartmental one where compartments are used to describe the different cell phases or combination of phases into clusters. The mathematical model consists of the mass balances of cells in each compartment of the model. The simplest mathematical model assumes that the entire cell cycle forms one compartment (Swierniak et al, 1994), whereas the most detailed model considers each phase as a separate compartment (Sherer et al., 2006).

However, compartmental models fail to account for system heterogeneity and a rigid population is assumed with common characteristics of size, age, mass etc. Population-based models (PBM) are another modelling type which describes the effect of the cell heterogeneity on the cell culture dynamics. In these models the cell cycle is organised in population balances differentiated over time and one other property that evolves in parallel with the cell cycle progression, i.e. mass for the mass-structured cell cycle (Sidoli, 2006).

Although the PBM are more robust and accurate than compartmental models, they introduce a considerable number of unknown parameters, some of which are difficult to be experimentally measured.

In general for both types of models (compartmental and PBM) the required parameters for the cell cycle mathematical model consist of the transition rates of cells between cell cycle phases, the proliferation rate of the cells, the distribution of cell populations (normal and abnormal) into the cell cycle phases and the natural apoptotic rate of each cell cycle phase. For the calculation of these parameters, the experimental measurement available is the duration of the cell cycle phases. If the time-history profile of each cell cycle phase is known, thereafter the distribution of cell population into phases, proliferation and transition rates can be estimated (Basse et al., 2003). As far as the natural cellular apoptotic rate is concerned, since the model purpose is chemotherapy action on cells, a valid assumption often used is that there is only a small probability that the cell will follow the path of natural apoptosis and the apoptotic rate equals zero (Basse et al., 2003). In that sense, the prevailing system measurement required is the duration of each phase in the mitotic cycle.

Models in the literature assume constant cell cycling times and transition rates between the phases which make the model purely deterministic (Dua et al., 2005; Fister, Paneta, 2000; Ledzewicz, Schattler, 2002; Swierniak et al., 2003). These models fail to capture the intra-patient variability in the duration of the cycle phases and are adequate only at capturing the behaviour of a mean cell cycle function. Work with a more accurate approach considers the cycle duration as a stochastic distribution between a minimum and maximum range (Basse et al., 2003; Kimmel, Swierniak, 2003; Sherer et al., 2006). In this approach, cells of the same population have different distribution characteristics. However, a large window still remains for the improvement of the compartmental models to account for intra-patient variability, let alone the PBM that should include this variability as functions over both time and another system characteristic.

2.4.2 Pharmacology of anti-leukemic drugs

The in-depth knowledge of individual cell dynamics will demonstrate the level of system malfunction and will suggest the optimal treatment requirements for patient treatment, i.e., will suggest the time and effect that the treatment should reach. For these requirements to be achieved, management of the pharmacology information of available drugs is needed. The most crucial branches of pharmacology essential for both drug development and management of drug information are PK and PD. PK generally aims to give the time-concentration history of the drug throughout the body while PD aims to describe the drug effects on the body. PK and PD are intimately connected as the effects of the drug on the body depend on the drug concentration at the molecular site of action.

The combination of PK and PD characterise of the complete action of drug on the human body, i.e., the time-dependent procedure for a drug to reach the target (tumour location) and act. This information will provide the appropriate insight for the design of treatment with respect to the most efficient drug combination, the optimal route of dose administration (iv, sc, intrathecal etc.), and the appropriate dose regimens in terms of both efficacy and toxicokinetic information of the agents.

The steps of the drug action in the body are as follows and they are described in figure 2.5 (Ratain, Plunkett, 2003),

1. Drug administration
2. Drug absorption and metabolism through gastrointestinal tract in case of oral administration of a drug
3. Metabolism of the drug in the liver
4. Drug delivery in cell environment and protein-binding to act on the cell
5. Drug action (PD)
6. Drug returned either to the liver or to the kidney and excreted by biliary or urinary excretion

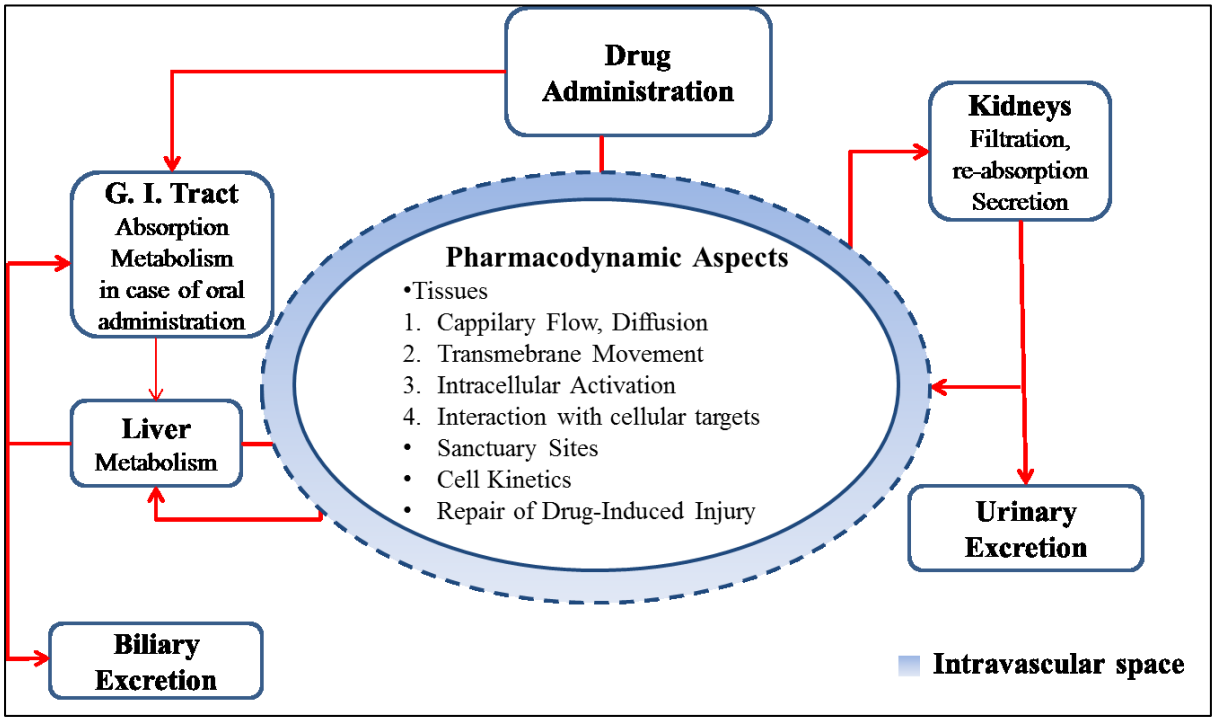

Figure 2.5: Schematic diagram of PK and PD: blue boxes are for the PK model and they are connected to the red cycle that represents the PD part of drug action. Adapted from (Ratain, Plunkett, 2003)

Initially the drug is dispensed into the patient's body. There is a variety of drug administration methods such as IV infusion, intraperitoneal infusion, intrathecal administration, intra-arterial infusion, oral administration, sc or intramuscular drug injection. The means of drug administration mainly affects the PK model as for example for the case of iv infusion the drug is directly injected into the blood and so the PK is described by the blood flow, whereas for intrathecal administration, the drug is injected into the spinal canal and the PK is different. The route of administration is chosen with the main goal to inject the drug as close as possible to the tumour site, if practical.

After its administration the drug has to be delivered to the tumour site. The drug delivery begins with absorption and metabolism from the liver and, in the case of oral administration, the gastrointestinal tract contributes to the drug metabolism. The active metabolites reach the systemic circulation and through distribution they are delivered to the desired site of action. Drug distribution mainly depends on the degree of blood flow in the vicinity of the tumour (vascularisation). It also depends on the flow across micro-vessel walls and the interstitial compartment from where it will finally be transferred to the site of action, that is inside the cell (Workman et al., 1993).

When the drug reaches the cell, transmembrane movement transports it into the cell where it acts. At the end of drug action, the drug is deactivated and is excreted from the human body mainly through urinary excretion and/or by biliary excretion. Drugs may also be excreted through lungs, breast milk, saliva and sweat.

In summary, the procedures of the drug being administrated, metabolised, delivered and excreted from the body comprise the PK part of the modelling while the drug action on cell level is the PD part.

2.4.3 Pharmacokinetic (PK) modelling

2.4.3.1 PK modelling principles

The major mechanisms of the **PK drug action** in the body consist of the drug absorption, distribution, metabolism and excretion (figure 2.6). Drug absorption is considered in cases of non-iv dose administration (sc, oral etc.) where the drug inflow reaches the systemic circulation with a certain time delay (absorption rate) and in a decreased amount (bioavailability) as some of the initial drug given is bound during absorption. Thereafter, the drug is distributed throughout the fluids and tissues of the body and is then metabolised in the liver and the kidneys. Finally, the drug is eliminated and excreted either by urinary (kidneys) or biliary (liver) route (Saltzman, 2001).

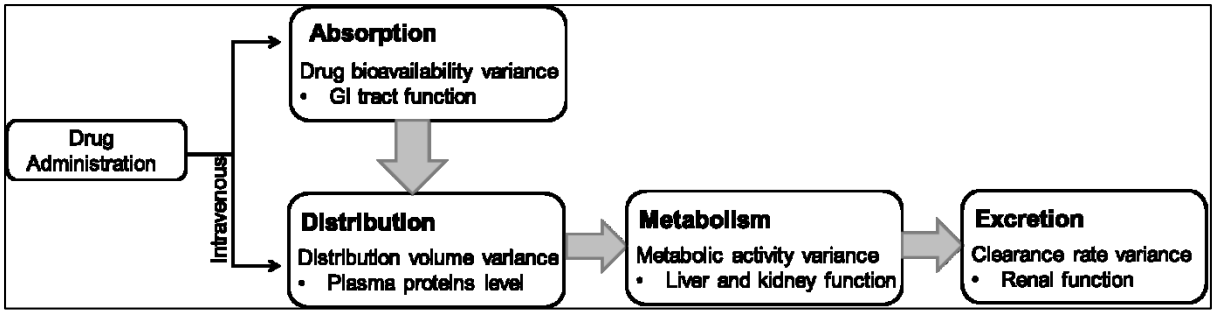

Figure 2.6: The process of drug delivery. Drug delivery is governed by four mechanisms: absorption, distribution, metabolism and excretion, each derived of further mechanisms. Inter- and intra-patient variability in these mechanisms is the probable source of PK variability.

High inter-patient variability exists in the amount of drug concentration produced by the same dose administered. This inter-patient variability is certainly correlated to the above described PK mechanisms although the exact source of variability is yet to be defined. Extensive works (Undevia et al., 2007; Garattini, 2006) review the probable patient information that could correlate with drug concentration at the tumour site and consequently in treatment outcome.

To begin with, absorption depends on the drug absorption rate and bioavailability. Absorption rate represents the time delay from the time of administration until the drug reaches the systemic circulation when it is given non-intravenously. This term has meaning mainly for the case of oral administration where the drug is firstly inserted to the gastrointestinal (GI) tract, while for the case of sc dosage, this rate represents a drug leak from the sc tissues into the blood. Bioavailability refers to the final amount of drug reaching the blood compartment. Again this term is mostly applied to oral administration where drug losses occur in the GI tract. Both bioavailability and absorption rate vary between different patients and depend on factors such as the absorptive area, the transition time of the drug into the blood, the blood flow and the GI environment, which are all probable sources of patient variability.

Moreover, drug distribution involves drug transition from the intravascular to the extravascular space. The amount of distributed drug will define the distribution volume of drug and depends on the level of binding proteins where proportion of the drug is bound and the amount of free drug is reduced. The drug metabolism takes place on the remaining free drug that reaches the liver and in some cases the kidney. The metabolism kinetics depends on the patient hepatic blood uptake and enzymatic activity. Lastly, excretion is related to kidney

action to eliminate and remove the inactive drug and will again differ between patients, resulting in varying drug clearance rates.

In summary, there is patient variability in all four mechanisms of drug delivery described above. This patient variability definitely contributes to an extent to the different treatment outcomes between patients. Especially for the anticancer agents, the variability in the amount of active drug that reaches the tumour location (without the drug bound during absorption and distribution) will finally affect the concentration of the active metabolite produced and the drug intra-cellular activation.

2.4.3.2 PK mathematical modelling

Currently two types of PK model are used, the compartmental and the physiological models.

In compartmental modelling, body organs are grouped into compartments and drug is assumed to be absorbed, distributed and eliminated in these compartments. For the case of the one compartmental model, body organs form one compartment and the model equations are as indicated below (Gardner, Fernandes, 2002):

$$C_i(t) = \left\{ \begin{array}{l} \frac{y_i}{\lambda} \cdot (1 - \exp(-\lambda \cdot (t - t_{AD,i})) + C_{residual}(t) \\ C_{residual}(t) = \sum_{i=1}^{PA} \frac{y}{\lambda} \cdot \exp(-\lambda \cdot (t - t_{AD,i})) \cdot (\exp(\lambda \cdot h_i) - 1) \end{array} \right\}$$

In this example, “i" is the number of dose applications and the drug is injected into the patient with a rate “y”. Dose duration is “h” and the total drug concentration in the body is calculated as the sum of the current dose plus the residual dose from the previous drug administration given “t_{AD}” hours ago. The drug concentration declines exponentially at a rate “λ”, the drug decay characteristic coefficient. The residual concentration is calculated as the sum of the concentration in the body from the first application (i=1) until the last of the previous applications (i=PA).

A case of a higher compartmental model is the two-compartmental model (figure 2.7). Another term should be added to the concentration equation that will account for the mass balance between these two compartments but the principles of the model will remain unchangeable. In general, compartmental models group organs with the same action towards the drug into compartments and the mathematical algorithm includes the mass balances

between these compartments. More information could be added, for example to account for blood concentration in each compartment or include absorption and distribution rates. However, the level of detail depends on the purpose of the model and the data availability.

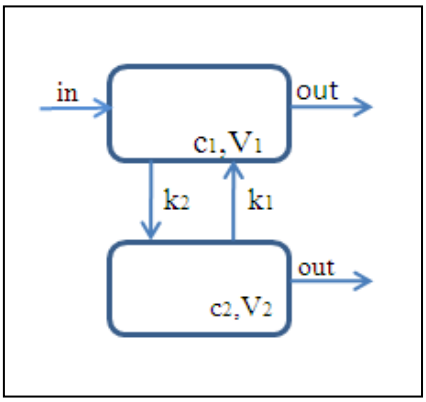

Figure 2.7: Representation of a two-compartment pharmacokinetic model. Adapted from (Saltzman, 2001)

Compartmental models represent the body as a set of compartments where the drug is inserted, diffused and then excreted. Empirical expressions relating drug concentration to time are afterwards derived for the hypothetical system. The parameters of these expressions are then estimated using the available system information that consists of drug dose, plasma drug concentration and drug clearance rate.

These are standardised models in great use by pharmaceutical companies and commercial tools exist for the development of this type of model for a variety of drugs (http://www.iconplc.com/technology/products/nonmem/;http://www.pharsight.com/products/prod_winnonlin_home.php;http://www.mathworks.co.uk/products/simbiology/; http://www.lixoft.eu/products/monolix/product-monolix-overview/). A large variety in PK and PD modelling software exists either as commercial or free available software packages for training purposes. Most software packages focus on one type of drug, or specific drug delivery, such as intravenous or oral doses. An overview of PK/PD software can be found here: http://www.boomer.org/pkin/soft.html. These tools use methods such as Monte Carlo expectation-maximization and Markov Chain Monte Carlo Bayesian next to classical likelihood to fit models to many different types of data. Some of the tools allow only non-compartmental analysis (Winnonlin, Nonmem) whereas others allow for the fit of physiological based PK models (Simbiology, Monolix). Most of these software (Nonmem, Winnonlin) benefit from the integration of inter-individual variability allowing the consideration of a large pool of data for the estimation of the PK model parameters.

However, the ability of these models to accurately predict the drug profile for a newly studied patient is rather questionable. The major source of model uncertainty is due to the fact that the values of the variables are based on the interpretation of the mean concentration profile of a group of patients. This "mean-concentration" profile in most cases is not representative of the behaviour of patients in the group studied let alone the whole patient population. Furthermore, since these models are empirical and include the concentration profile in the body as a totality, they do not account for more detailed phenomena taking place at the tumour location, for example, by linking the concentration profile to a detailed PD model of drug mechanism when it is activated intracellularly and acts.

These drawbacks are satisfied to a certain extend by the physiological based PK (PBPK) models. A physiological model is a high compartmental model that considers all the organs reacting with the drug. The model is derived from the equilibrium balances in these organs. The entire physiological model is described in figure 2.8 while for each drug the organs that do not affect the drug are neglected. PBPK models depend on two types of information; the patient physiological and the drug biochemical information. Physiological parameters consist of the body organ volume (Vi) and the blood flow rate in the body organs (Q_i). These parameters have been extensively measured and are correlated to patient characteristics such as sex, age, body mass index and cardiac output (Chouker et al., 2004; Pichardo et al., 2007; Brody, 1945; Brown et al, 1962; Wennesland et al., 1959). Moreover, the biochemical parameters are the parameters for the calculation of the drug metabolism rate. One common assumption in PBPK models is that the metabolism follows Michaelis-Menten kinetics and the required parameters are the drug maximal velocity (V_{max}) and the Michaelis affinity constant (k_m).

In the last decades, remarkable progress has been noted regarding the experimental design for the parameters of PBPK models. Initially for the PK model, metabolism information was only available from animal experiments and scaling was used afterwards for the approximation of the equivalent human values. However, there is a level of uncertainty in this method as humans are much more complex than other species and such a comparative relationship can only give a rough estimate of a human value and not the accuracy required. Established methods now exist to correlate PBPK parameters to *in vitro* and allometric data (Jones et al., 2009; Chaturvedi et al., 2001) with commercial tools for the calculation of these parameters for given drugs (http://www.cyprotex.com/home/, http://www.simulations-plus.com/, http://www.simcyp.com/).

A level of detail can be added to the PBPK models by further separating each compartment (i.e. organ) into vascular, interstitial and intracellular components. The vascular component consists of the part of the organ with the blood vessels from which the drug transists within the organ (interstitial) and before it reaches the cell (intracellular). This tri-partite modification would introduce a multitude of parameters, including the physiochemical characteristics of drug chemicals within the interstitial and vascular components (Schmitt, 2008, Peyret, Krishnan, 2012; Yun, Edginton, 2013). More elegant future models would combine this level of information with cellular information to provide cellular-level PBPK models that would be able to give insight of probable correlation between patient cell characteristics and the different PK profile (Caldwell et al., 2012).

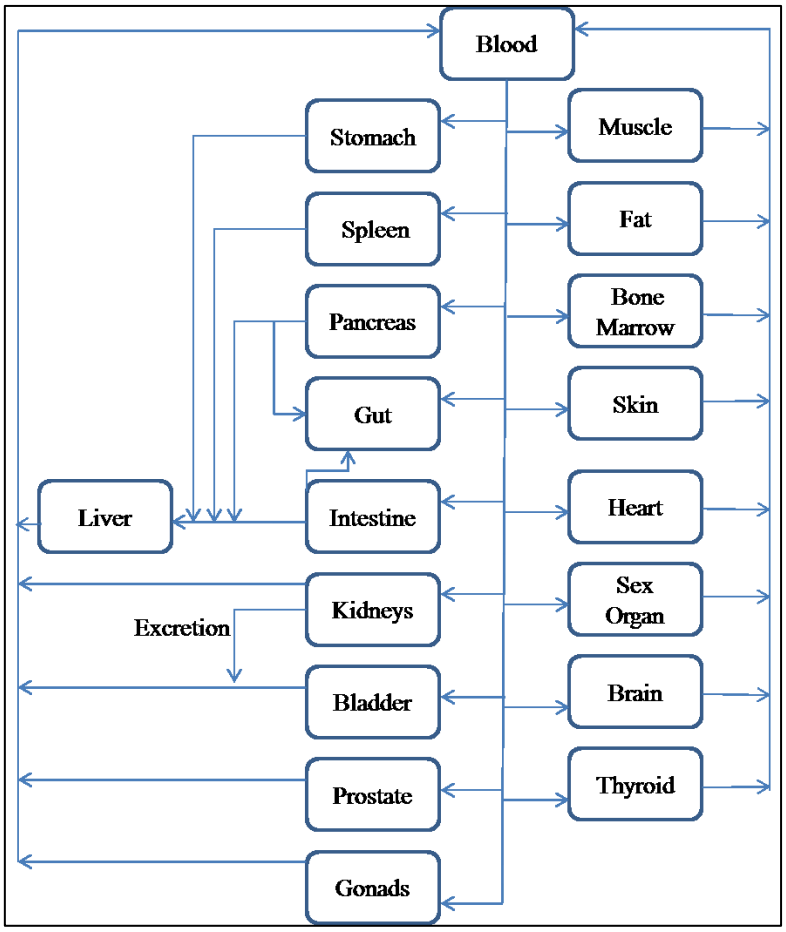

Figure 2.8: Representation of a physiological PK model with organs represented as one-compartment models. Adapted from (Saltzman, 2001).

In the literature, both compartmental and physiological models for cancer drugs are available and some references are listed in Table 2.3. Both compartmental and physiological models range from simple to more detailed models that are based on fewer assumptions. For

example for the case of Ara-C anti-leukemic agent, 1-compartmental model is developed and presented in the work of (Hijiya et al., 2006). This model describes 1 state, the drug concentration in the entire body, and includes two parameters i.e. the elimination rate constant and the systemic volume. On the other hand, for the same drug a physiological PK model is presented in the work of (Dedrick, 1972). This model describes the concentration state in 7 compartments including the liver, the kidney, the heart, the blood, the bone marrow, the gut and the lean muscle. The model depends on 21 parameters that comprise of the blood flow rate, volume, metabolism rate and clearance of each considered compartment. This example is used to explain that physiological models allow for a greater window of model accuracy and states inclusion, however, they require a larger amount of information for the accurate estimation of the model parameters. The level of detail added to the model depends on the data availability and the model purpose.

Table 2.3: PK models for cancer drugs

Compartmental Models	
Eight-compartmental model for methotrexate (MTX)	(Reich et al.,1977)
Multicompartmental model for doxorubicin	(Reich et al., 1977)
Three-compartmental model for idarubicinol	(Looby et al., 1997)
Two-compartmental model for methotraxate	(Hijiya et al., 2006)
Two-compartmental model for etoposide	(Hijiya et al., 2006)
Two-compartmental model for teniposide	(Hijiya et al., 2006)
One-compartmental model for Ara-C	(Hijiya et al., 2006)
Two-compartment model for etoposide	(Relling et al., 1998)
Two-compartmental pharmacokinetic model for etoposide	(Panetta et al., 2002)
Compartmental modelling of cyclosporine, etoposide and mitoxantrone	(Lacayo et al., 2002)
Two-compartment model of idarubicin	(Gillies et al., 1987)
Three-compartment model of mitoxantrone	(Richard et al., 1992)
Physiological Models	
Physiological model for Ara-C	(Morrison et al., 1975)
Physiological model for Ara-C (Ara-C)	(Dedrick et al., 1972)
Physiological model for thriopental	(Bischoff, Dedrick, 1968)
Physiological model for methotrexate	(Himmelstein, Lutz, 1979)
Physiologican model for adriamycin / doxorubicin	(Himmelstein, Lutz, 1979)
Physiological model for actinomycin-d	(Lutz et al., 1977)
Physiological model for adriamycin	(Chen et al., 1979)
Physiological model for cis-dichlorodiammine-platinum	(Chen et al., 1979)
Physiological model for cyclotidine	(Chen et al., 1979)

2.4.4 Pharmacodynamic (PD) modelling

PD models of anticancer drugs describe the effect of drugs that enter the cell and affect its function. Because of the complexity of the drug mechanism of action, detailed PD models are not in use. Empirical expressions relating drug concentration to drug effect are preferable (Holford, 1982) and the accuracy of the PD model is highly dependent on precision of the PK model.

In general, PD is the study of dose-response relationships. For the development of PD models for anti-cancer agents, tumour cells are exposed *in vitro* in different drug concentrations and drug effect curves are obtained. These data are then used to fit empirical PD models which are listed in Table 2.4 below. An example of a common dose-response curve is presented in figure 2.9. The drug effect curves are of utmost importance, especially for the early clinical trial phases, for the determination of maximal dose effect as well as for estimation of the effective drug dosing window.

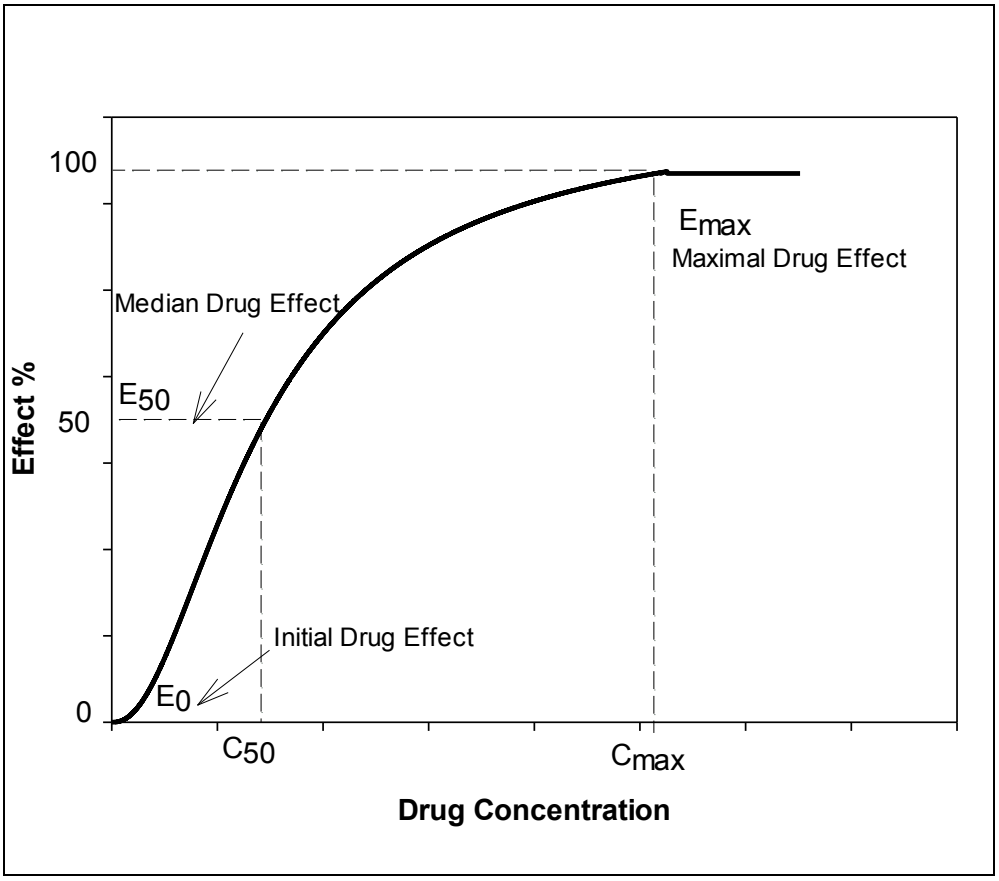

Figure 2.9: Schematic representation of an illustrative example of PD dose-response curves

The most widely used models are the drug effect models. These models relate drug concentration to drug effect which, for the purposes of this study, is the number of dead cells. These models contain estimated parameters from real-life data and drug effect depends only on the drug concentration (Table 2.4).

Table 2.4: Formulas of PD models (Holford et al., 1982)

Model	Model Equations	Description
Linear Model	$E = S \cdot C + E_o$	E: drug effect C: drug concentration S: slope parameter E_o: initial drug effect
Log-linear Model	$E = S \cdot \log C + I$	E: drug effect C: drug concentration S: slope parameter I: constant
E_{max} Model	$E = E_o - \frac{E_{max} \cdot C}{EC_{50} + C}$	E: drug effect C: drug concentration E_{max}: maximum drug effect E_o: initial drug effect from previous application EC_{50} : concentration producing half of the maximum drug effect
Sigmoid E_{max} model	$E = \frac{E_{max} \cdot C^n}{EC_{50}^n + C^n}$	E: drug effect C: drug concentration E_{max}: maximum drug effect E_o: initial drug effect from previous application EC_{50}: concentration producing half of the maximum drug effect n: constant affecting the shape of the drug effect-concentration curve

PART I:

Chemotherapy Treatment as a Process Systems Application

Chapter 3[1]

Mathematical Model Formulation

3.1 Introduction

In this chapter, chemotherapy treatment is presented and analysed from a process systems viewpoint. Section 3.2 presents framework for the design of personal optimised chemotherapy protocols by combining drug information together with patient and disease characteristics in order to develop the proper optimal dosing schedule for each individual. A major objective of the current project is to develop a mathematical model able to capture disease dynamics under chemotherapy for a patient case study. Section 3.3 presents the developed mathematical model for two chemotherapy protocols, the LDAC and the DA protocols as presented in section 2.3. The mathematical model depends on patient and disease characteristics that are analysed in detail, as well. Section 3.4 presents the sensitivity analysis results of the system, where the ranges of the inter-patient variability of the parameters considered in the model are collected from the literature and analysed with aim to identify the most crucial patient/disease dependent information that controls the treatment outcome, i.e. the level of leukemic cell population. After the sensitivity analysis, simulation results of two hypothetical patient case studies are presented and analysed in section 3.5 for the treatment of these patients under the two analysed chemotherapy protocols (LDAC and DA protocols).

[1] Work in this chapter has been published in Pefani E., Panoskaltsis N., Mantalaris A., Georgiadis M. C., Pistikopoulos E. N.. Design of optimal patient-specific chemotherapy protocols for the treatment of Acute Myeloid Leukemia (AML). Computers and Chemical Engineering Journal, 2013; 57: 187-195.

3.2. Framework for the development of optimal personalised chemotherapy protocols

Models aiming to describe the actions of chemotherapy should consist of mathematical expressions for all steps of drug treatment, from administration to intracellular action. The general framework for the derivation and function of such a mathematical model is described in figure 3.1.

To start, the initial dose load given to the patient in combination with the administration route and injection rate will be used for the calculation of treatment inflow (figure 3.1: box 1), the main input for the PK model.

The PK model (figure 3.1: box 2) depends on patient-specific characteristics and is comprised of the set of drug mass balances in patient organs for the calculation of the drug concentration profile. This profile is the main input for the PD model.

The PD model (figure 3.1: box 3) calculates the number of both normal and cancer cells which have died due to drug administration which are then successively subtracted from the starting number of cells (figure 3.1: box 4) in order to calculate the number of each cell type which remain following the chemotherapy cycle.

Thereafter, a new optimisation problem will be introduced and solved only if there are tumour cells still present (in this model) and normal cells are in sufficient number such that the patient can tolerate another chemotherapy cycle.

Within this framework, optimal chemotherapy cycles will be designed which aim to effectively control the treatment schedule (inflow, dose load) in order to eradicate the maximum possible number of cancer cells while maintaining normal cells within predefined limits. The optimal treatment will be different, defined case-by-case, based on physiological characteristics of the patient (determining drug kinetics) and cell characteristics (determining the diseased and normal population dynamics).

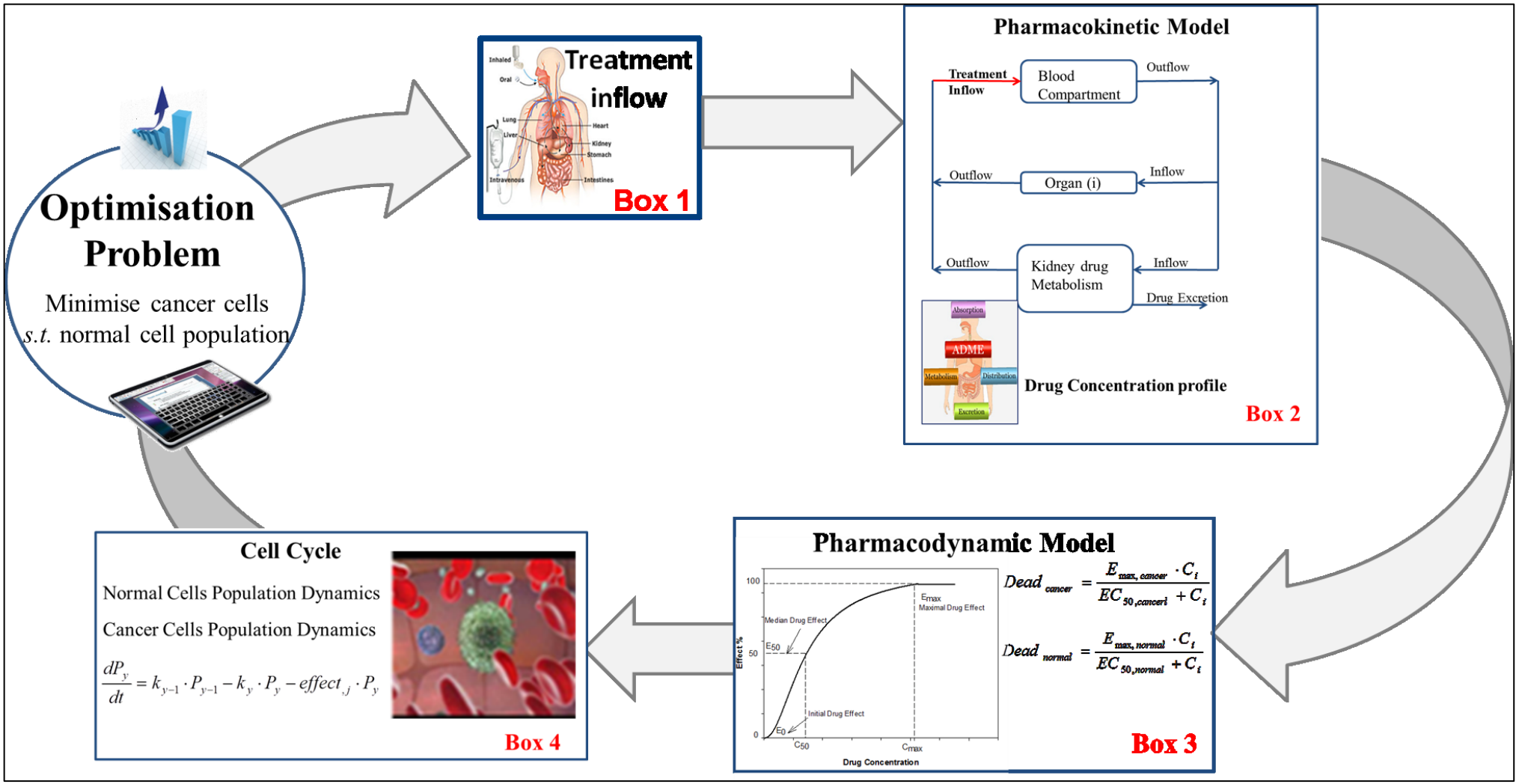

Figure 3.1: Framework for the derivation of optimal personalised chemotherapy protocols.

3.3 Physiologically based patient model for the treatment of AML with DNR and Ara-C

The need for more personalised treatment design has been previously presented (Undevia et al., 2007; Garattini, 2006; Essers, Trumpp, 2010). The main sources of inter- and intra-patient variability are in the cellular kinetics of the tumour and normal cell populations and the kinetics of the anti-cancer agents upon entering the human body. Thus, the desired mathematical model for the simulation of patient behaviour and tumour response during chemotherapy should consist of three parts: (i) the cell cycle model, which is the target of drug action, (ii) PK and (iii) PD aspects that provide the complete description of drug diffusion and action after administration.

In this section, a mathematical model is formulated to simulate the chemotherapeutic action of two anti-leukemic drugs, DNR and Ara-C, commonly used in clinical practice for the treatment of AML. The model describes the dynamic interactions of leukemic and normal cells exposed to chemotherapeutic drugs by a system of ordinary differential equations.

3.3.1 Mathematical model for IV and SC dose applications of DNR and Ara-C anti-leukemic agents

In this section the developed mathematical model is described in subsections I to VI. Table 3.1 lists the model parameters and includes the unit of the parameters and their description.

Table 3.1: List of model parameters

Symbol	Unit	Description
dose	mg	Drug dose in mg
duration	min	Dose duration
u	mg/m^2	Drug dose in mg/m^2
weight	kg	Patient weight
height	cm	Patient height
k_a	min^{-1}	Absorption rate
k_b	-	Bioavailability
$k_{l,Ara\text{-}C}$	min^{-1}	Ara-C liver elimination rate
$k_{k,Ara\text{-}C}$	L/min	Ara-C clearance rate by the kidneys
$k_{k,DNR}$	L/min	DNR clearance rate by the kidneys
$k_{l,DNR}$	min^{-1}	DNR elimination rate in liver
Vi	L	Volume of body organs B: blood, H:heart,Li:liver, K:kidney, M:bone marrow, Le: lean muscle
V_{iT}	L	Volume of organ tissue
Qi	L/min	Blood flow rate of body compartments i
$E_{max,Ara\text{-}C}$	-	Ara-C maximum drug effect
$E_{50,Ara\text{-}C}$	mg/L	Ara-C concentration at half drug effect
$E_{max,DNR}$	-	DNR maximum drug effect
$E_{50,DNR}$	Mg/L	DNR concentration at half drug effect
$slope_{DNR}$	-	slope scaling factor for DNR PD action
γ	min^{-1}	the death rate of cells in proliferation phase
δ	min^{-1}	the death rate of cells in non-proliferation phase
τ	min	the duration of proliferation phase
β_o	min^{-1}	the maximum recruitment rate
θ	cells/kg	cell population of growth phase when $\beta = \frac{\beta_o}{2}$
n	-	Scale factor depicting the sensitivity of the transition rate to the cell population of growth phase
k_1	min^{-1}	Transition rate of cells from G_1- to S- phase
k_2	min^{-1}	Transition rate of cells from S- to G_2M- phase
k_3	min^{-1}	Transition rate of cells from G_2M- to G_1- phase
μ_{G1}, μ_S, μ_{G2M}	min	natural apoptosis time constants for each cell cycle phase
T_{G1}, T_S, T_{G2M}	min	Duration constants for each cell cycle phase
T_c	min	Duration of the whole cell cycle

I. Treatment Inflow

$$In_{,j} = \frac{dose_{,j}}{duration_{,j}} \quad \text{(equation 3.1)}$$

$$dose_{,j} = u_{,j} \cdot bsa \quad \text{(equation 3.2)}$$

$$bsa = \sqrt{\frac{height \cdot weight}{3600}} \quad \text{(equation 3.3)}$$

The inflow rate ($In_{,j}$) is the rate of the administered dose applied over the dosage duration. The dose is adjusted to the patient by its multiplication with the body surface area (bsa), calculated by Mosteller empirical equation 3.3 as is currently done in clinical practice. These equations are used for the calculation of the inflow rate given the treatment schedule characteristics i.e. the dose load and duration of administration. Moreover, these two characteristics comprise the control variables for the optimisation problem.

II. Pharmacokinetic model

For both drugs, DNR and Ara-C, physiologically based PK models are used to calculate drug concentration of the active metabolite in specific human organs at each time point. Initially, the drug is injected into the blood and circulates to the whole body. The mass balance for the blood compartment is:

$$V_B \cdot \frac{dC_{B,j}}{dt} = \sum_{\substack{i:H,Li,M,Le \\ j:ara-C,DNr}} Q_i \cdot C_{i,j} + Q_K \cdot C_{K,j} - Q_B \cdot C_{B,j} + In_{,j} \quad \text{(equation 3.4)}$$

where $C_{B,j}$ is the concentration of drug j in the blood compartment, V_B is the total patient blood volume, Q_i is the blood flow in organs i: heart (H), liver (Li), BM (M), Le (lean), $C_{i,j}$ is the concentration of drug j in organs i, Q_K is the kidney blood flow, $C_{K,j}$ is the drug concentration in the kidneys and inflow is the treatment inflow as calculated in equation 3.1.

The metabolic action takes place in the liver and then the active metabolite is circulated in the body via the blood. The mass balance in body organ i is as follows:

$$V_i \cdot \frac{dC_{i,j}}{dt} = Q_i \cdot C_{B,j} - Q_i \cdot C_{i,j} - k_{i,j} \cdot C_{i,j} \cdot V_{iT} \quad \text{(equation 3.5)}$$

The drug is transmitted via the blood to the organs. The term $k_{,i,j}$ is the elimination rate of the drug j in the body organs i and has a non-zero value only for the liver.

After drug elimination and action, the drug is excreted through urine with clearance rate ($k_{K,j}$) from the kidneys. An extra factor is introduced in the mass balance of the kidneys (equation 3.6) to account for the drug clearance ($k_{K,j}$) . The cumulative excretion is calculated by (equation 3.7).

$$V_i \cdot \frac{dC_{i,j}}{dt} = Q_i \cdot C_{B,j} - Q_i \cdot C_{i,j} - k_{kKj} \cdot C_{B,j} \cdot V_{iT} \qquad \text{(equation 3.6)}$$

$$U_{,j} = \int_0^t k_{K,j} \cdot C_{B,j} dt \qquad \text{(equation 3.7)}$$

III. Pharmacodynamic model

The PD model is used for the calculation of drug effect, i.e. is the fraction of cells killed due to drug action per unit time. The PD model is shown in equation 3.8 where the main input is drug concentration at the location of the tumour, which for AML is the concentration in BM ($C_{M,j}$) and is calculated by the PK model.

$$effect_{,j} = \frac{E_{\max,j} \cdot C_{M,j}^{slope,j}}{E_{50,j} + C_{M,j}^{slope,j}} \qquad \text{(equation 3.8)}$$

$E_{max,j}$, $E_{50,j}$ and slope are the PD parameters that depend on the drug j and are validated using clinical data.

IV. Cancer Cell cycle model

A dynamic model is used for the description of the cell cycle through chemotherapy treatment. The selected compartments are the cells in G_1 phase, S-phase, and combined G_2 and M phases. G_1 is the first compartment after the starting point of the cell cycle and lasts T_{G1} hours. Afterwards, the cell proceeds to S-phase (DNA replication). This phase lasts T_S hours and the cell is transferred to the last compartment, G_2 and M that last T_{G2M} hours and results in two newborn cells. The mathematical model consists of the mass balances between these compartments and is described by the following equations,

$$\frac{dG_1}{dt} = 2 \cdot k_3 \cdot G_2M - k_1 \cdot G_1 - effect_{,j} \cdot G_1 \quad \text{(equation 3.9)}$$

$$\frac{dS}{dt} = k_1 \cdot G_1 - k_2 \cdot S - effect_{,j} \cdot S \quad \text{(equation 3.10)}$$

$$\frac{dG_2M}{dt} = k_2 \cdot S - k_3 \cdot G_2M - effect_{,j} \cdot G_2M \quad \text{(equation 3.11)}$$

where G_1, S, G_2M represent the cell population in cell cycle compartments, k_1, k_2, k_3 are the transition rates between cell phases and $effect_{,j}$ is calculated by the PD model (equation 3.8) and is the percentage of each cell cycle population killed by the anticancer drug. This parameter has physical meaning only if a drug acts on a particular cell phase i.e. for drug Ara-C the effect will be 0 for phases G_1 and G_2M, whereas for DNR the effect will be 0 only for phase G_2M. The transition rates are functions of the duration of the cell cycle phases and are calculated by the following equations,

$$k_1 = \frac{1}{T_{G1} + \mu_{G1}} \quad \text{(equation 3.12)}$$

$$k_2 = \frac{1}{T_S + \mu_S} \quad \text{(equation 3.13)}$$

$$k_3 = \frac{1}{T_{G2M} + \mu_{G2M}} \quad \text{(equation 3.14)}$$

where μ_{G1}, μ_S, μ_{G2M} are the natural apoptosis time constants for each cell cycle phase.

As the cell cycle is a dynamic model, the solution depends on the initial state. The initial distribution of the cell population in the cell phases is difficult to measure and will be estimated by the following equations,

$$G_1\big|_{t=0} = \frac{T_{G1}}{Tc} \cdot N(0) \quad \text{(equation 3.15)}$$

$$S\big|_{t=0} = \frac{T_S}{Tc} \cdot N(0) \quad \text{(equation 3.16)}$$

$$G_2M\big|_{t=0} = \frac{T_{G2M}}{Tc} \cdot N(0) \quad \text{(equation 3.17)}$$

where T_C is the total cell cycle time and N(0) is the initial number of cancer cells in the modelled cell cycle population.

V. Normal cell cycle model

The normal stem cell reserve contains cells which can replicate, differentiate or die. These cells are grouped into two compartments, proliferating (P) and non-proliferating (Q) cells. Non-proliferating cells are G_1 phase cells grouped together with quiescent cells. These cells are activated and transmitted to the proliferating compartment at a rate (β(Q)) that is reciprocal to the number of quiescent cells (equation 3.20), i.e. when the number of cells is low, more cells will be activated in order to preserve the stem cell population. The set of mathematical equations expressing the behaviour of normal cells are as follows,

$$\frac{dQ}{dt} = -\delta \cdot Q - \beta(Q) \cdot Q + 2 \cdot e^{-\gamma \cdot \tau} \cdot \beta(Q) \cdot Q - effect_{,j} \cdot Q \qquad \text{(equation 3.18)}$$

$$\frac{dP}{dt} = -\gamma \cdot P + \beta(Q) \cdot Q - e^{-\gamma \cdot \tau} \cdot \beta(Q) \cdot Q - effect_{,j} \cdot P \qquad \text{(equation 3.19)}$$

$$\beta(Q) = \beta_o \cdot \frac{\theta^n}{\theta^n + Q^n} \qquad \text{(equation 3.20)}$$

Where γ is the death rate in proliferative phase, δ is the death rate in non-proliferative phase, τ is the duration of proliferation, β_o is the maximum recruitment rate, θ is the cell population of growth phase when $\beta = \frac{\beta_o}{2}$ and n is a positive parameter depicting the sensitivity of the transition rate to the cell population of growth phase.

VI. Drug subcutaneous route

Sc route is an alternative route of drug delivery where the drug is injected into the individual's subcutaneous tissue. In this type of drug administration, the drug inflow reaches the systemic circulation with a certain time delay (absorption rate) and in a decreased amount (bioavailability) as some of the initial drug given is being bound during drug absorption from the sc to the blood compartment (figure 3.2).

For the case of sc dosing, two main differences are included in the model:

- An absorption rate
- A bioavailability term.

For the model of the SC route, equation 3.4 will be replaced by equations 3.4a and 3.4b that account for drug bioavailability (k_b) and absorption delay (k_a).

$$\frac{dS}{dt} = In - k_a \cdot S \qquad \text{(equation 3.4a)}$$

$$V_B \cdot \frac{dC_B}{dt} = \sum_{i:H,Li,M,Le,K} Q_i \cdot C_{i,j} - Q_B \cdot C_{B,j} + k_a \cdot k_b \cdot S \qquad \text{(equation 3.4b)}$$

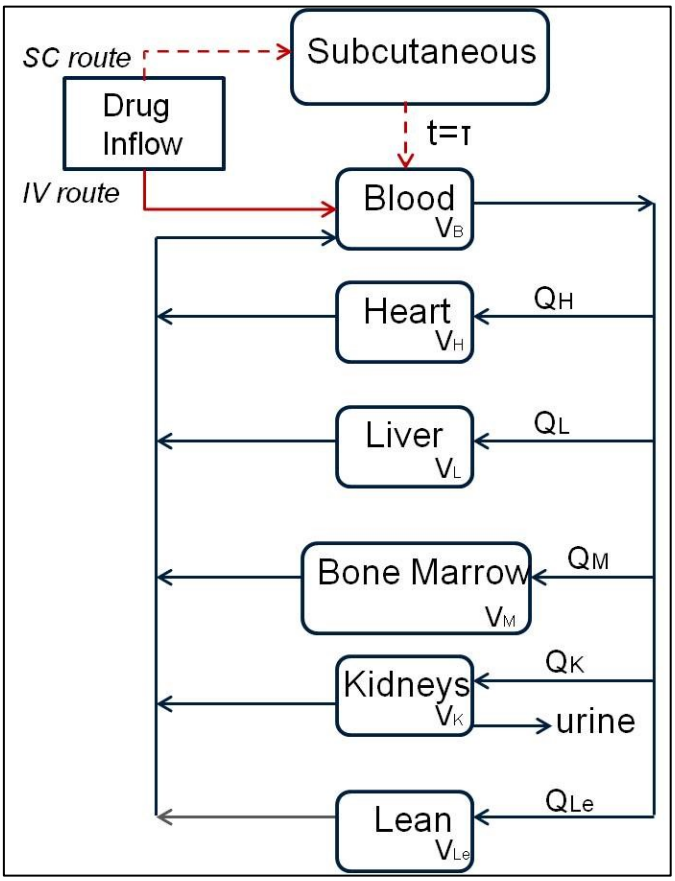

Figure 3.2: Schematic representation of Ara-C PK model following either i.v. or sc administration route

3.3.2 Patient and disease characteristics

The available patient information consists of the patient physiological characteristics i.e. patient sex, age, height and weight. These characteristics are used in the current model for the calculation of organ blood flow (Qi) and organ volume (Vi), variables used by the PK model

(equations 3.4-3.7). These variables are varying for patients with different anatomical and age characteristics and empirical expressions exist in the literature, which relate these patient characteristics to the two variables, Qi and Vi. The expressions incorporated in the current presented model are listed below.

Blood flow equals the cardiac output and is distributed to the body organs. The expression used for the calculation of cardiac output is adapted from the work of (Brody, 1945) and depends on the body weight,

$$CardiacOutput(lt/\min) = 0.2 \cdot weight(kg)^{\frac{3}{4}} \quad \text{(equation 3.21)}$$

Data provided by (Dedrick et al., 1971) are then used to calculate the percentage of cardiac output reaching various body organs (Table 3.2).

Table 3.2: Organ blood flow variability (Dedrick et al., 1971)

Body Organ	Blood flow (L/min)
Heart	0.06·CO*
Kidneys	0.31·CO*
Liver	0.36·CO*
BM	0.044·CO*
Lean	(1-0.2-0.07-0.044)·CO*=0.686·CO*

*CO: cardiac output

The heart volume depends on the number of heart chambers and the stroke volume (SV), that is the volume pumped from each chamber of the heart at each heartbeat and is calculated by equation 3.22.

$$V_H = chamber \cdot SV \quad \text{(equation 3.22)}$$

Both for males and females, the number of chambers is 4; for males, stroke volume is 70ml and for females 60ml. Thus, the calculated heart volumes will be 0.28 L and 0.24 L for males and females, respectively.

The blood volume depends on patient physiological characteristics of height and weight and separate expressions exist for female blood volume ($V_{B,F}$) (Brown et al., 1962) and for male blood volume ($V_{B,M}$) (Wennesland et al., 1959) as shown in equations 3.23 and 3.24, respectively.

$$V_{B,F}(ml) = 16.52 \cdot height(cm) + 38.46 \cdot weight(kg) - 1369 \quad \text{(equation 3.23)}$$

$$V_{B,M}(ml) = 28.5 \cdot height(cm) + 31.6 \cdot weight(kg) - 2820 \quad \text{(equation 3.24)}$$

Liver volume is calculated by equation 3.25 and depends on the body surface area and an age factor that is calculated depending on the age range an individual belongs to, as described in equation 3.25 (Yuan et al., 2008)

$$V_L(ml) = 949.7 \cdot BSA - 48.3 \cdot age - 247.4 \quad \text{(equation 3.25)}$$

where, $age = \begin{cases} 1, & years \le 40 \\ 2, & 40 \le years \le 60 \\ 3, & years \ge 60 \end{cases}$

Kidney volume is dependent on the weight factor of an individual (Cohen et al., 2007) and is calculated by equation 3.26 below,

$$V_K(ml) = 2.96 \cdot weight(kg) + 113 \quad \text{(equation 3.26)}$$

Equations for the BM and the lean muscle are not available as expressions of individual characteristics and the mean values will be used, V_M=2 L and V_{lt}=27 L, as found in (Dedrick et al.et al., 1971). Moreover, for the individual volumes of liver and kidney tissue, values used are as reported in (Dedrick et al., 1971).

As far as disease-specific information is concerned, the current presented model is a dynamic model, hence it depends on the initial state which depends on the blast percentage and the BM cellularity at the beginning of each chemotherapy cycle (explained later in this chapter). Moreover, the proliferation rate and the duration of each cell cycle phase are important factors that affect tumour expansion and characterise the aggressiveness of the disease which differs between different patients.

3.3.3 Model Assumptions

Cell cycle

Cell cycle is the process under which the cell replicates its genetic material to divide into two daughter cells. This is a complex process where numerous phenomena take place and cell-cycle phases serve only as checkpoints between the different states of the cells. Particularly

the cell cycle is separated into four phases: the G_1-phase, the S-phase, the pre-mitotic phase (G_2-phase) and the mitosis phase (M-phase) as has already been described in Chapter 2.

Compartmental cell cycle models, including cell cycle phases in separate compartments, are sufficient to describe cell kinetics under the effect of chemotherapy, that is the ultimate purpose of the current developed mathematical model. These compartmental models consist of the mass balances between compartments included in the model and the leading parameters are the initial condition of each cell cycle phase, the duration of each cell cycle phase and the transition rate between phases.

For purposes of chemotherapy optimisation, both the leukemic population (treatment objective) and the normal population (toxicity restriction) will have to be modelled. The major difference between these two populations lies on the different proliferation rate - leukemic cells exhibit a higher proliferative capacity that enables the cells to expand at a higher and faster rate compared with that of the normal population. In contrast, normal cells have a lower proliferation rate and a higher percentage of the population is in the non-proliferating state ready to be reactivated at times of population depletion.

This difference in population dynamics is mathematically expressed by consideration of different compartmental models and different transition rates between cell cycle phases. For the case of normal cell cycle, a two-compartmental model has been used including cells in non-proliferating and in proliferating state (figure 3.3). A feedback function is assumed for the transition rate of non-proliferating normal cells into proliferation. This transition rate is reciprocal to the number of non-proliferating normal cells, i.e. a decrease of proliferating cells exposed to chemotherapy provokes a higher transition rate of cells into proliferation in order to replenish the number of normal cells lost. This mathematical model for the normal cell population is a well-established model extensively used in the literature (Andersen, Mackey, 2001; Colijn, Mackey, 2005).

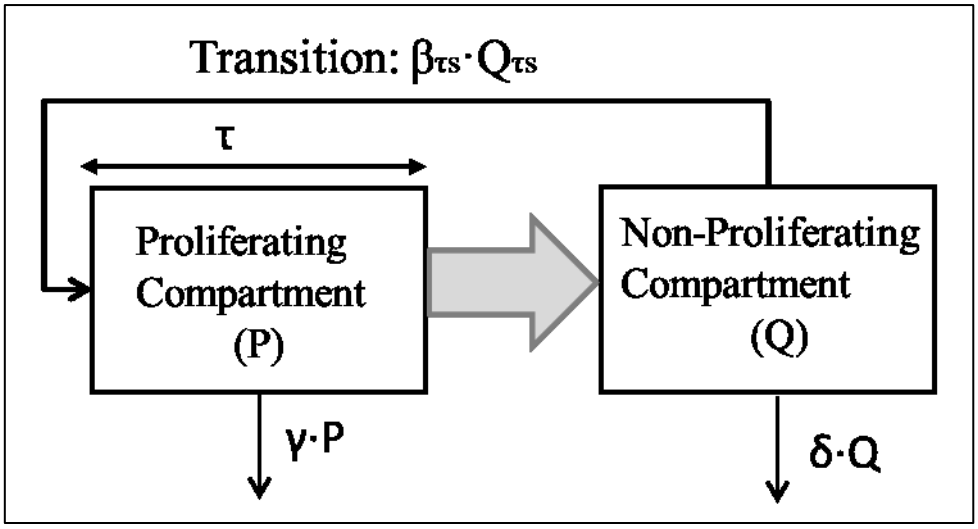

Figure 3.3: Representation of compartmental model for the normal cell population

However, this model is limited in the description of normal cell kinetics under the influence of chemotherapy and is not able to predict population recovery after treatment completion. For the case of AML, this recovery period ranges between patients and has mean duration of approximately 25 days. During this interval period, the normal population is recovering with dynamics that have not yet been examined and constitute a "black-box" process that is monitored through the level of platelets, leukocyctes and erythrocyte cells in patient blood samples.

Moreover, a three compartmental model is used for the leukemic population (figure 3.4). The first compartment includes cells in the G_0- and G_1- phases. Leukemic cells in their highest percentage will be proliferating, but this compartment of cells prior to proliferation will control proliferation as it adds a time delay in the proliferation process. The second compartment includes cells in S-phase and the third compartment merges cells in the G_2 - and M- phases. The transition rates between the succeeding cell phases are expressions of the duration of each cell-cycle phase.

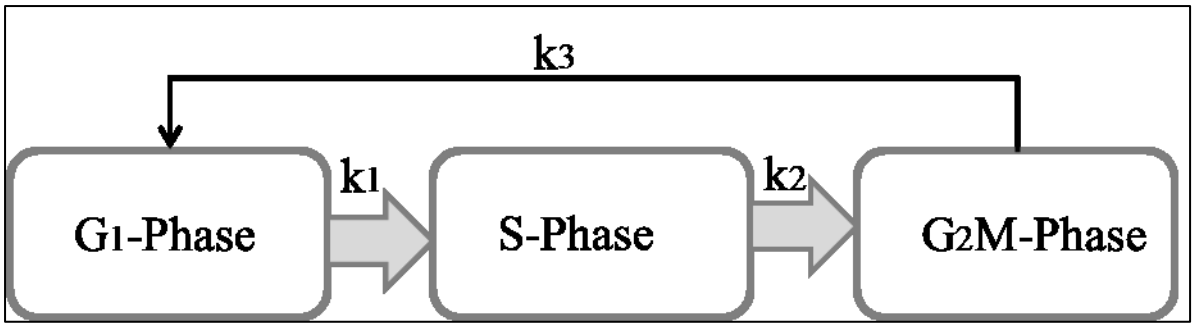

Figure 3.4: Representation of compartmental model for the AML cell population

Pharmacokinetics

A lumped compartmental model is used for the PK model development. This compartmental model includes body organs in compartments and a set of mass balances amongst them is constructed to describe the dynamic profile of drug concentration within the included organs. Flow-limitation formation is assumed for the description of the compartments, accepting that drug concentration in the blood outflow from a compartment will be in equilibrium with drug concentration in the tissue. This is a valid assumption often made for the development of PK models; however, it is not fundamental and is based on the lack of detailed physiological information, such as for membrane permeabilities, diffusion coefficients and tissue surfaces.

Moreover, for the incorporation of drug metabolism and elimination, parameters of elimination rate in the liver and the clearance rate through the kidneys are used. These parameters are calculated by using the drug concentration in plasma samples and the drug concentration in urine, respectively. The choice to include only these two types of parameters for purposes of the current analysis is because they are measured by well-established methods by pharmaceutical companies and are the only parameters provided in protocols of product characteristics. Undoubtedly, more complex phenomena take place from drug administration to drug distribution in the tumour location; however, patient variability determining in these phenomena would definitely be depicted in the drug plasma concentrations and the drug concentration in urine samples, which are the only two measurements available from the *in-vivo* system i.e. the human body undergoing treatment.

In summary, the leading principle behind the current model development is to include phenomena governed by parameters measured in clinical practice (patient physiological characteristics, treatment schedule, leukemic blast percentage in BM aspirate, BM cellularity) and parameters provided by pharmaceutical companies (drug half-life, elimination rate, clearance rate), with cell cycle duration times acquired from published literature.

3.4 Model Sensitivity Analysis

To gain a further understanding of the model and the crucial parameters that highly affect the treatment outcome i.e. the level of leukemic cells, a global sensitivity analysis and Quasi Monte-Carlo based high dimensional model representation using Sobol's indices was performed using the GUI-HDMR software (Ziehn, Tomlin, 2009). The output of interest is

the number of leukemic cells and the parameters checked are the cell cycle times, and the PK and PD parameters listed in Table 3.2.

Specifically, the drug elimination rates in the liver were included for the studied drugs as significant inter-patient variability has been reported as has patient variability for DNR kidney clearance rate(ULCH, 2009; BC cancer agency, 2007). However, there is no measured variability of the kidney clearance rate for Ara-C at the doses used in this protocol, and this parameter is not included in the sensitivity analysis. For the inter-patient variability of PD parameters, the work of (Quartino et al., 2007) has been used that includes analysis of PD action of DNR and Ara-C on BM samples of 179 patients with AML. Moreover, the cell cycle parameter ranges are as previously reported (Raza et al., 1990) with evaluation of the cell kinetics in 54 patients diagnosed with AML.

For the calculation of parameters sensitivity index (SI), 40,000 simulations were run of all the possible combinations of the tested parameters within their assigned ranges. The SI results are presented in Table 3.3. The SA results clearly indicate that the duration of the cell cycle phases is the most crucial parameter where Tc has an effect of 60.4% on the treatment outcome and Ts has 27.05% effect. The limit for a parameter is considered to be a crucial factor affecting the measured variable is at least 10%.

Table 3.3: PK, PD, cell cycle parameters and inter-individual ranges used for model sensitivity analysis and sensitivity index results

	Symbol	Default value	Range	Ref.	Sensitivity Index
PK	$k_{l,Ara\text{-}C}$	0.069	0.067-0.07	(UCLH, 2009)	0.0007
	$k_{k,DNR}$	1.5	0.036-1.7	(BC Cancer Agency, 2007)	0.017
	$k_{l,DNR}$	0.015	0.014-0.017	(BC Cancer Agency, 2007)	0.000085
PD	$E_{max,Ara\text{-}C}$	0.83	0.79-0.86	(Quartino, 2007)	0.0003
	$E_{50,Ara\text{-}C}$	0.29	0.25-0.33	(Quartino, 2007)	0.0049
	$E_{max,DNR}$	0. 91	0.88-0.93	(Quartino, 2007)	0.00925
	$E_{50,DNR}$	0.09	0.076-0.1	(Quartino, 2007)	0.0928
	$slope_{DNR}$	1.23	1.06-1.4	(Quartino, 2007)	0.000468
Cell Cycle	T_s	15	6-43	(Raza, 1990)	**0.2705**
	T_C	60	18-211	(Raza, 1990)	**0.604**

3.5 Simulation results for two hypothetical patient case studies

3.5.1 Model parameters for the patient case studies

The set of parameters used for all patient case studies are the drugs pharmacologic information, i.e. PK and PD for the two drugs, and the parameters for the normal cell population. Tables of these parts of the model are listed in Tables 3.4 and 3.5 below.

Table 3.4: Pharmacology (PK – PD) parameters for Ara-C and DNR anti-leukemic agents

	Symbol	Value	Description	Reference
PK	$k_{l,Ara\text{-}C}$	0.069 min^{-1}	Ara-C liver elimination rate	(UCLH, 2009)
	$k_{k,Ara\text{-}C}$	0.09	Ara-C clearance rate by the kidneys	(UCLH, 2009)
	$k_{k,DNR}$	1.5 $\frac{L}{min}$	DNR clearance rate by the kidneys	(BC Cancer Agency, 2007)
	$k_{l,DNR}$	0.015 min^{-1}	DNR elimination rate in liver	(BC Cancer Agency, 2007)
	ka	0.21 min^{-1}	Ara-C Absorption rate	(Slevin et al., 1981)
PD	$E_{max,Ara\text{-}C}$	0.83	Ara-C maximum drug effect	(Quartino et al., 2007)
	$E_{50,Ara\text{-}C}$	0.29 $\frac{mg}{L}$	Ara-C concentration at half drug effect	(Quartino et al., 2007)
	$E_{max,DNR}$	0. 91	DNR maximum drug effect	(Quartino et al., 2007)
	$E_{50,DNR}$	0.09 $\frac{mg}{L}$	DNR concentration at half drug effect	(Quartino et al., 2007)
	$slope_{DNR}$	1.23	slope scaling factor for DNR PD action	(Quartino et al., 2007)

Moreover, for the normal cell population published data (Andersen, Mackey, 2001) are used and listed in Table 3.5.

Table 3.5: Parameters of the compartmental model for the normal BM cell population

Symbol	Value	Description	Reference
γ	0.00007 min^{-1}	the death rate of cells in proliferation phase	(Andersen,Mackey, 2001)
δ	0.0001 min^{-1}	the death rate of cells in non-proliferation phase	(Fister, Panetta, 2000)
τ	4032 min	the duration of proliferation phase	(Andersen,Mackey, 2001)
β_o	0.0021 min^{-1}	the maximum recruitment rate	(Andersen,Mackey, 2001)
θ	$0.5 \cdot 10^6$ cells/kg	cell population of growth phase when $\beta = \frac{\beta_o}{2}$	(Andersen,Mackey, 2001)
n	4	Scale factor depicting the sensitivity of the transition rate to the cell population of growth phase	(Andersen, Mackey,2001)

The information that will be modified for each patient case study is as follows,

- Patient physiological characteristics (sex, age, weight)
- Patient disease characteristics (initial tumour burden, duration of cell cycle phases)
- Treatment schedule

The presented model is used for the simulation analysis of two different chemotherapy protocols, the LDAC and DA protocols, consistent with current clinical practice.

The LDAC protocol consists of (sc) Ara-C doses of 20 mg administered every 12 hrs for 10 days.The DA protocol includes DNR doses of 60 mg/m^2 administered for 1 hr IV infusion on days 1, 3 and 5 of the chemotherapy cycle and Ara-C doses of 100 mg/m^2 administered every 12 hrs for 10 days. These two protocols are simulated for two patient case studies using data previously reported (Clarkson et al., 1967). Table 3.6 lists the cell population and physiological characteristics of the two patient case studies.

Table 3.6: Hypothetical patient case study based on published data (Clarkson et al, 1967)

Physiological Patient Characteristics				
	Sex	**Age (yrs)**	**Height (m)**	**Weight (kg)**
Patient H1	F	61	1.60	70
Patient H2	F	68	1.60	70
AML population characteristics				
	Tumour burden (blasts/kg)	**G_0G_1-phase duration (hrs)**	**S-phase duration (hrs)**	**G_2M-phase duration (hrs)**
Patient H1	$2.6 \cdot 10^9$	61	19	3.62
Patient H2	$1.6 \cdot 10^9$	24	22	3.47

Induction treatment includes 4 chemotherapy cycles of either LDAC or DA with interval periods between chemotherapy cycles when no drug is supplied. As has already been mentioned, this period is a recovery period with mean duration of 25 days during which the patient receives no treatment. During this period, daily blood tests take place to monitor the patient's blood and immune system recovery, i.e. the recovery of the level of leukocytes, platelets and erythrocytes. It impossible to derive the same measurements for the leukemic/blast population as the number of BM aspirations must be limited for patient safety and ethical reasons. This "black box" period increases the uncertainty for the analysis of the clinical data as the behaviour of the leukemic cells is unknown.

Based on clinical experience, a valid assumption during this interval period is that a 1-log disease increase will occur. In our model, this is expressed by cell cycle times Ts and Tc equal to 40 hours and 211 hours, respectively. These values are taken from published work (Raza et al., 1990) and represent cell cycle times required for the leukemic cell population to have a slower proliferation rate. This assumption has been made, since post-chemotherapy administration, the BM microenvironment has been affected by the same drugs used to kill the tumour and is therefore more hostile towards the expansion of cells, including leukemic.

3.5.2 Simulation results of Patient H1 undergoing LDAC and DA induction treatments

- **Simulation results of the LDAC protocol for patient H1**

1st Chemotherapy Cycle

In this section simulation results are presented for Patient H1 with physiological and disease characteristics presented in Table 3.6. Figure 3.5 presents the normal and leukemic population dynamics for the 1st chemotherapy cycle with LDAC.

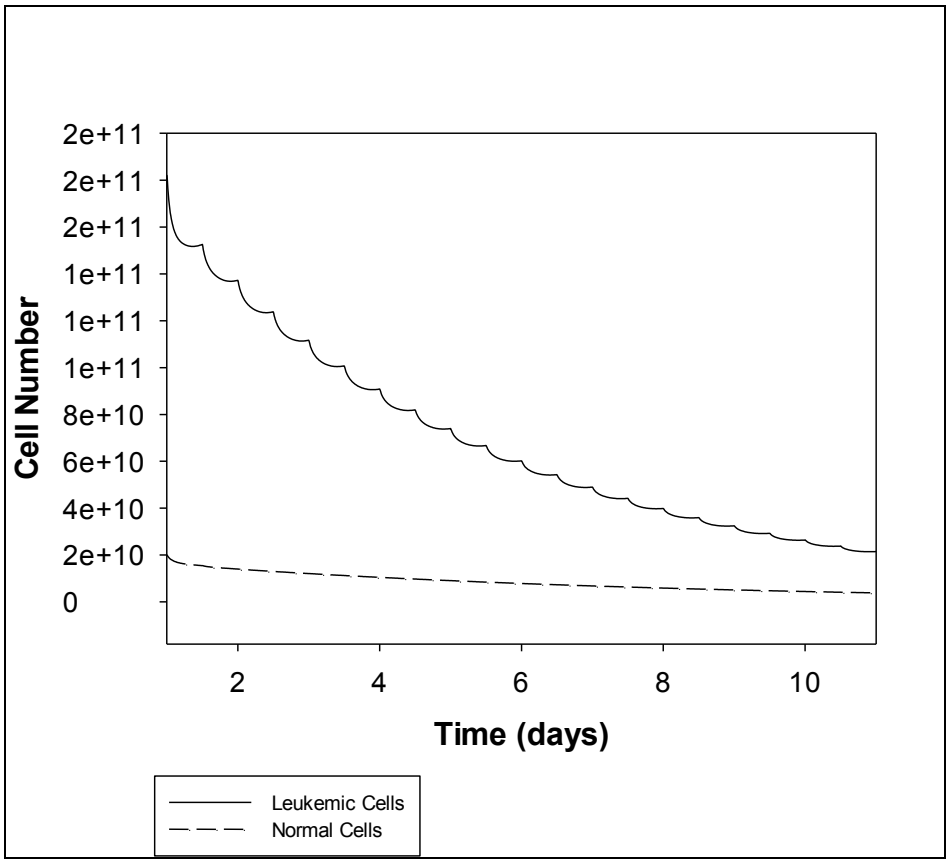

Figure 3.5: Patient H1 behaviour over the first cycle (days 1-11) of LDAC induction treatment

A decrease of $1.6 \cdot 10^{11}$ leukaemic cells results as the population declines from $1.82 \cdot 10^{11}$ to $2.14 \cdot 10^{10}$ cells. Normal cells decreases as well from $1.9 \cdot 10^{10}$ cells initially to $3.8 \cdot 10^{9}$ cells by cycle completion representing a $1.52 \cdot 10^{10}$ variance. The main objective, even from the 1st cycle of induction chemotherapy treatment, is to reduce the leukemic population to a level lower than that of the normal cell population. This objective is not achieved for Patient H1 after the 1st cycle of LDAC and the chemotherapy cycle is not successful.

2nd Chemotherapy Cycle

At the beginning of the 2nd chemotherapy cycle, the leukemic cell population equals $2.44 \cdot 10^{11}$ cells, which is already higher than that of the leukemic initial state at the point of diagnosis, i.e. the initial population at the beginning of the 1st cycle ($1.82 \cdot 10^{11}$ cells). The behaviour of the normal and leukemic cell populations over the 2nd chemotherapy cycle from day 36 to day 46 of treatment is presented in figure 3.6.

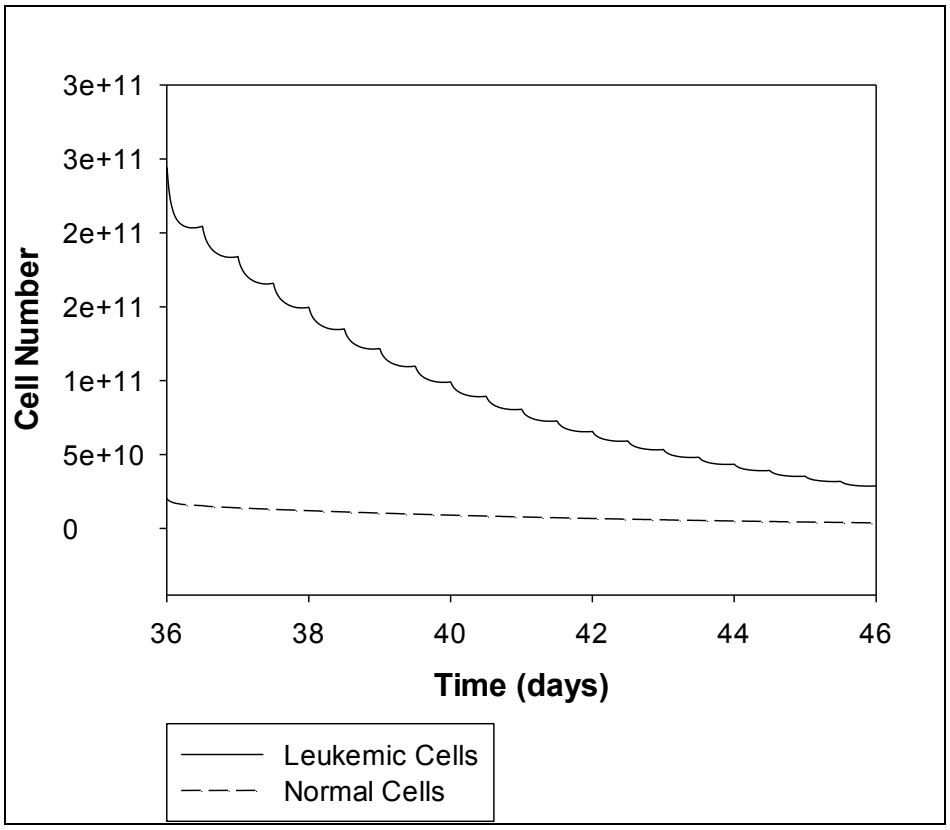

Figure 3.6: Patient H1 behaviour over the 2nd cycle (days 36-46) of LDAC induction treatment

Over the 2nd chemotherapy cycle, leukemic cell number decreases from $2.44 \cdot 10^{11}$ to $2.87 \cdot 10^{10}$ cells, with a variance of $2.15 \cdot 10^{11}$ cells. Moreover, normal cells will have the same dynamics as the initial population and the applied protocol is the same as that for the 1st chemotherapy cycle. At completion of the 2nd chemotherapy cycle, the leukemic population is still higher than that of the normal population with a difference of $2.5 \cdot 10^{10}$ cells.

3rd Chemotherapy Cycle

After the 2nd chemotherapy cycle, one more recovery period without chemotherapy treatment occurs for 25 days. Over this period, both normal and leukemic cell populations will increase, since cells are left without the effects of cytotoxic treatment. The normal population is

assumed to fully recover during this period i.e. the state at the beginning of the 3rd cycle will be similar that at the beginning of the 1st chemotherapy cycle ($1.9 \cdot 10^{10}$ cells). The estimated initial leukemic population at the beginning of the 3rd cycle is $3.27 \cdot 10^{11}$ cells. This cell population is even higher compared with that of the initiating populations at the start of chemotherapy cycles 1 and 2.

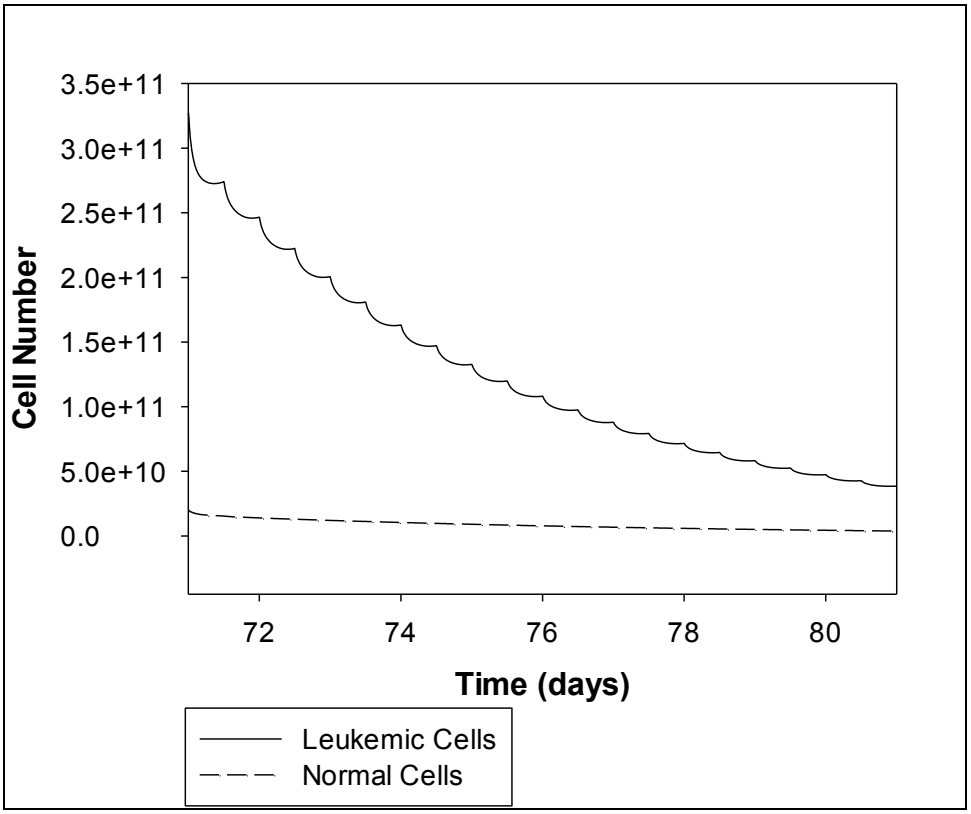

Figure 3.7: Patient H1 behaviour over the third cycle (days 71-81) of LDAC treatment

Over the 3rd chemotherapy cycle, leukemic population decreases down to $3.85 \cdot 10^{10}$ cells, with a variance of $2.88 \cdot 10^{11}$ cells. Moreover, normal cells will have the same dynamics as that over the 1st chemotherapy cycle since the initial normal population will be the same as well as when the chemotherapy schedule is administered (At completion of the 3rd chemotherapy cycle, the leukemic burden is still higher than that of the normal population with a difference of $3.47 \cdot 10^{10}$ cells, indicating that this cycle is not successful (figure 3.7).

4th Chemotherapy Cycle

The increasing leukemic population present at the beginning of all chemotherapy cycles together with the sustained difference between leukemic and normal cells (higher leukemic cell number than that of normal cells) are clear indicators that this protocol is not effective for

Patient H1. At the start of the 4th chemotherapy cycle, the leukemic population is higher than that of the previous cycles ($4.39 \cdot 10^{11}$ cells). Leukemic cells decrease over the 4th and last chemotherapy cycle but are still maintained to a level higher than that of the normal cell population (figure 3.8).

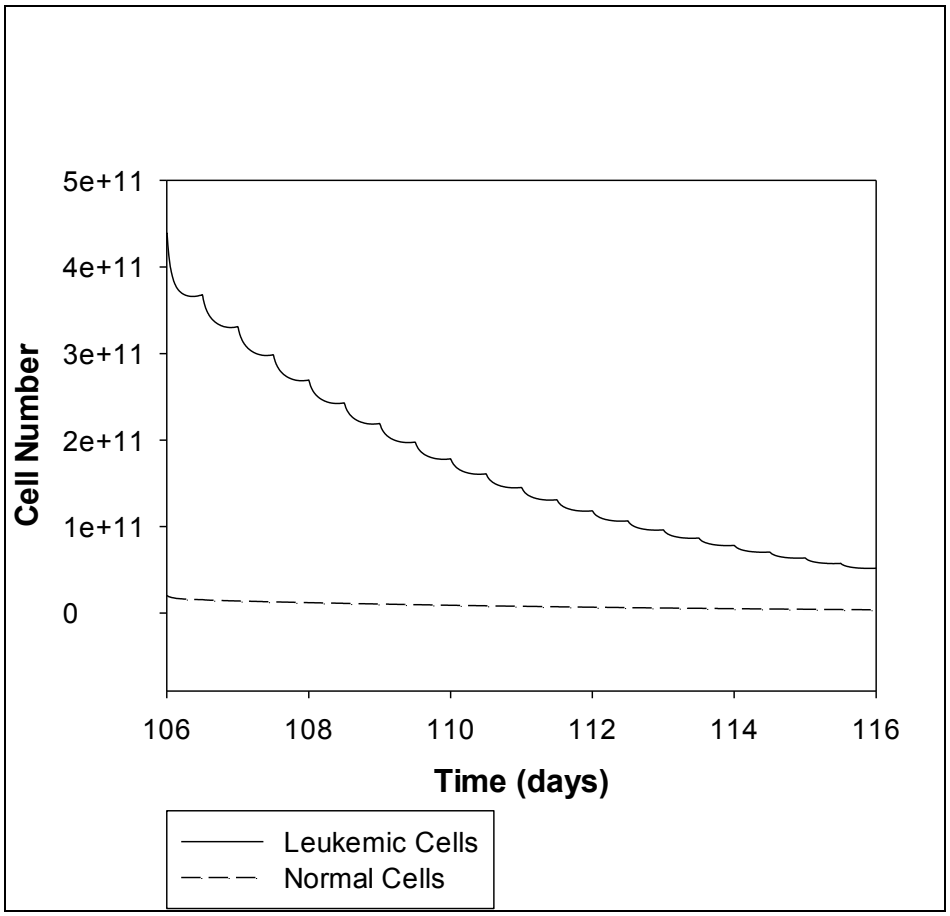

Figure 3.8: Patient H1 behaviour over the 4th cycle (days 106-116) of LDAC treatment

The simulated behaviour profile of Patient H1 undergoing the full course of standard LDAC treatment is presented in figure 3.9 and the numbers of leukemic and normal cell populations are listed in Table 3.7.

In summary, Patient H1 shows resistance to LDAC from the first chemotherapy cycle as the disease burden declines by less than 1-log during treatment. At the beginning of the 2nd chemotherapy cycle, the tumour load is $2.44 \cdot 10^{11}$ cells (Table 3.7), higher than that at diagnosis, i.e. $1.82 \cdot 10^{11}$ cells (Table 3.7). This trend is maintained throughout treatment and by the end of a course of LDAC, the disease burden is $5.89 \cdot 10^{11}$ cells indicating that this protocol is not efficient for this case study. The leukemic population is not decreasing to a

level lower than that of hypoplasia and the leukemic population is constantly higher than that of the normal.

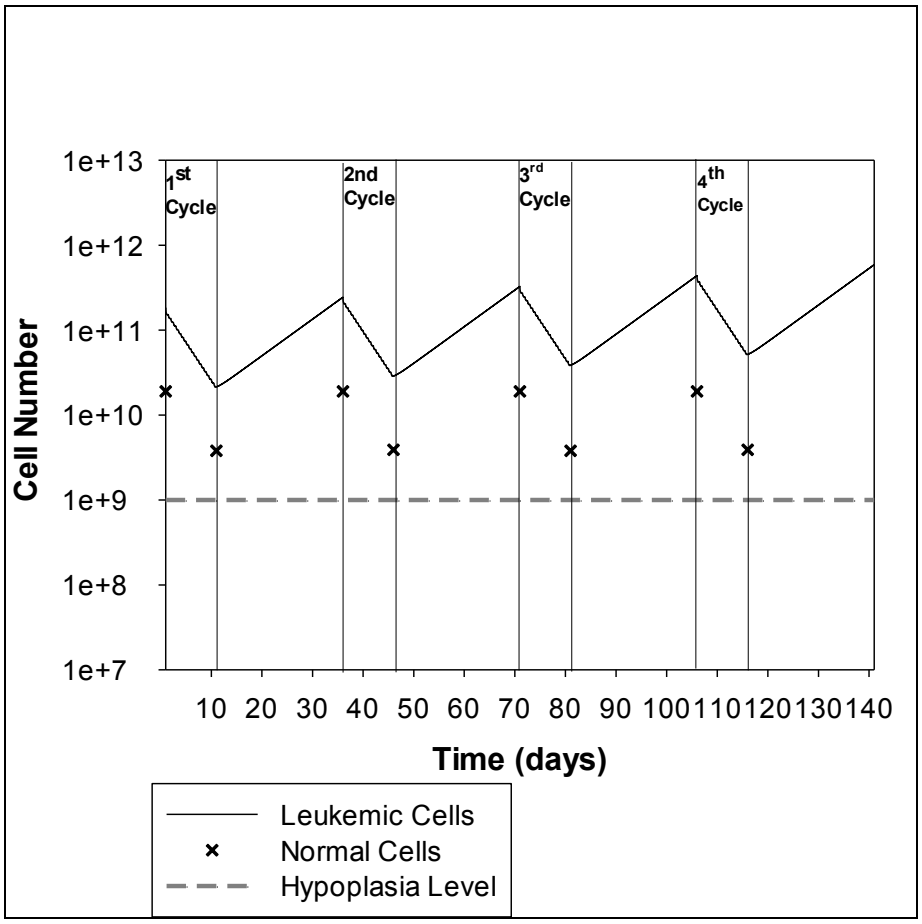

Figure 3.9: Patient H1 cell population dynamics during a course of treatment with LDAC

Table 3.7: Simulation results for the full course of treatment of Patient H1 with LDAC.

Date	Leukemic population over simulation with LD protocol	Normal population over simulation with LD protocol
Beginning of 1st cycle	$1.82 \cdot 10^{11}$	$1.9 \cdot 10^{10}$
End of 1st cycle	$2.14 \cdot 10^{10}$	$3.8 \cdot 10^{9}$
Beginning of 2nd cycle	$2.44 \cdot 10^{11}$	$1.9 \cdot 10^{10}$
End of 2nd cycle	$2.87 \cdot 10^{10}$	$3.8 \cdot 10^{9}$
Beginning of 3rd cycle	$3.27 \cdot 10^{11}$	$1.9 \cdot 10^{10}$
End of 3rd cycle	$3.85 \cdot 10^{10}$	$3.8 \cdot 10^{9}$
Beginning of 4th cycle	$4.39 \cdot 10^{11}$	$1.9 \cdot 10^{10}$
End of 4th cycle	$5.17 \cdot 10^{10}$	$3.8 \cdot 10^{9}$
BM aspirate after 4th cycle	$5.89 \cdot 10^{11}$	

- **Simulation results of the DA protocol for Patient H1**

1st Chemotherapy Cycle

As previously presented, Patient H1 shows resistance when treated with the LDAC protocol. This is due to the long duration of the G_0G1-phase (61 hrs) resulting in a high percentage of cells being in the inactive phase (G_oG_1-phase) unaffected by Ara-C (an S-phase specific drug). In this part, patient H1 will be treated with DA; the results are expected to be better since higher doses of chemotherapy will be applied and, more importantly, DNR will be administered which acts on cells in G_0-phase.

Figure 3.10 presents the leukemic and normal cell populations for the first cycle using the DA protocol. Leukemic cells decrease from $1.82 \cdot 10^{11}$ cells initially to $7.7 \cdot 10^{7}$cells. The resulting cell number at treatment completion is below the BM hypoplasia level ($1 \cdot 10^{9}$ cells). Normal cell number decreases from $1.9 \cdot 10^{10}$ to $3.7 \cdot 10^{8}$ cells and from the 5th day, the normal population is higher than the leukemic population, thereby reaching another important objective of induction chemotherapy treatment.

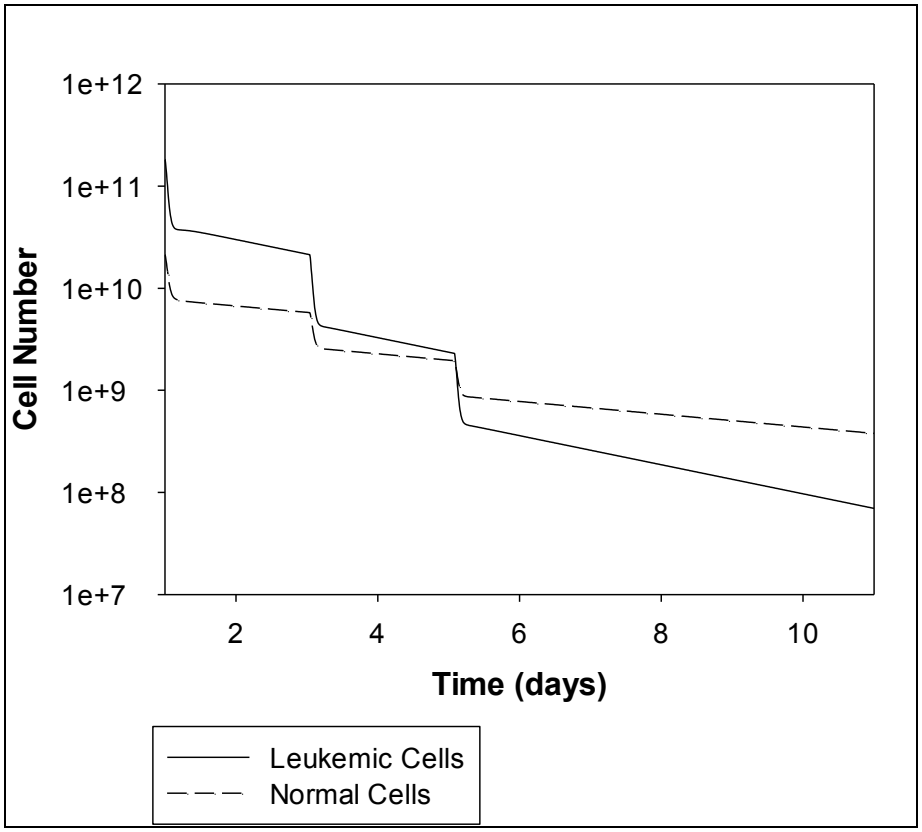

Figure 3.10: Patient H1 behaviour over the first cycle (days 1-11) of DA induction treatment

Over the cycle, the leukemic population undergoes a 3-log reduction, whereas normal cells show a 2-log reduction under the same applied chemotherapy protocol. This difference is due to the feedback mechanism which enables normal non-proliferating cells to replace the population loss by proceeding faster into the proliferation state.

Figure 3.11 presents the normal proliferating and non-proliferating cell populations during the 1st chemotherapy cycle of DA induction treatment. Cells undergoing proliferation are susceptible to the effects of chemotherapy and is the reason that the cell number declines quickly over the first three days when they become undetectable. After the 3rd day, the proliferating cell population starts increasing again and this is due to the higher population transitioning from the non-proliferating cell compartment.

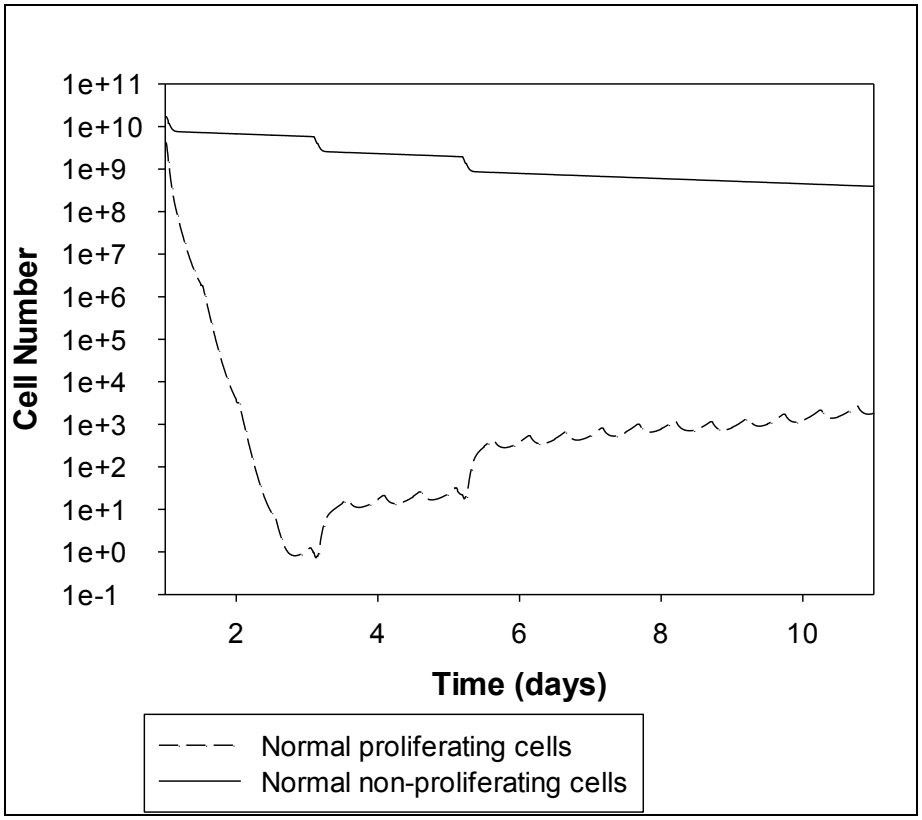

Figure 3.11: Normal proliferating and non-proliferating cell populations of Patient H1 undergoing the 1st cycle of DA induction treatment

The decrease rate of the normal population presents a peak on days 1, 3 and 5 when iv doses of both agents (Ara-C and DNR) are applied. This rapid decline in cell number will provoke a higher transition of non-proliferating cells to proliferate (figure 3.12).

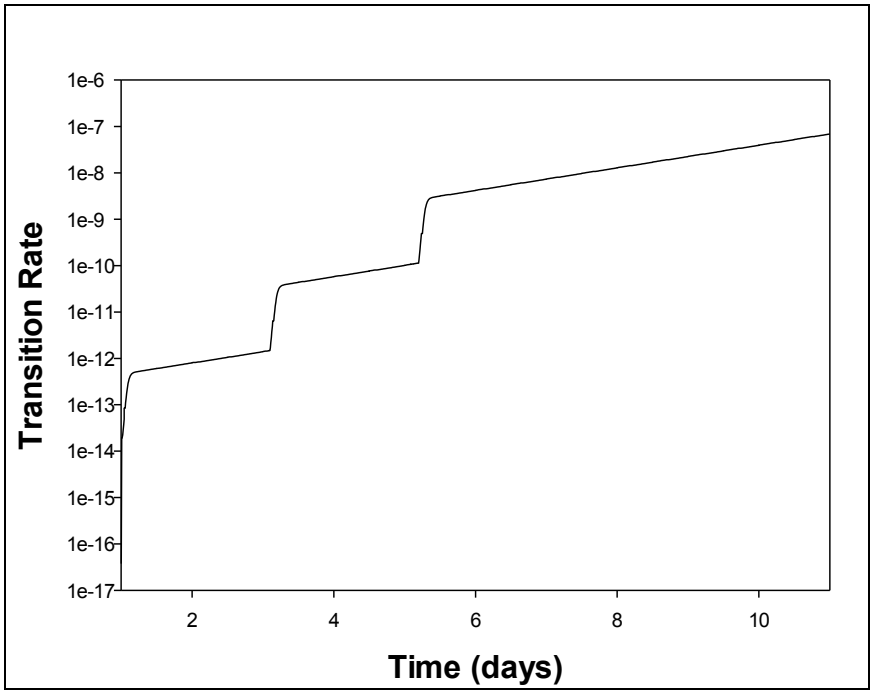

Figure 3.12: Transition rate from normal non-proliferating to proliferating cell population of Patient H1 under the 1st cycle of DA induction treatment

2nd Chemotherapy Cycle

The initiating leukemic cell number at the start of the 2nd chemotherapy cycle will be higher than the resulting leukemic population number at completion of the 1st chemotherapy cycle because of the 25-day recovery period during which the patient is left without chemotherapy treatment. Over the 2nd chemotherapy cycle, leukemic cells decrease from $7.8 \cdot 10^8$ to $3.3 \cdot 10^5$ cells. Normal cells will have the same response as during the 1st chemotherapy cycle since the population is assumed to fully recover during the 25-day interval period and the same protocol is applied. As shown in figure 3.13, the normal population is much higher than that of the leukemic population, which is one of the most important objectives of chemotherapy treatment since it will result in a healthier BM with normal function. Leukemic cells are lower than the hypoplasia and remission level of $1 \cdot 10^9$ cells and the two objectives of the induction treatment have already been achieved.

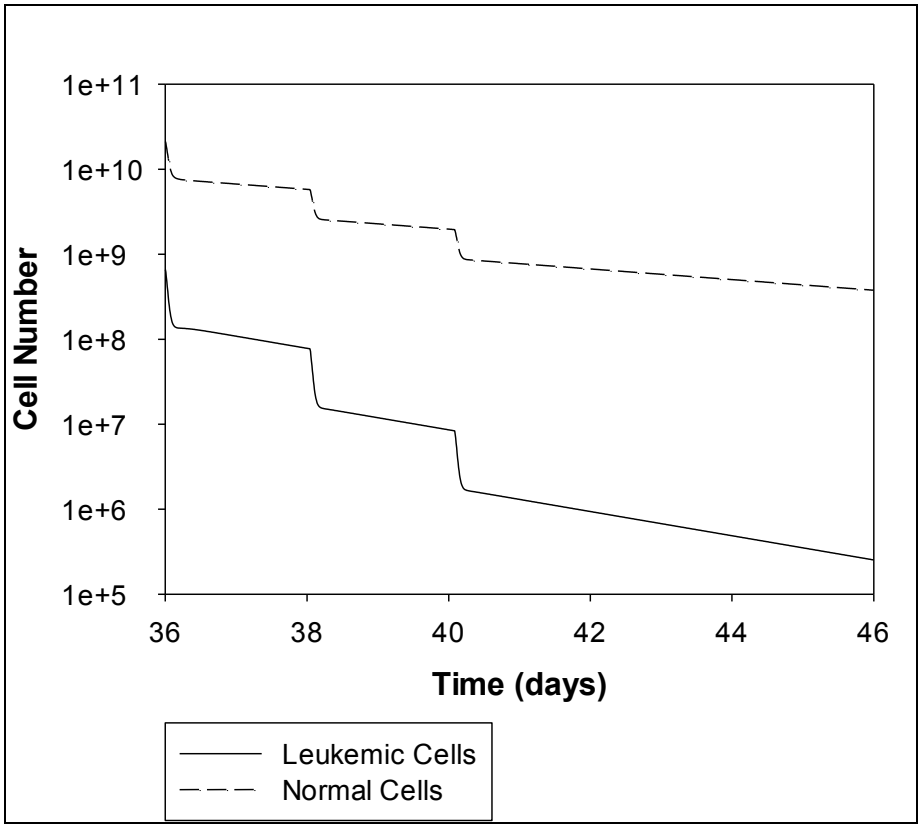

Figure 3.13: Patient H1 behaviour over the second cycle (days 36-46) of DA treatment.

3rd Chemotherapy Cycle

Although the treatment objectives have been achieved from the first two chemotherapy cycles, there is still residual disease left so simulation results will be presented for the full course of treatment. Figure 3.14 presents the normal and leukemic populations undergoing the 3rd chemotherapy cycle of DA.

Leukemic cells increase over the recovery period between the 2nd and 3rd chemotherapy cycles, and the initial population prior to the 3rd cycle is $3.4 \cdot 10^6$ cells. After completion of the 3rd cycle, leukemic cells are decreased to 1430 cells, whereas the normal cell population is much higher at $3.7 \cdot 10^8$ cells.

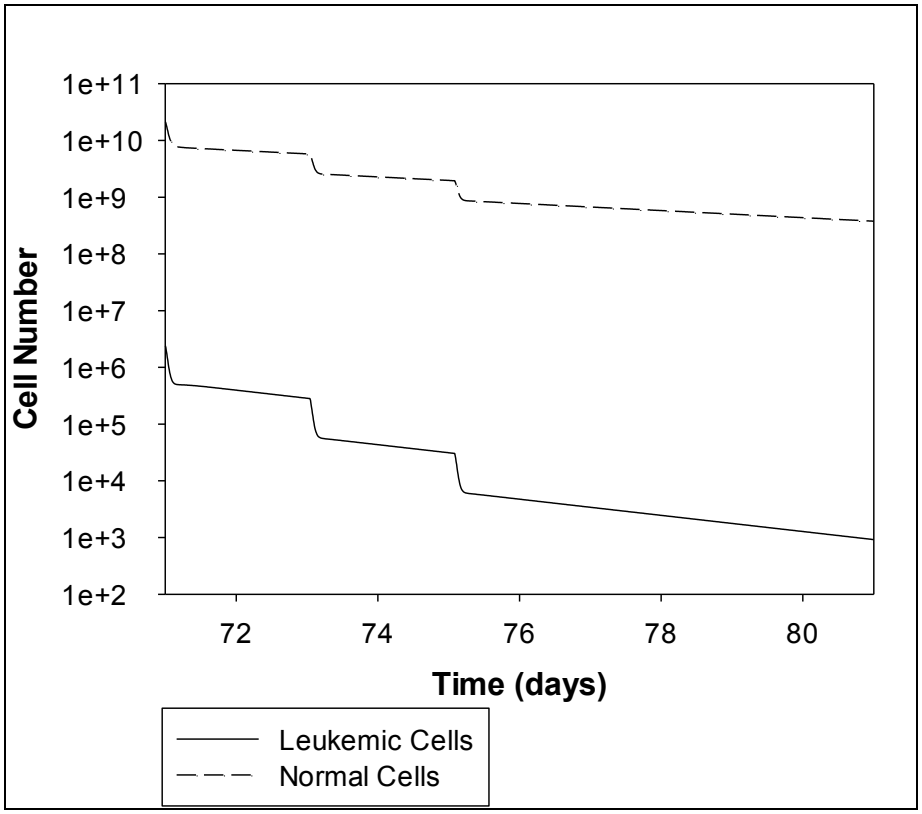

Figure 3.14: Patient H1 behaviour over the third cycle (days 71-81) of DA treatment.

4th Chemotherapy Cycle

By completion of the 3rd chemotherapy cycle, the leukemic population was decreased to 1430 cells which, after the 25-day recovery period increased to $1.5 \cdot 10^4$ cells, and represents the initial condition of the 4th and last chemotherapy cycle (figure 3.15). After the 4th chemotherapy cycle, only 6 leukemic cells are left and the disease is practically completely eradicated. Normal cells will have the same dynamics as for all the chemotherapy cycles i.e. to $3.7 \cdot 10^8$ cells, that is higher than the leukemic cell burden and will result in a healthy functioning BM.

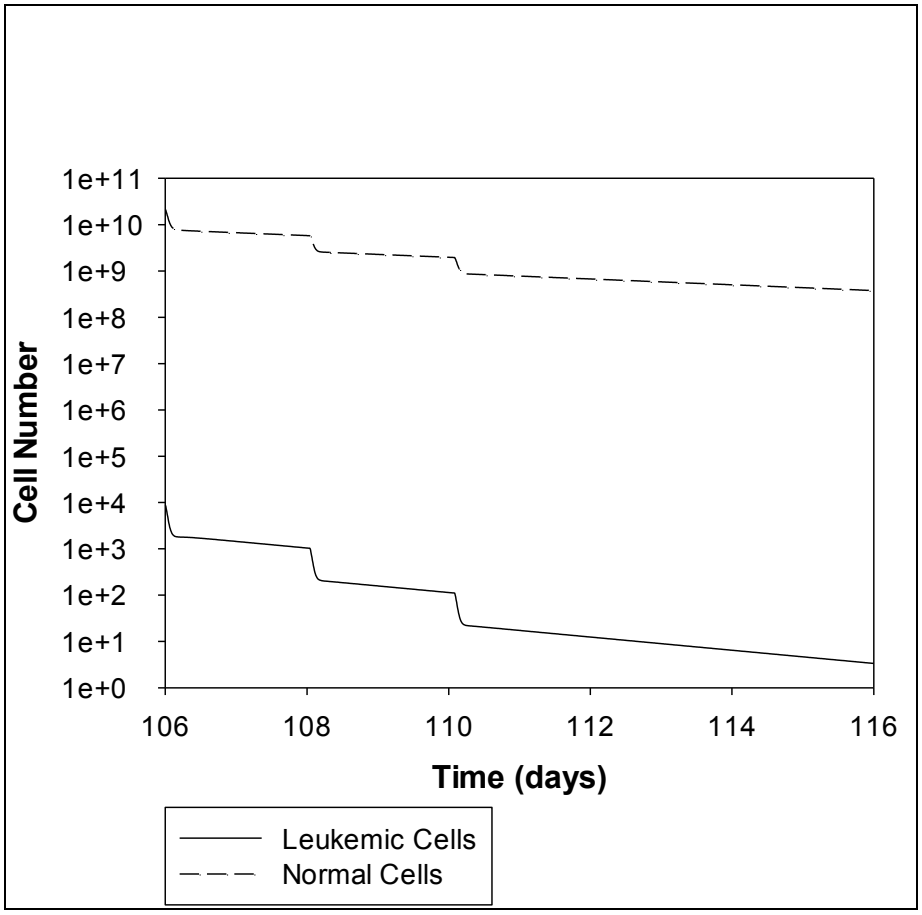

Figure 3.15: Patient H1 behaviour over the fourth cycle (days 106-116) of DA treatment.

The full length profile of patient H1 undergoing DA treatment is presented in figure 3.16 and the cell population numbers are listed in Table 3.8 below.

In summary, the DA protocol simulation results clearly demonstrate that this protocol is appropriate for Patient H1 case study. The disease is decreasing and BM hypoplasia is achieved from the 1st chemotherapy cycle as leukemic cells are less than 10^9 cells, the hypoplasia and remission level. Moreover, for this protocol, leukemic cells are decreased to a level wherein, even after the 1st cycle, their number is less than that of normal cells (Table 3.8) which is a major objective of chemotherapy treatment. After the full course of treatment (four cycles of chemotherapy), leukemic cells are near-fully eradicated and the normal population is high enough for the BM to start functioning normal to produce healthy blood cells.

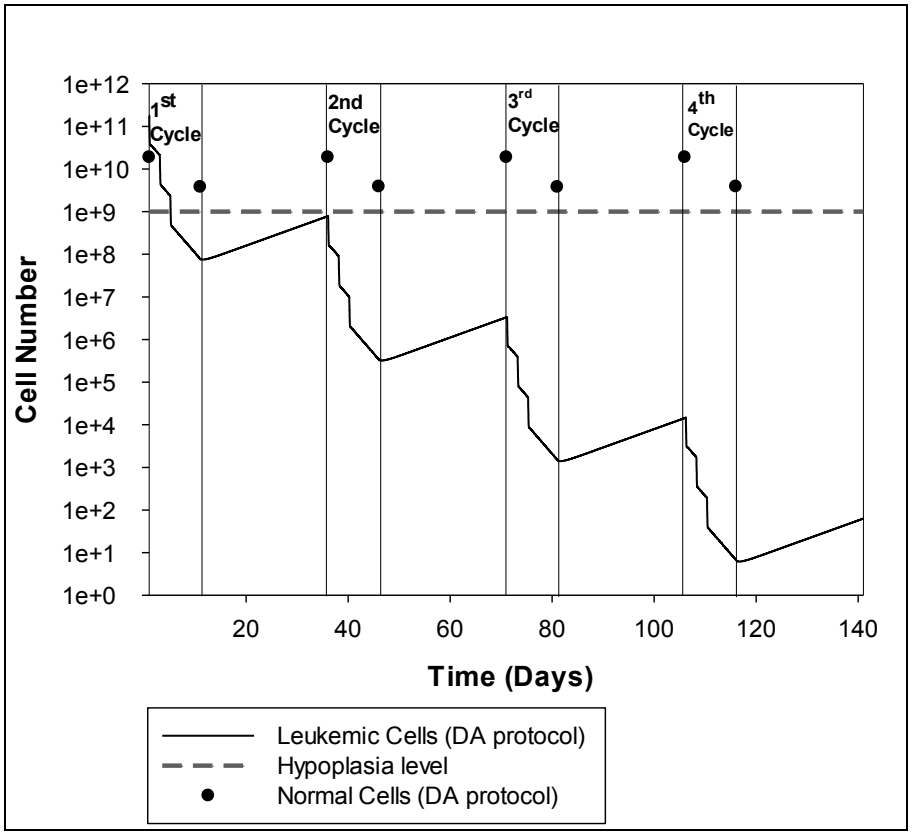

Figure 3.16: Patient H1 cell population dynamics under the full-length course of treatment with the DA clinical protocol

Table 3.8: Simulation results for the full course of treatment of patient H1 under the DA clinical protocol

Date	Leukemic population over simulation with DA protocol	Normal population over simulation with DA protocol
Beginning of 1st cycle	$1.82 \cdot 10^{11}$	$1.9 \cdot 10^{10}$
End of 1st cycle	$7.7 \cdot 10^{7}$	$3.7 \cdot 10^{8}$
Beginning of 2nd cycle	$7.8 \cdot 10^{8}$	$1.9 \cdot 10^{10}$
End of 2nd cycle	$3.3 \cdot 10^{5}$	$3.7 \cdot 10^{8}$
Beginning of 3rd cycle	$3.4 \cdot 10^{6}$	$1.9 \cdot 10^{10}$
End of 3rd cycle	1430	$3.7 \cdot 10^{8}$
Beginning of 4th cycle	$1.5 \cdot 10^{4}$	$1.9 \cdot 10^{10}$
End of 4th cycle	6	$3.7 \cdot 10^{8}$
BM aspirate after 4th cycle	64	

3.5.3 Simulation results of Patient H2 using LDAC and DA treatment protocols

- **Simulation results of the LDAC protocol for patient H2**

1st Chemotherapy Cycle

Figure 3.17 presents the normal and leukemic cells' behaviour after the 1st chemotherapy cycle of LDAC. Both populations decrease under the influence of drug action and, over the final days, the normal population is higher than that of the leukemic population. In particular, leukemic cell number decreases from $1.12 \cdot 10^{11}$ to $5.8 \cdot 10^{8}$ cells and the normal cell number decreases from $1.99 \cdot 10^{10}$ to $3.8 \cdot 10^{9}$ cells.

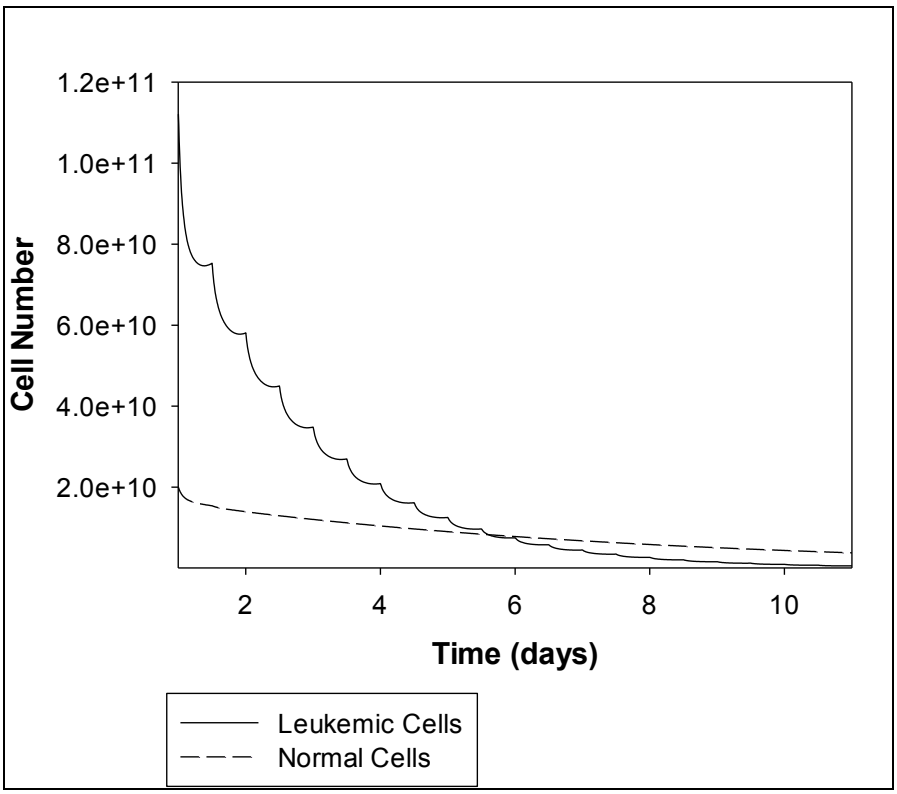

Figure 3.17: Patient H2 behaviour over the first cycle (days 1-11) of LDAC induction treatment

2nd Chemotherapy Cycle

Over the 25-day recovery period after the 1st chemotherapy cycle, both normal and leukemic populations increase and at the beginning of the 2nd chemotherapy cycle, there are $7.2 \cdot 10^{9}$ leukemic cells with a normal cell population of $1.99 \cdot 10^{10}$ cells. Figure 3.18 demonstrates the normal and leukemic populations over the 2nd chemotherapy cycle. Normal cells are higher than that of leukemic for the entire duration of the 2nd chemotherapy cycle. The dynamics of

the normal population are the same as that over the 1st chemotherapy cycle since the same protocol is applied i.e. the cell population decreases from $1.99 \cdot 10^{10}$ to $3.8 \cdot 10^{9}$ cells. Moreover, the leukemic population decreases from $7.2 \cdot 10^{9}$ to $3.74 \cdot 10^{7}$ cells, with a difference of $3.76 \cdot 10^{9}$ cells less than that of the normal cell population.

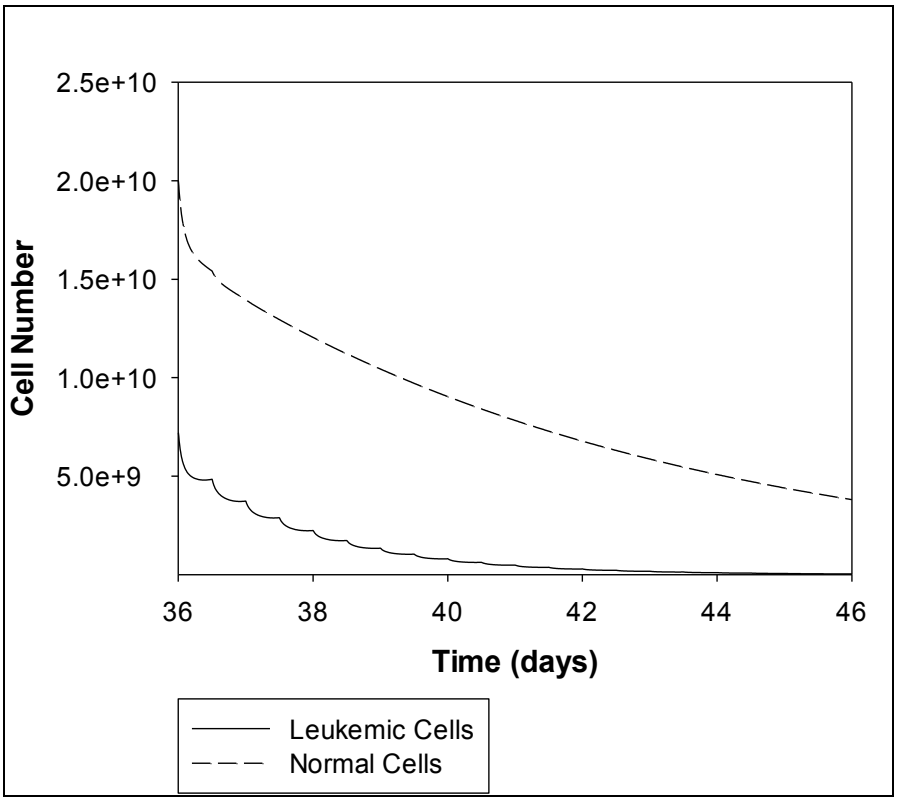

Figure 3.18: Patient H2 behaviour over the second cycle (days 36-46) of LDAC treatment.

3rd Chemotherapy Cycle

The leukemic population increases to $4.6 \cdot 10^{8}$ cells at the beginning of the 3rd chemotherapy cycle. The population thereafter decreases to $2.4 \cdot 10^{6}$ cells at completion of the 3rd chemotherapy cycle (figure 3.19). During the 3rd chemotherapy cycle, leukemic cells are maintained at a lower state compared with that of the normal cell population, which is an indicator of the efficiency of LDAC for the treatment of Patient H2.

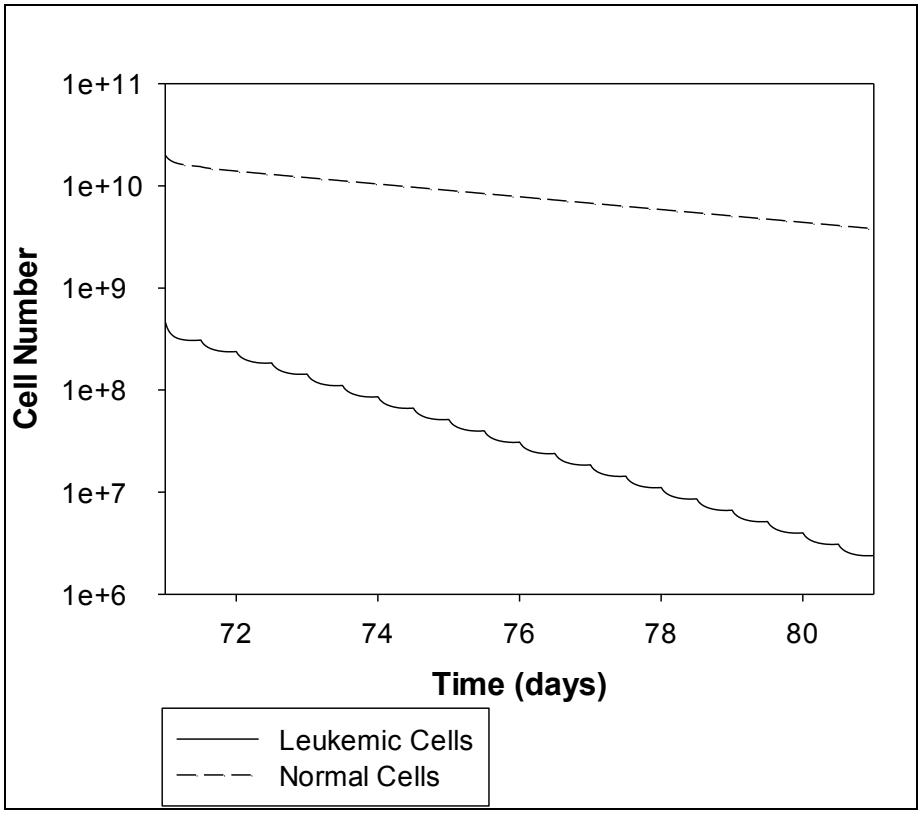

Figure 3.19: Patient H2 behaviour over the third cycle (days 71-81) of LDAC treatment.

4th Chemotherapy Cycle

The dynamics of normal and leukemic cell populations over the last cycle of the LDAC protocol are presented in figure 3.20, below. Leukemic cells are still lower than that of the normal population for the 4th cycle as they were from the last days of the 1st chemotherapy cycle and thereafter. In particular, the leukemic population increases to $2.96 \cdot 10^7$ cells during the recovery period between the 3rd and 4th cycles and then decreases to $1.5 \cdot 10^5$ cells. Normal cells will have the same dynamics as in the previous chemotherapy cycles since the initial population is assumed to be the same for all cycles and the same chemotherapy schedule is applied. In that sense, the normal population will decrease from $1.99 \cdot 10^{10}$ to $3.8 \cdot 10^9$ cells making a 4-log difference compared with that of the leukemic cell population in the BM.

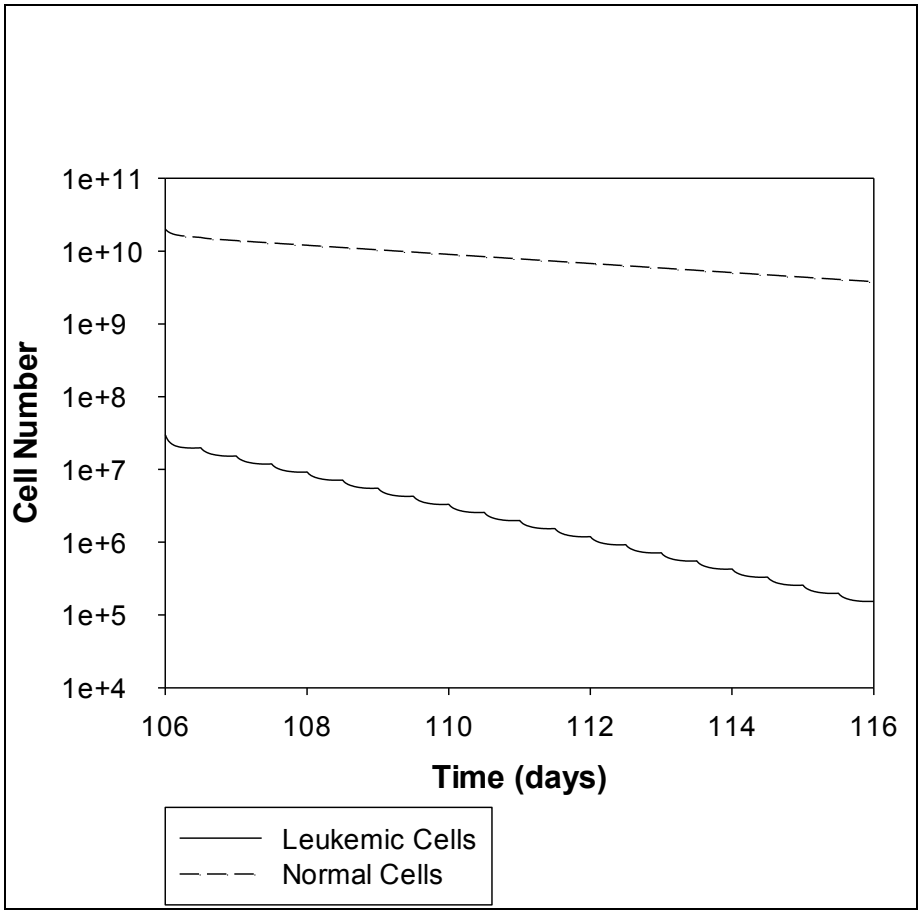

Figure 3.20: Patient H2 behaviour over the fourth cycle (days 106-116) of LDAC treatment

In summary, the presented simulation results demonstrate a successful treatment outcome for Patient H2 over the LDAC protocol. The leukemic cell population decreases from the first chemotherapy cycle to a lower level compared with that of the normal cell population. This is an important objective for the chemotherapy treatment as it will allow for normal cells to start proliferating and functioning normally resulting in an improved blood and immune system for the patient to be able to tolerate the remainder of chemotherapy treatment. Moreover, the disease decreases and BM hypoplasia is achieved from the 2^{nd} chemotherapy cycle as leukemic cells are less than 10^9 cells, the level of hypoplasia and morphologic remission.

The profile of Patient H2 undergoing the full course of standard LDAC treatment simulation is presented in figure 3.21 and the numbers of the leukemic and normal cell populations are listed in Table 3.9.

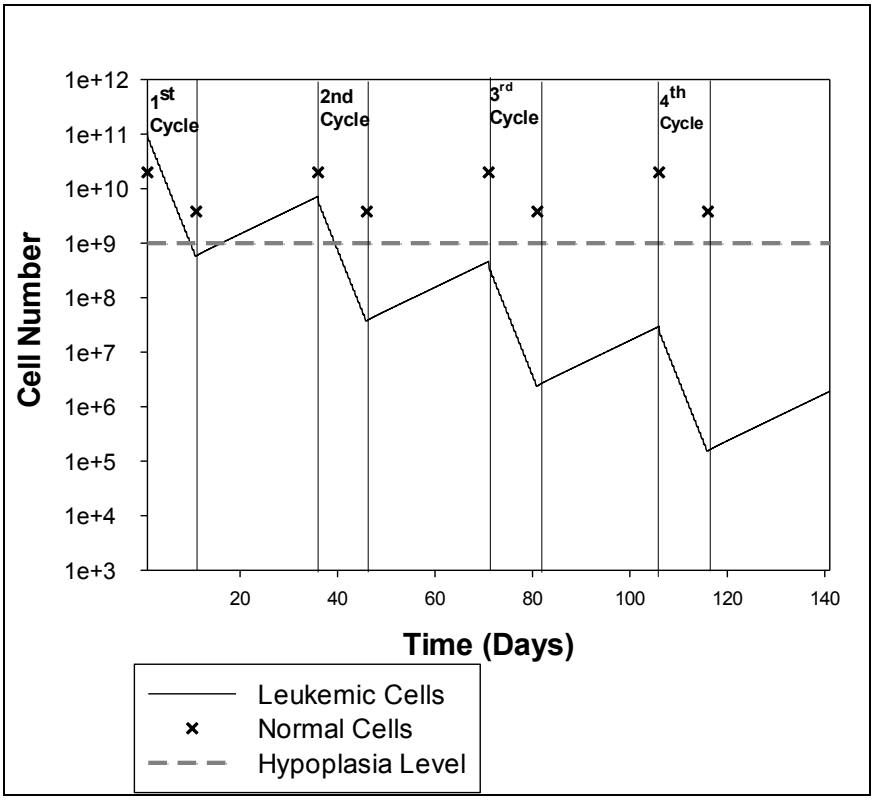

Figure 3.21: Patient H2 cell population dynamics under the full course of LDAC treatment.

Table 3.9: Simulation results for the full course of treatment of patient H2 using the LDAC clinical protocol

Date	Leukemic population over simulation with LD protocol	Normal population over simulation with LD protocol
Beginning of 1st cycle	$1.12 \cdot 10^{11}$	$1.99 \cdot 10^{10}$
End of 1st cycle	$5.8 \cdot 10^{8}$	$3.8 \cdot 10^{9}$
Beginning of 2nd cycle	$7.2 \cdot 10^{9}$	$1.99 \cdot 10^{10}$
End of 2nd cycle	$3.74 \cdot 10^{7}$	$3.8 \cdot 10^{9}$
Beginning of 3rd cycle	$4.6 \cdot 10^{8}$	$1.99 \cdot 10^{10}$
End of 3rd cycle	$2.4 \cdot 10^{6}$	$3.8 \cdot 10^{9}$
Beginning of 4th cycle	$2.96 \cdot 10^{7}$	$1.99 \cdot 10^{10}$
End of 4th cycle	$1.5 \cdot 10^{5}$	$3.8 \cdot 10^{9}$
BM aspirate after 4th cycle	$1.9 \cdot 10^{6}$	

- **Simulation results of the DA protocol for patient H2**

1st Chemotherapy Cycle

Figure 3.22 presents the leukemic and normal cell population dynamics during the 1st chemotherapy with combination of Ara-C and DNR drugs (DA protocol). The leukemic population decreases from $1.12 \cdot 10^{11}$ to $4.8 \cdot 10^{5}$ cells, whereas normal cells decrease from $1.99 \cdot 10^{10}$ to $3.7 \cdot 10^{8}$ cells. Induction treatment objectives are achieved from the 1st chemotherapy cycle as leukemic cells are below the $1 \cdot 10^{9}$ cells, the hypoplasia level, and the leukemic population is less than that of the normal population (figure 3.22).

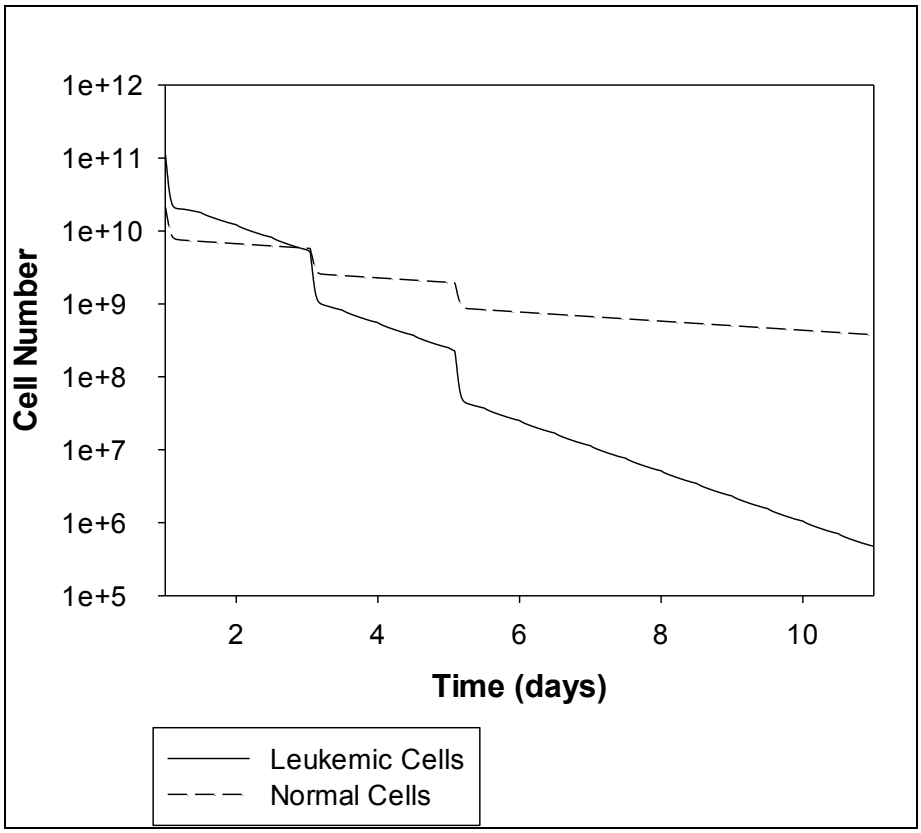

Figure 3.22: Patient H2 behaviour over the first cycle (days 1-11) of DA induction treatment.

2nd Chemotherapy Cycle

Consistent with clinical practice, a 25-day recovery period is allowed between the 1st and the 2nd chemotherapy cycle in order to enable recovery of the normal population. Over this period, leukemic cells increase to $4.8 \cdot 10^{6}$ cells and the normal cell population is assumed to have repopulated and equals $1.99 \cdot 10^{10}$ cells. Figure 3.23 presents the dynamics of the normal and leukemic populations during the 2nd chemotherapy cycle. Normal cell number is higher than that of the leukemic for the entire duration of the treatment cycle. In particular, the

normal cell population decreases to $3.7 \cdot 10^8$ cells, whereas the leukemic population decreases to 20 cells.

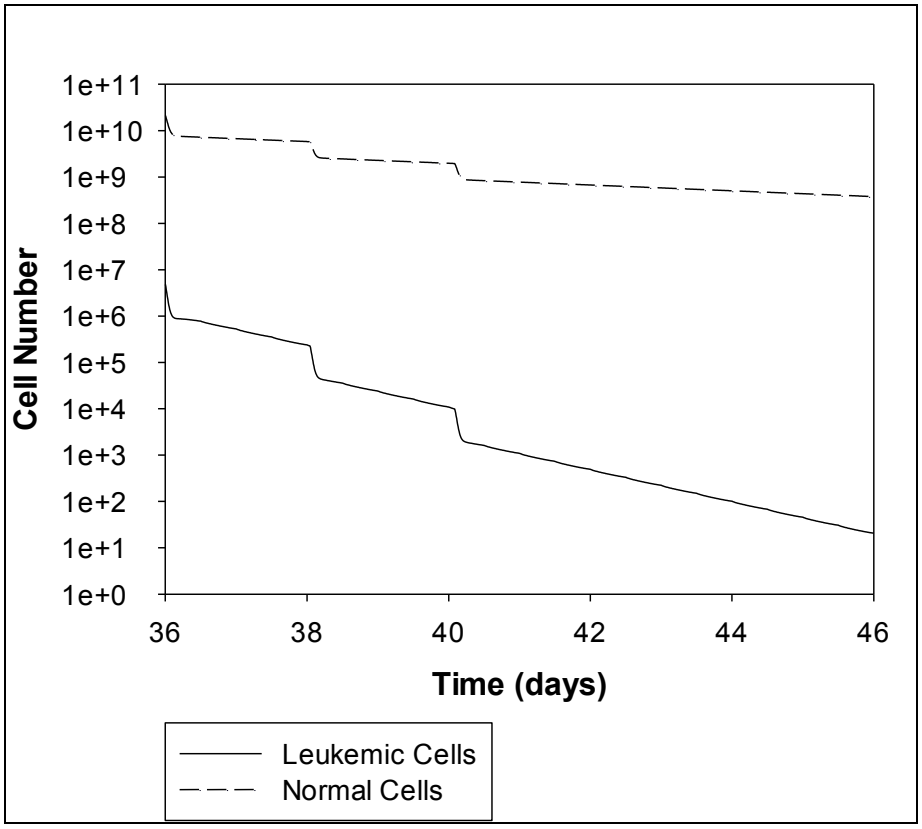

Figure 3.23: Patient H2 behaviour over the second cycle (days 36-46) of DA treatment.

3rd Chemotherapy Cycle

The leukemic population increases to 200 cells by the beginning of the 3rd chemotherapy cycle and one more chemotherapy cycle is applied. Over the 3rd chemotherapy cycle leukemic cells become undetectable and, according to the simulation results, the BM only consists of normal cells (figure 3.24).

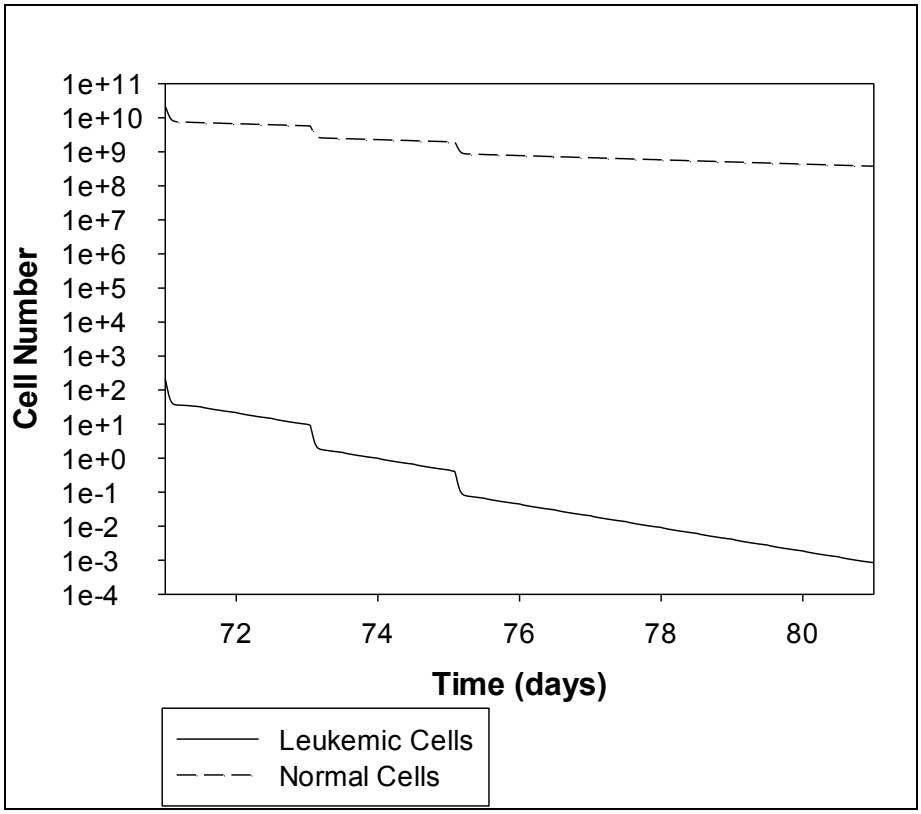

Figure 3.24: Patient H2 behaviour over the third cycle (days 71-81) of DA treatment.

The profile of Patient H2 undergoing the full course of standard DA treatment simulation is presented in figure 3.25 and the numbers of the leukemic and normal cell populations are listed in Table 3.10.

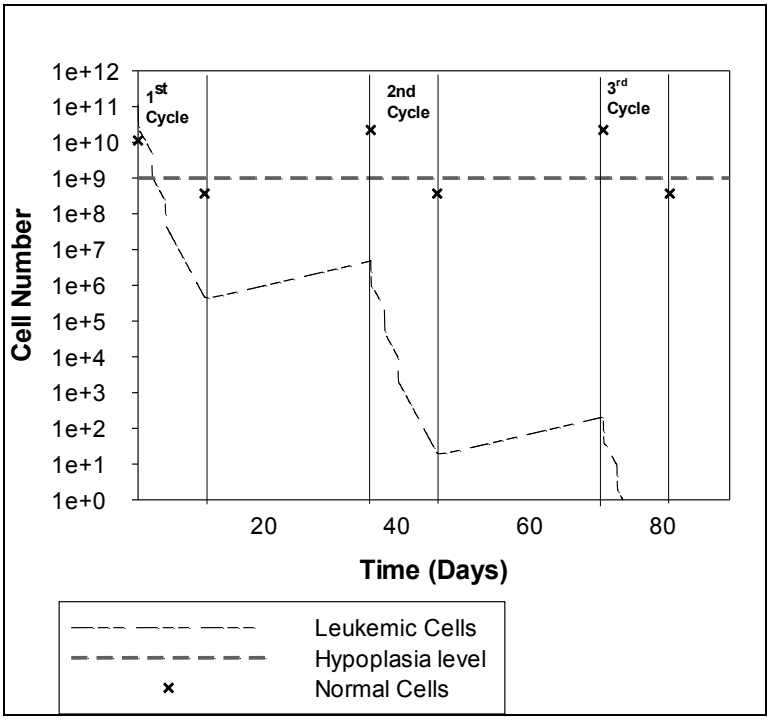

Figure 3.25: Patient H2 cell population dynamics under the full course of treatment with the DA clinical protocol

Table 3.10: Simulation results for the full course of treatment of Patient H2 with DA clinical protocol

Date	Leukemic population over simulation with LD protocol	Normal population over simulation with LD protocol
Beginning of 1st cycle	$1.12 \cdot 10^{11}$	$1.99 \cdot 10^{10}$
End of 1st cycle	$4.8 \cdot 10^{5}$	$3.7 \cdot 10^{8}$
Beginning of 2nd cycle	$4.8 \cdot 10^{6}$	$1.99 \cdot 10^{10}$
End of 2nd cycle	20	$3.7 \cdot 10^{8}$
Beginning of 3rd cycle	200	$1.99 \cdot 10^{10}$
End of 3rd cycle	0	$3.7 \cdot 10^{8}$
Beginning of 4th cycle	-	
End of 4th cycle	-	
BM aspirate after 4th cycle	-	

For Patient H2, both protocols are efficient at decreasing the level of leukemic cells to below the hypoplasia level of 10^9 cells, which is the ultimate purpose of chemotherapy treatment. However, over the DA protocol, the leukemic population becomes undetectable from completion of the 3rd cycle, whereas residual disease remains after completion of LDAC. The residual disease equals $1.9 \cdot 10^6$ cells, which is still less than the desired level of less than 10^9 cells. This difference in the leukemic population is due to the increased toxicity of the DA protocol that results in a decreased number of normal cells as well. The calculated normal population reduction is 1-log after the LDAC protocol and a 2-log reduction after the DA protocol. Moreover, for both chemotherapy protocols, the leukemic population is decreased from the very first chemotherapy cycle to a level at which the normal population is higher. This is an important objective for the chemotherapy process as it will allow the normal cells to start proliferating and functioning normally resulting in an improved blood and immune system in order to enable the patient to tolerate the remainder of chemotherapy treatment.

3.6 Discussion

A mathematical model is developed and presented for the full course of treatment using two chemotherapy protocols currently used in standard clinical practice i.e.

- the LDAC protocol of (sc) Ara-C doses of 20 mg applied every 12 hrs for 10 days
- the DA protocol of DNR doses of 60 mg/m^2 applied for 1-hr IV infusion on days 1, 3 and 5 of the chemotherapy cycle and Ara-C doses of 100 mg/m^2 IV administered every 12 hrs for 10 days, also starting from day 1.

Sensitivity analysis takes place in the current work using collectible data from the open literature in order to define the inter-patient variability of the PK, PD and the cell cycle parameters. The results show that the cell cycle times are crucial model parameters that highly affect the disease treatment outcome.

Simulation results are presented applying the two studied protocols to two patient case studies with characteristics published in (Clarkson et al., 1967). Patient H1 is a more difficult case study with more aggressive cell population kinetics. Specifically, this patient shows a higher initial tumour burden together with a lower proliferation phase and a prolonged non-proliferation state of cells unaffected by the chemotherapy agents. Simulation results of this

patient show successful treatment outcome for the DA protocol and unsuccessful for the LDAC protocol over which leukemic cells are still increasing. In contrast, patient H2 is a case study with successful treatment outcome for both protocols. Of note, complete disease eradication is simulated for this patient under the DA protocol.

The simulation results appear to suggest that the DA protocol should be applied for the treatment of both patients. This protocol affords more toxicity and leads to a greater reduction of leukemic burden while the normal population is within acceptable limits. However, considering solely the AML population kinetics is not sufficient for proper treatment design. In clinical practice, treatment preference also takes account of the patient physiologic state to determine whether the patient is able to tolerate the toxicity of chemotherapy. This patient physiologic state is determined by the clinician responsible for the treatment design who also relies on other parameters such as kidney and liver function together with the age and the health history of each individual. For this reason, the purpose of the current work is not to compare the two studied protocols but to optimise and analyse them separately in order to derive leukaemia-specific and patient-specific personalised treatments for AML. The optimisation algorithm of the chemotherapy process for AML is discussed in the next chapter and results are presented of the optimisation of the LDAC and DA protocols for the two hypothetical patients presented in this chapter.

Chapter 4[2]

Chemotherapy process as an optimisation problem

This chapter presents an algorithm for the optimization of the chemotherapy process as a scheduling problem. The algorithm is presented in section 4.1 and afterwards is solved for the two patients presented in Chapter 3 for both intensive and non-intensive treatment protocols with maximal and minimal thresholds set for efficacy and toxicity, respectively. For iv Ara-C, total drug administration is set between 50mg – 4000mg with infusion duration between 1 min to 24 hours. The window for DNR dose optimisation is stricter due to potential toxic effects and the only independent variable is the dose which varies between 30mg – 90mg per infusion. For sc Ara-C, the maximum dose per day is 40mg, and doses are permitted up to four times daily for a maximum period of 20 days.

This optimisation problem was formed and solved using gPROMS (gPROMS, 2003) and the optimised treatment protocols for the two studied patient case studies over the protocols are presented in section 4.2 of this chapter.

4.1 Optimisation scheduling algorithm of chemotherapy process

The aim of remission induction therapy is to achieve the rapid restoration of normal BM function. By treatment completion, the leukemic population should be reduced to a level of approximately 10^9 cells at which point BM hypoplasia is achieved. Moreover, the normal population should be higher than that of the leukemic population and a 3-log reduction is the maximum permissible level of population reduction. Treatment design will be mainly based on the control of four schedule parameters:

- the drug use,
- the dose load,
- the dose duration and
- the number of dose applications.

[2] Work in this chapter is presented in
Pefani E., Panoskaltsis N., Mantalaris A., Georgiadis M. C., Pistikopoulos E. N.. Chemotherapy Drug Scheduling for the Induction Treatment of patients diagnosed with Acute Myeloid Leukemia. Accepted for publication in the Transactions of Biomedical Engineering Journal.

The optimisation algorithm is presented below (table 4.1):

Table 4.1: Chemotherapy process optimisation algorithm

Objective function	$\min_{j,u_{n,j},t_{n,j},NA} Cells_{leuk}(t_f)$
Equality Constraints	$Cells_{nor,n,j} = f(effect_{n,j})$
	$Cells_{leuk,n,j} = f(effect_{n,j})$
	$effect_{n,j} = f(C_{M,n,j})$
	$C_{M,n,j} = f(In_{n,j})$
	$In_{n,j} = \sum_{n=1}^{n=NA} \frac{u_{n,j}}{t_{n,j}} \cdot (t - n \cdot \tau_n)$
Inequality Constraints	$Cells_{nor}(t_f) \geq Cells_{leuk}(t_f)$
	$Cells_{nor}(t) \geq 10^{-3} \cdot Cells_{nor}(0)$

*n is the number of dose application; j is the drug; $t_{n,j}$ is the duration of each dose application; $u_{n,j}$ is the dose load of each application; $Cells_{leuk,n,j}$ is the number of leukemic ; $Cells_{nor,n,j}$ is the number of normal cells; $effect_n$ is the the PD effect of drug j over application n; $C_{Mn,j}$: is the BM concentration; $Inflow_{n,j}$: is the inflow of drug j during application n; τ_n is the duration between two succeeding dose applications; NA is the total number of applications; t_f time at the end of last dose.

The objective function is the minimisation of the leukemic ($Cells_{leuk}$) cells at the end of the last dose subject to the treatment schedule that is defined by the drug use (j), the dose load ($u_{n,j}$), the dose duration ($t_{n,j}$) the number of applications (NA) and the interval period between two succeeding dose applications (τ_n). The four first parameters are the optimisation schedule variables, whereas the interval period between two doses is a design variable calculated by the frequency of doses i.e. if two or four doses will be applied daily as defined by clinicians. The control parameters define the drug inflow that has physical meaning only for the periods of chemotherapy treatment, whereas the value of the inflow is set to 0 for the periods between two succeeding chemotherapy cycles.

The feasible optimisation solutions are defined by the set of the equality and inequality constraints. Equality constraints consist of the expressions used to calculate the number of leukemic ($Cells_{leuk}$) and normal ($Cells_{nor}$) cells throughout the treatment. Both cell populations are functions of the drug PD effect ($effect_n$) that is defined by the drug concentration profile at the tumour location i.e. the BM ($C_{M,n,j}$). The drug concentration profile is determined by the treatment inflow, a variable calculated by the schedule and the

design parameters. Moreover, the inequality constraints consist of constraints on the number of normal cells that will have to be higher than a 3-log reduction throughout the treatment (path-constraint) and by treatment completion they will have to be higher than the number of leukemic cells (end-point constraint).

4.2 Optimisation Results for the two hypothetical patients

4.2.1 Optimisation results of Patient H1 over the LDAC and DA treatment protocols

- **Optimisation results of the LDAC protocol for patient H1**

Simulation results for Patient H presents resistance to LDAC and, at treatment completion, the disease burden is higher than at disease presentation (at the start of cycle 1). The optimisation problem for this case is formulated with a maximum dose load per day of 40 mg and up to four daily dose applications are permitted for a maximum period of 20 days. This optimisation problem is solved for the four chemotherapy cycles and the optimisation schedules are listed in Table 4.2.

Table 4.2: Optimal LDAC induction treatment protocol for Patient H1

Protocol	Dose Load	Dose Duration	Application route	Application Schedule
SC Ara-C				
1st Cycle	40 mg	24-hr	SC	1 daily application for days 1-20
2nd Cycle	40 mg	24-hr	SC	1 daily application for days 1-20
3rd Cycle	40 mg	24-hr	SC	1 daily application for days 1-10
4th Cycle	40 mg	24-hr	SC	1 daily application for days 1-10

1st Chemotherapy Cycle

The optimisation problem for the 1st chemotherapy cycle of patient H1 over the LDAC protocol suggests daily infusions of the same total dose i.e. 40 mg applied for double the time-period, 20 days in total (Table 4.2). The double dose load is therefore suggested with total Ara-C dose equal to 800 mg. Over the 1st chemotherapy cycle leukemic cells decrease from $1.82 \cdot 10^{11}$ cells to $1.2 \cdot 10^{9}$ cells and normal cells decrease from $1.9 \cdot 10^{10}$ to $8.9 \cdot 10^{8}$ cells. Figure 4.1 presents the leukemic and normal population dynamics over the optimisation and simulation protocols.

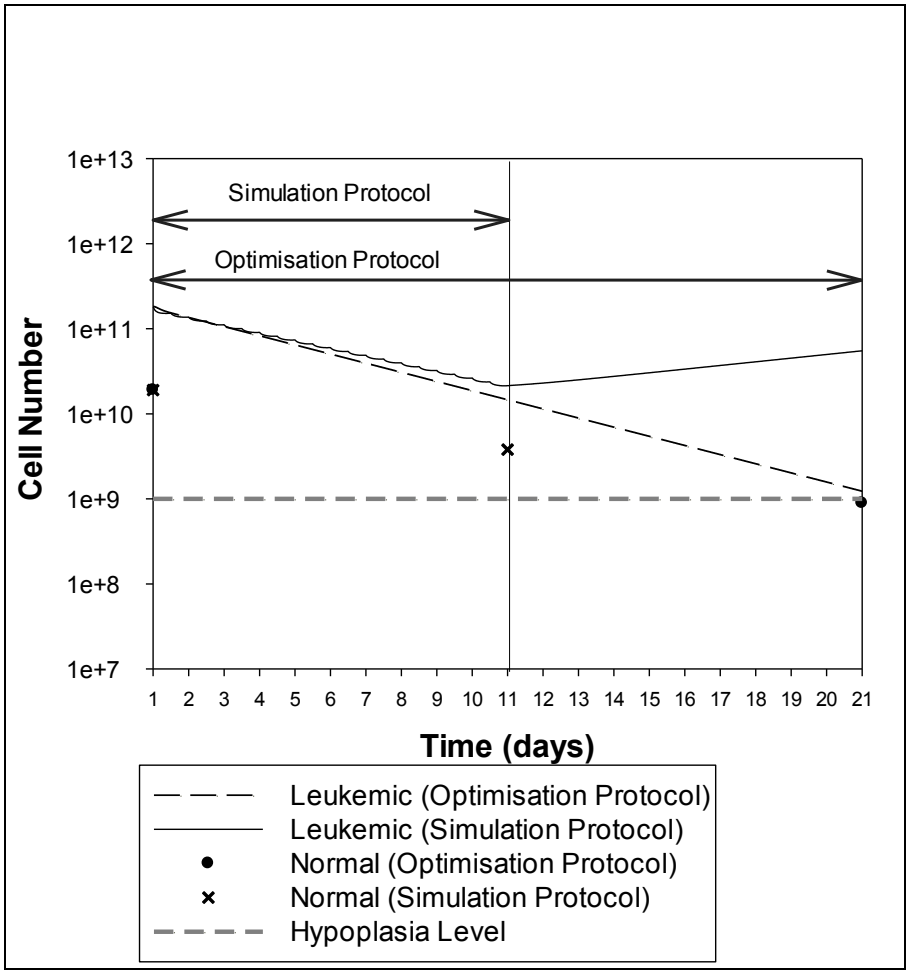

Figure 4.1: Optimisation results for patient H1 over the 1st cycle of LDAC. The black straight line represents the leukemic population over the simulation protocol with a duration of 10 days (day 1 to 11), whereas the dashed line is for the optimisation protocol with duration of 20 days (day 1 to 21).

Due to the increased toxicity of the optimisation protocol, leukemic and normal cell populations further decrease in the optimisation protocol. Particularly, there is a further decrease of $2.02 \cdot 10^{10}$ leukemic cells achieved at a cost of losing $2.9 \cdot 10^{9}$ normal cells. The optimisation objective is to achieve a BM with a higher normal population than leukemic population from the 1st chemotherapy cycle. However, due to the aggressiveness of the leukemic population of patient H1, such a solution is infeasible and this constraint had to be relaxed for an optimal solution to be found. Hence, for this patient, over the 1st cycle, the difference between the normal and leukemic population is decreased to the maximum possible level and over the 2nd cycle, the normal population is higher, indicating a healthier BM.

2nd Chemotherapy Cycle

The schedule of the 2nd chemotherapy cycle is the same as that of the 1st chemotherapy cycle i.e. 40 mg applied as daily infusions for 20 days (Table 4.2). The dynamics of the normal and leukemic cell populations are presented in figure 4.2. Due to the increased toxicity of the 1st chemotherapy cycle, the initial burden of the leukemic population over the optimisation protocol is lower. The leukemic population is further decreased by the 2nd chemotherapy cycle and by cycle completion, there is a further population reduction of $2.86 \cdot 10^{10}$ cells compared with that of the simulation protocol. Normal population dynamics are the same for the 1st and the 2nd chemotherapy cycles since the same schedule is applied. Moreover, during the optimisation protocol, BM hypoplasia is achieved since leukemic cells are less than the hypoplasia level ($1 \cdot 10^9$ cells).

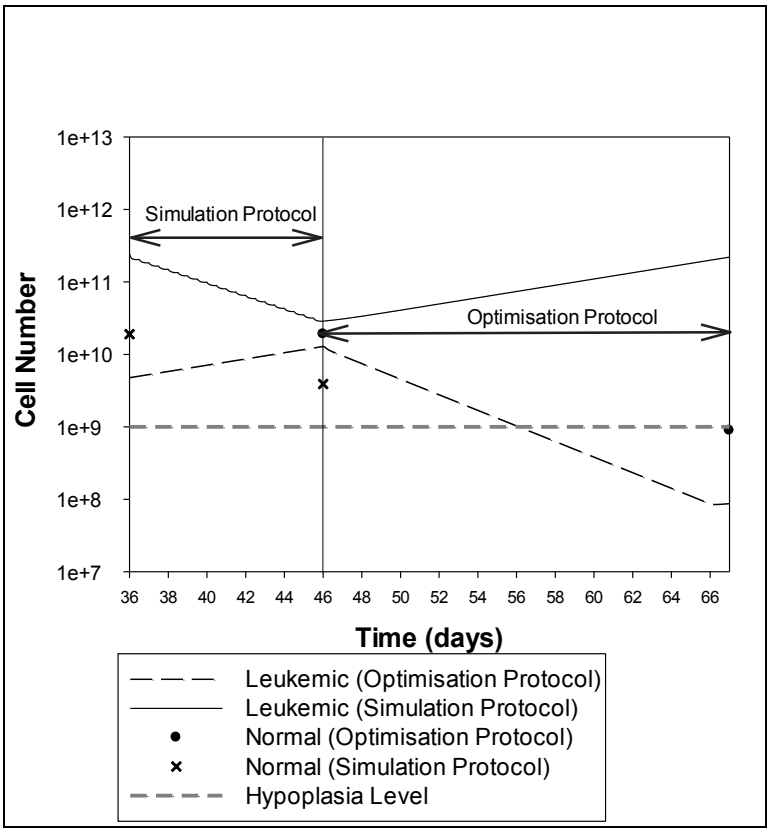

Figure 4.2: Optimisation results for patient H1 over the 2nd cycle of LDAC. The black straight line represents the leukemic population over the simulation protocol with a duration of 10 days (day 36 to 46), whereas the dashed line is for the optimisation protocol with duration of 20 days (day 46 to 66).

3rd Chemotherapy Cycle

The same total dose as with the simulation protocol is suggested for the 3rd chemotherapy cycle i.e. daily amount of 40 mg. The cycle duration is 10 days and the doses will be applied as daily infusions rather than rapid bolus doses. The comparison of the simulation and optimisation results for the 3rd cycle is presented in figure 4.3 below. Optimisation results are better since the leukemic population is below the hypoplasia level for the entire duration of the cycle.

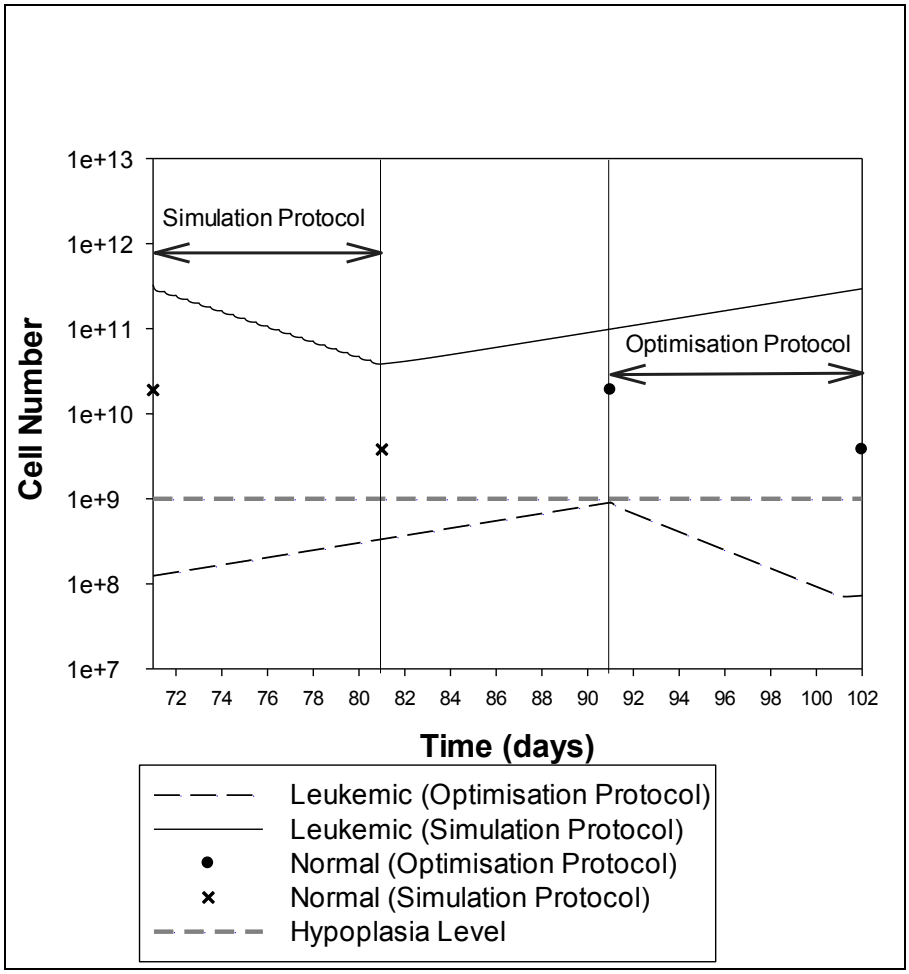

Figure 4.3: Optimisation results for patient H1 over the 3rd cycle of LDAC .The black straight line represents the leukemic population over the simulation protocol with a duration of 10 days (day 71 to 81), whereas the dashed line is for the optimisation protocol with duration of 10 days (day 91 to 101). There is a 20 day delay between the optimisation and simulation protocols due to the increased duration of the previous 2 cycles of 10 days each.

The leukemic population decreases from $9.06 \cdot 10^8$ cells to $7.2 \cdot 10^7$ cells and the normal population decreases from $1.9 \cdot 10^{10}$ cells to $3.79 \cdot 10^9$ cells. As compared with the simulation results, there is a further decrease of $3.8 \cdot 10^{10}$ cells, whereas the normal cell population is the same. This is expected if we consider that the normal population consists of proliferating cells susceptible to treatment and quiescent cells serving as back-up cells at times of BM depletion. Since the transition rate of quiescent cells depends on the population depletion, the population will be adjusted to account for the loss and the transition rate will be adapted to keep the population constant. For the optimal protocol, since dose injection rate is lower and constant over the optimal treatment protocol, it will enable a constant transition of quiescent cells to proliferation that will result in a more rigid normal cell population recovery over this protocol.

4^{th} Chemotherapy Cycle

The same schedule as for the 3^{rd} cycle is suggested for the 4^{th} and last cycle of the LDAC protocol. Total dose is kept constant and the schedule is changed to include daily dose infusion rather than the applied rapid dose applications over the simulation protocol. The leukemic population further decreases and at treatment completion, BM consists of $6 \cdot 10^7$ leukemic cells and $3.79 \cdot 10^9$ normal cells (figure 4.4).

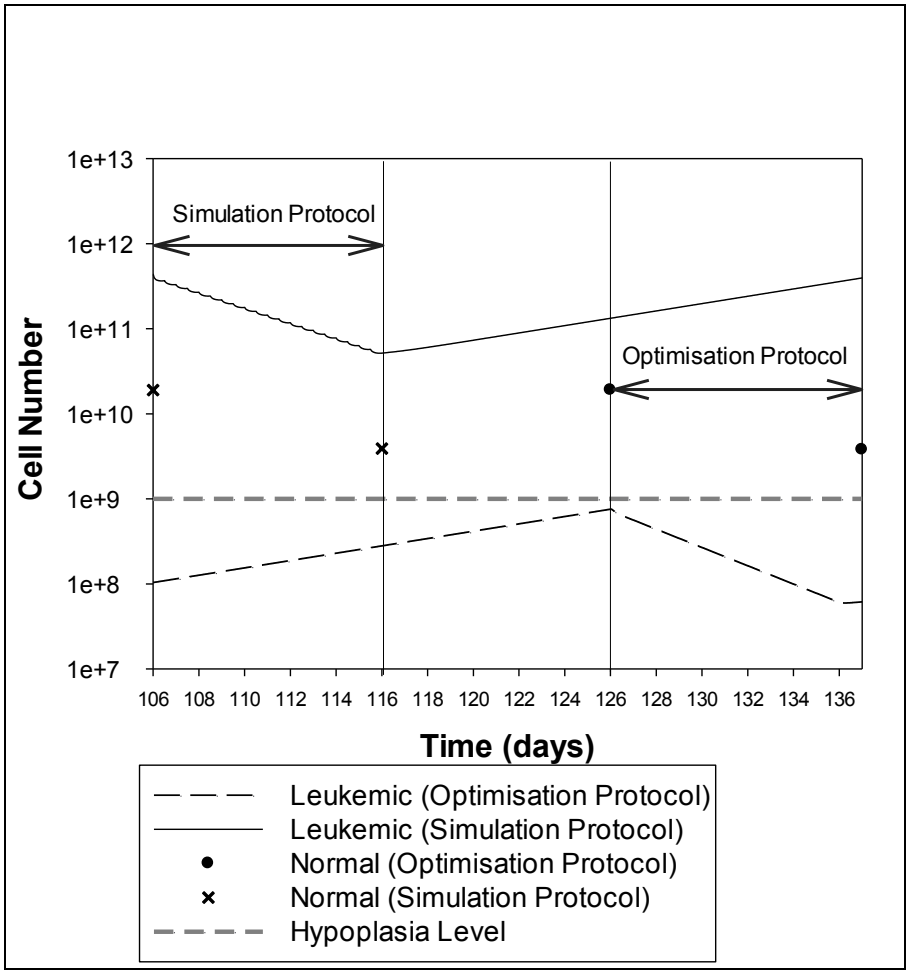

Figure 4.4: Optimisation results for patient H1 over the 4th cycle of the LDAC protocol. The black straight line represents the leukemic population over the simulation protocol with a duration of 10 days (day 106 to 116), whereas the dashed line is for the optimisation protocol with duration of 10 days (day 126 to 136). There is a 20 days delay between the optimisation and simulation protocols due to the increased duration of the previous 2 cycles of 10 days each.

In summary, Patient H1 shows resistance during the simulation with the LDAC protocol and disease burden is decreased over each chemotherapy cycle but over the interval period is increasing and by treatment completion the final leukemic population is higher than that at diagnosis. For this reason, the optimisation protocol suggests for the two first chemotherapy cycles, extended treatment duration to 20 days rather than the 10 days of the simulation protocol. For the first two cycles, a total dose increase of 400 mg is suggested and doses are administered as continuous daily infusions. Over these two more toxic cycles, the disease burden is decreasing more rapidly and, after the 2nd cycle, the leukemic population is below the desired hypoplasia level (figure 4.5). For cycles 3 and 4, the total dose is kept at the same levels as that for the simulation protocol i.e. 40 mg, but given as continuous 24 hour infusions

SC, as well. At treatment completion of the full course of the optimised protocol, there is a total 3-log reduction of leukemic cells that equals $6.4 \cdot 10^8$ cells (Table 4.3). This population is below the level of hypoplasia and below the level of normal cells, which is the treatment objective. Normal cells are also reduced more over the first two chemotherapy cycles compared with the last two cycles (Table 4.3) as is expected since the first cycles are of increased toxicity. Finally, as is presented in figure 4.5, with a total dose increase of 800 mg over the entire chemotherapy course, compared with that of the simulation protocol, the leukemic population is reduced to a level below the hypoplasia level, whereas the same patient was resistant to the simulated LDAC protocol used in current clinical practise.

Table 4.3: Optimisation results for the full course of LDAC treatment for Patient H1

Date	**Leukemic population over optimisation with LD protocol**	**Normal population over optimisation with LD protocol**
Beginning of 1st cycle	$1.82 \cdot 10^{11}$	$1.9 \cdot 10^{10}$
End of 1st cycle	$1.2 \cdot 10^9$	$8.9 \cdot 10^8$
Beginning of 2nd cycle	$1.28 \cdot 10^{10}$	$1.9 \cdot 10^{10}$
End of 2nd cycle	$8.58 \cdot 10^7$	$8.9 \cdot 10^8$
Beginning of 3rd cycle	$9.06 \cdot 10^8$	$1.9 \cdot 10^{10}$
End of 3rd cycle	$7.2 \cdot 10^7$	$3.79 \cdot 10^9$
Beginning of 4th cycle	$7.58 \cdot 10^8$	$1.9 \cdot 10^{10}$
End of 4th cycle	$6 \cdot 10^7$	$3.79 \cdot 10^9$
BM aspirate after 4th cycle	$6.4 \cdot 10^8$	

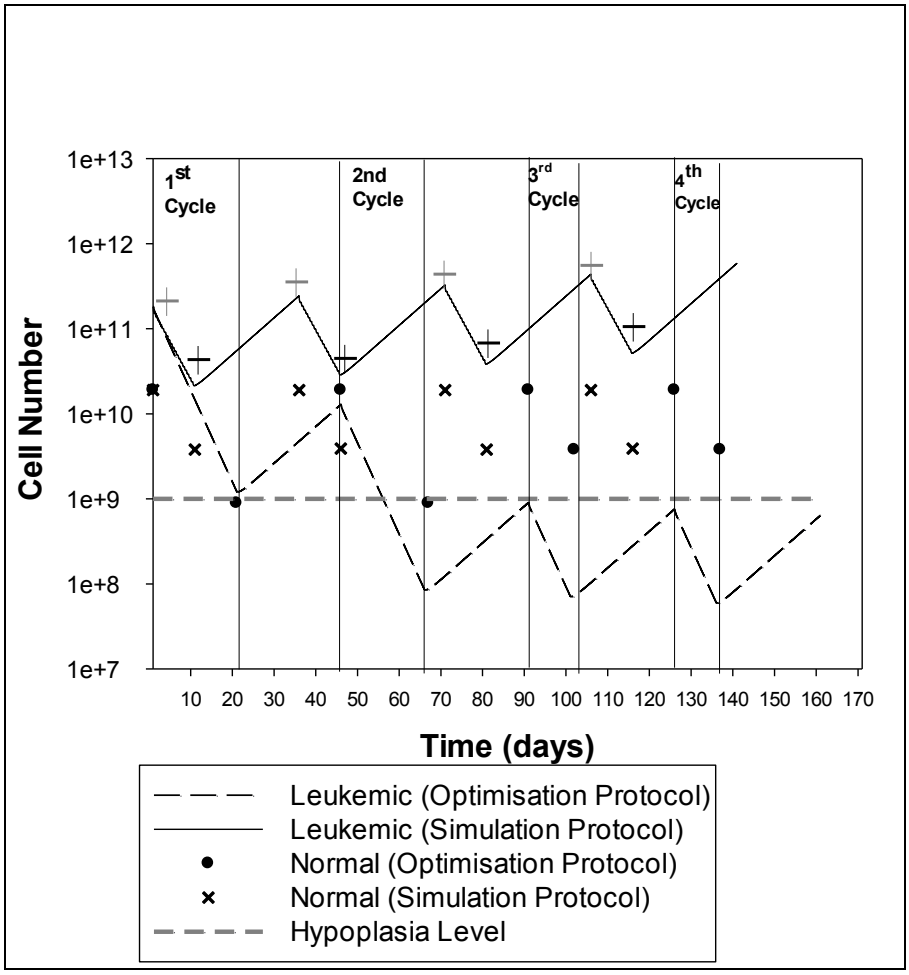

Figure 4.5: Simulation and optimisation results for Patient H1 over the LDAC protocol. The straight line represents the simulation results and the black dashed line represents the optimisation results. The figure is separated for the 4 cycles of the optimisation treatment that present a lag period compared with the simulation protocol as the first 2 cycles last 10 days more for each optimised cycle. Grey cross symbols indicate the start date of each chemotherapy cycle for the simulation protocol and black cross symbols indicate the end of each cycle.

- **Optimisation results of the DA protocol for Patient H1**

As has already been mentioned, the purpose of induction chemotherapy treatment is to reduce the leukemic population below the hypoplasia level and also below the level of normal cells while suffering a maximum 3-log reduction in the number of normal cells. With these constraints at the end of the induction treatment, a BM with recovering normal cells and a weakend leukemic cell population will be achieved. Simulation results for Patient H1 indicate that treatment with DA is successful. For this reason the aim of the optimisation of the current protocol should not be to increase the dose load i.e. treatment toxicity, but to use the same total dose and optimise in order to identify the optimal schedule of this dose load. This

optimisation problem is solved and the optimal protocol suggests daily continuous doses, i.e. 24 hour iv infusion, of 200 mg/m^2 instead of 2 doses of 100 mg/m^2 twice a day, whereas the same schedule for DNR is maintained since the toxicity of this drug does not allow for the flexibility to find alternative optimisation solutions. Figure 4.6 presents the disease dynamics of Patient H1 over the simulation and optimisation results for the DA protocol and Table 4.4 summarises the results over the optimisation DA treatment protocol.

Table 4.4: Optimisation results for the full course of treatment of protocol DA for Patient H1

Date	Leukemic population over optimisation with DA protocol	Normal population over optimisation with DA protocol
Beginning of 1st cycle	$1.82 \cdot 10^{11}$	$1.9 \cdot 10^{10}$
End of 1st cycle	$6.97 \cdot 10^{7}$	$3.78 \cdot 10^{8}$
Beginning of 2nd cycle	$6.6 \cdot 10^{8}$	$1.9 \cdot 10^{10}$
End of 2nd cycle	$2.5 \cdot 10^{5}$	$3.78 \cdot 10^{8}$
Beginning of 3rd cycle	$2.4 \cdot 10^{6}$	$1.9 \cdot 10^{10}$
End of 3rd cycle	912	$3.78 \cdot 10^{8}$
Beginning of 4th cycle	8749	$1.9 \cdot 10^{10}$
End of 4th cycle	0	$3.78 \cdot 10^{8}$
BM aspirate after 4th cycle	-	

As illustrated in figure 4.6, the optimal treatment protocol is more effective since leukemic cells are further decreased over the full course of treatment. After completion of the 1st chemotherapy cycle for Patient H1, the leukemic population is further reduced making a difference of $7.3 \cdot 10^6$ cells less. This reduction will successively affect the initial conditions of the subsequent chemotherapy cycles resulting in further reduction of the leukemic population that is finally undetectable at completion of the optimal treatment schedule (Table 4.4).

Moreover, the normal population is kept at the same order of magnitude for both the simulation and optimisation protocols (Tables 3.7 and 4.4). This is expected if we consider

that the normal population consists of proliferating cells susceptible to the treatment and quiescent cells kept in reserve for use at times of BM depletion. Since the transition rate of quiescent cells depends on the population depletion, the population will be adjusted to account for the loss and the transition rate will be adapted to keep the population constant. For the optimal protocol, since dose administration rate is lower and constant over the optimal treatment protocol, it will enable a constant transition of quiescent cells to enter proliferation and will result in a more rigid normal cell population recovery over this protocol.

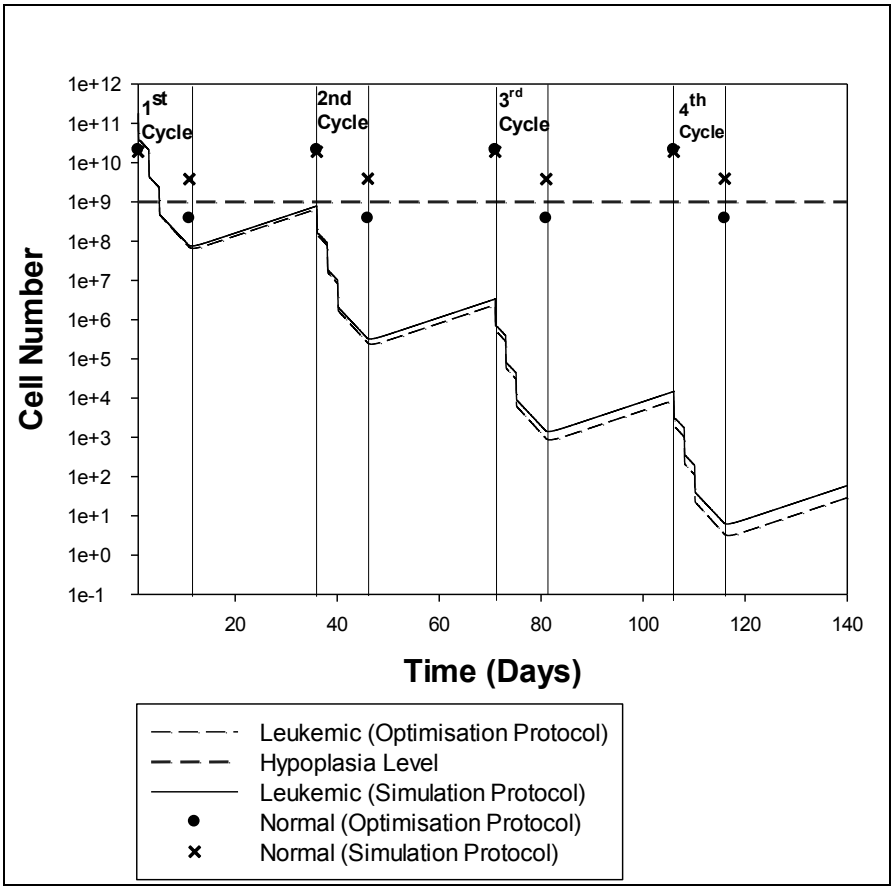

Figure 4.6: Simulation and optimisation results for Patient H1 over the DA protocol. The straight line represents the simulation results and the black dashed line represents the optimisation results.

4.2.2 Optimisation results of Patient H2 with LDAC and DA treatment protocols

- **Optimisation results of the LDAC protocol for Patient H2**

As has already been presented in the simulation results section, Patient H2 has a successful treatment with the LDAC protocol since leukemic cells are successfully lowered to a level less than the BM hypoplasia level and the number of normal cells. For this patient, the optimisation problem will be to keep the total dose constant i.e. 400 mg total and check if there is an improved treatment schedule. This optimisation problem is solved and the optimised protocol suggests daily continuous infusions sc of 40 mg for 10 days rather than 2 doses of 20 mg daily for 10 days that is applied in current clinical practice.

The comparison of the Patient H2 cell populations over the simulation and optimisation treatment protocols is presented in figure 4.7 and the resulted populations are listed in detail in Table 4.5.

Table 4.5: Optimisation results for the full course treatment of LDAC for Patient H2

Date	Leukemic population over optimisation with LDAC	Normal population over optimisation with LDAC
Beginning of 1st cycle	$1.12 \cdot 10^{11}$	$1.99 \cdot 10^{10}$
End of 1st cycle	$2.25 \cdot 10^{8}$	$3.79 \cdot 10^{9}$
Beginning of 2nd cycle	$2.42 \cdot 10^{9}$	$1.99 \cdot 10^{10}$
End of 2nd cycle	$4.8 \cdot 10^{6}$	$3.79 \cdot 10^{9}$
Beginning of 3rd cycle	$5.23 \cdot 10^{7}$	$1.99 \cdot 10^{10}$
End of 3rd cycle	$1.05 \cdot 10^{5}$	$3.79 \cdot 10^{9}$
Beginning of 4th cycle	$1.1 \cdot 10^{6}$	$1.99 \cdot 10^{10}$
End of 4th cycle	3400	$3.79 \cdot 10^{9}$
BM aspirate after 4th cycle	$3.6 \cdot 10^{4}$	

As presented in figure 4.7, over the optimal protocol, a reduction of the leukemic population is achieved although the total dose is kept constant. This difference is increasing as the chemotherapy cycles are accumulating and is due to the lower initial leukemic numbers of cycles 2 to 4. By treatment completion, the leukemic population is further reduced to $1.86 \cdot 10^6$ cells fewer than that of the simulation protocol. Moreover, the normal population is kept to the same order of magnitude for both protocols. This is expected if we consider that the normal population consists of proliferating cells susceptible to the treatment and quiescent cells serving as back-up in times of BM depletion. Since the transition rate of quiescent cells depends on the population depletion, the population will be adjusted to the loss and the transition rate will be adapted to keep the population constant. For the optimal protocol, since dose administration rate is lower and more frequent over the optimal treatment protocol, it will enable a lower and constant transition of quiescent cells to the proliferating state that will result in a more rigid normal cell population recovery over this protocol.

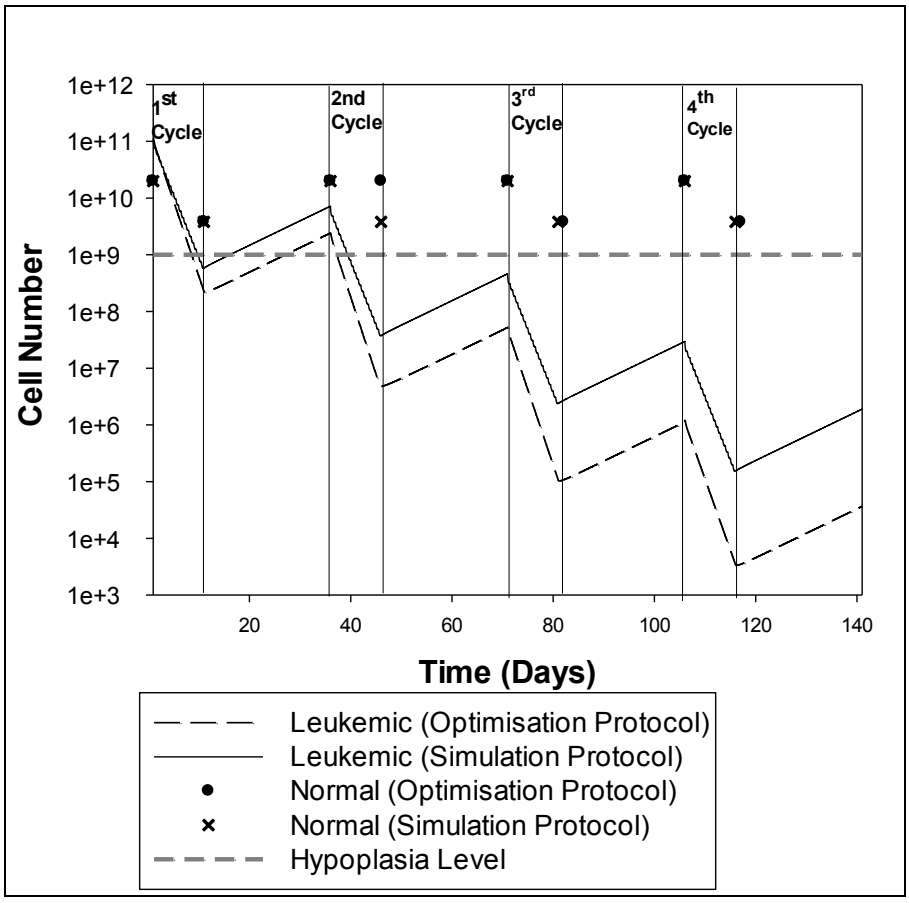

Figure 4.7: Optimisation results for Patient H2 over the LDAC protocol with daily continuous infusions sc of 40 mg for 10 days (optimisation results: black dashed line) instead of doses every 12 hrs of 20 mg for 10 days (simulation results: straight line).

- **Optimisation results of the DA protocol for Patient H2**

Simulation results of Patient H2 over the DA protocol show that the patient reached the desired BM state. For this reason, the aim of the optimisation of the current protocol would not be to increase the dose load i.e. treatment toxicity, but to use the same total dose and optimise in order to identify the optimal schedule of this dose load. This optimisation problem is solved and the optimal protocol suggests daily continuous infusion doses of 200 mg/m^2 iv Ara-C instead of 2 doses of 100 mg/m^2 twice a day, whereas the same schedule for DNR is kept since the toxicity of this drug does not allow flexibility for alternative optimisation solutions.

Figure 4.8 presents the disease dynamics of Patient H2 over the simulation and optimisation results for the DA protocol and Table 4.6 summarises the results over the optimisation DA treatment protocol.

Table 4.6: Optimisation results for the throughout treatment of protocol DA for Patient H2

Date	**Leukemic population over optimisation with DA protocol**	**Normal population over optimisation with DA protocol**
Beginning of 1st cycle	$1.12 \cdot 10^{11}$	$1.99 \cdot 10^{10}$
End of 1st cycle	$3.6 \cdot 10^{5}$	$3.78 \cdot 10^{8}$
Beginning of 2nd cycle	$3.4 \cdot 10^{6}$	$1.99 \cdot 10^{10}$
End of 2nd cycle	0	$3.78 \cdot 10^{8}$
Beginning of 3rd cycle	-	
End of 3rd cycle	-	
Beginning of 4th cycle	-	
End of 4th cycle	-	
BM aspirate after 4th cycle	-	

As illustrated in figure 4.8, the optimal treatment protocol is more effective as leukemic cells are further reduced during the full course of treatment. After completion of the 1st

chemotherapy cycle for Patient H2, the leukemic population is further reduced to $1.2 \cdot 10^5$ cells. This difference leads to a decreased number of the initial leukemic population for the 2nd chemotherapy cycle over which the disease becomes undetectable and there is no need for a 3rd chemotherapy cycle.

Moreover, the normal population is kept to the same order of magnitude for both protocols. This is expected if we consider that the normal population consists of proliferating cells susceptible to the treatment and quiescent cells serving as back-up cells in times of BM depletion. Since the transition rate of quiescent cells depends on the population depletion, the population will be adjusted to the loss and the transition rate will be adapted to keep the population constant. For the optimal protocol, since dose injection rate is lower and constant over the optimal treatment protocol, it will allow a constant transition of quiescent cells to the proliferating state that will result in a more rigid normal cell population recovery over this protocol.

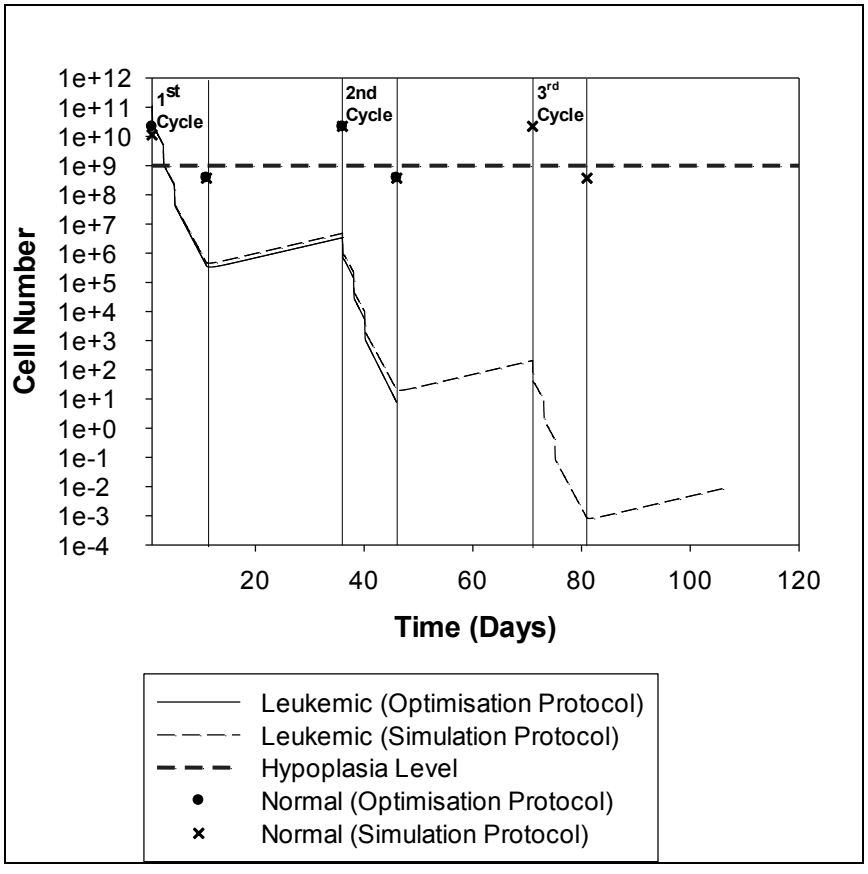

Figure 4.8: Optimisation results for Patient H2 over the DA protocol with continuous daily infusion doses of 200 mg/m^2 iv Ara-C for 10 days (optimisation results: straight line) instead of doses every 12 hrs of 100 mg/m^2 for 10 days (simulation results: dashed line).

4.3 Discussion

In this chapter, the mathematical model presented in Chapter 3 is used as an optimisation problem application. The benefits of optimisation are presented and a scheduling optimisation problem is developed for the optimisation of chemotherapy process.

The objective is to reduce the leukemic population to a level of approximately 10^9 cells at which BM hypoplasia and morphologic remission is achieved. Moreover, the normal population should be higher than the leukemic population and a 3-log reduction is the maximum level of population reduction permitted per chemotherapy cycle. In this way, rapid restoration of normal BM function will be achieved which is the aim of remission-induction therapy.

This optimisation problem is solved using gPROMS for the two patient case studies. For the DA protocol, the optimisation problem is comprised of scheduling problem with the same total dose as the simulation protocol but with possibly an improved schedule. This is due to the fact that both patients receive a successful treatment after this protocol and there is no need for dose load increase. The optimisation schedule suggests that Ara-C should be administered in continuous iv infusion of 200 mg/m^2 daily for 10 days instead of a rapid bolus of 100 mg/m^2 applied twice a day for 10 days as is used in standard clinical practice. The resulting protocol shows improvement of the treatment outcome where Patient H1 has complete disease eradication at completion of the 4 cycles and Patient H2 has full disease eradication after the 2nd cycle.

For the LDAC protocol, two optimisation problems were solved, one for each patient. For Patient H1, increased dose intensity was suggested since this patient had unsuccessful treatment outcome over the simulation results. A total dose increase of 400 mg in each of the first two cycles is suggested given as 40 mg daily continuous infusions sc over 20 days. Moreover, for cycles 3 and 4 the total dose is similar to that in the simulation protocol, i.e. 400 mg, but with different treatment schedule that includes daily continuous sc infusions of 40 mg. Following this protocol, Patient H1 has a successful treatment with leukemic cells reduced to a level lower than the hypoplasia level as desired.

Lastly, a scheduling optimisation problem was formed and solved for the LDAC protocol of Patient H2. This patient has a successful treatment over the simulation results so the aim of

optimisation is to use the same total dose but optimise the applied treatment schedule. The resulted schedule suggests 4 cycles of chemotherapy with daily continuous sc infusional doses of 40 mg applied for 10 days instead of 20 doses of 20 mg applied every 12 hrs sc as used in the simulation protocol. Under this optimised protocol, the leukemic population is further reduced compared with that of the simulation results.

Treatment outcome is highly dependent on the duration of the S-phase (Ts) and the total cycle duration (Tc). For this reason, in Appendix A, the dynamics of the leukemic cell population in the particular cell phases are presented for the two patients. Patient H1 is characterised by a high duration of the GoG_1-phase which results in a high percentage of cells being in this phase. Under the LDAC protocol, only Ara-C is applied and therefore does not affect cells in the GoG_1-phase. For this reason, this treatment is unsuccessful for this patient case study as it is not able to kill cells in the most abundant cell phase resulting in disease relapse (Appendix A: figures A1 – A4). In contrast, when the DA protocol is applied to the same population, the treatment outcome is successful. The reason for this is that DNR acts on and reduces cells in the GoG_1-phase, and also a higher dose of Ara-C is administered, which results in the reduction of more S-phase cells and GoG_1- G_2M- cells successively (Appendix A: figures A5-A8). Patient H2 is characterised by a lower duration of the GoG_1-phase and thus a lower population exists in this phase. For this reason, the LDAC protocol presents a better treatment outcome results for this case study compared to Patient H1. Moreover, the DA protocol is more efficient for this patient, as well, due to its increased toxicity (Appendix A: figures A9-A15).

For the optimisation results, the common trend across all results is that continuous infusional doses (iv or sc) are preferred for both protocols. The most interesting case is the optimisation of Patient H1 under the LDAC protocol. As discussed earlier, this protocol was unsuccessful for Patient H1; however, optimisation allows the desired results to be obtained. The optimisation protocol suggests prolonging cycles 1 and 2 by 10 more days compared with that in the simulation protocol and doubling the total dose load i.e. 800 mg total dose increase over the course of therapy. Moreover, cycles 3 and 4 use the same total dose as for the simulation but continuously applied. For the optimisation protocol, cells in S-phase are continuously decreasing faster than in the simulation protocol. This decrease will successively affect cells in the other two phases as fewer cells will be transitioned from the S-phase. Treatment outcome is much improved over the first two chemotherapy cycles where more toxic doses are applied but, overall, the results for this protocol are better and the

desired induction treatment objectives are achieved (Appendix A: figures A16-A19). For the optimisation of the remaining patient case studies i.e. Patient H1 under the DA protocol and Patient H2 under both protocols, the optimisation problem was to use the same total dose but under optimal dosing schedule. For all these cases, the suggested schedule is to use the same dose load but continuously infused for Ara-C and the same schedule for DNR. Under this schedule a lower but constant concentration is applied to cells in S-phase which results in a higher reduction of cells in this phase and in succession leads to the reduction of cells in all phases (Appendix A: figures A19 – A30).

In summary, the optimisation protocols appear to be more efficient disease management than the simulated protocols applied in clinical practice. Under these optimised protocols, according to model results, BM hypoplasia is achieved for all patients and the normal population is higher than that of the leukemic for all the applied chemotherapy cycles.

PART II:

Model Analysis with Patient Data

Chapter 5[3]

Model Analysis with Patient Data

5.1 Introduction

A mathematical model and an optimisation algorithm have been developed and presented in the previous chapter which is able to capture normal and leukemic cell population dynamics under induction chemotherapy treatment for AML. For the personalisation of treatment design, individual parameters are used in the model that consists of physiological patient characteristics (sex, age, body mass index) and disease characteristics (initial tumour burden, cell population kinetic information). Sensitivity analysis of the model parameters is also performed and the results identify that cell cycle parameters are the critical parameters that control the treatment outcome.

In this chapter, the anonymised health records of 6 patients diagnosed with AML and treated under the LDAC and DA protocols are used for purposes of model analysis. In particular, patient characteristics (sex, age, BMI) are used together with disease characteristics (blast percentage measurements from BM aspirates, BM cellularity factor) for the estimation of cell cycle distribution times for each patient. Moreover, the already presented optimisation problem is solved for the two types of chemotherapy protocols, the low dose Ara-C protocol where sc low doses of Ara-C are applied as twice daily short doses and the DA protocol where short intravenous doses of Ara-C and DNR are applied daily. These protocol types are optimised for all the patients studied in this work.

Section 5.2 presents the clinical data used for model analysis, then section 5.3 presents the parameter estimation results for the calculation of the patient specific cell cycle times. Moreover, optimisation results are presented and analysed in section 5.4 of this chapter. Section 5.5 presents the explanation of the optimisation results by illustrating the different

[3] Work in this chapter has been submitted for publication to *Cancer Research*.
Pefani E., Panoskaltsis N., Mantalaris A., Georgiadis M. C., Pistikopoulos E. N.. Mathematical modelling and optimal scheduling of induction chemotherapy treatment of Acute Myeloid Leukemia (AML) with Daunorubicin (DNR) and Cytarabine (Ara-C) agents.

concentration profiles for the optimisation and simulation protocol and their effect on the cell population. Lastly, concluding remarks of this chapter are discussed in section 5.6.

5.2 Patient data and model analysis assumptions

5.2.1 Patient Data

The project was submitted to and approved by the North West London Hospitals Trust (RD12.012) for the provision of anonymised health records of patients diagnosed with AML and treated within Northwick Park Hospital using DNR and Ara-C anti-leukemic agents under either i.v. or sc doses applied as per standard clinical practice (protocols available in Appendix B).

5.2.2 Model Analysis Assumptions

The required input data for a treatment protocol simulation consists of patient, disease, drug and treatment schedule information. Patient information includes the physiological patient characteristics of sex, age, weight and height that are used in order to calculate the volume of the body organs and the organ blood flow rate. Both the volume and the blood flow rate of the organs are important parameters that differ between patients and affect the drug PK profile. Disease information includes the blast percentage in the marrow aspirate and the BM cellularity, both of which are pieces of information acquired in routine clinical practice during the course of AML diagnosis and during the course of treatment. As extra information to what is currently used in clinical practice, the cell cycle characteristics of S-phase duration and the total cell cycle duration will be assessed. Moreover, for model simulation, drug information is required of the drugs that will be used for the treatment protocol. The required drug information is available in the product specification provided by the pharmaceutical company producing each drug. The PK drug information includes the elimination rate in the kidneys and the liver and the clearance rate by the kidneys. The PD drug response is defined by parameters that relate the drug concentration to the PD effect. PD model parameters include the drug concentration at the half drug effect, the concentration at the maximum drug effect as well as the slope scaling factor. Lastly, the treatment schedule for each chemotherapy cycle for the drugs applied is needed. Schedule information consists of the dose load, the dose duration, the number of dose applications and the duration of the chemotherapy cycle applied.

The clinical data of the 6 patients under LDAC and DA treatment protocols were used for model analysis purposes. The clinical data is comprised the patient physiological characteristics, the blast percentage and cellularity in the BM aspirate at diagnosis, the chemotherapy treatment protocol and the blast percentage together with marrow cellularity of the marrow examinations after the applied chemotherapy protocol (Appendix B).

Since the model involves the number of leukemic cells, assumptions were made in order to convert the blast % into the number of leukemic cells:

i. Conversion of % blast into leukemic cells is calculated by the formula,

$$Cells_{leukemic} = CF \cdot BP \cdot DB$$

where CF is the cellularity factor of each patient, BP is the measured blast percentage in the BM aspirate and DB is the disease burden. For the calculation of these factors the below assumptions are used.

$$CF = \begin{cases} 0.2 \ , \ hypocellular \\ 0.4 \ , normocellular \ , \ years > 65 \\ 0.5 \ , normocellular \ , \ years \le 65 \\ 0.95 , \ hypercellular \end{cases}$$ (Williams et al., 1983; Bennett, Orazi, 2009)

$DB = 1 \cdot 10^{12} Cells$ (Williams et al., 1983)

ii. Leukemic cell population is assumed to be constant from the biopsy sampling point until the first application of chemotherapy. At the point of disease diagnosis, the leukemic cell population is assumed to have already reached its maximum, and until the first cycle of treatment, the leukemic population will preserve the same order of magnitude of leukemic cells.

iii. BM at the point of diagnosis is hypercellular.

iv. The tumour cell burden in AML is 1 trillion cells (Williams et al., 1983). BM hypoplasia is the objective of induction chemotherapy, with 2- 3-log reduction in cell number.

As far as the drug information is concerned, the PK parameters for DNR and Ara-C agents were as reported in the latest reports of the British Cancer agency and the University College of London Hospital NHS Foundation Trust (BC cancer agency, 2007; ULCH, 2009).

Moreover, for the PD information, the published results of PD action of DNR and Ara-C on BM samples of 179 patients with AML were used (Quartino et al., 2007).

These are the assumptions made in order to use the available data for model analysis. The next section presents the method and the results of the estimation of the cell cycle distribution times for each patient.

5.3 Estimation of patient cell cycle distribution parameters

In this section, data presented in Appendix B of the health record of 6 AML patients are used for the estimation of leukemic cell cycle parameters that are the critical model parameters as indicated by the sensitivity analysis results. One important assumption the estimation is based on is the cell cycle times during the interval period between two successive chemotherapy cycles. As has already been mentioned, this period is a recovery period lasting 20-30 days during which the patient receives no treatment.

Under this assumption, for the interval period between two cycles when no treatment is applies the leukemic cell cycle parameters are set to Ts=40hrs and Tc=211hrs. The provided leukemic population measurement at the end of this interval period together with the duration of this period are then used for the calculation of the leukemic population at the beginning of the recovery period, that is the leukemic population at completion of the last applied chemotherapy cycle.

The calculated leukemic population at the end of the chemotherapy cycle together with the provided initial tumour burden at the beginning of each chemotherapy cycle and the treatment schedule are subsequently used to estimate the leukemic cell cycle parameters (Ts, Tc) under chemotherapy.

This parameter estimation problem is solved using gPROMS (gPROMS, 2003) and the fitted cell cycle for the 6 patients are listed in Table 5.7 and are presented in figures 5.1 to 5.6, whereas the leukemic cells in exact numbers for all patients are listed in Tables 5.1 to 5.6.

5.3.1 Cell cycle estimation for Patient P001

P001 is a female patient with a diagnosis of secondary AML. Physiological characteristics are 75 years old, 152 cm height and 56kg. BM aspirate shows a 21% blast percentage and the designed treatment for this patient is the LDAC protocol with 4 cycles of 10 days.Two doses of 20mg are administered sc to the patient daily. Patient reaction to this chemotherapy protocol is very promising for the first three cycles where the blast percentage is reduced to 14% after the first chemotherapy cycle, then is reduced to 4% after the second cycle and to 5% after the third cycle. However, after the 4th cycle, the leukemic population is recovering and there is a disease relapse with a blast percentage as high as 15% by induction treatment completion.

The fitted cell cycle times for P001 are listed in Table 5.7. For the 1st cycle, Ts is equal to 13 hrs and Tc is 45 hrs. For the second cycle Ts equals 16 hrs and Tc 40 hrs, whereas for the 3rd cycle Ts is fitted to 11 hrs and the whole cell cycle time to 45 hrs. Lastly, over the 4th cycle Ts equals 18 hrs and there is an increase of the Tc hrs to 65 hrs, an indicator of disease relapse over this chemotherapy cycle. Figure 5.1 presents the leukemic cell dynamics over the full course of treatment for this patient and Table 5.1 lists the leukemic cell populations for P001 for model simulation compared with the clinical data.

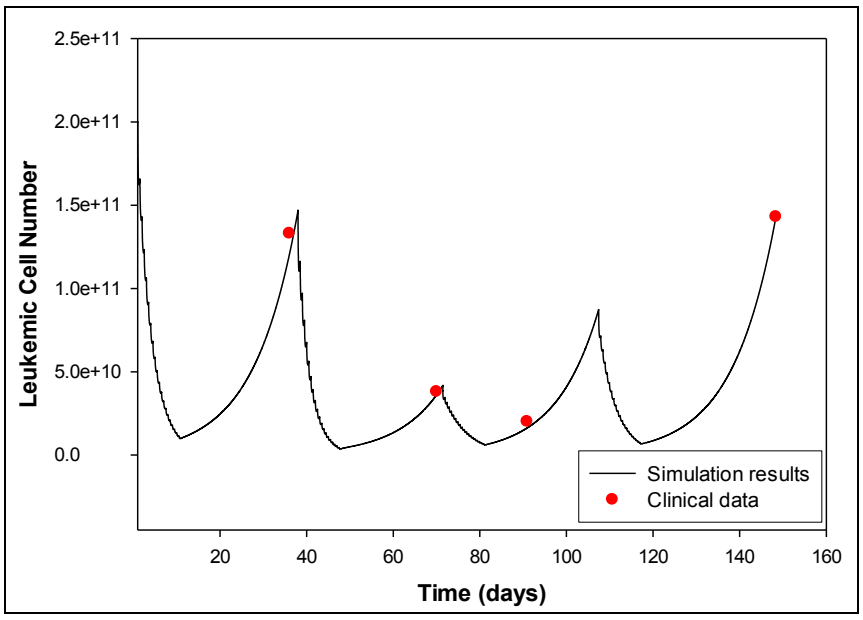

Figure 5.1: Comparison of simulation results and clinical data for Patient P001.

Table 5.1: Leukemic population of Patient P001 based on model analysis and clinical data

Date	Leukemic Population (simulation)	Leukemic Population (data)
1st cycle start date: Day 1	$2 \cdot 10^{11}$ cells	
1st cycle end date: Day 10	$9.95 \cdot 10^{9}$ cells	
BM Aspirate after 1st Cycle Day 36	$1.33 \cdot 10^{11}$ cells	$1.33 \cdot 10^{11}$ cells
2nd cycle start date: Day 37	$1.47 \cdot 10^{11}$ cells	
2nd cycle end date: Day 47	$3.8 \cdot 10^{9}$ cells	
BM Aspirate after 2nd Cycle Day 70	$3.84 \cdot 10^{10}$ cells	$3.8 \cdot 10^{10}$ cells
3rd cycle start date: Day 69	$3.82 \cdot 10^{10}$ cells	
3rd cycle end date: Day 79	$6.13 \cdot 10^{9}$ cells	
BM Aspirate after 3rd Cycle Day 91	$2 \cdot 10^{10}$ cells	$2 \cdot 10^{10}$ cells
4th cycle start date: Day 105	$8.7 \cdot 10^{10}$ cells	
4th cycle end date: Day 115	$6.7 \cdot 10^{9}$ cells	
BM Aspirate after 4th Cycle Day 146	$1.44 \cdot 10^{11}$ cells	$1.43 \cdot 10^{11}$ cells

5.3.2 Cell cycle estimation for patient P002

The second patient case study is Patient P002. P002 is a female patient 72 years old with 150 cm height and 47 kg weight. This patient is diagnosed with secondary AML and the blast percentage in the BM aspirate is 83%. The designed treatment for this patient is the LDAC protocol and due to clinical complications, this patient received only the 1st out of the 4 planned chemotherapy cycles. Data available for the 1st chemotherapy cycle reveal that the patient responded well to the treatment since the leukemic population is reduced and the blast percentage is 4% after the completion of the 1st chemotherapy cycle.

The fitted cell cycle times are listed in Table 5.7 for this patient. The resulting Ts parameter is 21 hrs, whereas the whole cell cycle duration is 45 hrs. Figure 5.2 presents the leukemic cell dynamics for the full treatment this patient received in comparison with the available clinical data. Moreover, Table 5.2 lists the leukemic cell population numbers after model simulation together with the clinical data measurements.

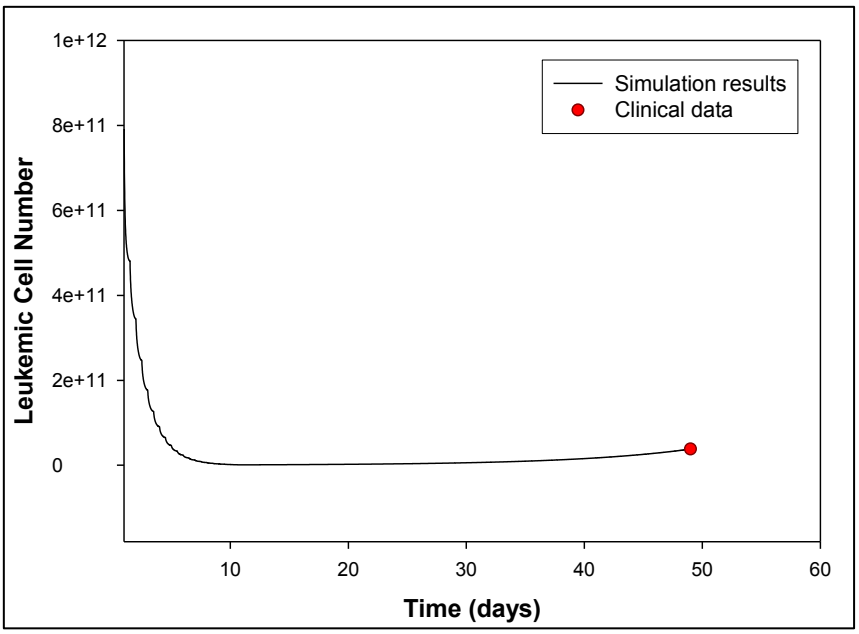

Figure 5.2: Comparison of simulation results and clinical data for Patient P002

Table 5.2: Leukemic population of Patient P002 based on model analysis and clinical data.

Date	Leukemic Population (model)	Leukemic Population (data)
1st cycle start date: Day 1	$7.9 \cdot 10^{11}$ cells	
1st cycle end date: Day 10	$8.6 \cdot 10^{8}$ cells	
BM Aspirate after 1st Cycle Day 48	$3.\ 8 \cdot 10^{10}$ cells	$3.\ 8 \cdot 10^{10}$ cells

5.3.3 Cell cycle estimation for Patient P006

Patient P006 is a female patient 71 years old, 160 cm height and 57 kg weight. This patient is diagnosed with de novo AML and the blast percentage in the BM aspirate at disease diagnosis is 36%. This patient received 4 chemotherapy cycles of LDAC and the treatment outcome was successful. Specifically, after the 1st chemotherapy cycle the blast percentage is reduced to 3%, after the 2nd cycle it is further reduced to 2% and after the 3rd cycle is

maintained at 2% with an increased cellularity factor (from 1 to 3) showing that the cellularity is increased but the disease is still maintained to the same order of magnitude. Lastly, after the 4th chemotherapy cycle complete remission is achieved, with leukemic cells dropping to the hypoplasia level.

For the 1st chemotherapy cycle, the S-phase duration of the leukemic population is fitted to 20 hrs and the whole cell cycle duration to 33 hrs. Moreover, for the 2nd chemotherapy cycle the fitted cell cycle times are 14 hrs duration of the S-phase and 46 hrs of the whole cell cycle. Over the 3rd chemotherapy cycle there is disease relapse as discussed earlier which results in increase of the cell cycle duration to 68 hrs, whereas Ts is 14 hrs. Lastly, for the 4th chemotherapy cycle Ts is fitted to 20 hrs and Tc to 40 hrs. Figure 5.3 presents the leukemic cell dynamics compared to the clinical data for the full length treatment of this patient and Table 5.3 lists the leukemic population cell number and the clinical data for all the chemotherapy cycles.

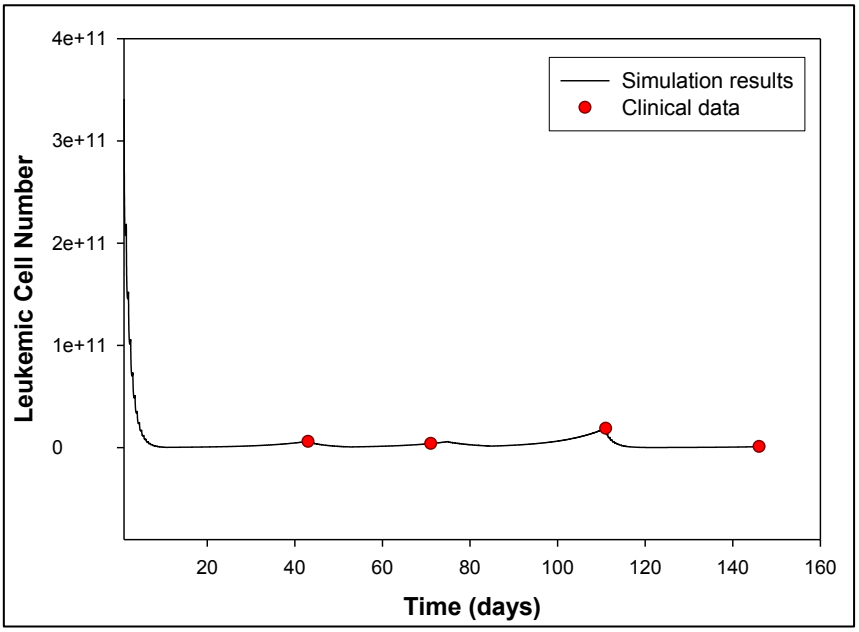

Figure 5.3: Comparison of simulation results and clinical data for Patient P006

Table 5.3: Leukemic population of Patient P006 based on model analysis and clinical data

Date	Leukemic Population (model)	Leukemic Population (data)
1st cycle start date: Day 1	$3.42 \cdot 10^{11}$ cells	
1st cycle end date: Day 10	$2.15 \cdot 10^{8}$ cells	
BM Aspirate after 1st Cycle Day 42	$6.1 \cdot 10^{9}$ cells	$6 \cdot 10^{9}$ cells
2nd cycle start date: Day 42	$6.1 \cdot 10^{9}$ cells	
2nd cycle end date: Day 52	$6.4 \cdot 10^{8}$ cells	
BM Aspirate after 2nd Cycle Day 70	$3.95 \cdot 10^{9}$ cells	$4 \cdot 10^{9}$ cells
3rd cycle start date: Day 74	$5.87 \cdot 10^{9}$ cells	
3rd cycle end date: Day 84	$1.46 \cdot 10^{9}$ cells	
BM Aspirate after 3rd Cycle Day 110	$1.89 \cdot 10^{10}$ cells	$1.89 \cdot 10^{10}$ cells
4th cycle start date: Day 109	$1.89 \cdot 10^{10}$ cells	
4th cycle end date: Day 119	$6.77 \cdot 10^{7}$ cells	
BM Aspirate after 4th Cycle Day 145	$9.7 \cdot 10^{8}$ cells	$1 \cdot 10^{9}$ cells

5.3.4 Cell cycle estimation for Patient P011

P011 is a male 24 years of age with 170 cm height and 59.5 kg weight. The diagnosis is secondary AML with a leukemic blast percentage in the BM of 56%. This patient received one cycle of DA induction with combination Ara-C and DNR anti-leukemic agents. Two daily doses (at 12 hour intervals) of 100 mg/m^2 of Ara-C were administered by iv bolus for 10 days combined with 3 doses of 60 mg/m^2 DNR applied on days 1, 3 and 5 by 1 hour iv

infusion. Treatment outcome is positive in terms of leukemic population reduction for this patient and the blast percentage is reduced to 3% at completion of the 1st chemotherapy cycle.

The fitted cell cycle times for the one cycle this patient received are listed in Table 5.7. Ts duration is fitted to 9 hrs and the whole cell cycle duration is fitted to 53 hrs. Figure 5.4 presents the leukemic population dynamics for the simulation results and the clinical data available. Moreover, Table 5.4 lists the leukemic population numbers for the simulation and the available clinical data.

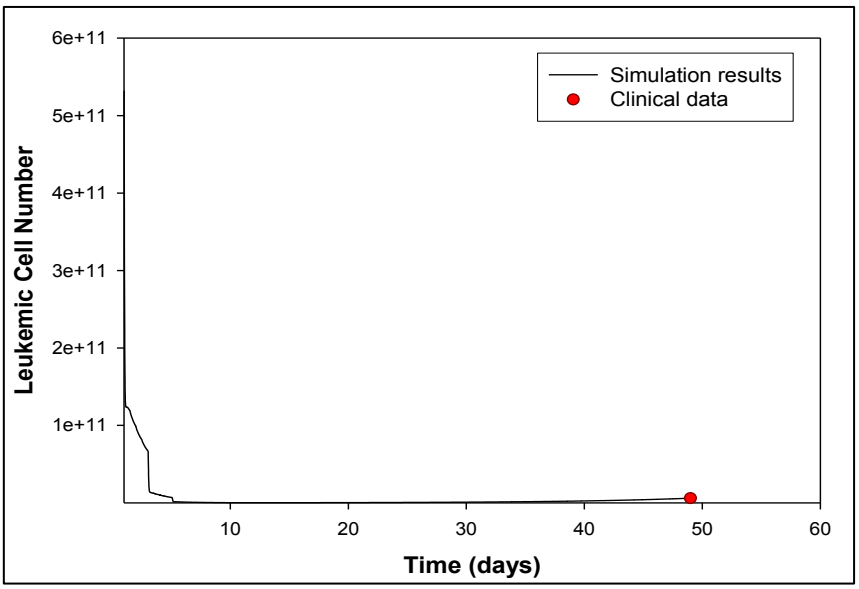

Figure 5.4: Comparison of simulation results and clinical data for Patient P011

Table 5.4: Leukemic population of Patient P011 based on model analysis and clinical data

Date	Leukemic Population (model)	Leukemic Population (data)
1st cycle start date: Day 1	$5.32 \cdot 10^{11}$ cells	
1st cycle end date: Day 10	$1.62 \cdot 10^{8}$ cells	
BM Aspirate after 1st Cycle Day 48	$6.06 \cdot 10^{9}$ cells	$6 \cdot 10^{9}$ cells

5.3.5 Cell cycle estimation for Patient P016

P016 is the 5th patient case study. P016 is a male patient with a diagnosis of secondary AML. Physiological characteristics are 80 years old, 167.5 cm height and 79.3kg. BM aspirate

shows a leukemic blast percentage of 90% and the treatment for this patient is a combination of the DA and LDAC treatment protocols, due to complications during treatment. Specifically, treatment design combined one cycle of the DA protocol as the 1st chemotherapy cycle and one cycle of LDAC as the 2nd and last cycle for this patient case. The patient responded well to the induction treatment as blast percentage reduced to 1% after the 1st cycle and after the 2nd cycle leukemic population was maintained at 1% with a lower cellularity factor. Although the disease was reduced BM hypoplasia was not achieved for this patient.

The fitted cell cycle times for the one cycle this patient received are listed in Table 5.7. Ts duration is fitted to 10 hrs and the whole cell cycle duration is fitted to 54 hrs. For the 2nd chemotherapy cycle, Ts is fitted to 14 hrs and the whole cell cycle duration to 45 hrs. Figure 5.5 presents the leukemic population dynamics for the simulation results and the clinical data available. Moreover, Table 5.5 lists the leukemic population numbers for the simulation and the available clinical data.

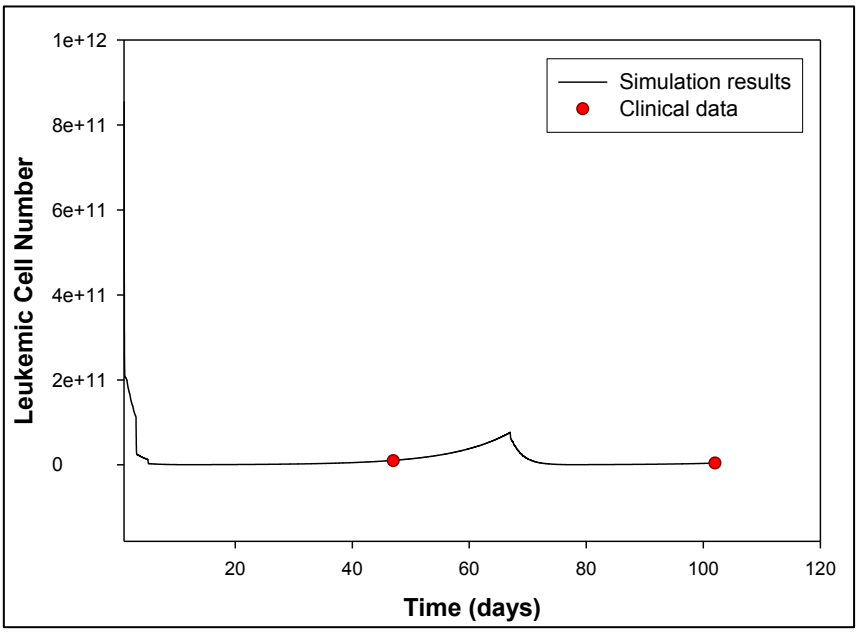

Figure 5.5: Comparison of simulation results and clinical data for Patient P016.

Table 5.5: Leukemic population of Patient P016 based on model analysis and clinical data

Date	Leukemic Population (model)	Leukemic Population (data)
1st cycle start date: Day 1	$8.55 \cdot 10^{11}$ cells	
1st cycle end date: Day 10	$3.29 \cdot 10^{8}$ cells	
BM Aspirate after 1st Cycle Day 45	$9.46 \cdot 10^{9}$ cells	$9.5 \cdot 10^{9}$ cells
2nd cycle start date: Day 66	$7.62 \cdot 10^{10}$ cells	
2nd cycle end date: Day 76	$3.96 \cdot 10^{8}$ cells	
BM Aspirate after 2nd Cycle Day 101	$4 \cdot 10^{9}$ cells	$4 \cdot 10^{9}$ cells

5.3.6 Cell cycle estimation for patient P026

Lastly, the last patient case is patient P026. This patient is a female patient 45 years old, of 169.3 cm height and 94.8 kg weight. The patient is diagnosed with *de novo* AML and a blast percentage of 71% is reported at diagnosis. P026 received two chemotherapy cycles of the DA protocol. The 1st cycle combined doses of 80 mg/m^2 of Ara-C applied twice a day as iv applications for 10 days, with doses of 70 mg/m^2 of DNR applied on days 1, 3 and 5. Reduced toxicity is applied on the 2nd chemotherapy cycle for which same dose of Ara-C is applied but for 8 days duration and also the dose of DNR is reduced to 40 mg/m^2 applied same days as for the 1st chemotherapy cycle. This patient had a successful treatment outcome as BM hypoplasia is achieved from the 1st chemotherapy cycle and maintained after the 2nd chemotherapy cycle.

For the 1st chemotherapy cycle, the S-phase duration of the leukemic population is fitted to 15 hrs and the whole cell cycle duration to 47 hrs. Moreover, for the 2nd chemotherapy cycle the fitted cell cycle times are 15 hrs duration for S-phase and 40 hrs for the whole cell cycle. Figure 5.6 presents the leukemic cell dynamics compared with the clinical data for the full length treatment of this patient and Table 5.6 lists the leukemic population cell number and the clinical data for all the chemotherapy cycles.

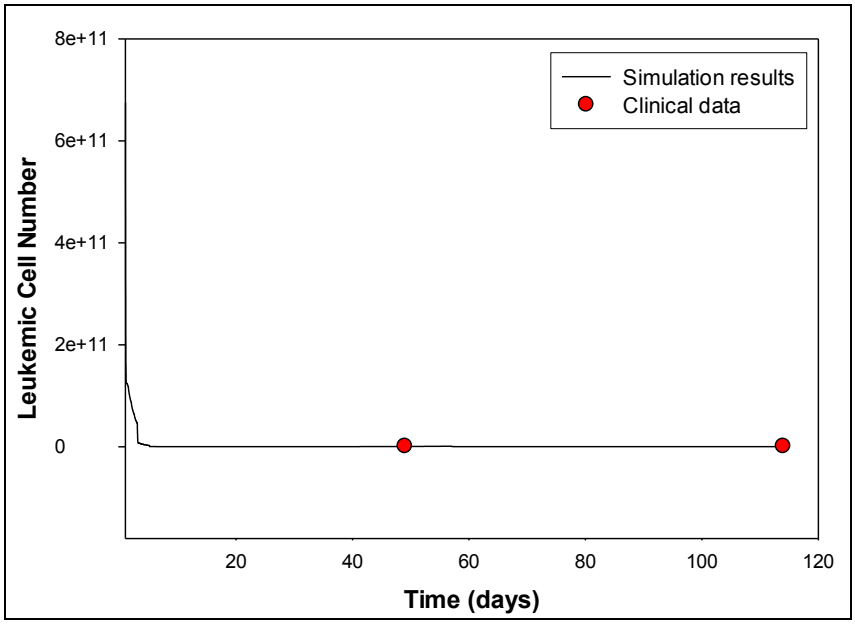

Figure 5.6: Comparison of simulation results and clinical data for Patient P026

Table 5.6: Leukemic population of Patient P026 based on model analysis and clinical data

Date	Leukemic Population (model)	Leukemic Population (data)
1st cycle start date: Day 1	$6.75 \cdot 10^{11}$ cells	
1st cycle end date: Day 10	$1.24 \cdot 10^{7}$ cells	
BM Aspirate after 1st Cycle Day 48	$4.7 \cdot 10^{8}$ cells	$<1 \cdot 10^{9}$ cells
2nd cycle start date: Day 56	$1.05 \cdot 10^{9}$ cells	
2nd cycle end date: Day 64	$3.8 \cdot 10^{4}$ cells	
BM Aspirate after 2nd Cycle Day 116	$2 \cdot 10^{6}$ cells	$<1 \cdot 10^{9}$ cells

Table 5.7: Cell cycle times fitted for the clinical data of 6 patients undergoing LDAC and DA protocols (Appendix B)

	Patient number	Ts (hrs)*	Tc (hrs)*
Patients under LD protocol			
	001 (1st cycle)	13	45
	001 (2nd cycle)	16	40
	001 (3rd cycle)	11	45
	001 (4th cycle)	18	65
	002 (1st cycle)	21	45
	006 (1st cycle)	20	33
	006 (2nd cycle)	14	46
	006 (3rd cycle)	14	68
	006 (4th cycle)	20	40
	016 (2nd cycle)	14	45
Patients under DA protocol			
	011 (1st cycle)	9	53
	026 (1st cycle)	15	47
	026 (2nd cycle)	15	40
	016 (1st cycle)	10	54
mean		**15**	**47.5**
range		**(9 – 21)**	**(33 – 68)**

The results show inter- and intra-patient variability of the cycling times that are different between patients and between the chemotherapy cycles of the same patient. The mean calculated time for Ts is 15 hrs with a range between (9 -21) hrs and for Tc the mean value is 47.5 hrs with variability within (33 – 68) hrs.

Another observation from the fitted cell cycle results is that the longer Tc times were indicative of disease relapse (P001 4^{th} cycle, P006 3^{rd} cycle). This relation between Tc and disease increase has a scientific explanation as the longer cycling times are indicative of longer GoG_1-phase. It is well-reported (Lewin et al., 2007; Komarova, Wodarz, 2005; Michor, 2008) that GoG_1-phase is a factor related to disease resistance and relapse since cells in this phase are not affected by the drugs and they form residual disease after treatment completion. The reverse relationship was observed for Ts time where the longer Ts indicated lower numbers of leukemic cells. The longer S-phase duration is linked to a higher percentage of cells in this phase that respectively increases the probability of the leukemic cells to be affected and eradicated by anti-leukemic S-phase specific drugs as DNR and Ara-C.

Moreover, a very interesting point in the cell cycle distributions is that patients successfully treated under the LDAC protocol are characterised by a shorter Tc duration as compared with patients undergoing DA protocol. An interesting fact in clinical practice is that patients who receive a low dose of sc treatment may present as good treatment results (that is, induction of remission) as do patients who receive much higher doses of DNR and Ara-C intravenously administered and who undergo greater toxicity. In order to capture this fact, the model uses a lower duration of non-proliferating phase for the cases of patients with successful results of low dose Ara-C treatment. Physically, this means that for a patient to be successfully treated by a low dose treatment an explanatory scenario is that the majority of his/her cells will be in proliferation, thus, susceptible to the drug.

5.4 Optimal induction treatment design for the studied patients

The aim of remission induction therapy described by the current presented model is to achieve the rapid restoration of normal BM function. By treatment completion, the leukemic population should be reduced to a level of approximately 10^9 cells at which point BM hypoplasia is achieved. Moreover, the normal population should be higher than that of the leukemic population and a 3-log reduction is the maximum permissible level of normal population reduction. This optimisation problem is formulated and solved for the patient case studies who failed the induction treatment according to the provided clinical data i.e. P001, P002, P011, P016, for the case of the DA and LDAC protocols, as well as for the patients

with acceptable treatment outcome for whom the optimisation objective is to seek an alternative and optimal dosing schedule.

The required information for each patient case study is the physiological patient characteristics and tumour characteristics (initial tumour burden) which are clinically provided. Moreover, the cell cycle kinetic information of the S-phase and total cycle duration is required which is estimated using the available clinical data and the parameters for each patient are listed in Table 5.7 in the previous section.

For iv Ara-C, total drug administration is set between 50mg – 4000mg, with infusion duration between 1 min to 24 hours. The window for DNR dose optimisation is stricter due to potential toxic effects and the only independent variable is dose with 30mg – 90mg per infusion. For sc Ara-C, the maximum dose per day is 40mg and doses are permitted up to four times daily for a maximum period of 20 days (BC cancer agency, 2007; Milligan et al, 2006).

This optimisation problem was formed and solved using gPROMS (gPROMS, 2003) and the optimised treatment protocols for the six studied patient case studies are presented and analysed below.

5.4.1 Optimal personalised chemotherapy protocol for Patient P001

P001 is a patient case study treated with LDAC protocol. Treated according to standard clinical practice, this patient's disease burden decreased over the first 3 chemotherapy cycles. However, over the last cycle there is disease relapse and at the point of the BM aspirate done at treatment completion, leukemic cells are as high as at diagnosis. For this patient, the optimisation problem is solved and results are listed below for all chemotherapy cycles.

1st Chemotherapy Cycle

The optimisation problem for this patient is solved and the suggested protocol for the four chemotherapy cycles is to administer 40 mg of Ara-C as daily continuous infusions for 10 days (Table 5.8). Over this optimal protocol, the total dose will be constant but the dose schedule will differ.

Although the same total dose is used per cycle the optimised protocol succeeds in further reducing the leukemic population. Specifically, after the 1st chemotherapy cycle, the leukemic

population is further reduced by $6.25 \cdot 10^9$ cells and the population equals $3.7 \cdot 10^9$ cells. This reduced population is less than that of the normal population with a difference of $1 \cdot 10^8$ cells (Figure 5.7).

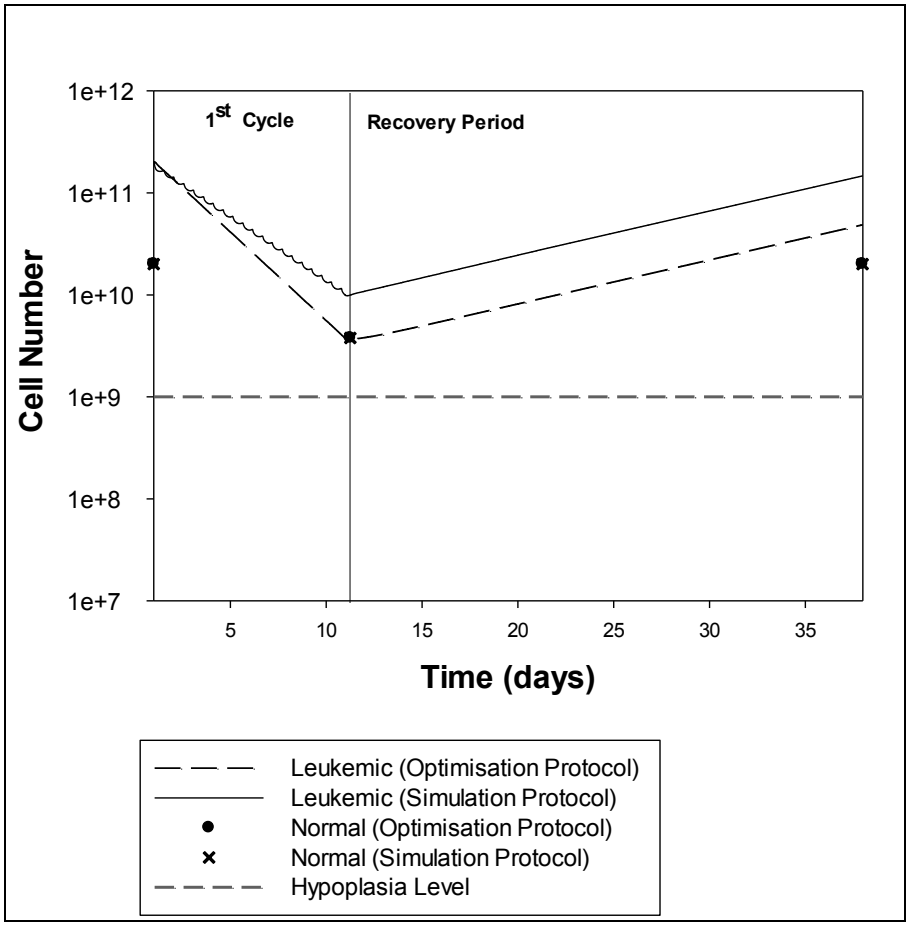

Figure 5.7: Patient P001 behaviour over the 1st chemotherapy cycle (days 1-11) and the recovery period afterwards (days 11-38) for the simulation and optimisation chemotherapy protocols. The dashed line is for the leukemic cell population over the optimised protocol; the straight black line is for the leukemic cell over the simulation of the clinical applied protocol; the circle signs are for the normal population at the start and end date of the optimisation protocol; the x signs are for the normal population at the start and end date of the simulation protocol and the grey line represents the BM hypoplasia objective.

Table 5.8: Optimal LDAC induction treatment protocol for Patient P001

Protocol	Dose Load	Dose Duration	Application route	Application Schedule
SC Ara-C				
1st Cycle	40 mg	24-hr	SC	One daily application for days 1-10
2nd Cycle	40 mg	24-hr	SC	One daily application for days 1-10
3rd Cycle	40 mg	24-hr	SC	One daily application for days 1-10
4th Cycle	40 mg	24-hr	SC	One daily application for days 1-10

2nd Chemotherapy Cycle

The leukemic population is increased to $4.86 \cdot 10^{10}$ cells after completion of the 1st chemotherapy cycle due to the necessary recovery period with no treatment between the two cycles. This population is decreased over the 2nd optimised chemotherapy with daily infusional doses of 40 mg for 10 days. Leukemic cells are further decreased in the optimal protocol compared with that of the simulation protocol and for the optimal schedule, the level of leukemic cells is below the hypoplasia level (figure 5.8). In particular, at the end of the 2nd cycle, the leukemic and normal populations have $9.34 \cdot 10^{7}$ and $3.8 \cdot 10^{9}$ cells respectively..

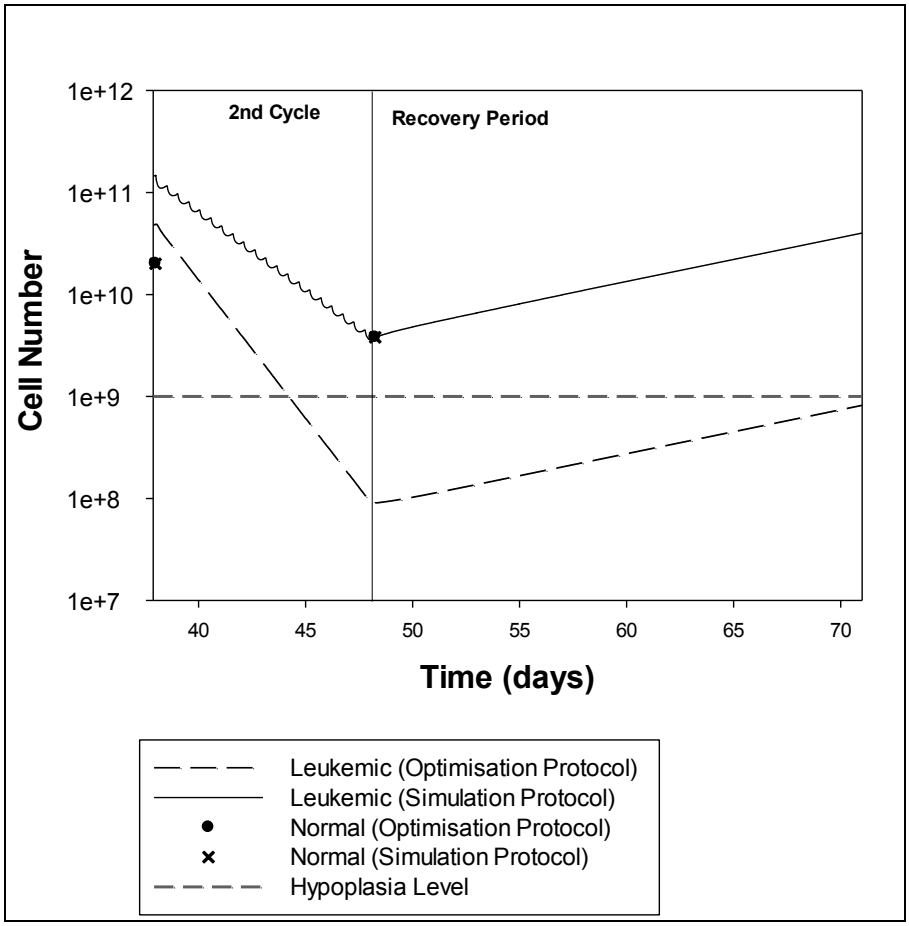

Figure 5.8: Patient P001 behaviour over the 2nd chemotherapy cycle (days 38-48) and the recovery period afterwards (days 38-71) for the simulation and optimisation chemotherapy protocols. The dashed line is for the leukemic cell population over the optimised protocol; the straight black line represents leukemic cells over the simulation of the clinically applied protocol; the circle signs are for the normal population at the start and end date of the optimisation protocol; the x signs are for the normal population at the start and end date of the simulation protocol and the grey line represents the BM hypoplasia objective.

3rd Chemotherapy Cycle

Figure 5.9 illustrates the cell population dynamics over the simulation and optimisation of the 3rd chemotherapy cycle. For the simulation protocol, the leukemic population is reduced but is higher than that of the normal population indicating that the cycle purpose is not achieved. Moreover, BM hypoplasia is not achieved as cells are above the $1 \cdot 10^9$ cells target. In contrast, over the optimisation cycle, the leukemic population is further reduced and is lower than the hypoplasia level for the whole length of the treatment and interval period. At cycle completion, the leukemic population equals $3.68 \cdot 10^7$ cells and the normal population is $3.8 \cdot 10^9$ making a 2-log difference between the 2 populations.

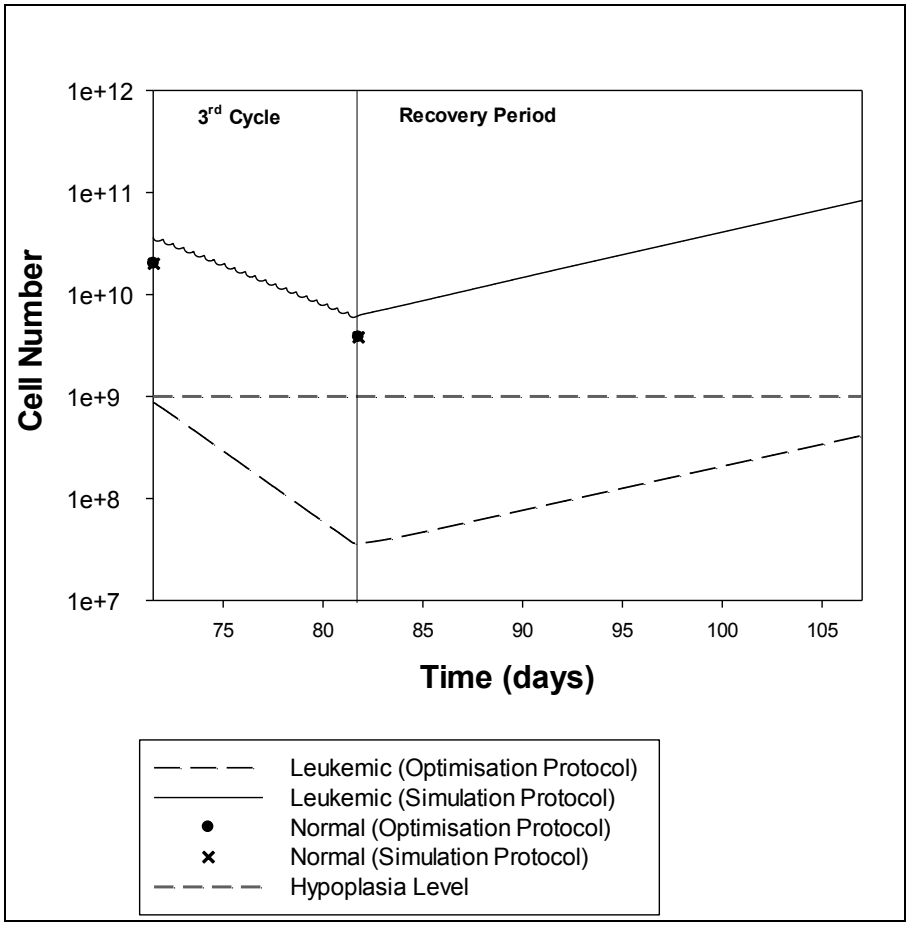

Figure 5.9: Patient P001 behaviour over the 3rd chemotherapy cycle (days 71-81) and the recovery period afterwards (days 81-107) for the simulation and optimisation chemotherapy protocols. The dashed line represents the leukemic cell population over the optimised protocol; the straight black line represents the leukemic cells over simulation of the clinically applied protocol; the circle signs are for the normal population at the start and end date of the optimisation protocol; the x signs are for the normal population at the start and end date of the simulation protocol and the grey line represents the BM hypoplasia objective

4th Chemotherapy Cycle

Figure 5.10 presents the normal and leukemic cell population dynamics after the simulation and optimisation chemotherapy protocol for the last cycle. Over the optimisation protocol, patient treatment outcome is much improved and induction treatment is successful, whereas treatment relapse is noted over the simulation protocol. In particular, over the simulation protocol, the leukemic population is higher than that of the normal and higher than the BM hypoplasia level. At simulation treatment completion, the leukemic population equals $6.7 \cdot 10^9$ cells. However, after the optimisation chemotherapy protocol, the leukemic population is

further decreased and equals $1.53 \cdot 10^7$ cells. This population is lower than the desired hypoplasia level and also lower than the normal population that equals $3.8 \cdot 10^9$ cells.

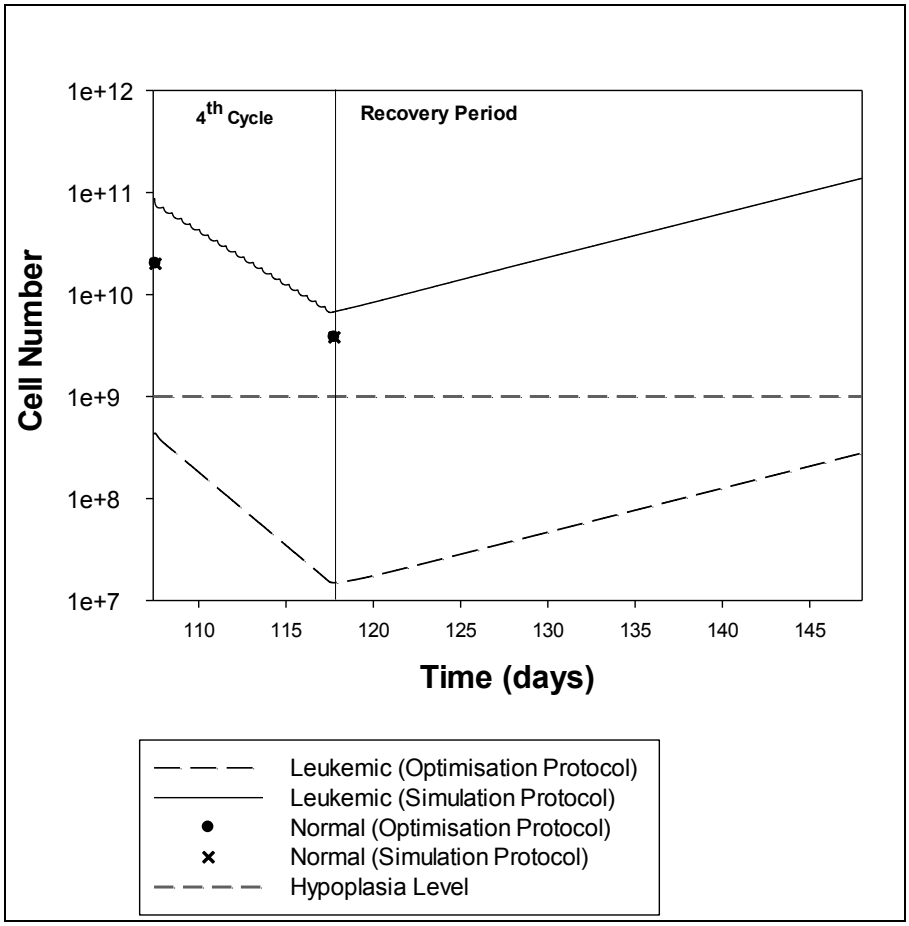

Figure 5.10: P001 behaviour over the 4th chemotherapy cycle (days 107-117) and the recovery period before the last BM aspirate (days 117-150). The dashed line represents the leukemic cell population over the optimised protocol; the straight black line represents the leukemic cells during simulation of the clinically applied protocol; the circle and x signs are for the normal population at the start and end date of the optimisation and the simulation protocol, respectively.

In summary, for P001, the same total dose is used per cycle for the optimised protocol that suggests total doses of 40 mg applied as daily 24 hour sc infusions for 10 days instead of 2 daily sc bolus doses of 20 mg applied over the clinically applied protocol. This optimisation protocol succeeds in further reducing the leukemic population. Specifically, after the 1st chemotherapy cycle, the leukemic population is further reduced by $6.25 \cdot 10^9$ cells. This reduced population is less than the normal population with a difference of $1 \cdot 10^8$ cells. The reduced leukemic population at completion of the 1st cycle successively affects the initial state of the 2nd cycle, that is $4.86 \cdot 10^{10}$ cells instead of $1.47 \cdot 10^{11}$ cells that was obtained during

the simulation results. This reduced population will be further reduced over the remaining chemotherapy cycles. By treatment completion, the leukemic population equals $2.9 \cdot 10^8$ cells that is less than the level of BM hypoplasia, equal to $1 \cdot 10^9$ cells, the objective of induction treatment. In contrast, over the simulation results disease relapse is noticed and the leukemic population increased to its initial state at diagnosis. Figure 5.11 presents the comparison of the simulation and optimisation protocols for the full course of treatment and Table 5.9 lists the leukemic and normal cell numbers for each chemotherapy cycle.

Table 5.9: Leukemic and normal cell populations for P001, over the simulation and optimisation treatment protocols

Date	Leukemic population over simulation	Normal population over simulation	Leukemic population over optimisation	Normal population over optimisation
Beginning of 1st cycle	$2 \cdot 10^{11}$	$2 \cdot 10^{10}$	$2 \cdot 10^{11}$	$2 \cdot 10^{10}$
End of 1st cycle	$9.95 \cdot 10^9$	$3.8 \cdot 10^9$	$3.7 \cdot 10^9$	$3.8 \cdot 10^9$
Beginning of 2nd cycle	$1.47 \cdot 10^{11}$	$2 \cdot 10^{10}$	$4.86 \cdot 10^{10}$	$2 \cdot 10^{10}$
End of 2nd cycle	$3.8 \cdot 10^9$	$3.8 \cdot 10^9$	$9.34 \cdot 10^7$	$3.8 \cdot 10^9$
Beginning of 3rd cycle	$3.8 \cdot 10^{10}$	$2 \cdot 10^{10}$	$8.6 \cdot 10^8$	$2 \cdot 10^{10}$
End of 3rd cycle	$6.13 \cdot 10^9$	$3.8 \cdot 10^9$	$3.68 \cdot 10^7$	$3.8 \cdot 10^9$
Beginning of 4th cycle	$8.7 \cdot 10^{10}$	$2 \cdot 10^{10}$	$4.35 \cdot 10^8$	$2 \cdot 10^{10}$
End of 4th cycle	$6.7 \cdot 10^9$	$3.8 \cdot 10^9$	$1.53 \cdot 10^7$	$3.8 \cdot 10^9$
BM aspirate after 4th cycle	$1.44 \cdot 10^{11}$		$2.9 \cdot 10^8$	

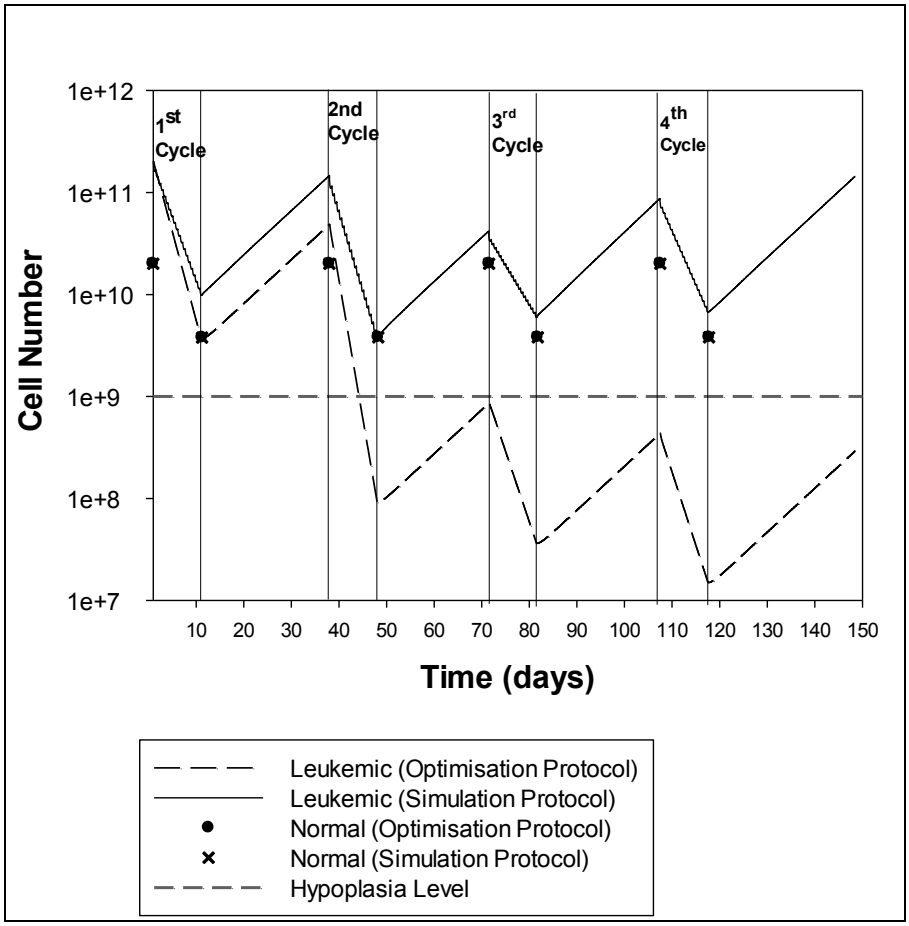

Figure 5.11: Patient P001 behaviour for the full course of treatment over the simulation and optimisation chemotherapy protocols. The dashed line represents the leukemic cell population over the optimised protocol; the straight black line represents leukemic cells during simulation of the clinically applied protocol; the circle signs are for the normal population at the start and end date of the optimisation protocol; the x signs are for the normal population at the start and end date of the simulation protocol and the grey line represents the BM hypoplasia objective

5.4.2 Optimal personalised chemotherapy protocol for Patient P002

P002 is a patient case study treated with the LDAC protocol. For this patient, data are available only for the 1st chemotherapy cycle (Appendix B). Over this cycle, leukemic cells are decreasing and by cycle completion, normal cells are higher than leukemic cells as shown in the simulation results in Table 5.2. The optimisation problem for this case study would be to possibly achieve BM hypoplasia from the 1st chemotherapy cycle.

This optimisation problem is solved and the protocol suggests 40 mg of Ara-C as daily 24 hour continuous infusions sc for 13 days (Table 5.10).

Table 5.10: Optimal LDAC induction treatment protocol for Patient P002

Protocol	Dose Load	Dose Duration	Application route	Application Schedule
SC Ara-C				
1st Cycle	40 mg	24-hr	SC	One daily application for days 1-13

This protocol suggests an increase of the total dose by 120 mg (i.e. total dose of 520 mg). This increased dose load and the optimal continuous drug schedule results in a further reduction of the leukemic population (Figure 5.12). Specifically, a further reduction of the leukemic population is achieved with a difference of $5.6 \cdot 10^8$ cells (Table 5.11). The normal population is reducing as well and there is a cost of $1.2 \cdot 10^9$ cells less over the optimised protocol. However, BM hypoplasia is achieved with $1 \cdot 10^9$ cells making a difference of $3.68 \cdot 10^{10}$ cells less when compared with that of the simulation results (Table 5.11).

Table 5.11: Leukemic and normal cell populations for P002, over the simulation and optimisation induction treatment protocols

Date	Leukemic population over simulation	Normal population over simulation	Leukemic population over optimisation	Normal population over optimisation
Beginning of 1st cycle	$7.9 \cdot 10^{11}$	$1.68 \cdot 10^{10}$	$7.9 \cdot 10^{11}$	$1.68 \cdot 10^{10}$
End of 1st cycle	$8.6 \cdot 10^8$	$3.2 \cdot 10^9$	$3 \cdot 10^8$	$2 \cdot 10^9$
BM aspirate after 1st cycle	$3.78 \cdot 10^{10}$		$1 \cdot 10^9$	

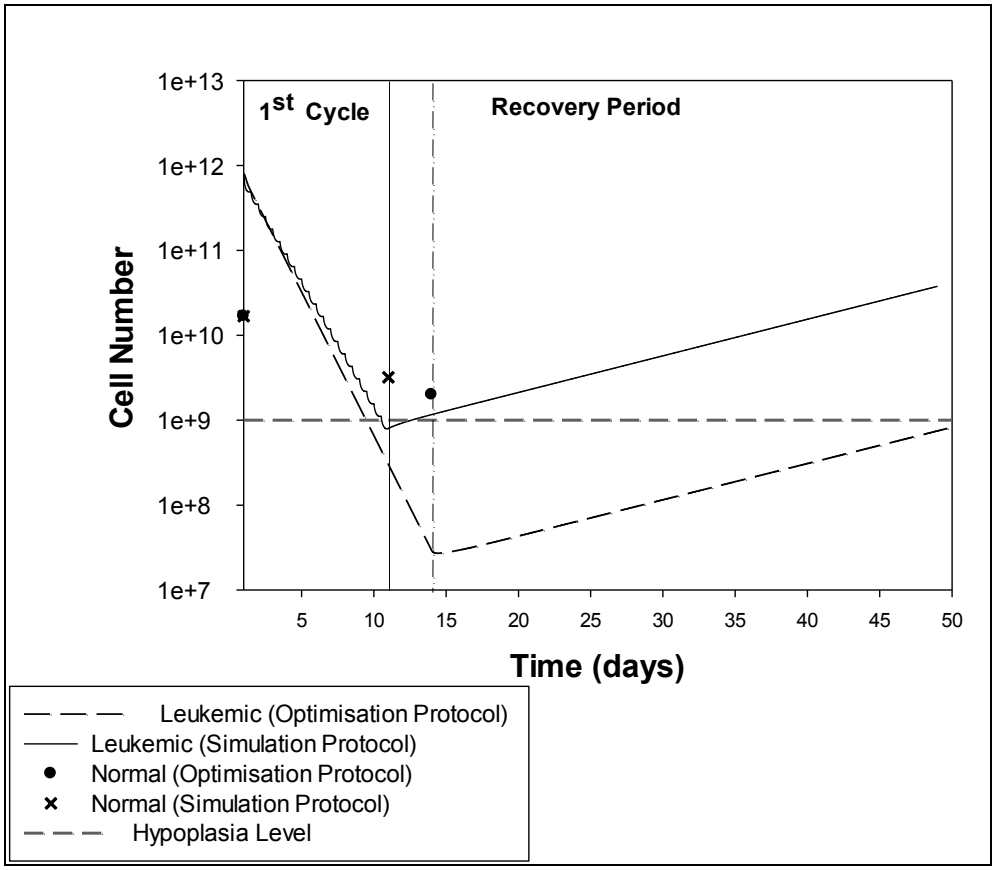

Figure 5.12: Patient P002 behaviour for the full length treatment over the simulation and optimisation chemotherapy protocols. Duration of the simulation protocol is 10 days from days (1-11) and the end is indicated by a vertical straight line. The vertical dashed line indicates the end of the optimisation cycle with 13 days duration. The dashed line represents the leukemic cell population over the optimised protocol; the straight black line represents leukemic cells during the simulation of the clinically applied protocol; the circle signs are for the normal population at the start and end date of the optimisation protocol; the x signs are for the normal population at the start and end date of the simulation protocol and the grey line represents the BM hypoplasia objective

5.4.3 Optimal personalised chemotherapy protocol for Patient P006

P006 has a successful treatment outcome with the LDAC protocol. This patient presents a 3-log leukemic population reduction over the 1st chemotherapy cycle where leukemic cells are reduced to $2.15 \cdot 10^8$ cells and the normal population is reduced to $5 \cdot 10^9$ cells. Therefore, treatment is effective from the 1st cycle since leukemic cells are below the desired hypoplasia level and below the normal population level. For the succeeding three chemotherapy cycles, the leukemic population is further reduced and by the time of the BM aspirate after the 4th

chemotherapy cycle, the leukemic population equals $9.7 \cdot 10^8$ cells which is close to, but less than, the desired hypoplasia level.

Since, treatment is successful for this patient, the objective of the optimisation is to optimise the treatment schedule while keep the same total drug load as that used in the clinically applied protocol i.e. 40 mg of sc Ara-C daily for 10 days. As in the case of the previously optimised patients undergoing LDAC treatment, the optimisation results suggest that for the 4 chemotherapy cycles a daily sc continuous infusion of 40 mg for 10 days is ideal (Table 5.12).

Table 5.12: Optimal LDAC induction treatment protocol for Patient P006

Protocol	Dose Load	Dose Duration	Application route	Application Schedule
SC Ara-C				
1st Cycle	40 mg	24-hr	SC	One daily application for days 1-10
2nd Cycle	40 mg	24-hr	SC	One daily application for days 1-10
3rd Cycle	40 mg	24-hr	SC	One daily application for days 1-10
4th Cycle	40 mg	24-hr	SC	One daily application for days 1-10

Table 5.13: Leukemic and normal cell populations for P006, over the simulation and optimisation induction treatment protocols

Date	Leukemic population over simulation	Normal population over simulation	Leukemic population over optimisation	Normal population over optimisation
Beginning of 1st cycle	$3.4 \cdot 10^{11}$	$2.64 \cdot 10^{10}$	$3.4 \cdot 10^{11}$	$2.64 \cdot 10^{10}$
End of 1st cycle	$2.15 \cdot 10^{8}$	$5 \cdot 10^{9}$	$6.9 \cdot 10^{6}$	$5 \cdot 10^{9}$
Beginning of 2nd cycle	$6.13 \cdot 10^{9}$	$2.64 \cdot 10^{10}$	$1.55 \cdot 10^{8}$	$2.64 \cdot 10^{10}$
End of 2nd cycle	$6.4 \cdot 10^{8}$	$5 \cdot 10^{9}$	$3.1 \cdot 10^{6}$	$5 \cdot 10^{9}$
Beginning of 3rd cycle	$5.87 \cdot 10^{9}$	$2.64 \cdot 10^{10}$	$2.56 \cdot 10^{7}$	$2.64 \cdot 10^{10}$
End of 3rd cycle	$1.46 \cdot 10^{9}$	$5 \cdot 10^{9}$	$2.5 \cdot 10^{6}$	$5 \cdot 10^{9}$
Beginning of 4th cycle	$1.89 \cdot 10^{10}$	$2.64 \cdot 10^{10}$	$3 \cdot 10^{7}$	$2.64 \cdot 10^{10}$
End of 4th cycle	$6.77 \cdot 10^{7}$	$5 \cdot 10^{9}$	8641	$5 \cdot 10^{9}$
BM aspirate after 4th cycle	$9.7 \cdot 10^{8}$		$1.05 \cdot 10^{5}$	

Table 5.13 lists the leukemic and normal population cell number throughout the simulation and optimisation protocols and figure 5.13 presents the cell dynamics over the two protocols (simulation and optimisation).

At the end of the 1st chemotherapy cycle using the optimisation protocol, the leukemic population is further reduced to $6.9 \cdot 10^6$ cells, making a difference of $2.08 \cdot 10^8$ cells less compared with that of the simulation protocol. In contrast, the normal population is similar under both the simulation and the optimisation protocol. This is a result noted and explained for all the previous patient case studies for which no increase of dose load was suggested. This is due to the assumption made for the normal cell population that the majority of cells exist in the non-proliferating state with the ability to enter the cell proliferation state when population depletion occurs. For the cases when the same dose load is administered with changed schedule, proliferating cells will reduce more quickly but non-proliferating cells will replace this loss. Thus difference in the population of normal cells is noticed only for a different dose load.

After, the interval period, the leukemic population is increased and equals $1.55 \cdot 10^8$ cells for the optimisation case, whereas the normal population is equal to the initial population (at diagnosis) since full population recovery is assumed for the interval period. During the 2nd chemotherapy cycle, the leukemic population is reduced and at cycle completion equals $3.1 \cdot 10^6$ cells, that is $6.4 \cdot 10^8$ cells less compared with that of the simulation protocol. The reduced leukemic population combined with successive rounds of optimal chemotherapy cycles results in a difference in the initiating leukemic population burden at the beginning of the 3rd chemotherapy cycle. For the optimisation protocol, the leukemic cell population equals $2.56 \cdot 10^7$ cells, whereas for the simulation protocol it is $5.87 \cdot 10^9$ cells. At completion of the optimisation cycle, the leukemic population for the optimisation protocol equals $2.5 \cdot 10^6$ cells making a difference of $1.45 \cdot 10^9$ cells compared with that of the simulation protocol. By completion of the 4th and last chemotherapy cycle, the leukemic population equals 8641 cells for the optimisation protocol and $6.8 \cdot 10^7$ for the simulation protocol. Moreover, at the last BM aspirate sample analysis, the leukemic population will be $1.05 \cdot 10^5$ cells for the optimisation protocol and $9.7 \cdot 10^8$ cells for the simulation protocol. This difference in the cell population is impressive especially if we consider that the same dose load is applied with a different dosing schedule and demonstrates the usefulness of optimisation technique for treatment design. Comparison of P006 cell dynamics for the two protocols is illustrated in figure 5.13.

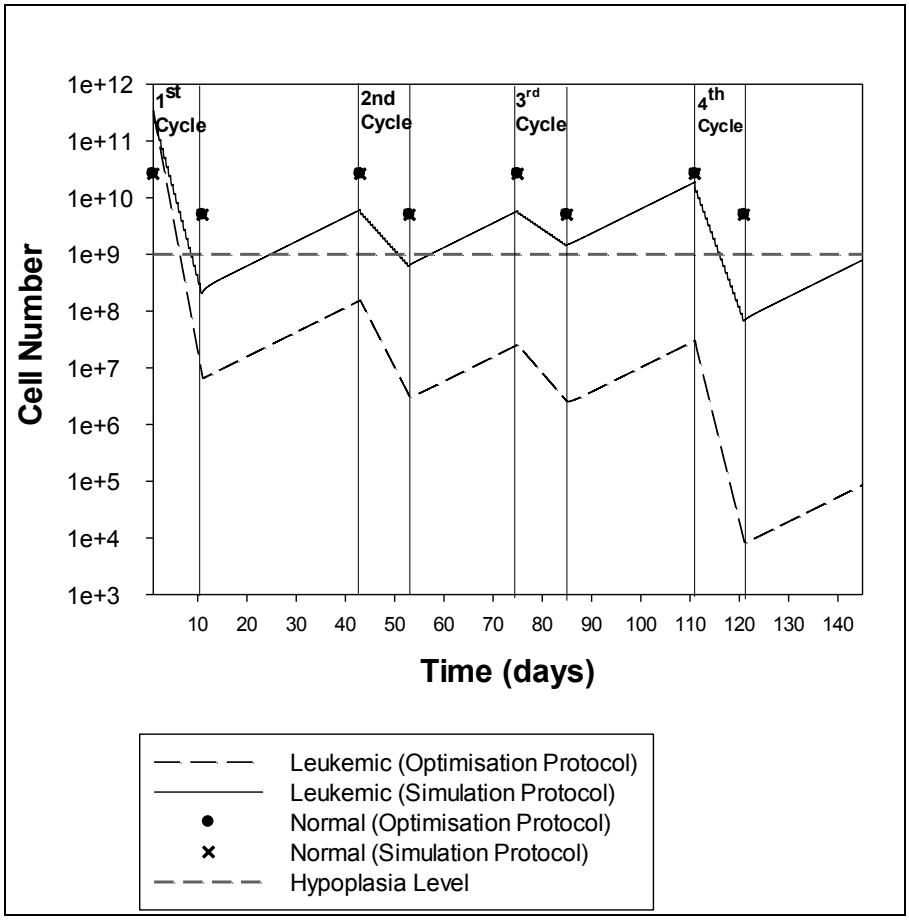

Figure 5.13: Patient P006 behaviour for the full length treatment over the simulation and optimisation chemotherapy protocols. The dashed line represents the leukemic cell population over the optimised protocol; the straight black line represents leukemic cells during simulation of the clinically applied protocol; the circle signs are for the normal population at the start and end date of the optimisation protocol; the x signs are for the normal population at the start and end date of the simulation protocol and the grey line represents the BM hypoplasia objective

5.4.4 Optimal personalised chemotherapy protocol for Patient P011

Patient 011 is a patient case study treated with the DA protocol and results of the 1st chemotherapy cycle are only available for model analysis. As shown in the simulation results (Table 5.15), with the clinically applied protocol, this patient case study shows reduction of the leukemic population and leukemic cells are less than normal cells. The optimisation problem for this case study is to further minimise the leukemic population in order to reach BM hypoplasia from the 1st chemotherapy cycle. This problem is solved and the optimal protocol suggests 250 mg/m^2 of continuous daily iv infusions of Ara-C for 10 days combined with 90 mg/m^2 of DNR administered as bolus doses on days 1,3 and 5 (Table 5.14).

Table 5.14: Optimal DA induction treatment protocol for Patient P011

Protocol	Dose Load	Dose Duration	Application route	Application Schedule
DA protocol				
DNR	90 mg/m^2	1 hr	IV	One daily applications on days 1, 3 and 5
Ara-C	250 mg/m^2	24-hr	IV	1 daily application, for days 1-10

This is a more toxic chemotherapy protocol as the daily amount of Ara-C is increased by 50 mg/m^2, which gives a total dose load increase of 500 mg/m^2 over 10 days and the total increase for DNR is 90 mg/m^2. By chemotherapy cycle completion over the optimised protocol, a further reduction of the leukemic population is achieved with a difference of $1.02 \cdot 10^8$ cells (Table 5.15). The normal population is reducing as well and there is a cost of $1.29 \cdot 10^8$ cells less over the optimised protocol. However, BM hypoplasia is achieved (figure 5.14) at the point of the BM aspirate where leukemic cells equal $1 \cdot 10^9$ cells and there is a difference of $5 \cdot 10^9$ cells less compared with that of the simulation results (Table 5.15).

Table 5.15: Leukemic and normal cell populations for P011, over the simulation and optimisation induction treatment protocols

Date	Leukemic population over simulation	Normal population over simulation	Leukemic population over optimisation	Normal population over optimisation
Beginning of 1st cycle	$5.32 \cdot 10^{11}$	$2.12 \cdot 10^{10}$	$5.32 \cdot 10^{11}$	$2.12 \cdot 10^{10}$
End of 1st cycle	$1.63 \cdot 10^{8}$	$3.79 \cdot 10^{8}$	$6.1 \cdot 10^{7}$	$2.5 \cdot 10^{8}$
BM aspirate after 1st cycle	$6 \cdot 10^{9}$		$1 \cdot 10^{9}$	

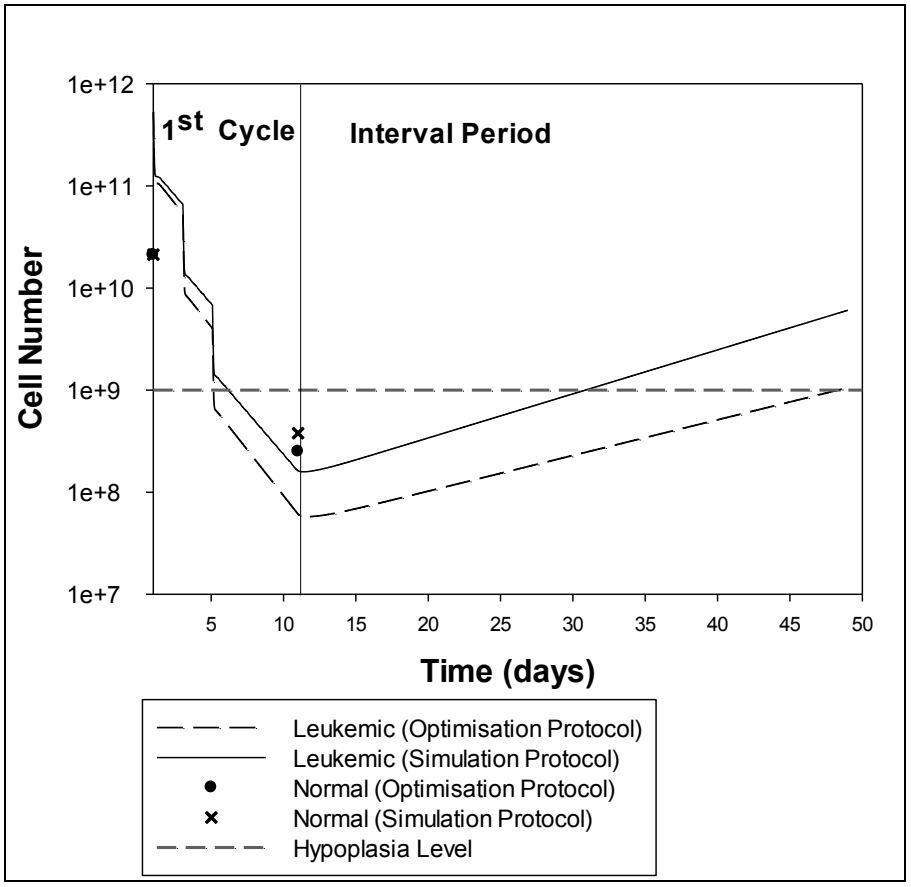

Figure 5.14: Patient P011 behaviour for the full length treatment over the simulation and optimisation chemotherapy protocols. The dashed line represents the leukemic cell population over the optimised protocol; the straight black line represents leukemic cells during simulation of the clinically applied protocol; the circle signs are for the normal population at the start and end date of the optimisation protocol; the x signs are for the normal population at the start and end date of the simulation protocol and the grey line represents the BM hypoplasia objective

5.4.5 Optimal personalised chemotherapy protocol for Patient P016

Patient 016 was treated with the DA protocol for the 1st chemotherapy cycle and with LDAC for the 2nd cycle due to clinical complications during treatment. As shown in the simulation results, this patient has a reduction of the leukemic burden from the 1st chemotherapy cycle and normal cells are higher than leukemic cells. However, by the completion of the 2nd cycle, residual disease exists and BM hypoplasia is not achieved. For this reason the optimisation problem is solved for both chemotherapy cycles.

1st Chemotherapy Cycle

For the 1st chemotherapy cycle, Ara-C is suggested to be continuously administered over 24 hour daily infusions iv. The total dose of Ara-C is kept constant to what was used in the simulation protocols i.e. 200 mg/m^2 daily dose load. For DNR the same schedule is followed with a dose increase to 90 mg/m^2 (Table 5.16).

Table 5.16: Optimal schedule of the 1st chemotherapy cycle for Patient P016

Protocol	Dose Load	Dose Duration	Application route	Application Schedule
DA protocol				
DNR	90 mg/m^2	1 hr	IV	One daily applications on days 1,3 and 5
Ara-C	200 mg/m^2	24-hr	IV	1 daily application, for days 1-10

Under this chemotherapy protocol, the leukemic population is further minimised and by completion of the 1st cycle, the leukemic population is $2.43 \cdot 10^8$ cells less with a cost of $2.3 \cdot 10^8$ normal cells (figure 5.15).

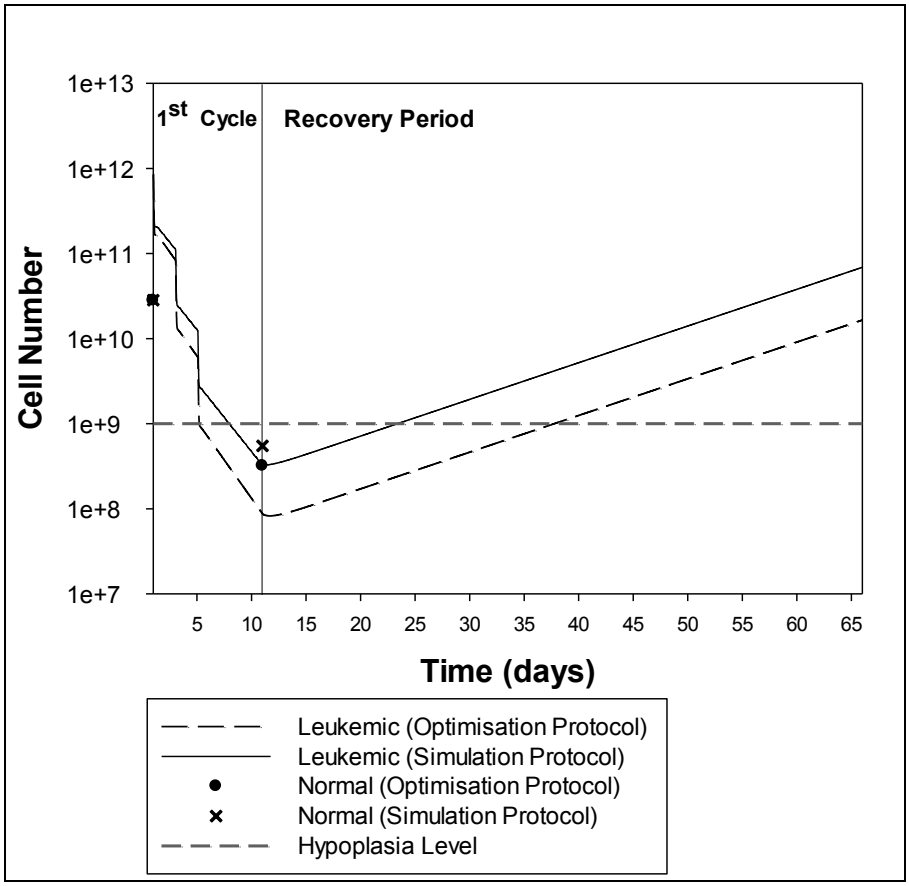

Figure 5.15: Patient P016 behaviour over the 1st chemotherapy cycle (days 1-11) and the recovery period prior the 2nd chemotherapy cycle (days 11-67). The dashed line represents the leukemic cell population over the optimised protocol; the straight black line represents leukemic cells during simulation of the clinically applied protocol; the circle signs are for the normal population at the start and end date of the optimisation protocol; the x signs are for the normal population at the start and end date of the simulation protocol and the grey line represents the BM hypoplasia objective

2nd Chemotherapy Cycle

For the 2nd chemotherapy protocol, the schedule suggested includes daily doses of 40 mg of Ara-C applied as daily 24 hour sc continuous infusions for 10 days (Table 5.17).

Table 5.17: Optimal LDAC induction treatment protocol for Patient P016

Protocol	Dose Load	Dose Duration	Application route	Application Schedule
SC Ara-C				
1st Cycle	40 mg	24-hr	SC	One daily application for days 1-10

Figure 5.16 presents the normal and leukemic cell dynamics. The leukemic population has a further decrease of $3.2 \cdot 10^8$ cells and the normal population remains at the same order of magnitude. This is expected if we consider that the normal population consists of proliferating cells susceptible to the treatment and quiescent cells serving as back-up cells at times of BM depletion. Since the transition rate of quiescent cells depends on the population depletion, the population will be adjusted to the loss and the transition rate will be adapted to keep the population constant. For the optimal protocol, since dose injection rate is lower and constant over the optimal treatment protocol, it will enable a constant transition of quiescent cells to enter proliferation that will result in a more rigid normal cell population recovery over this protocol. Moreover, by treatment completion, the leukemic population is reduced by $3.3 \cdot 10^9$ cells resulting in BM hypoplasia as the final population is lower than the $1 \cdot 10^9$ cells limit (Table 5.18).

Table 5.18: Leukemic and normal cell populations for P016, over the simulation and optimisation DA followed by LDAC treatment protocols

Date	Leukemic population over simulation	Normal population over simulation	Leukemic population over optimisation	Normal population over optimisation
Beginning of 1st cycle	$8.55 \cdot 10^{11}$	$2.83 \cdot 10^{10}$	$8.55 \cdot 10^{11}$	$2.83 \cdot 10^{10}$
End of 1st cycle	$3.29 \cdot 10^8$	$5.5 \cdot 10^8$	$8.6 \cdot 10^7$	$3.2 \cdot 10^8$
Beginning of 2nd cycle	$7.62 \cdot 10^{10}$	$2.83 \cdot 10^{10}$	$1.82 \cdot 10^{10}$	$2.83 \cdot 10^{10}$
End of 2nd cycle	$3.96 \cdot 10^8$	$5.39 \cdot 10^9$	$7.6 \cdot 10^7$	$5.35 \cdot 10^9$
BM aspirate after 2nd cycle	$4 \cdot 10^9$		$7 \cdot 10^8$	

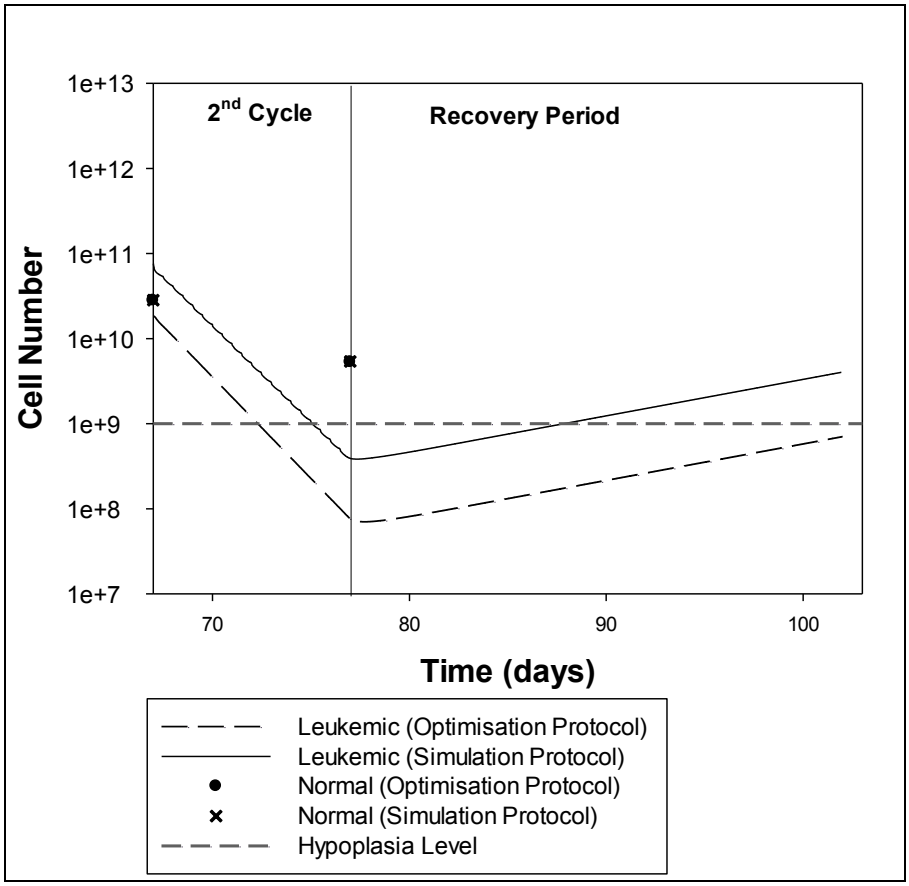

Figure 5.16: Patient P016 behaviour over the 2nd chemotherapy cycle (days 67-77) and the recovery period prior to the BM aspirate at treatment completion (days 77-100). The dashed line represents the leukemic cell population over the optimised protocol; the straight black line represents leukemic cells during simulation of the clinically applied protocol; the circle signs are for the normal population at the start and end date of the optimisation protocol; the x signs are for the normal population at the start and end date of the simulation protocol and the grey line represents the BM hypoplasia objective

5.4.6 Optimal personalised chemotherapy protocol for Patient P026

Patient 026 received two chemotherapy cycles of the DA protocol and had a successful treatment outcome. Specifically, this patient received one cycle of 10 days with rapid infusion boluses of 80 mg/m^2 of Ara-C twice a day for 10 days and doses of 70 mg/m^2 of DNR iv over 1 hour on days 1, 3 and 5. The 2nd chemotherapy cycle lasted for 8 days with doses of Ara-C 80 mg/m^2 administered every 12 hours iv bolus and a decreased dose of DNR equal to 40 mg/m^2 administered again on days 1, 3 and 5 by iv infusion over 1 hour. The leukemic population according to the clinical data is decreasing and by completion of the 2nd chemotherapy cycle BM hypoplasia is achieved. Since chemotherapy treatment is successful for this patient, the optimisation problem is to use the same dose load and propose the optimal treatment schedule. As in the previous patient case studies, the results of this optimisation problem suggest continuous dose administration of Ara-C by 24 hour infusion and the same 3 day iv schedule for DNR (Table 5.19).

Table 5.19: Optimal schedule of the full-length treatment for Patient P026

Protocol	Dose Load	Dose Duration	Application route	Application Schedule
1st Cycle				
DNR	70 mg/m^2	1 hr	IV	One daily applications on days 1,3 and 5
Ara-C	160 mg/m^2	24-hr	IV	1 daily application, for days 1-10
2nd Cycle				
DNR	40 mg/m^2	1 hr	IV	One daily applications on days 1,3 and 5
Ara-C	160 mg/m^2	24-hr	IV	1 daily application, for days 1-8

Table 5.20 below lists the leukemic and normal cell population in numbers during the simulation and the optimisation protocol, whereas figure 5.17 demonstrates the cell population dynamics during the two protocols.

Table 5.20: Leukemic and normal cell populations for P026, during the simulation and optimisation DA treatment protocols

Date	Leukemic population over simulation	Normal population over simulation	Leukemic population over optimisation	Normal population over optimisation
Beginning of 1st cycle	$6.75 \cdot 10^{11}$	$3.38 \cdot 10^{10}$	$6.75 \cdot 10^{11}$	$3.38 \cdot 10^{10}$
End of 1st cycle	$1.25 \cdot 10^{7}$	$4.52 \cdot 10^{8}$	$8.05 \cdot 10^{6}$	$4.52 \cdot 10^{8}$
Beginning of 2nd cycle	$1 \cdot 10^{9}$	$3.38 \cdot 10^{10}$	$2.66 \cdot 10^{8}$	$3.38 \cdot 10^{10}$
End of 2nd cycle	$3.8 \cdot 10^{4}$	$9.97 \cdot 10^{8}$	6030	$9.97 \cdot 10^{8}$
BM aspirate after the 2nd cycle	$2 \cdot 10^{6}$		$8.4 \cdot 10^{5}$	

As shown in figure 5.17, the optimisation protocol leads to a better treatment outcome compared with that of the simulation protocol. After the 1st chemotherapy protocol, the leukemic population is reduced to $8.05 \cdot 10^{6}$ cells, making a difference of $4.4 \cdot 10^{6}$ cells less than the clinically applied (simulation) protocol. Furthermore, the residual disease after the 2nd cycle with the optimisation protocol is 6030 cells and with the simulation is $3.8 \cdot 10^{4}$ cells. At the point of the BM aspirate after treatment completion, the leukemic population for the optimisation protocol is $8.4 \cdot 10^{5}$ cells making a difference of $1.16 \cdot 10^{6}$ cells less than the final outcome from the simulation protocol. As far as the normal population is concerned, the simulation and optimisation cycles present the same results. As explained earlier, the normal cell population is dose-dependent i.e. the population dynamics will differ for protocols of different toxicity and not for protocols with same dose load and different schedule of administration. This point is apparent in this patient case study where normal population dynamics differ between the simulation and optimisation results for the 1st chemotherapy cycle where there is a dose increase for the optimisation protocol. However, normal population results are the same for the simulation and optimisation of the 2nd chemotherapy cycle where the same dose load is applied under different schedule.

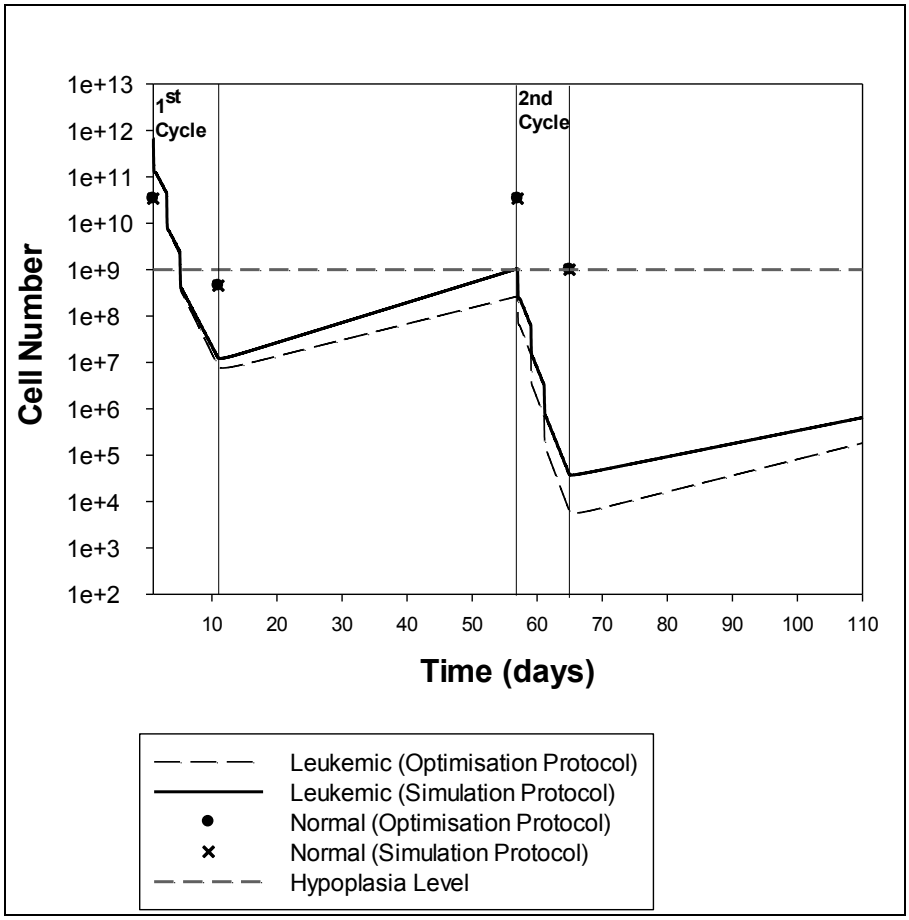

Figure 5.17: Patient P026 behaviour for the full course of treatment over the simulation and optimisation chemotherapy protocols. The dashed line represents the leukemic cell population over the optimised protocol; the straight black line represents leukemic cells during simulation of the clinically applied protocol; the circle signs are for the normal population at the start and end date of the optimisation protocol; the x signs are for the normal population at the start and end date of the simulation protocol and the grey line represents the BM hypoplasia objective

5.5 Cytarabine (Ara-C) is more effective when given in continuous daily 24-hour infusions than in short 12-hourly infusions

For all the patient case studies undergoing treatment simulations with both the LDAC and the DA protocols, the optimal schedule for administration of Ara-C is the daily continuous 24 hour infusions of the drug rather than the short bolus 12-hourly doses. The difference in the effectiveness of the two protocols (continuous vs short bolus doses) is due to the different concentration profiles in the BM.

In figure 5.18, the concentration profile of Ara-C in BM is presented for the first day after the administration of two short bolus doses of 20 mg every 12-hrs and after the application of 1

daily dose of 40 mg as continuous 24 hour infusion, both schedules given sc. In the standard protocol, there are high concentration peaks at the point of dose administration which thereafter exponentially decrease (figure 5.18). In contrast, during the optimised treatment protocol a constant infusion rate is suggested for Ara-C that is lower compared with the peaks of the standard treatment protocol but is of longer duration. This difference in the schedule will provoke different dynamics in the cell population and especially the cells in S-phase where the drug acts.

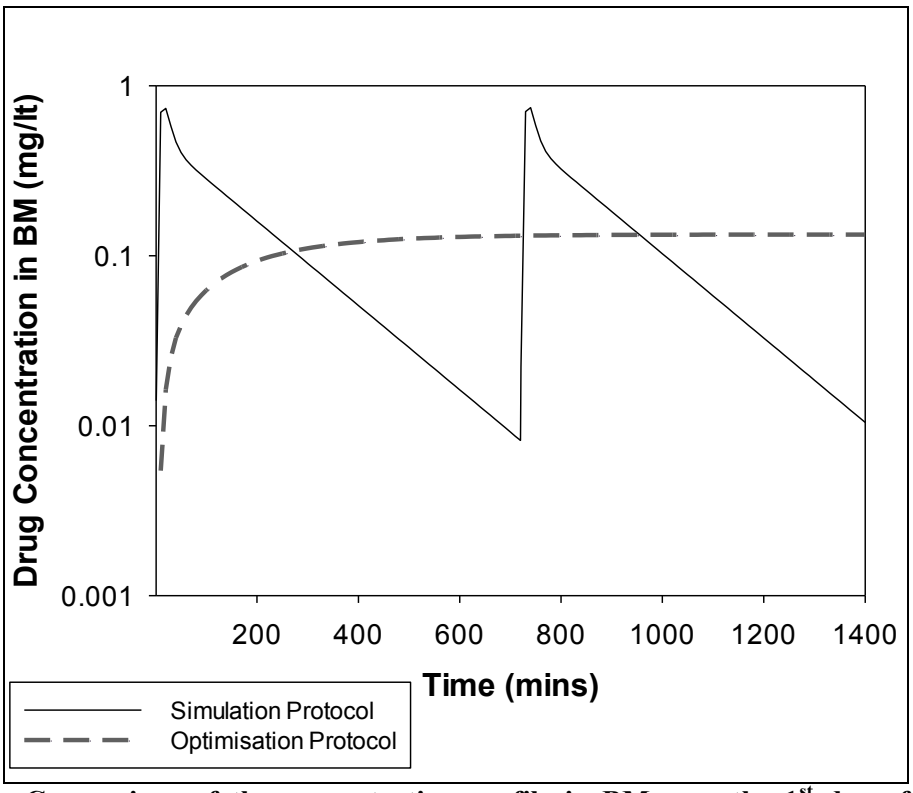

Figure 5.18: Comparison of the concentration profile in BM over the 1st day of the LDAC standard protocol and over the optimised protocol

In figure 5.19, the dynamics of cells in S-phase are presented for the 1st day of the standard and optimised protocols. Cells in S-phase are decreasing sharply after the first dose application but as the drug concentration declines, the cell population starts increasing and thereafter decreases again due to the second dose application. In contrast, during the optimised protocol, the cell population decreases at a slower rate compared with that of the standard protocol. However, the drug concentration is constantly present in the S-phase population that results in a constant death rate due to drug action and so there are no oscillations in the dynamics of the S-phase population. Leukemic cells in this phase over the optimised protocol are continuously decreasing and by the end of the 1st day, the leukemic cell population reaches a lower state compared with that of the standard treatment protocol.

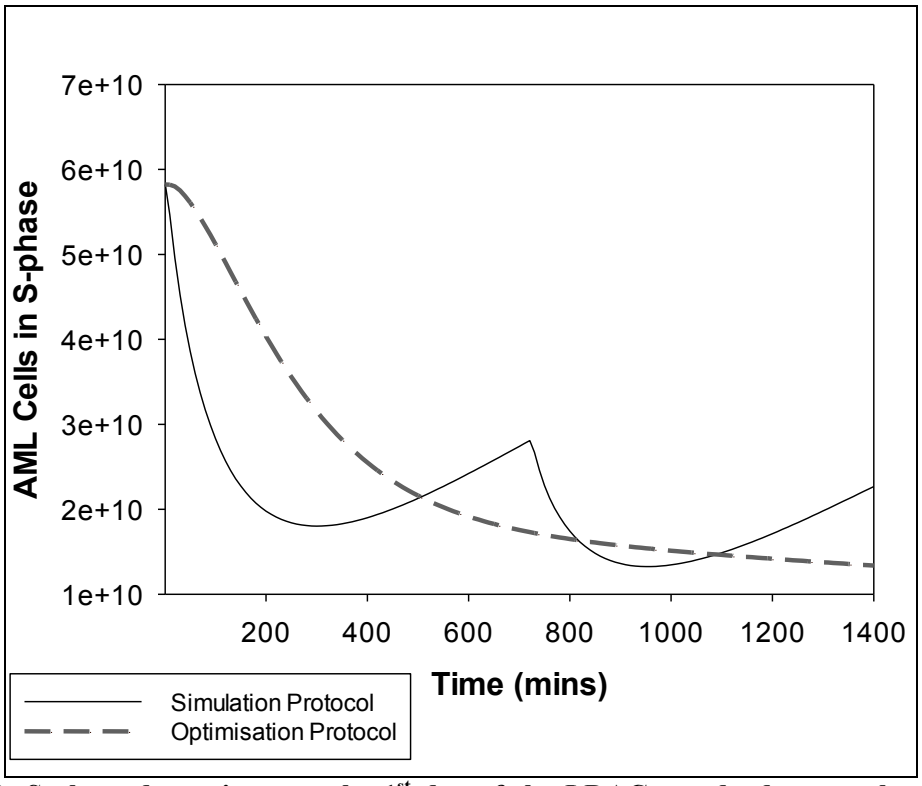

Figure 5.19: S-phase dynamics over the 1st day of the LDAC standard protocol and over the optimised protocol. The straight black line represents the model simulation of the standard protocol and the grey dashed line represents the optimisation results. Over the continuous daily infusions of Ara-C for the optimised protocol, a constant concentration profile is maintained that results in a continuous death rate of cells in S-phase which, from the end of the 1st day, reach a lower state compared with that of the simulation results of standard treatment.

5.6 Concluding Remarks

For model analysis, clinical data of 6 patients who underwent chemotherapy are used for the estimation of cell cycle time distribution. The patient data is comprised of disease characteristics (tumour burden, cell cycle times, normal cell population) as well as patient-specific characteristics (gender, age, weight and height). The estimated mean S-phase duration (Ts) is 15 hrs (range: 9-21 hrs) and mean whole cell cycle duration (Tc) is 47.5 hrs (range: 33-68 hrs).

The estimated data reveals a clear relationship of cell cycle times to treatment outcomes. Specifically, low Ts duration combined with high Tc duration indicates worse treatment

outcomes, whereas the reverse combination is indicative of a good response to treatment. This patient variability in tumour kinetics and its effect on the diverse patient clinical outcome has been experimentally tested and proven elsewhere (Stryckmans et al., 1970; Cheung et al., 1972; Hayes et al., 1977; Raza et al., 1987; Lampkin et al., 1969; Preisler et al., 1993; Chiorino, Lupi, 2002).

In order to improve the effectiveness of AML therapy and reduce its toxicity, treatment with chemotherapy is presented as an optimal control problem with the main aim of obtaining a treatment schedule which maximises leukemic cell, kill yet minimises death of the normal cell population in the BM. By the end of treatment, the leukemic population should be reduced to a level of approximately 10^9 cells at which point BM hypoplasia is also achieved.

Out of the 6 patients studied, 2 patients had a successful treatment with leukemic hypoplasia achieved, 2 had a reduction of leukemic cells without achieving the hypoplasia target and two had disease progression on chemotherapy. The optimisation algorithm is formulated and solved for all patients for both intensive and non-intensive treatment protocols with maximal and minimal thresholds set for efficacy and toxicity, respectively. For iv Ara-C, total drug administration is set between 50mg – 4000mg with infusion duration between 1 min to 24 hours. The window for DNR dose optimisation is stricter due to potential toxic effects and the only independent variable is dose with 30mg – 90mg per infusion. For sc Ara-C, the maximum dose per day is 40mg and doses are permitted up to four times daily for a maximum period of 20 days.

Optimisation results obtained for the 6 patients indicate that continuous infusions are more effective for leukemia cell kill than are rapid infusions. For non-intensive chemotherapy, 40mg of Ara-C in continuous infusion sc is better than daily divided doses with BM leukemic hypoplasia achieved for all patient case studies. For the intensive protocol, dose increase of DNR to 90 mg/m^2 combined with Ara-C daily infusion iv is the optimal chemotherapy regimen. Ara-C doses differ between patients and the optimal dose range is between 200 to 250 mg/m^2.

Using the optimisation protocol, the leukemic cell population is further reduced and the treatment outcome is improved. The reason for this difference in the cell population dynamics for the different dosing schedule is due to the effect that schedule has on the Ara-C concentration profile. For the Ara-C continuous infusion, the concentration profile will increase and reach a peak that will be constant for the full length treatment. The existence of

sufficient drug concentration constantly at the tumour location causes constant cell death which, according to the model, leads to higher death of the leukemic population in total as compared with that of the simulation results in which short bolus doses of higher dose load are used. Appendix C includes the cell population profiles of cells in the S-phase, GoG_1-phase and G_2M-phase for all patients. This difference in the cell dynamics of the cell phases is clearly shown since, during the constant drug dosing, the cells in S-phase are further minimised which in turn reduces cells in the two other cell cycle compartments successively.

Chapter 6

Conclusions and Future Directions

6.1 Project Summary

We have developed a model for the simulation of patients with AML undergoing treatment with two standard chemotherapy protocols, one intensive and the other non-intensive: (a) Daunarubicin (DNR) and Cytosine Arabinoside (Ara-C) used in standard intravenous (iv) doses (DA 3+10) and (b) low dose Ara-C (LDAC) administered subcutaneously (sc).

The model has been implemented in the gPROMS environment (gPROMS, 2003) and consists of a model simulator and an optimiser. The requiring information as input for both the simulator and the optimiser consist of patient, disease and drug information. Patient information includes the physiological patient characteristics of sex, age, weight, height, whereas disease information is the clinically available BM information such as the blast percentage in the marrow aspirate and the BM cellularity. As extra information to what is currently used in clinical practice, the cell cycle characteristics of the S-phase duration and the total cell cycle duration were used. Moreover, PK information of drug elimination rate in the liver and kidneys is required as is available in the product specification supplied by the pharmaceutical company producing this drug. PD information is also required that consist of the fitted parameters of the measured drug effect on the cell cycle population and are the drug concentration at the maximum PD effect together, the concentration at the half of the maximum effect and the slope parameter that is a scale factor affecting the shape of the curve.

The developed mathematical model is afterwards used as a system for sensitivity analysis between the cell cycle, the PK and PD parameters in order to identify the crucial factor that mainly affects the clinical treatment outcome. Inter-patient variability bounds are collected from the literature for the cell cycle, PK and PD parameters. Sensitivity analysis results show the cell cycle times as the crucial model parameters that highly affect the disease treatment outcome.

The developed mathematical model is used for various simulation analyses under two chemotherapy protocols of chemotherapy induction treatment for AML, one intensive and the

other non-intensive: (a) DNR and Ara-C used in standard intravenous (iv) doses (DA 3+10) and (b) low dose Ara-C (LDAC) administered sc.

For the clinical data, the project is submitted and approved by the North West London Hospitals Trust for the provision of health records of patients diagnosed with AML and treated within Northwick Park Hospital using DNR and Ara-C anti-leukemic agents under either i.v. or sc doses applied (protocols available in Appendix B). For the patient data, the duration of the cell cycle phases were fitted using the leukemic cell population numbers derived by the given patient blast percentage of the BM aspirate. The patient data is comprised of disease characteristics (tumour burden, cell cycle times, normal cell population) as well as patient-specific characteristics (gender, age, weight and height). The estimated mean S-phase duration (Ts) is 15 hrs (range: 9-21 hrs) and mean whole cell cycle duration (Tc) is 47.5 hrs (range: 33-68 hrs). The estimated data reveal a clear relationship of cell cycle times to treatment outcomes. Specifically, low Ts duration combined with high Tc duration indicates worse treatment outcomes, whereas the reverse combination is indicative of a good response to treatment. This patient variability in tumour kinetics and its effect on the diverse patient clinical outcome has been experimentally tested and proven elsewhere (Stryckmans et al., 1970; Cheung et al., 1972; Hayes et al., 1977; Raza et al., 1987; Lampkin et al., 1969; Preisler et al., 1993; Chiorino, Lupi, 2002). This relationship between Tc and disease increase has a scientific explanation as the longer cycling times indicate longer GoG1-phase. It is well-reported (Lewin et al., 2007; Komarova, Wodarz, 2005; Michor, 2008) that GoG1-phase is a factor related to disease resistance and relapse since cells in this phase are not affected by the chemotherapy drugs and form residual disease after treatment completion. The reverse relationship was observed for Ts time where the longer Ts indicated lower leukemic cell numbers. The longer S-phase duration is linked to a higher percentage of cell population in this phase that respectively increases the probability of the leukemic cells to be affected and eradicated by anti-leukemic S-phase specific drugs as DNR and Ara-C.

The aim of remission-induction therapy described by the current presented model is to achieve the rapid restoration of normal BM function. By treatment completion, the leukemic population should be reduced to a level of approximately 10^9 cells, at which point BM hypoplasia is achieved. Moreover, the normal population should be higher than the leukemic population and a 3-log reduction is the maximum permissible level of population reduction. This optimisation problem is formulated and solved for both of the chemotherapy protocols studied, the intensive and non-intensive protocols.

The optimisation results suggest that continuous dose infusions are more effective than short bolus doses in terms of the treatment outcome. This is due to the fact that over the continuous dose administration, the anti-leukemic agent is constantly present at the site of the tumour population resulting in a constant death rate due to drug action.

However, the purpose of the current work is not to make an implication for improvement of the current medical processes but to show the benefits of an automated system for the chemotherapy treatment design. This automated system would give the opportunity to the clinician to insert the required information in terms of patient and disease characteristics then select the drug and regimen used for the treatment and either simulate an existing protocol or use the optimisation option to derive an optimal suggested treatment protocol.

The end-user of such an automated system will have a tool (a) to simulate and compare the endpoints of specific treatment protocols, (b) to track and audit a patient's real-time outcome with treatment, (c) to empower and enable patients to directly input and influence their own treatment programme (e.g. input of side effects and real-time quality of life data) and, (d) to calculate and apply the optimal treatment schedule using the integrated optimiser based on patient- and leukemia-specific input data with the ultimate result of improved treatment outcomes.

6.2 Key Contributions

The contributions of the work presented in this thesis can be summarised as follows:

- A mathematical model able to capture AML and normal cell dynamics under chemotherapy has been developed. Tumour-specific characteristics, such as tumour burden and cell cycle times, as well as patient-specific characteristics, such as gender, age, weight and height, are incorporated into the model to gain insights into the cell dynamics for the studied patients during treatment.

- Simulation results are obtained for patients with AML undergoing treatment with two standard chemotherapy protocols, one intensive and the other non-intensive: (a) DNR and Ara-C used in standard intravenous (iv) doses (3+10) and (b) low dose Ara-C (LDAC) administered subcutaneously (sc).

- Sensitivity analysis has been used to identify cell cycle times as the critical personal parameters that control the treatment outcome.

- The project is submitted and approved by the North West London Hospitals Trust for the provision of health records of patients diagnosed with AML and treated within Northwick Park Hospital using DNR and Ara-C anti-leukemic agents under either intravenous (i.v.) or subcutaneous (sc) doses applied. The patient data is comprised of disease characteristics (tumour burden, cell cycle times, normal cell population) as well as patient-specific characteristics (gender, age, weight and height).

- The clinical data are used for parameter estimation of the cell cycle times for each patient case. The estimated data reveal a clear relationship of cell cycle times to treatment outcomes. Specifically, low Ts duration combined with high Tc duration indicates worse treatment outcomes, whereas the reverse combination is indicative of a good response to treatment.

- Treatment with chemotherapy is presented as an optimal control problem with the main aim of obtaining a treatment schedule which could maximise leukemic cell kill yet minimise death of the normal cell population in the BM. By the end of treatment, the leukemic population should be reduced to a level of approximately 10^9 cells at which point BM hypoplasia is achieved. The optimisation problem is solved for all the studied patients and an optimal treatment protocol is proposed for each case study revealing the potential for improved treatment design in AML therapy, dependent on disease and patient characteristics, defined on a case-by-case basis.

6.3 Future Directions

6.3.1 Model elaboration

To obtain a more specific and validated model that is further individually adapted to the patient, extra experimental data sets gained by experiments on primary leukemic samples are needed. The outcome of these experiments will be specific knowledge concerning the cell cycle times of each patient sample together with the pharmacodynamics, toxicity and efficacy, of the drugs used. The core of such an experimental design is the leukemic

biomimicry, 3D hollow fibre bioreactor, that has been already designed by the group of Prof. Mantalaris and Dr Panoskaltsis, BSEL group in Imperial College of London. This bioreactor is able, by using a patient BM sample to analyse and estimate *in vitro* the cell cycle distribution and the duration of each cycling phase for a particular patient. In that sense the measured cell cycle data will be used together with the clinical performance of the patient in order to validate the developed mathematical model.

Moreover, experiments in the 3D bioreactor will allow the patient's BM samples to be tested undergoing chemotherapy. Such an experiment would mimic the chemotherapy process *in vitro* and would provide the PD action of the drug on the patient sample that could further validate the PD model used. From the acquired knowledge on the pharmacodynamic properties of the drugs and the cell cycle, a validated patient–specific and leukaemia–specific model will be derived. To close-the-loop, the experimental device can be used for the design of an experiment where the optimal personalised protocol will be applied *in vitro* and the optimisation results will be validated.

Lastly experimental analysis of the patient BM sample will provide the necessary insight into the cell cycle, the drug metabolic activity when it enters the cell and the drug mechanism of action. These data are not yet available from clinical practice and the information is not sufficient in order to develop a detailed mathematical model. Therefore *in vitro* experiments are required to obtain individual properties of the dominating phenomena (toxicities and efficacies).

The combination of mathematical modelling and experimental design will lead to a more elaborate version of the developed mathematical model describing cell dynamics during chemotherapy treatment for AML which can be expanded to analyse all different types of leukemia i.e. ALL, CLL and CML. The proposed platform, illustrated in figure 6.1, would help (a) to validate the developed model, (b) to further elaborate this model by including more complex phenomena, e.g. drug resistance, that relate patient and disease characteristics to treatment outcome and (c) develop this system for other types of leukemia disease, such as CLL, CML and ALL.

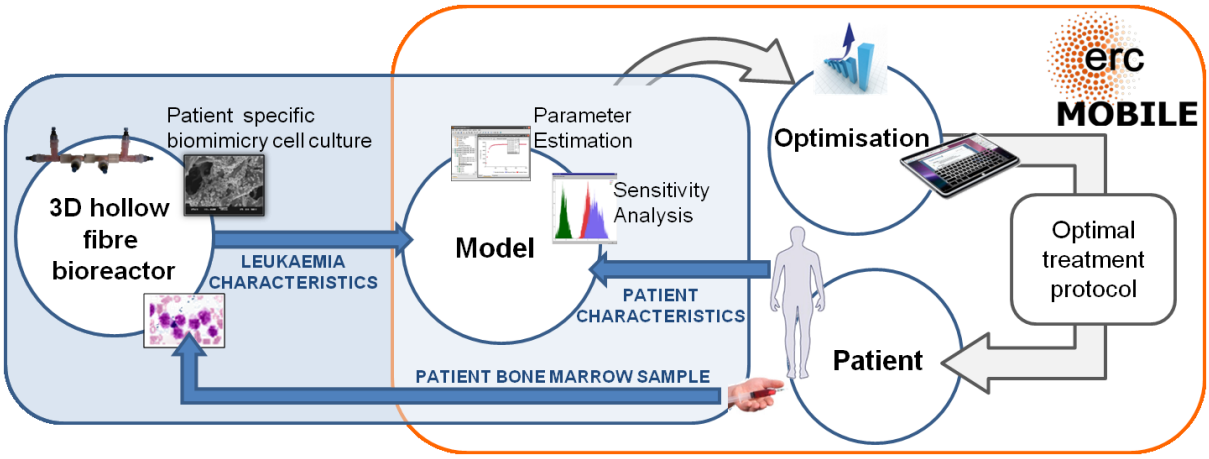

Figure 6.1: Schematic representation of the proposed closed loop system for the design of optimal patient- and leukaemia-specific chemotherapy protocols

6.3.2 The ChemoApp

More than $50b (£32b) is spent annually by large pharmaceutical companies to develop and bring new drugs to market (Paul et al., 2010), a process which on average takes 13.5 years (in 2007). Pre-clinical development accounts for approximately 32% of this cost with approximately 63% attributed to bringing the new drug through Phase I-III clinical trials (not including costs for exploratory discovery research, post-launch expenses or overheads (Paul et al., 2010)). Even if a drug is found to be effective in a clinical trial setting, the efficacy in clinical practice may be quite different (Eichler et al., 2010). More than half of pharmaceutical drugs coming through the pipeline do not pass Phase I clinical trials either due to failure of drug, failure of clinical trial design or failure of drug dose and schedule (Thomas, Baker, 2007). These failures not only represent a high cost to the pharmaceutical industry and the international healthcare economy, but more importantly also incur high personal cost to patients with incurable and debilitating illnesses, such as cancers, which currently have inadequate therapy. ***An ordered and cost-effective strategy to bring such drugs to market and use them in appropriately selected patients, e.g. in appropriate model systems with the use of molecular and genomic data from the patient and the tumour (Rooij, Marsh, 2011; Gonzalez-Angulo, 2010), would enable and justify healthcare costs in a market that desperately needs rationalisation.***

Towards this objective, a mathematical tool has been developed and presented in the current project as the result of an Advanced ERC grant award (MOBILE-ERC Advanced Grant, No:226462), that integrates patient and disease characteristics, to determine the

chemotherapeutic effect of a treatment schedule on the patient. The already developed model and more elaborated versions will serve as basis for ***the development of an automated advanced tool, i.e., ChemoApp, for the design of optimal personalised treatment protocols for acute and chronic leukemia***. This tool will provide the ability to simulate and compare different treatment protocols, generate an optimal treatment schedule for a patient case study and audit patient performance under treatment. Such software will benefit through the:

(i) Provision to the physician with advice during the treatment design as well as investigating the progress of the disease.
(ii) Ability to the patients to follow their treatment step by step.
(iii) Improvement in the nationalised healthcare system and the private sector by the reduced cost stemming from the more accurate calculated drug doses, the limitation of hospital stays, reduction of hospital resources and long-term health effects of treatment.
(iv) Personalisation of the treatment based on tumour and patient-specific data.

The proposed ChemoApp will be a tool containing:

- ***A library of models for both types of leukemia, acute and chronic;***
- ***Computational engines for optimisation, simulation and parameter estimation;***
- ***Analytical library for the available individual data provision such as cyclin expressions analysis, clinical and experimental data from apparatus for cell cycle modelling.***

The current developed model will serve as version 0.1 (v.0.1) of the ChemoApp tool and its function is illustrated in figures 6.2 to 6.4. The required input information for both the simulator and the optimiser consist of patient, disease and drug information. Patient information includes the physiological patient characteristics of sex, age, weight, height, whereas disease information is the clinically available BM information such as the blast percentage in marrow aspirate and the BM cellularity. Extra information to what is currently used in clinical practice will be the cell cycle characteristics of S-phase duration and the total cell cycle duration. This extra information can be either provided by the analytical library of the ChemoApp Tool or can be measured by immunophenotyping on the BM aspirates and trephine biopsies taken from each patient at diagnosis (Ki-67 and cyclin analysis). Moreover, ChemoApp requires the product names of the drugs that will be used for the treatment

protocol. For the selected drugs, ChemoApp will automatically generate PK and PD values as given in the product specification by the pharmaceutical company producing this drug. However, the end-user will have access to these data and will be able to change the information if required. All of this information may be filed and stored in patients' electronic records for local and central audit purposes as well as for research programmes.

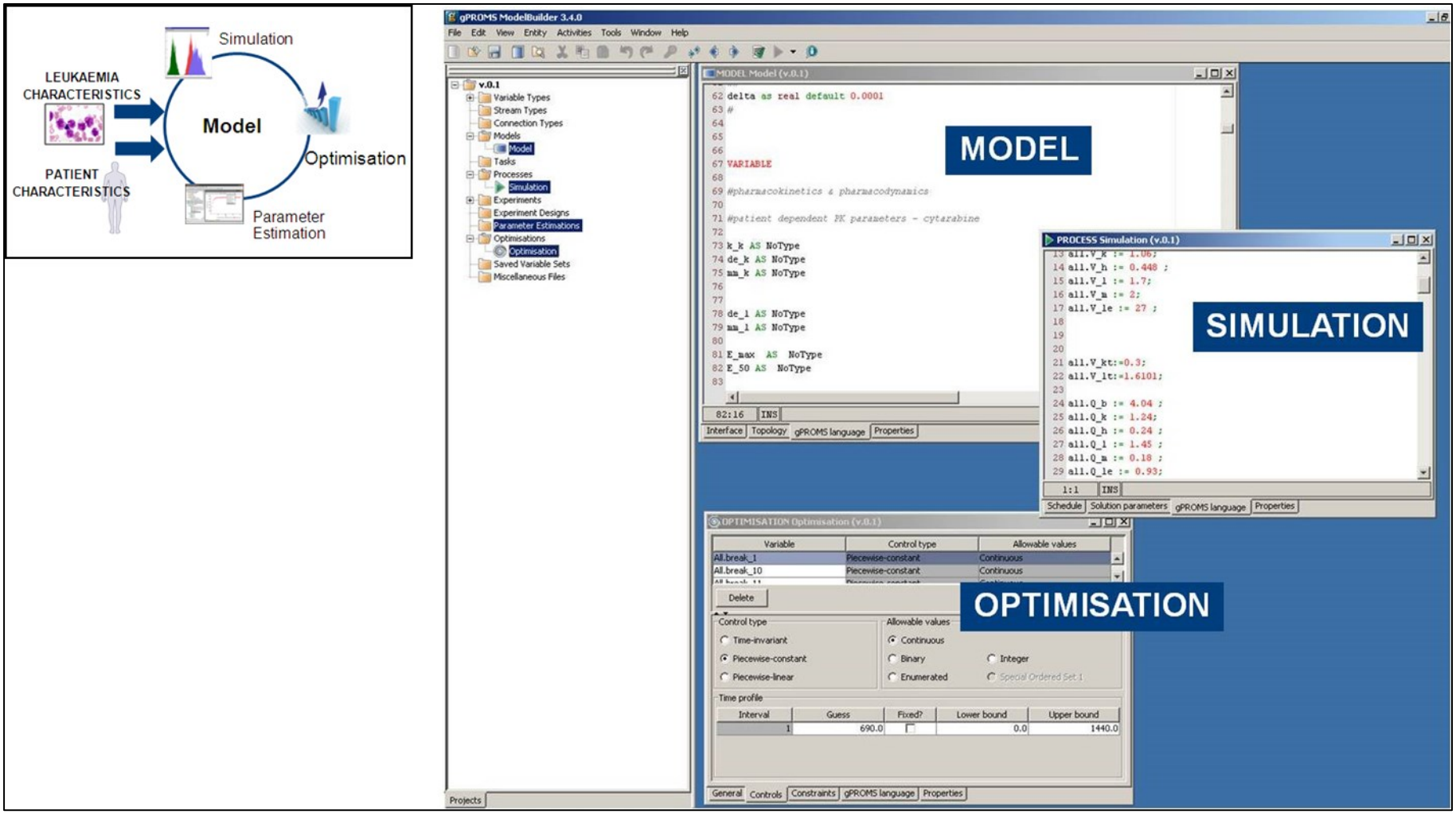

Figure 6.2: ChemoApp – Library model version 0.1 (v.0.1)

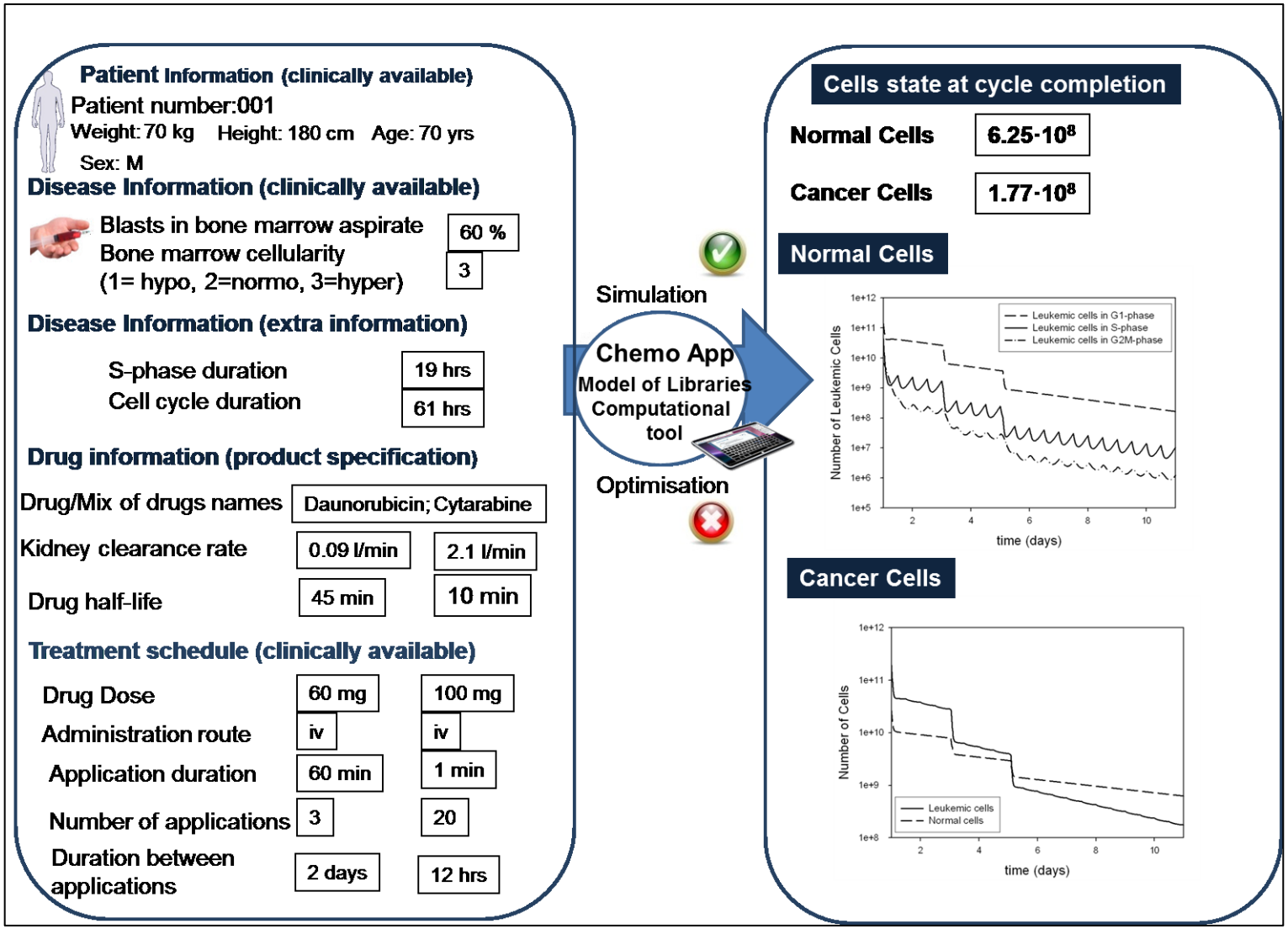

Figure 6.3: ChemoApp – Illustration of simulator for version v.0.1

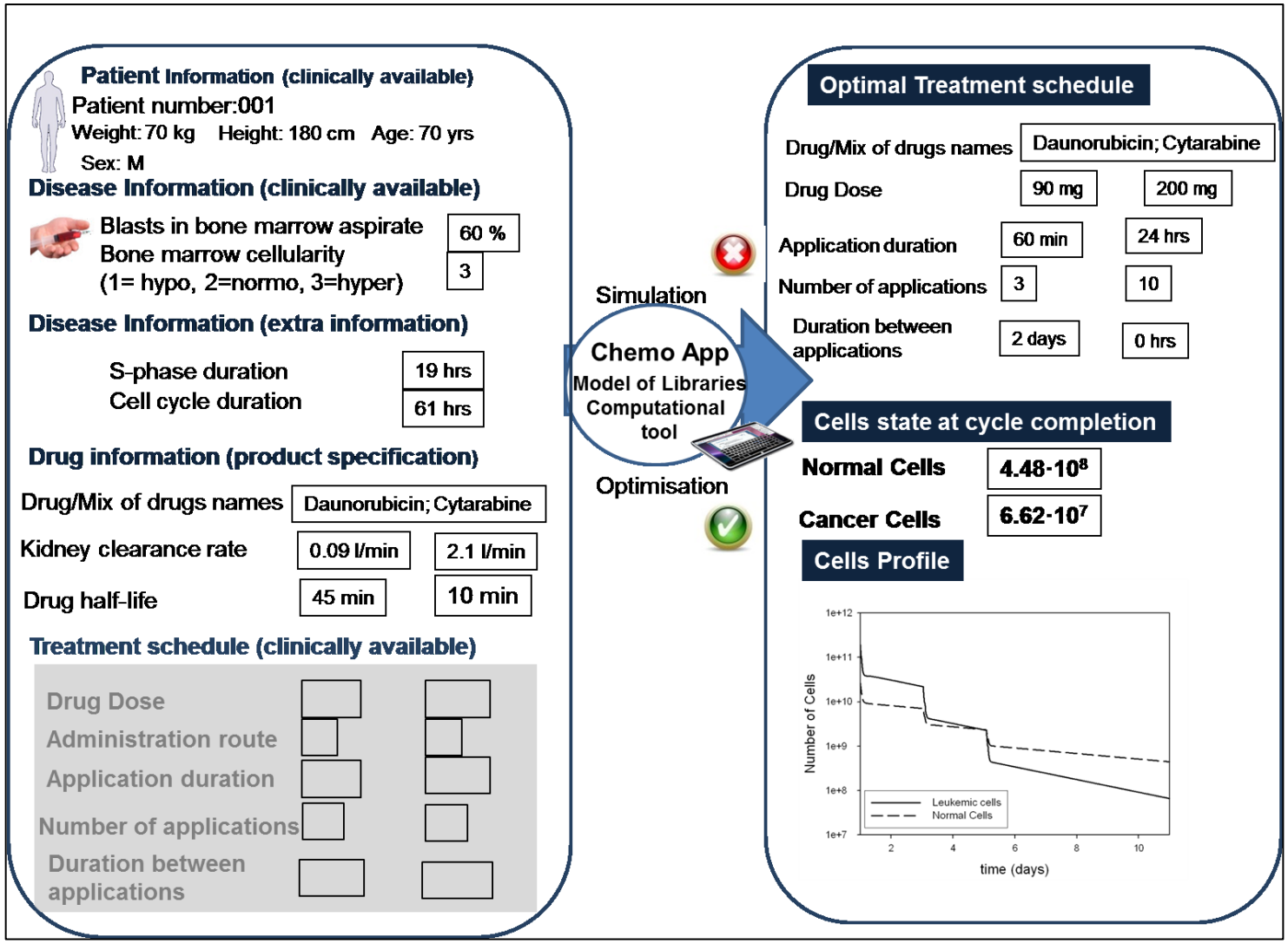

Figure 6.4: ChemoApp – Illustration of optimiser for version v.0.1

ChemoApp, has a variety of patient related benefits, benefits to the national economy and NHS as well as benefits to the pharmaceutical industry and societal benefits. More specifically, as an advanced intelligent computational tool, ***ChemoApp*** will enable ***audit analysis***, i.e., giving a framework which will enable process improvement via creating a database on actions that should be done and on those that are done in practice. Moreover, audit analysis provided by ***ChemoApp***, will enable ***patient involvement in the treatment*** via provision of the possibility of following up his/her clinical case on-line and potentially in real-time. Additionally, the ***optimisation application of ChemoApp***, will enable the definition of an optimal personalised treatment protocol – based on specific patient characteristics - and will provide better insight into disease dynamics as well as the drug desired summary of product characteristics (SPC), therefore, increasing the efficiency of the treatment. This is crucial both for the patient, i.e., higher efficiency of chemotherapy (personalised) treatment as well as for the national economy and the NHS, i.e., accurate prediction of optimal treatment will enable more cost-efficient drug use and cost-savings for hospital care for these patients, enabling value-for-money in both nationalised and privatised healthcare sectors. Moreover, the tool will also provide the possibility of ***rapid, accurate and cost effective design of Clinical Trial phases I & II***, therefore, facilitating new drug development and faster release of new drugs to market. The latter is of great importance as currently, more than $50b (£32b) is spent annually by large pharmaceutical companies to develop and bring new drugs to market. Societal benefits originate from improved treatment design for patients with AML and limitation of toxicities which can impact on long-term survivorship due to the secondary effects of chemotherapy later in life, as well as by reduced overall costs of drugs due to less money spent by the pharmaceutical industry during the drug development phase.

In summary, the benefits from the development of the software proposed in this project are as listed below:

(i) ***ChemoApp*** provides the physician with advice in real-time during the decision making process of leukemia treatment and has the potential to monitor and audit progress and amielioration of the disease during treatment. It can also integrate quality of life parameters within the system to improve toxicity profile and patient satisfaction during and post-treatment.

(ii) ***ChemoApp*** enables patients to follow their own treatment step by step and potentially can enable and empower them to drive their own treatment plan, with their treating team. This may in itself have positive outcomes both physically and psychologically for patients as they will remain in some control of their environment and what has happened to them after such a devastating diagnosis has been made – it is one of the most difficult things for patients to come to terms with during treatment.

(iii) Potential improvement in healthcare (both nationalised and private systems) in terms of reduced cost of drugs/treatment and secondary effects due to excessive toxicities of treatment. Since therapy will be based on patient- and disease- specific characteristics, rather than empirical therapy currently employed, it is anticipated that there will be less treatment toxicity, a reduction in hospital resources and long-term toxicity of treatment.

(iv) Personalised treatment based on tumour and patient-specific data leading to better survival outcomes.

Publications from this thesis

Journal Publications

[1] Pefani E., Panoskaltsis N., Mantalaris A., Georgiadis M. C., Pistikopoulos E. N.. Design of optimal patient-specific chemotherapy protocols for the treatment of Acute Myeloid Leukemia (AML). Computers and Chemical Engineering Journal, 2013; 57: 187-195.

[2] Pefani E., Panoskaltsis N., Mantalaris A., Georgiadis M. C., Pistikopoulos E. N.. Chemotherapy Drug Scheduling for the Induction Treatment of patients diagnosed with Acute Myeloid Leukemia. Accepted for publication in the Transactions of Biomedical Engineering Journal.

[3] Pefani E., Panoskaltsis N., Mantalaris A., Georgiadis M. C., Pistikopoulos E. N.. Mathematical modelling and optimal scheduling of induction chemotherapy treatment of Acute Myeloid Leukemia (AML) with Daunorubicin (DNR) and Cytarabine (Ara-C) agents. To be submitted in the Cancer Research Journal.

Conference Proceedings

[1] Pefani E., Panoskaltsis N., Mantalaris A., Georgiadis M. C., Pistikopoulos E. N.. Towards a high-fidelity model for model based optimisation of drug delivery systems in acute myeloid Leukemia. Proceedings of the 21st European symposium on computer Aided Process Engineering (ESCAPE 21), Halkidi, Greece, 2011.

[2] Pefani E., Panoskaltsis N., Mantalaris A., Georgiadis M. C., Pistikopoulos E. N.. Modelling and Simulation of Drug Delivery Systems for the treatment of Acute Myeloid Leukemia. 5th European Conference of the International Federation for Medical and Biological Engineering IFMBE proceedings, Budapest, 2011: Volume 37, p.259.

[3] Pefani E., Panoskaltsis N., Mantalaris A., Georgiadis M. C., Pistikopoulos E. N.. A decision tool for the design of optimal personalized chemotherapy protocols for the treatment of Acute Myeloid Leukemia (AML). Annals of Oncology, 2012; Volume 23 (supplement 5): p. 33.

[4] Pefani E., Panoskaltsis N., Mantalaris A., Georgiadis M. C., Pistikopoulos E. N.. Design of optimal patient-specific chemotherapy protocols for the treatment of Acute Myeloid

Leukemia (AML). Proceeding of the International Symposia of Process Systems Engineering, Singapore, 2012.

[5] Pefani E., Panoskaltsis N., Mantalaris A., Georgiadis M. C., Pistikopoulos E. N.. A decision tool for the design of optimal personalized chemotherapy protocols for the treatment of Acute Myeloid Leukemia (AML).Proceedings of the 2012 American Institute of Chemical Engineers (AIChE), Pittsburg, PA, 2012.

[6] Pefani E., Velliou E., Panoskaltsis N., Mantalaris A., Georgiadis M. C., Pistikopoulos E. N.. An automated system for the design of optimal personalized chemotherapy protocols for the treatment of Leukemia. Proceedings of the 2013 American Institute of Chemical Engineers (AIChE), San Francisco, 2013.

[7] Pefani E.,Panoskaltsis N., Mantalaris A., Georgiadis M. C., Pistikopoulos E.N. Optimized patient- and leukemia-specific chemotherapy protocols for the treatment of Leukemia. Proceedings of the 2013 American Society of Haematology (ASH), New Orleans, LA, 2013.

Oral presentations

[1] **Pefani E**., Panoskaltsis N., Mantalaris A., Georgiadis M. C., Pistikopoulos E. N.. Modelling and Simulation of Drug Delivery Systems for the treatment of Acute Myeloid Leukemia. 5th European Conference of the International Federation for Medical and Biological Engineering IFMBE proceedings, Budapest, 2011: Volume 37, p.259.

[2] Pefani E., Panoskaltsis N., Mantalaris A., Georgiadis M. C., **Pistikopoulos E. N**.. Design of optimal patient-specific chemotherapy protocols for the treatment of Acute Myeloid Leukemia (AML). International Symposia of Process Systems Engineering, Singapore, 2012.

[3] **Pefani E**., Panoskaltsis N., Mantalaris A., Georgiadis M. C., Pistikopoulos E. N.. A decision tool for the design of optimal personalized chemotherapy protocols for the treatment of Acute Myeloid Leukemia (AML). 2012 American Institute of Chemical Engineers (AIChE), Pittsburg, PA, 2012.

[4] Pefani E., **Velliou E**., Panoskaltsis N., Mantalaris A., Georgiadis M. C., Pistikopoulos E. N.. An automated system for the design of optimal personalized chemotherapy protocols for the treatment of Leukemia. 2013 American Institute of Chemical Engineers (AIChE), San Francisco, 2013.

References

Afenya, E. K., (2001). Recovery of normal hemopoiesis in disseminated cancer therapy-a model. *Mathematical biosciences*, 172, 15-32.

Adimy M., Crauste F., Ruan S., (2005). A mathematical study of the hematopoiesis process with applications to Chronic Myelogenous Leukemia. *SIAM Journal of Applied Mathematics*, 65, 1328-1352.

Andersen, L. K., Mackey, M C., (2001). Resonance in periodic chemotherapy: a case study of acute myelogenous leukemia. *Journal of theoretical biology*, 209, 113-30.

Bain, B.J., (2003). *Leukemia Diagnosis*. 3rd ed. Blackwell Publishing: Oxford,UK.

Basse, B., Baguley, B. C., Marshall, E. S., Joseph, W. R., Brunt, B. V., Wake, G., Wall, D. J. N., (2003). A mathematical model for analysis of the cell cycle in cell lines derived from human tumours. *Mathematical Biology*, 47, 295-312.

BC Cancer Agency,(2007). Cancer drug manual: Cytarabine. Available at: http://www.bccancer.bc.ca/HPI/DrugDatabase/DrugIndexPro/Cytarabine.htm

Bennett, J. M., Orazi, A., (2009). Diagnostic criteria to distinguish hypocellular acute myeloid leukemia from hypocellular myelodysplastic syndromes and aplastic anemia: recommendations for a standardised approach. *Haematologica*, 94, 264-268.

Bischoff, K. B., Dedrick, R L., (1968). Thiopental pharmacokinetics. *Journal of pharmaceutical sciences*, *57*(8), 1346-51.

Bonnet D., Dick J. E., (1997). Human acute myeloid leukemia is organized as a hierarchy that originates from primitive hematopoietic stem cell. *Nature medicine*, 3, 730-737.

Borojevic, R, (2004). BM stroma in childhood myelodysplastic syndrome: composition, ability to sustain hematopoiesis in vitro, and altered gene expression. *Leukemia Research*,**28**(8), 831-844.

Brody, S. (1945), Bioenergetics and Growth, Reinhold Publications Corp., New York.

Brown, E., Hopper, J., Hodges, J. L., Bradley, B., Wennesland, R. and Yamauchi, H. (1962), Red cell, plasma, and blood volume in healthy women measured by radiochromium cell labeling and hematocrit*, Journal of Clinical Investigation,* 41(12), 2182–2190.

Caldwell J. C., Evans M. V., Krishnan K., (2012). Cutting edge PBPK models and analyses: providing the basis for future modelling efforts and bridges to emerging toxicology paradigms. *Journal of Toxicology,* 1-10.

Catlin S. N., Busque L., Gale R. E., Guttrop P., Abkowitz J. L., (2011). The replication rate of human hematopoietic stem cells in vivo. *Blood,* 117, 4460-4466.

Chaturvedi P. R., Decker C. J., Odinecs A. (2001). Prediction of pharmacokinetic properties using experimental approaches during early drug discovery. *Current Opinion in Chemical Biology*, 5, 452-463.

Chen, H. G.,Gross, J. F., (1979). Physiologically Based Pharmacokinetic Models for Anticancer Drugs. *Cancer Chemotherapy and Pharmacology*, 2, 85-94.

Cheung W. H., Rai K. R., Sawitsky A., (1972). Characteristics of cell proliferation in acute leukemia. *Cancer research*, 32, 939-942.

Chiorino, G., Lupi, M., (2002). Variability in the timing of G1/S transition. *Mathematical biosciences*, 177 & 178, 85-101.

Chouker A., Martignoni A., Dugas M., Eisenmenger W., Schauer R., Kaufmann I., Schelling G., Lohe F., Jauch K., Peter K., Thiel M., (2004). Estimation of liver size for liver transplantation:the impact of age and gender. *Liver transplantation*, 10, 678-685.

Clarkson B., Ohkita T., Ota K., Fried J. (1967). Studies of cellular proliferation in human leukemia. I. Estimation of growth rates of leukemic and normal hematopoietic cells in two adults with Acute leukemia given single injections of triatiated thymidine. *Journal of clinical investigation*, 46, 506-529.

Cohen, E. I., Kelly, S. A., Edyeb, M., Mitty, H. A., Bromberg, J. S., (2009). MRI estimation of total renal volume demonstrates significant association with healthy donor weight. *European Journal of Radiology*, 71, p283-287.

Coldman A. J., Murrary J. M., (2000). Optimal control for a stochastic model of cancer chemotherapy. *Mathematical biosciences*, 168, 187-200.

Colijn C., Mackey M. C., (2005). A mathematical model of hematopoiesis – I. Periodic chronic myelogenous leukemia. *Journal of Theoritical Biology*, 237, 117-132

Colmone, A., (2008). Leukemic Cells Create BM Niches That Disrupt the Behaviour of Normal Hematopoietic Progenitor Cells. *Science*, **322**(5909), 1861-1865.

Dedrick, R.L., Forrester, D. D., Ho, D. H. W.,(1972). In Vitro-in vivo correlation of drug metabolism-deamination of 1-b-D-Arabinofuranosylcytosine. *Biochemical Pharmacology*, 21, 1-16.

DeVita V., Chu E., (2008). A history of cancer chemotherapy. *Cancer Research*, 68, 8643-8653.

Doan, P.L. and J.P. Chute, (2012). The vascular niche: home for normal and malignant hematopoietic stem cells. *Leukemia*, 26(1), p. 54-62.

Dua, P., V. Dua, and E.N. Pistikopoulos, (2008). Optimal delivery of chemotherapeutic agents in cancer. Computers & Chemical Engineering, 32(1-2), 99-107.

Eichler H., Abadie E., Breckenriddge A., Flamion B., Gustafsson, Leufkens H., Rowland M., Schneider C. K., Bloechl-Daum B., (2011). Bridging the efficacy – effectiveness gap : a regulator's perspective on addressing variability of drug response. Nature Reviews, 10, 495-506.

Eisen M., Mathematical models in cell biology and cancer chemotherapy. Lecture notes in biomathematics, vol. 30. 1st edition. New York: Springer-Verlag Berlin Heidelberg; 1979.

Essers, M.A.G. and A. Trumpp, (2010). Targeting leukemic stem cells by breaking their dormancy. *Molecular Oncology*, 4(5), 443-450.

Ezoe S., Matsumura I., Satoh Y., Tanaka H., Kanakura Y. (2004). Cell cycle regulation in Hematopoietic Stem/Progenitor Cells. *Cell Cycle*, 3, 314-318.

Fister, K.R. and J.C. Panetta, (2000). Optimal control applied to cell-cycle-specific cancer chemotherapy. *Siam Journal on Applied Mathematics*, 60(3), 1059-1072.

Garattini S., (2007). Pharmacokinetics in cancer chemotherapy. *European journal of cancer,* 43, 271-282.

Gardner S. N., Fernandes M., (2003). New tools for cancer chemotherapy: computational assistance for tailoring treatments. *Molecular cancer therapeutics*, 2, 1079-1084.

Gillies, H. C., Herriott, D., Liang, R., Ohashi, K., Rogers, H. J.,Harper, P. G., (1987). Pharmacokinetics of idarubicin (4-demethoxydaunorubicin; IMI-30; NSC 256439) following intravenous and oral administration in patients with advanced cancer. *British journal of clinical pharmacology*, *23*, 303-10.

Gonzalez-Angulo A. M., Hennessy B. T. J., Mills G. B., (2010). Future of personalised medicine in oncology: A systems biology approach. *Journal of Clinical Oncology*, 28, 2777-2783.

gPROMS, (2003). Introductory user's guide, release 2.2, Process Systems Enterprise Limited, London, U.K.

Harrold J. M, Parker R. S., (2009). Clinically relevant cancer chemotherapy dose scheduling via mixed-integer optimisation. *Computers and chemical engineering*, 33, 2042-2054.

Hayes F. A., Green A. A., Mauer A. M. (1977). Correlation of cell kinetic and clinical response to chemotherapy in disseminated neuroblastoma. *Cancer research*, 37, 3766-3770.

Hijiya, N., Panetta, J. C, Zhou, Y., Kyzer, E. P., Howard, S. C., Jeha, S., Razzouk, B. I., Ribeiro, R. C., Rubnitz, J. E., Hudson, M. M., Sandlund, J. T., Pui, C.H., Relling, M.V., (2006). Body mass index does not influence pharmacokinetics or outcome of treatment in children with acute lymphoblastic leukemia. *Childhood A Global Journal Of Child Research*, 108, 3997-4002.

Himmelstein, K. J.,Lutz, R. J., (1979). A review of the applications of physiologically based pharmacokinetic modelling. *Journal of pharmacokinetics and biopharmaceutics*, 7(2), 127-45.

Hoffbrand,A.V. Moss, P.A.H. Pettit, J.E., (2006). *Essential Haematology.* 5th ed. Blackwell Publishing: Oxford,UK.

Hoffmann M. H., Klausen T. W., Boegsted M., Larsen S. F., Schmitz A., Leinoe E. B., Schmiegelow K., Hasle H., Bergmann O. J., Sorensen S., Nyegaard M., Dybkaer K., Johnsen H. E., (2012). Clinical impact of leukemic blast heterogeneity at diagnosis in cytogenetic intermediate-risk acute myeloid leukemia. *Clinical Cytometry*, 82B, 123-131.

Holford N. H. G., Sheiner L. B., (1982). Kinetics of pharmacologic response. *Pharmacology & Therapeutics*, 16, 143-166.

Horton S. J., Huntly B. J. P., (2012). Recent advances in acute myeloid leukemia stem cell biology. *Haematologica*, 97, 966-974.

Huffman D. H., Bachur N. R., (1972). Daunorubicin metabolism in acute myelocytic leukemia. *Blood,* 39, 637-643.

Jones H. M., Gardner I. B., Watson K. J., (2009). Modelling and PBPK simulation in drug discovery. *The AAPS Journal*, 11, 155-166.

Kennedy, J.A. and F. Barabe, (2008). Investigating human leukemogenesis: from cell lines to in vivo models of human leukemia. *Leukemia*, 22(11), 2029-2040.

Kimmel, M., Swierniak, A.,(2003). Using Control Theory to Make Cancer Chemotherapy Bene ficial from Phase Dependence and Resistant to Drug Resistance. *Mathematical Biosciences*, 1-44.

Komarova, N. L., Wodarz, D.,(2005). Drug resistance in cancer: principles of emergence and prevention. *Proceedings of the National Academy of Sciences of the United States of America*, 102, 9714-9.

Krieger,A.,Panoskaltsis N., Mantalaris A., Georgiadis M., Pistikopoulos E. N., (2013). Modelling and analysis of individualized pharmacokinetics and pharmacodynamics for volatile anaesthesia, *IEEE Transactions on Biomedical Engineering* (Accepted for publication on 22/07/2013).

Kufe D., Spriggs D., Egan EM., Munroe D., (1984). Relationships among ara-CTP pools, formation of (Ara-C)DNA, and cytotoxicity of human leukemic cells. *Blood*, 64, 54-58.

Lacayo, N. J., Lum, B. L., Becton, D. L., Weinstein, H., Ravindranath, Y., Chang, M. N.,Bomgaars, L., Lauer, S.J., Sikic, B.I., Dahl, G.V., (2002). Pharmacokinetic interactions of cyclosporine with etoposide and mitoxantrone in children with acute myeloid leukemia. *Leukemia*, 920-927.

Lampkin B. C., Nagao T., Mauer A. M., (1969). Drug effect in acute leukemia. *The journal of clinical investigation*, 48, 1124-1130.

Ledzewicz, L., Schattler, H., (2002). Optimal Bang-Bang Controls for a Two-Compartment Model. *Optimisation*, 114, 609-637.

Ledzewicz, U., Schättler, H., (2007). Optimal controls for a model with pharmacokinetics maximizing BM in cancer chemotherapy. *Mathematical biosciences*, *206*, 320-342.

Lewin B., Cassimeris L., Lingappa V. R., Plopper, G. Cells. 2nd edition.United States: Jones and Bartlett Publishers; 2007.

Looby, M., Linke, R., Weiss, M., (1997). Pharmacokinetics and tissue distribution of idarubicin and its active metabolite idarubicinol in the rabbit.*Cancer Chemotherapy & Pharmacology*, 39,554 - 556.

Lutz, R. L., Galbraith, W. M. Dedrick, R. L., Shrager, R., Mellett, L. B., (1977). A model for the kinetics of distribution of actinomycin-d in the beagle dog.The Journal of *Pharmacology and Experimental Therapeutics,*200,469-478.

Marcucci G., Mrozek K., Bloomfield, (2005). Molecular heterogeneity and prognostic biomarkers in adults with acute myeloid leukemia and normal cytogenetics. Current Opinion in Hematology, 12, 68-75.

Michor, F., (2008). Mathematical models of cancer stem cells. *Journal of clinical oncology : official journal of the American Society of Clinical Oncology*, 26, 2854-61.

Milligan D. W., Grimwade D, Cullis J. O., Bond L., Swirsky D., Craddock C., Kell J., Homewood J., Campbell K., McGinley S., Wheatley K., Jackson G., (2006). Guidelines on the management of acute myeloid Leukemia in adults. *British Journal of Haematology*, 135, 470-474.

Morrison, P. F., Lincoln, T. L., Aroesty, J., (1975). Rand Report: The disposition of Ara-C and its metabolites: a pharmacokinetic simulation. *Santa Monica: Rand Corparation*.

Coldman, A., Murray, J. M., (2000). Optimal control for a stochastic model of cancer chemotherapy. *Mathematical Biosciences*, 168, 187-200.

Nair, R.R., J. Tolentino, and L.A. Hazlehurst, (2010). The bone marrow microenvironment as a sanctuary for minimal residual disease in CML. *Biochemical Pharmacology*, 80(5), 602-612.

Nakase K., Bradstock K., Sartor M., Gottlieb D., Byth K., Kita K., Shiku H., Kamada N., (2000). Geographic heterogeneity of cellular characteristics of acute myeloid leukemia: a comparative study of Australian and Japanese adult cases. *Leukemia*, 4, 163-168.

Nurse P., Masui Y., Hartwell L., (1998). *Understanding the cell cycle*. Nature, 10, 1103-1106.

Olsen, R.J., et al., (2008). *Acute Leukemia Immunohistochemistry: A Systematic Diagnostic Approach.* Archives of Pathology & Laboratory Medicine, 132(3), 462-475.

Panetta, J. C., Wilkinson, M., Pui, C.H., Relling, M. V., (2002). Limited and optimal sampling strategies for etoposide and etoposide catechol in children with leukemia. *Journal of pharmacokinetics and pharmacodynamics*, *29*(2), 171-88.

Panoskaltsis N, Reid CDL, Knight SC., (2003). Quantification and cytokine production of circulating lymphoid and myeloid cells in acute myelogenous leukemia (AML). *Leukemia*, 17, 716-730.

Panoskaltsis, N., A. Mantalaris, and J.H.D. Wu, (2005). Engineering a mimicry of bone marrow tissue ex vivo. *J Biosci Bioeng*, 100(1), 28-35.

Parker R. S., Doyle F. J., (2001). Control relevant modelling in drug delivery. *Advanced drug delivery reviews*, 48, 211-228.

Paul S. M., Mytelka D. S., Dunwiddie C. T., Persinger C. C., Munos B. H., Lindborg S. R., Schacht A. L., (2010). How to improve R&D productivity: the pharmaceutical industry's grand challenge. *Nature Reviews*, 9, 203-214.

Peyret T., Krishnan K., (2011). QSARs for PBPK modelling of environmental contaminants. *SAR and QSAR in Environmental Research*, 22, 129-169.

Pichardo J. C., Trindade A. A., Brindle J. M., Bolch W. E., (2007). Method for estimating skeletal spongiosa volume and active marrow mass in adult male and adult female. *The journal of nuclear medicine*, 48, 1880-1888.

Preisler, H. D., Raza, A., Gopal, V., Ahmad, S., Bokhari, J., (1993). Distribution of cell cycle times amongst the leukemia cells within individual patients with acute myeloid leukemia. *Leukemia research*, 19, 693-698.

Quartino A., Karlsson M. O., Freijs A., Jonsson N., Nygren P., Kristensen J., Lindhagen E., Larsson R., (2007). Modelling of in vitro drug activity and prediction of clinical outcome in acute myeloid leukemia. *Journal of clinical pharmacology*, 47, 1014-2.

Ratain M., Plunkett W. K., (2003). Chapter 64: Pharmacology, Holland-Frei Cancer Medicine. 6th ed. Hamilton: BC Decker Inc.

Raza, A., Maheshwari, Y., Preisler, H. D., (1987). Differences in cell cycle characteristics among patients with acute nonlymphocytic leukemia. *Blood*, 69, 1647-1653.

Raza A., Preisler HD., Day R., Yasin Z., White M., Lykins J., Kukla C., Barcos M., Bennett J., Browman G., (1990). Direct relationship between remission duration in acute myeloid leukemia and cell cycle kinetics: a leukemia intergroup study. *Blood*, 76, 2191-2197.

Reich, S. D., Bachur, N. R., Goebel, R. H., Berman, M., (1977). A pharmacokinetic model for high-dose methotrexate infusions in man. *Journal of pharmacokinetics and biopharmaceutics*, *5*(5), 421-33.

Relling, M V, Yanishevski, Y., Nemec, J., Evans, W. E., Boyett, J. M., Behm, F. G., Pui, C.H., (1998). Etoposide and antimetabolite pharmacology in patients who develop secondary acute myeloid leukemia. *Leukemia*, 346-352.

Richard, B., Launay-Iliadis, M. C., Iliadis, A., Just-Landi, S., Blaise, D., Stoppa, A. M., Viens, P., Gaspard, M.H., Maraninchi, D., Cano, J.P., Carcassonne, Y., (1992). Pharmacokinetics of mitoxantrone in cancer patients treated by high-dose chemotherapy and autologous bone marrow transplantation. *British journal of cancer*, *65*, 399-404.

Rooij T. V., Marsh S., (2011). Improving oncology outcomes through targeted therapeutics will require electronic delivery systems, Future Oncology, 5, p. 649-656.

Saltzman, W. M., (2001). *Drug Delivery: Engineering principles for drug therapy*. Oxford: University Press.

Sidoli F. R., Asprey S. P., Mantalaris A., (2006). A coupled single cell-population-balance model for mammalian cell cultures. *Industrial and Engineering Chemistry Research*, 45, 5801-5811.

Slevin M. L., Piall E. M., Aherne G. W., Johnston A., Sweatman M.C., Lister T. A., (1981). The pharmacokinetics of subcutaneous cytosine arabinoside in patients with AML. Br J Clin Pharmacol, 12, 507-510.

Schmitt W., (2008). General approach for the calculation of tissue to plasma partition coefficients. Toxicology in vitro, 22, 457-467.

Sherer, E., Hannemann, R. E., Rundell, A., Ramkrishna, D., (2006). Analysis of resonance chemotherapy in leukemia treatment via multi-staged population balance models. *Journal of theoretical biology*, 240, 648-61.

Somayaji M. R., Xenos M., Zhang L., Mekarski, Linninger A. A., (2008). Systematic design of drug delivery therapies. Computers and chemical engineering, 32, 89-98.

Stryckmans P., Delalieux G., Manaster J., Socquet M., (1970).The potentiality of out-of-cycle acute leukemic cells to synthesize DNA. *Blood*, 36, 697-703.

Swan G. W., (1985). Optimal control applications in the chemotherapy of multiple myeloma. Journal of mathematics applied in medicine and biology, 2, 139-160.

Swierniak A., Kimmel M.m Smieja J., (2009). Mathematical modelling as a tool for planning anticancer therapy. European journal of pharmacology, 625, 108-121.

Thomas C. S., Baker M., (2007). Overhauling clinical trials. *Nature Biotechnology*, 25, 287 - 292 .

UCLH - Dosage Adjustment for Cytotoxics in Renal Impairment (Version 3 - updated January2009) Available at: http://www.eastmidlandscancernetwork.nhs.uk/Library/RenalDosageAdjustments.pdf

Undevia S. D., Gomez-Abuin CG., Ratain M. J., (2005). Pharmacokinetic variability of anticancer agents. *Nature reviews*, 5, 447-458.

Vo T., Ryan J., Carrasco R., Neuberg, Rossi D., Stone R. M., DeAngelo D. J., Frattini M. G., Letai., (2012). Relative mitochondrial priming of myeloblasts and normal HSCs determines chemotherapeutic success in AML. *Cell*, 151, 344-355.

Weinberg O. K., Seethram M., Ren L., Seo K., Ma L., Merker J. D., Gotlib J., Zehnder J. L., Arber D. A.,(2009). Clinical characterisation of acute myeloid leukemia with myelodyspalsia-related changes as defined by the 2008 WHO classification system. *Blood*, 113, 1906-1908.

Wennesland, R., Brown, E., Hopper, J., Hodges, J. L., Guttentag, O. E., Scott, K. G., Tucker,I. N. and Bradley, B. (1959), 'Red cell, Plasma and Blood Volume in Healthy Men measured by Radiochromium (Cr51) Cell Tagging and Hematocrit: Influence of Age, Somatotype and Habits of Physical Activity on the Variance after Regression of Volumes to Height and Weight combined', *Journal of Clinical Investigation,* 38(7), 1065–1077.

Williams, W.J., Beutler, E., Erslev, A. J., Lichtman, M. A., (1983). *Hematology.* 3rd ed. USA: McGraw-Hill.

Workman, P. & Graham, M.A., Sidebottom, E., (1993). *Pharmacokinetics and cancer chemotherapy*. New York: CSHL Press.

Yuan, D., Lu, T., Wei, Y.G., Li, B., Yan, L. N., Wen, T. F., Zhao, J. C., (2008). Estimation of standard liver volume for liver transplantation in the Chinese population. *Transplantation proceeding*, 40, 3536-3540.

Yun Y. E., Edginton., (2013). Correlation-based prediction of tissue-to-plasma partition coefficients using readily available input parameters. *Xenobiotica*, 1-14.

Ziehn, T., Tomlin, A.S., (2009). GUI–HDMR – A software tool for global sensitivity analysis of complex models. *Environmental modelling and software*, 24, 775-785.

Appendix A:

Treatment outcome is highly dependent on the duration of the S-phase (Ts) and the total cycle duration (Tc). For this reason in this Appendix the dynamics of the leukemic cell population in the particular cell phases are presented for the two patients studied and analysed in Part I.

A1: Patient H1 under simulation with LDAC protocol

Table A1: Cells in S-phase, G_1-phase and G_2M-phase of patient H1 under simulation with LDAC protocol

	Cells in S-phase	Cells in G_1-phase	Cells in G_2M - phase
Beginning of 1st Cycle	4.17E+10	1.34E+11	6.58E+09
End of 1st Cycle	2.09E+09	1.92E+10	2.43E+08
Beginning of 2nd Cycle	5.59E+10	1.79E+11	8.82E+09
End of 2nd Cycle	2.80E+09	2.57E+10	3.26E+08
Beginning of 3rd Cycle	7.49E+10	2.40E+11	1.18E+10
End of 3rd Cycle	3.75E+09	3.44E+10	4.36E+08
Beginning of 4th Cycle	1.00E+11	3.23E+11	1.59E+10
End of 4th Cycle	5.03E+09	4.62E+10	5.86E+08

*The initial population of cells in the separate phases is calculated by the multiplication of the leukemic population at the beginning of each cycle times the percentage of cell population in each phase for each cycle (equations 3.15-3.17 section 3.3.1).

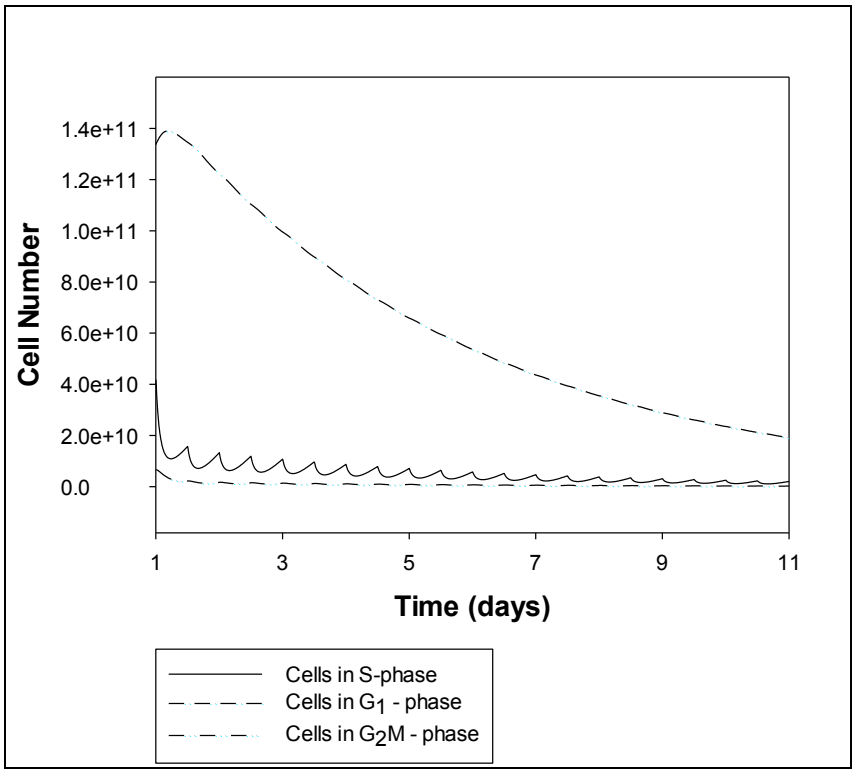

Figure A1: Patient H1 Cells in S-phase, G1-phase and G2M-phase over the 1st cycle of the LDAC simulation protocol

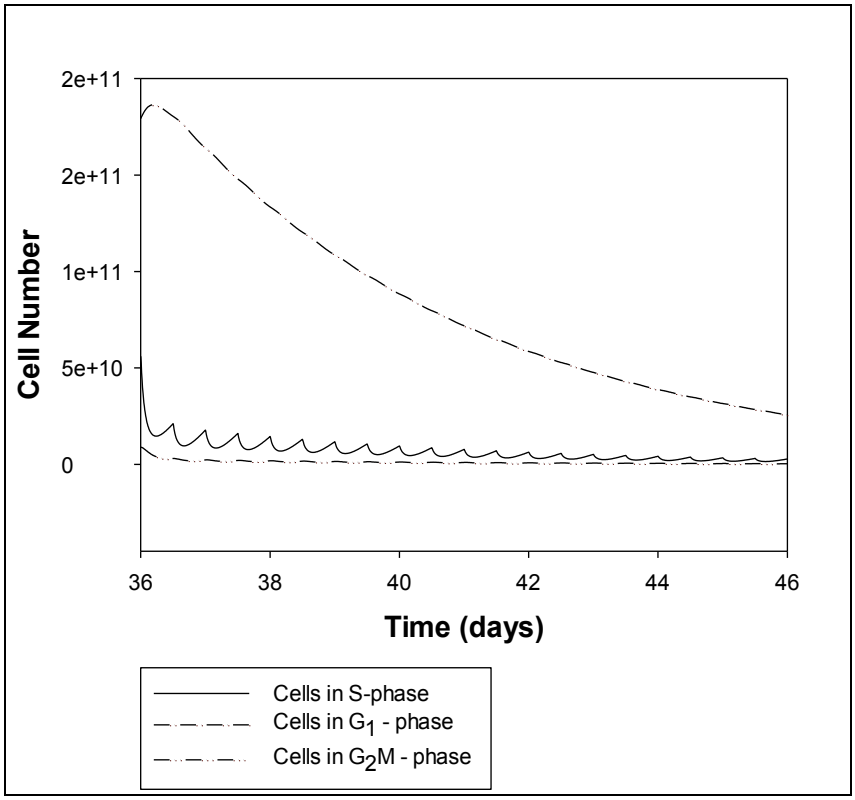

Figure A2: Patient H1 Cells in S-phase, G1-phase and G2M-phase over the 2nd cycle of the LDAC simulation protocol

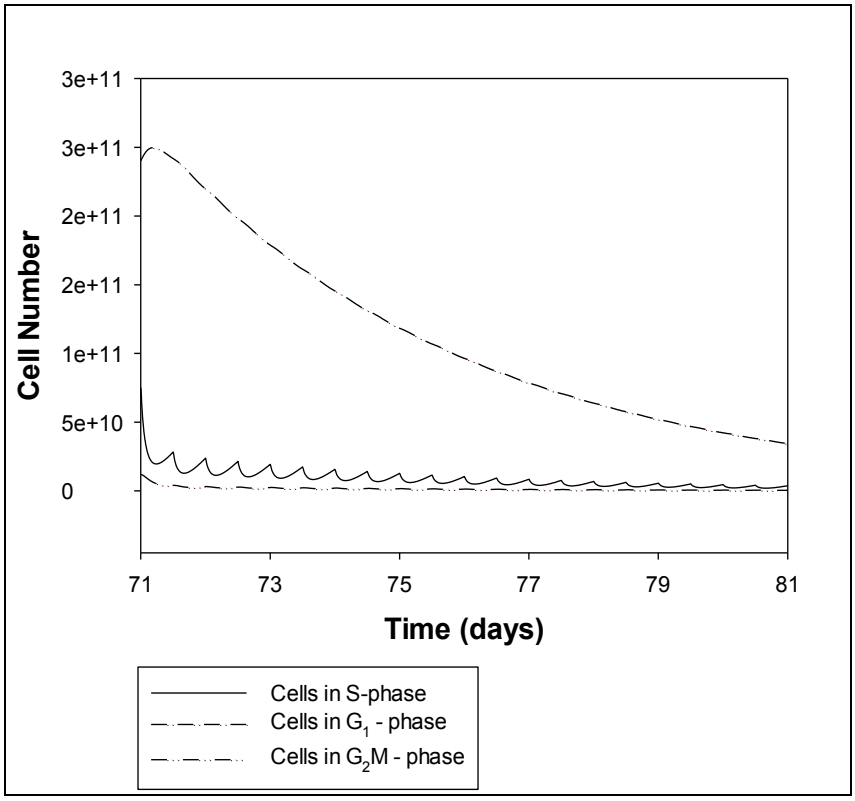

Figure A3: Patient H1 Cells in S-phase, G1-phase and G2M-phase over the 3rd cycle of the LDAC simulation protocol

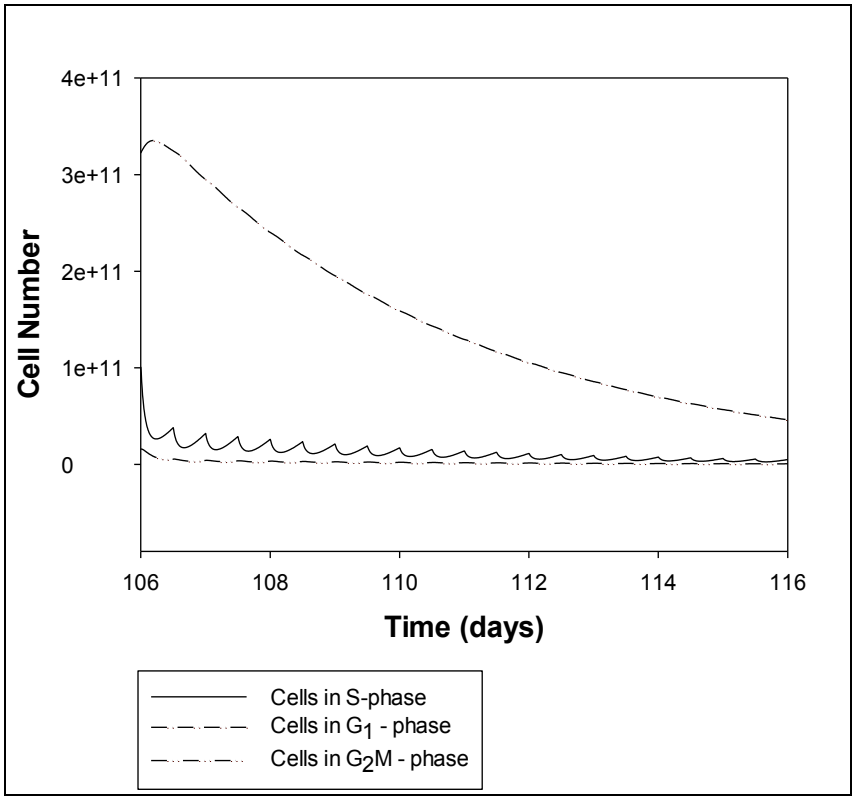

Figure A4: Patient H1 Cells in S-phase, G1-phase and G2M-phase over the 4th cycle of the LDAC simulation protocol

A2: Patient H1 under simulation with DA protocol

Table A2: Cells in S-phase, G_1-phase and G_2M-phase of Patient H1 under simulation with DA protocol

	Cells in S-phase	Cells in G_1-phase	Cells in G_2M - phase
Beginning of 1st Cycle	4.12E+10	1.34E+11	6.50E+09
End of 1st Cycle	2574654.2	7.46E+07	348131.75
Beginning of 2nd Cycle	1.76E+08	5.76E+08	2.79E+07
End of 2nd Cycle	11034.237	319812.78	1491.9939
Beginning of 3rd Cycle	769047.6	2509523.8	121428.57
End of 3rd Cycle	48.097878	1394.0555	6.503553
Beginning of 4th Cycle	3392.8572	11071.429	535.7143
End of 4th Cycle	0.21219935	6.1502643	0.02869239

*The initial population of cells in the separate phases is calculated by the multiplication of the leukemic population at the beginning of each cycle times the percentage of cell population in each phase for each cycle (equations 3.15-3.17 section 3.3.1).

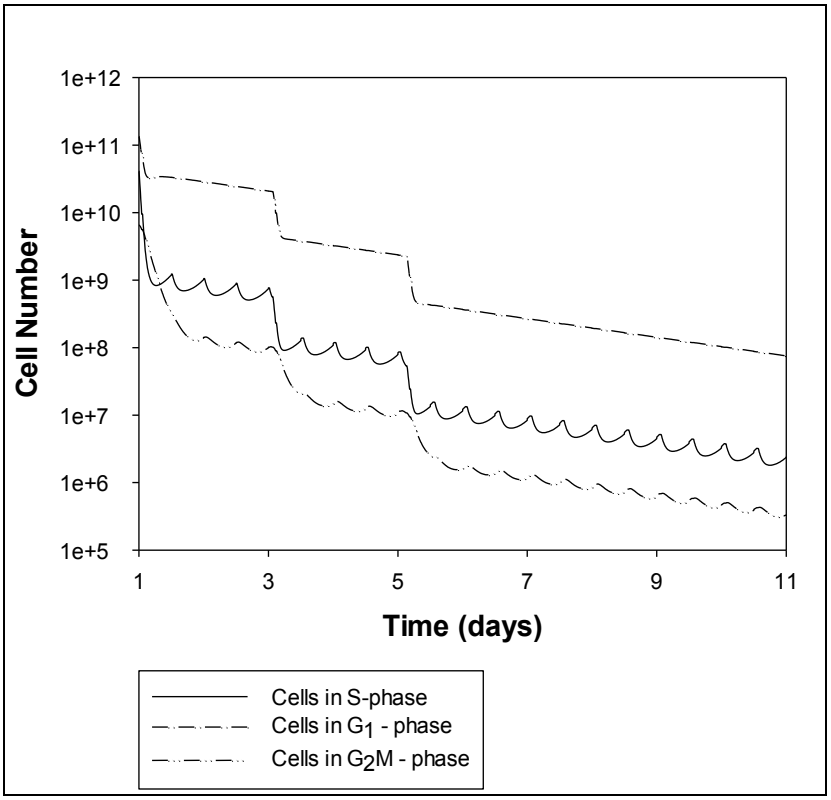

Figure A5: Patient H1 Cells in S-phase, G1-phase and G2M-phase over the 1st cycle of the DA simulation protocol

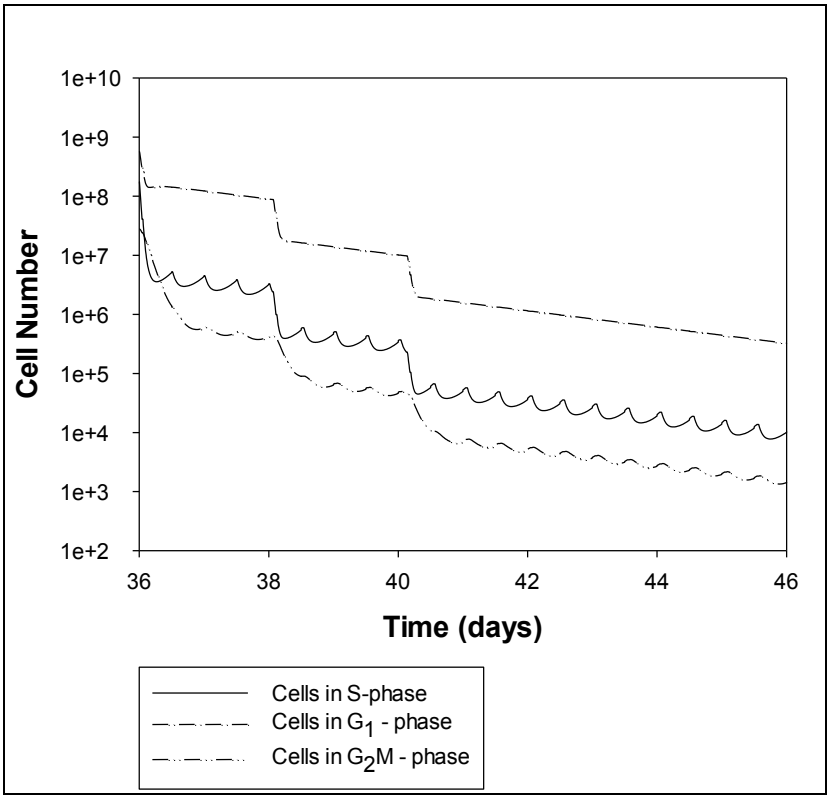

Figure A6: Patient H1 Cells in S-phase, G1-phase and G2M-phase over the 2nd cycle of the DA simulation protocol

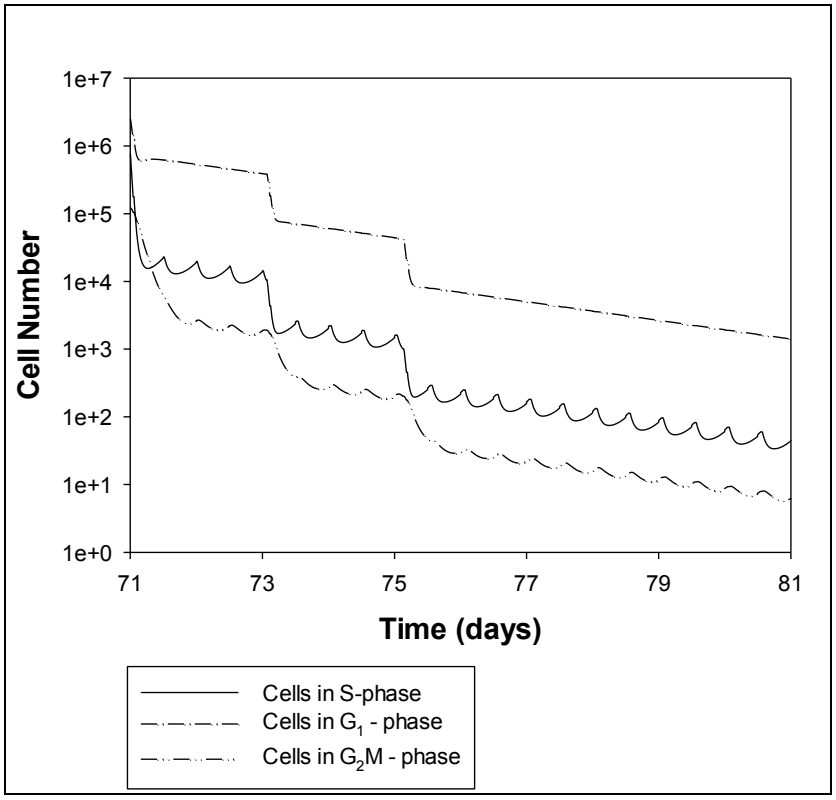

Figure A7: Patient H1 Cells in S-phase, G1-phase and G2M-phase over the 3rd cycle of the DA simulation protocol

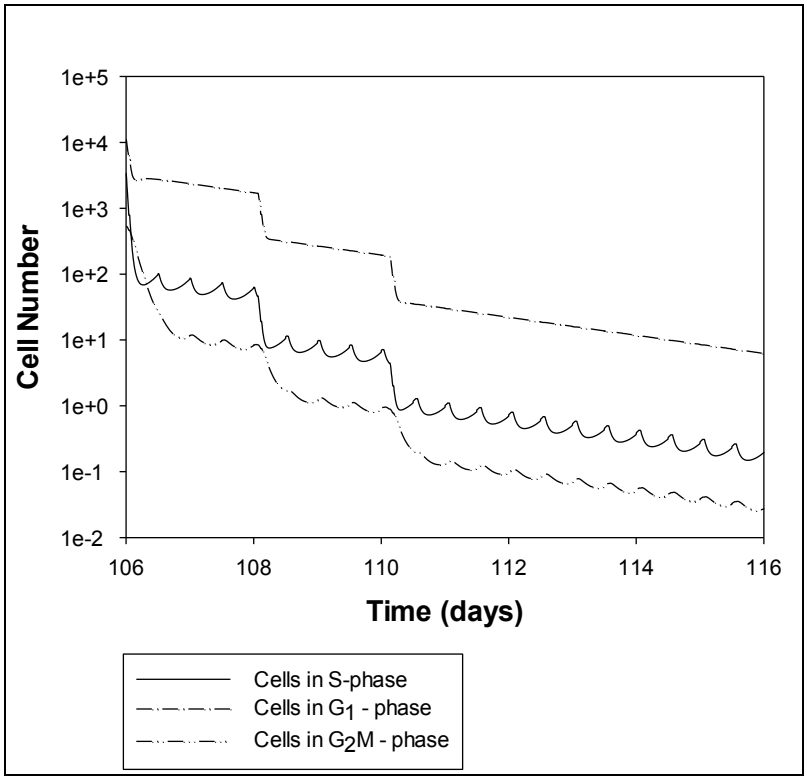

Figure A8: Patient H1 Cells in S-phase, G1-phase and G2M-phase over the 4th cycle of the DA simulation protocol

A3: Patient H2 under simulation of LDAC protocol

Table A3: Cells in S-phase, G_1-phase and G_2M-phase of Patient H2 under simulation with LDAC protocol

	Cells in S-phase	Cells in G_1-phase	Cells in G_2M - phase
Beginning of 1st Cycle	4.93E+10	5.60E+10	6.72E+09
End of 1st Cycle	1.26E+08	4.45E+08	1.35E+07
Beginning of 2nd Cycle	3.17E+09	3.60E+09	4.32E+08
End of 2nd Cycle	8119624.5	2.86E+07	870052.2
Beginning of 3rd Cycle	2.02E+08	2.30E+08	2.76E+07
End of 3rd Cycle	518754.6	1826699	55586.76
Beginning of 4th Cycle	1.30E+07	1.48E+07	1776000
End of 4th Cycle	33380.617	117543.71	3576.8752

*The initial population of cells in the separate phases is calculated by the multiplication of the leukemic population at the beginning of each cycle times the percentage of cell population in each phase for each cycle (equations 3.15-3.17 section 3.3.1).

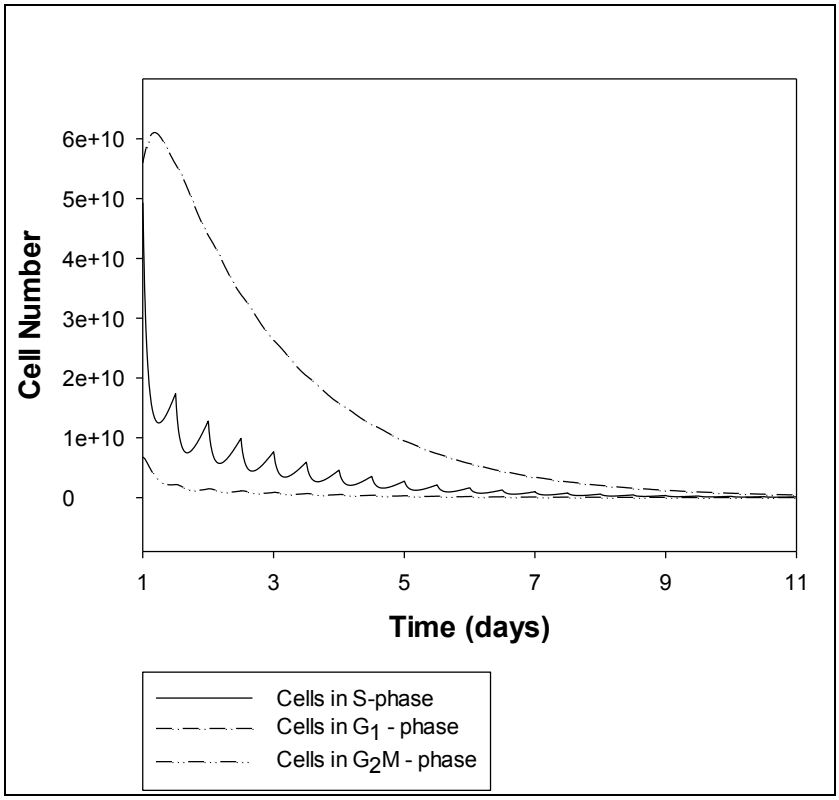

Figure A9: Patient H2 Cells in S-phase, G1-phase and G2M-phase over the 1st cycle of the LDAC simulation protocol

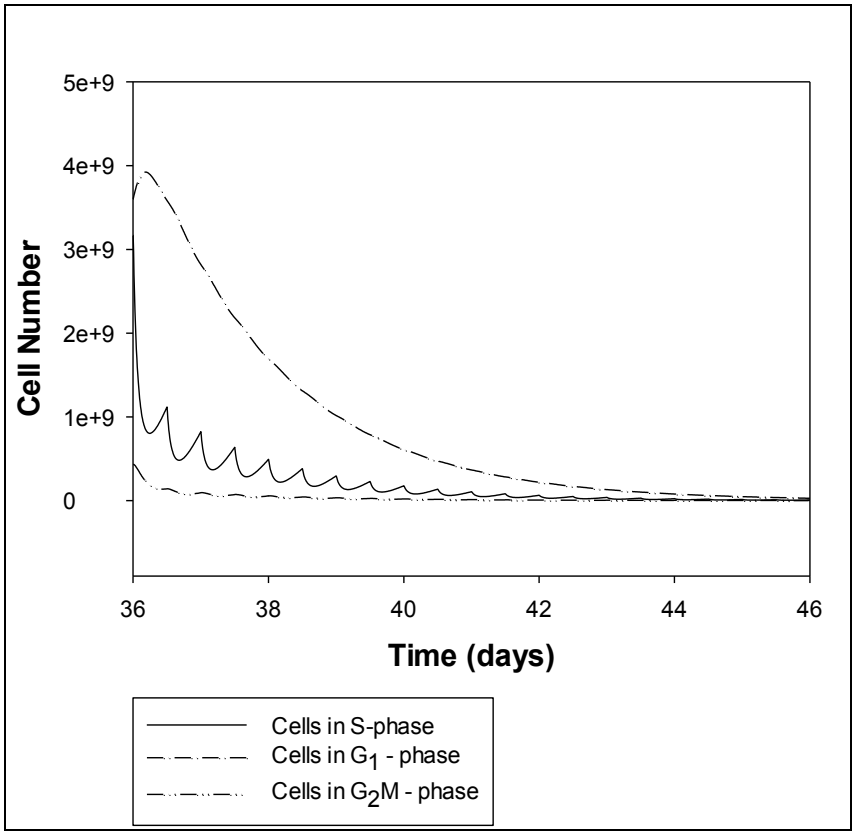

Figure A10: Patient H2 Cells in S-phase, G1-phase and G2M-phase over the 2nd cycle of the LDAC simulation protocol

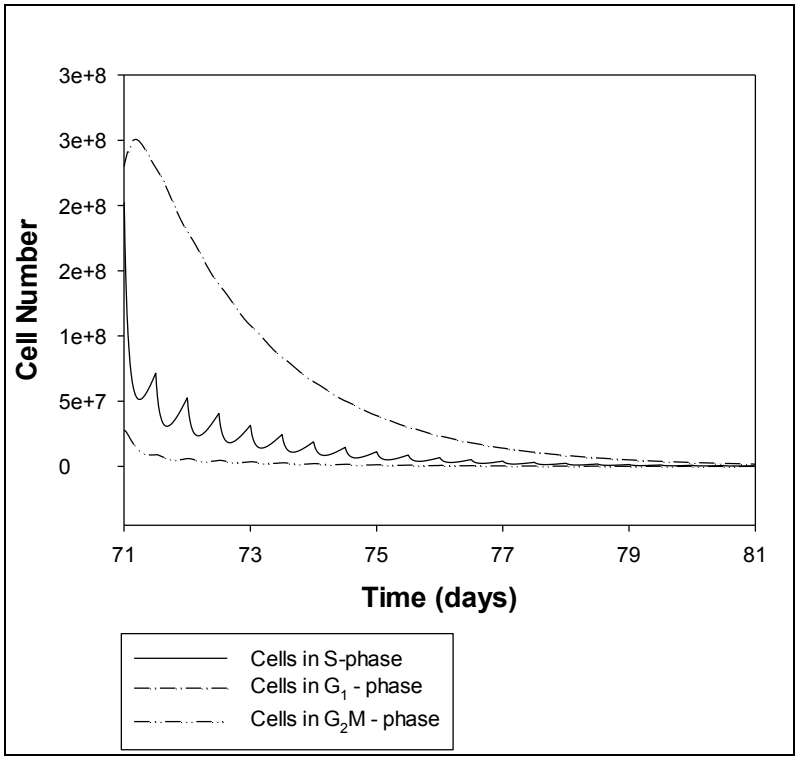

Figure A11: Patient H2 Cells in S-phase, G1-phase and G2M-phase over the 3rd cycle of the LDAC simulation protocol

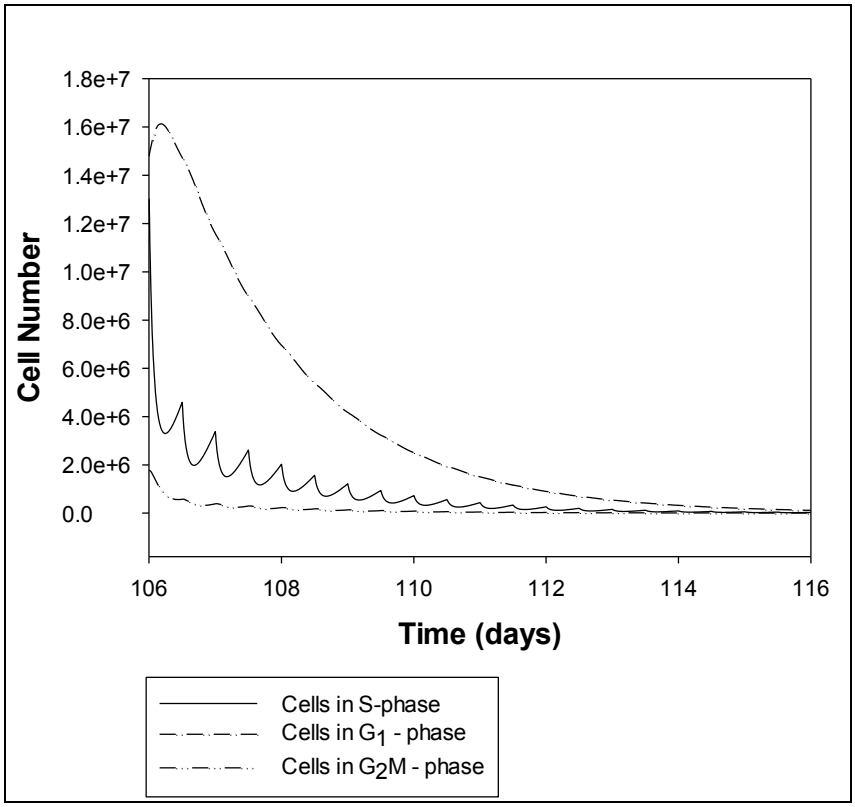

Figure A12: Patient H2 Cells in S-phase, G1-phase and G2M-phase over the 4th cycle of the LDAC simulation protocol

A4: Patient H2 under simulation of DA protocol

Table A4: Cells in S-phase, G_1-phase and G_2M-phase of Patient H2 under simulation with DA protocol

	Cells in S-phase	Cells in G_1-phase	Cells in G_2M - phase
Beginning of 1st Cycle	4.93E+10	5.60E+10	6.72E+09
End of 1st Cycle	39524.688	439012.44	4868.7617
Beginning of 2nd Cycle	2138400	2430000	291600
End of 2nd Cycle	1.7151027	19.049969	0.21127135
Beginning of 3rd Cycle	88	100	12
End of 3rd Cycle	7.06E-05	7.84E-04	8.69E-06

*The initial population of cells in the separate phases is calculated by the multiplication of the leukemic population at the beginning of each cycle times the percentage of cell population in each phase for each cycle (equations 3.15-3.17 section 3.3.1).

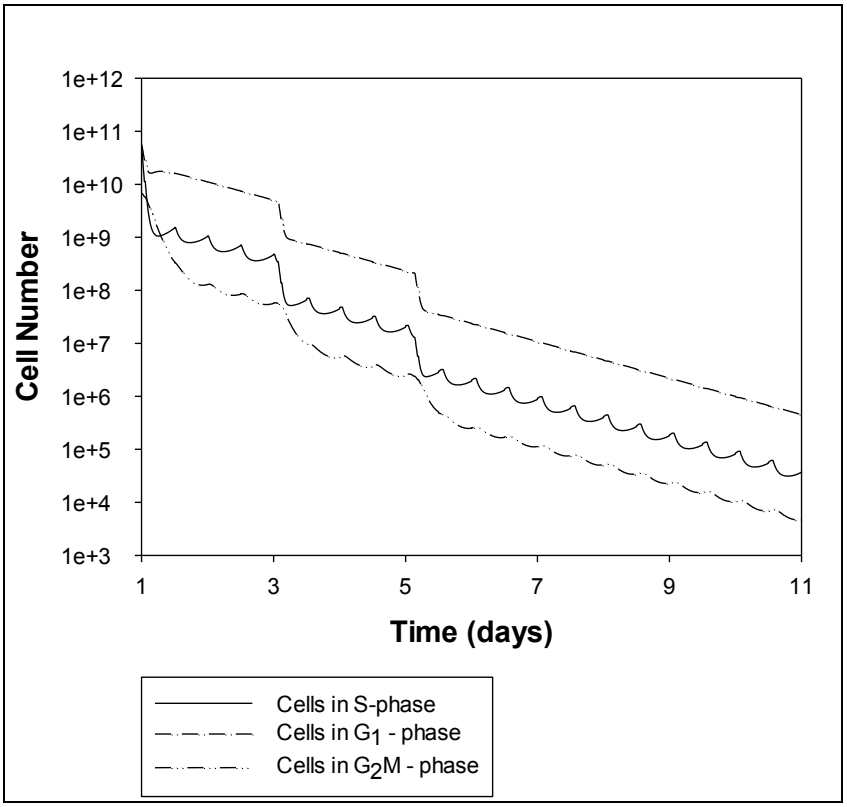

Figure A13: Patient H2 Cells in S-phase, G1-phase and G2M-phase over the 1st cycle of the DA simulation protocol

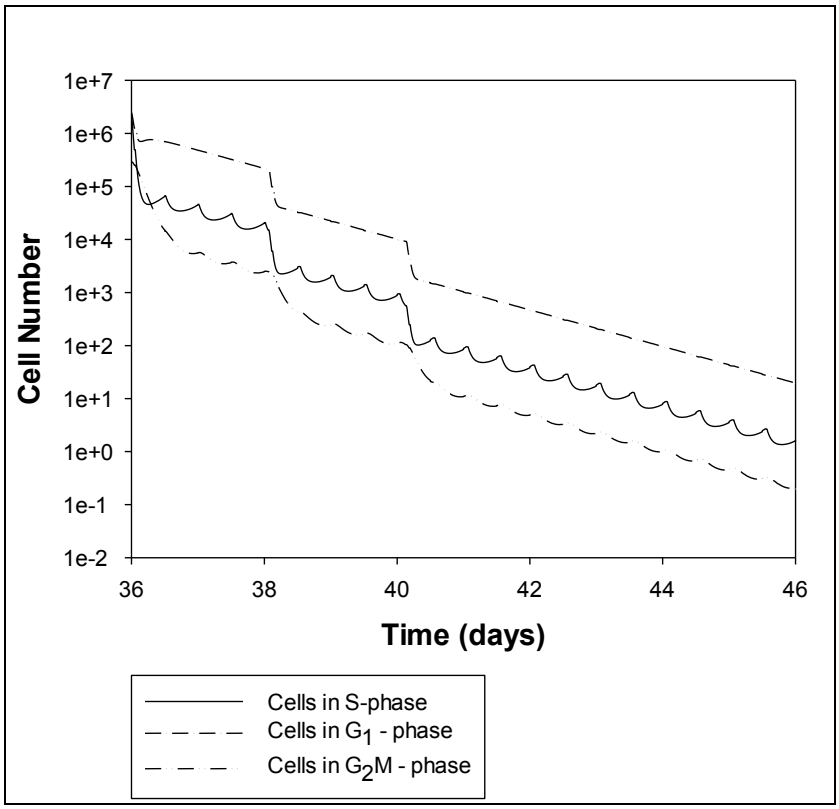

Figure A14: Patient H2 Cells in S-phase, G1-phase and G2M-phase over the 2nd cycle of the DA simulation protocol

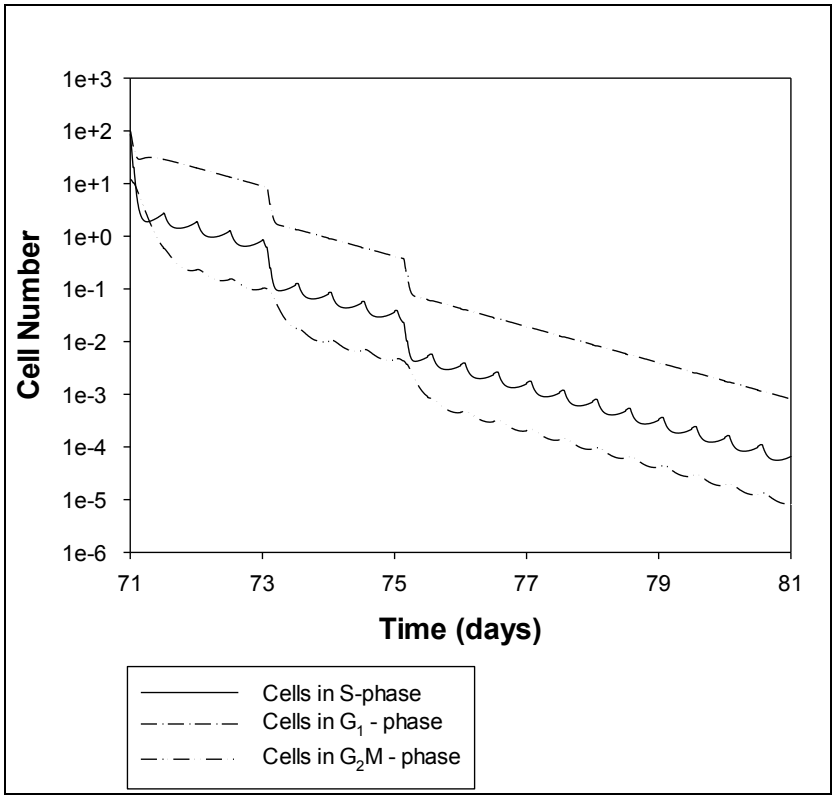

Figure A15: Patient H2 Cells in S-phase, G1-phase and G2M-phase over the 3rd cycle of the DA simulation protocol

A5: Patient H1 under optimisation of LDAC protocol

Table A5: Cells in S-phase, G_1-phase and G_2M-phase of Patient H1 under optimisation of LDAC protocol

	Cells in S-phase	Cells in G_1-phase	Cells in G_2M - phase
Beginning of 1st Cycle	4.17E+10	1.34E+11	6.58E+09
End of 1st Cycle	5.77E+07	1.16E+09	8290762.5
Beginning of 2nd Cycle	2.93E+09	9.41E+09	4.63E+08
End of 2nd Cycle	3909514.2	8.14E+07	587558.56
Beginning of 3rd Cycle	9.00E+08	6.61E+08	3.25E+07
End of 3rd Cycle	7.10E+07	6.70E+07	287523.97
Beginning of 4th Cycle	1.73E+08	5.56E+08	2.74E+07
End of 4th Cycle	3296483	5.63E+07	253690.77

*The initial population of cells in the separate phases is calculated by the multiplication of the leukemic population at the beginning of each cycle times the percentage of cell population in each phase for each cycle (equations 3.15-3.17 section 3.3.1).

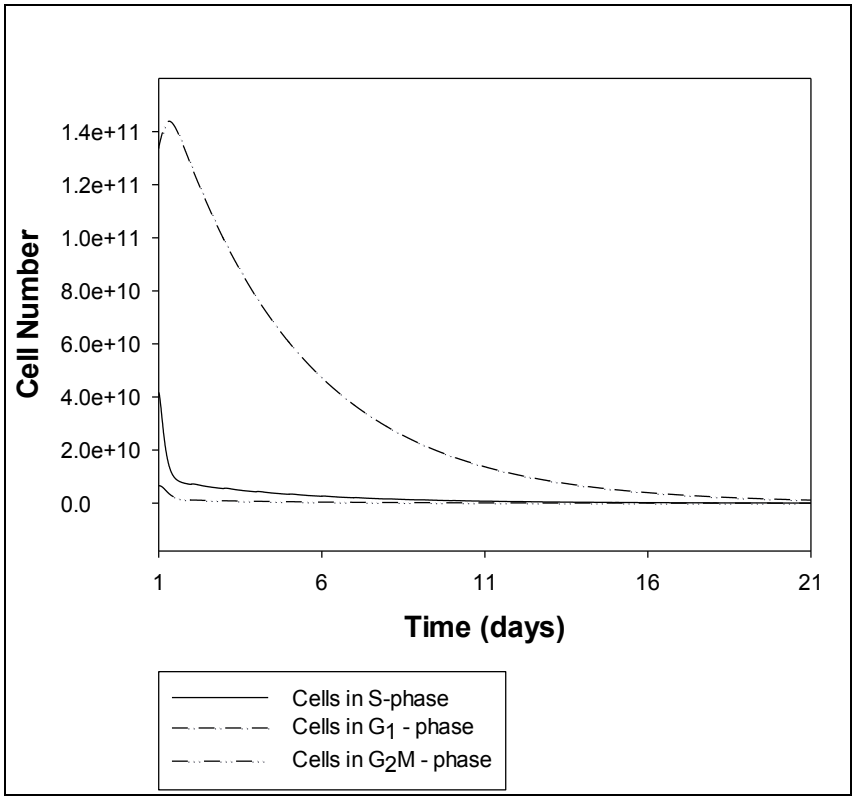

Figure A16: Patient H1 Cells in S-phase, G1-phase and G2M-phase over the 1st cycle of the LDAC optimisation protocol

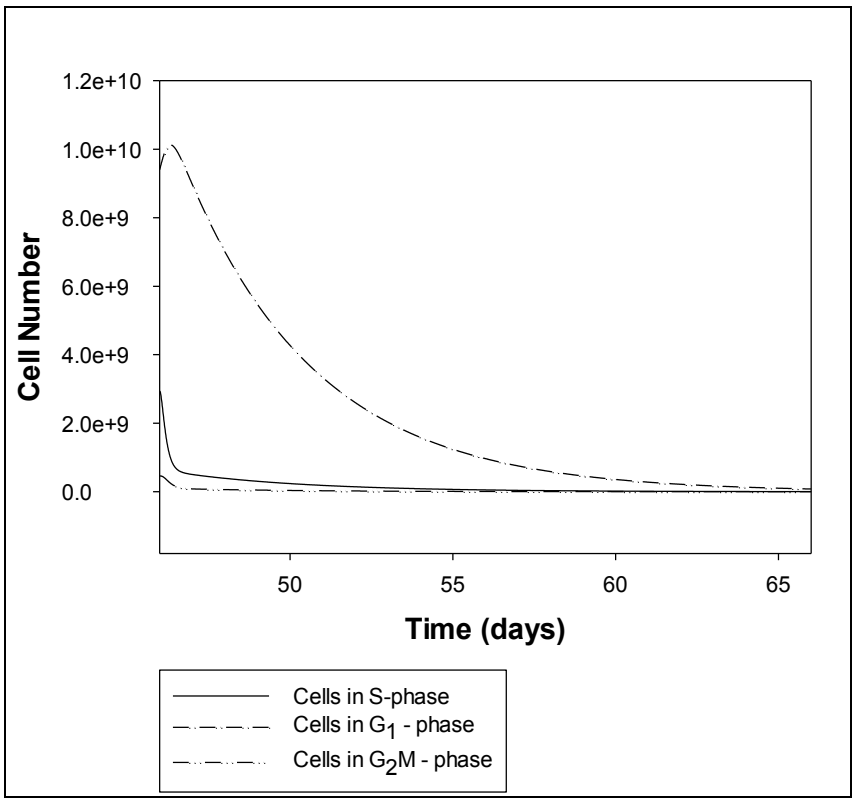

Figure A17: Patient H1 Cells in S-phase, G1-phase and G2M-phase over the 2nd cycle of the LDAC optimisation protocol

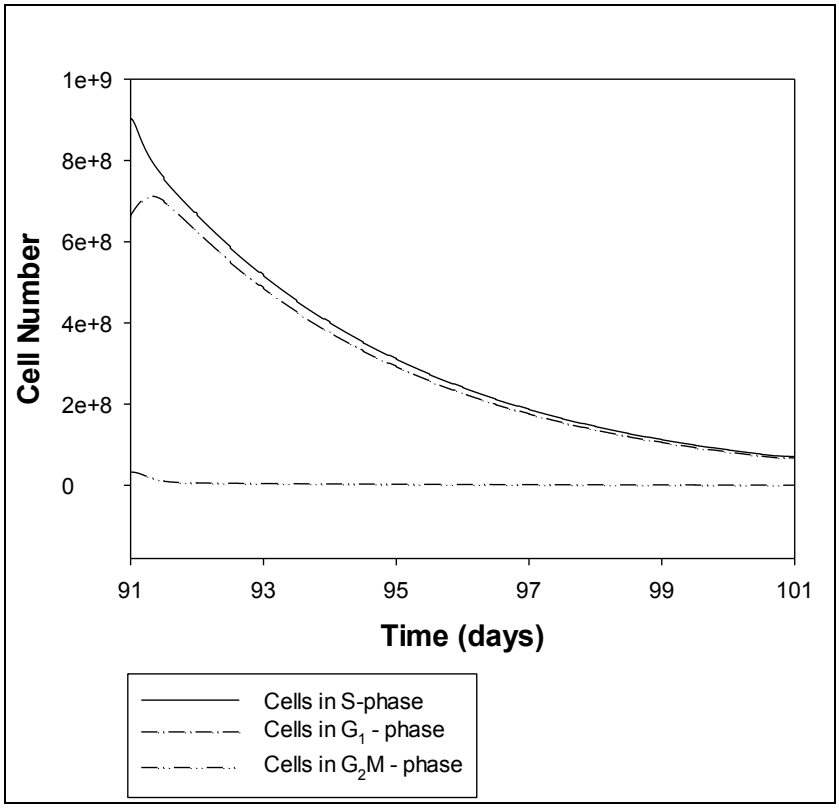

Figure A18: Patient H1 Cells in S-phase, G1-phase and G2M-phase over the 3rd cycle of the LDAC optimisation protocol

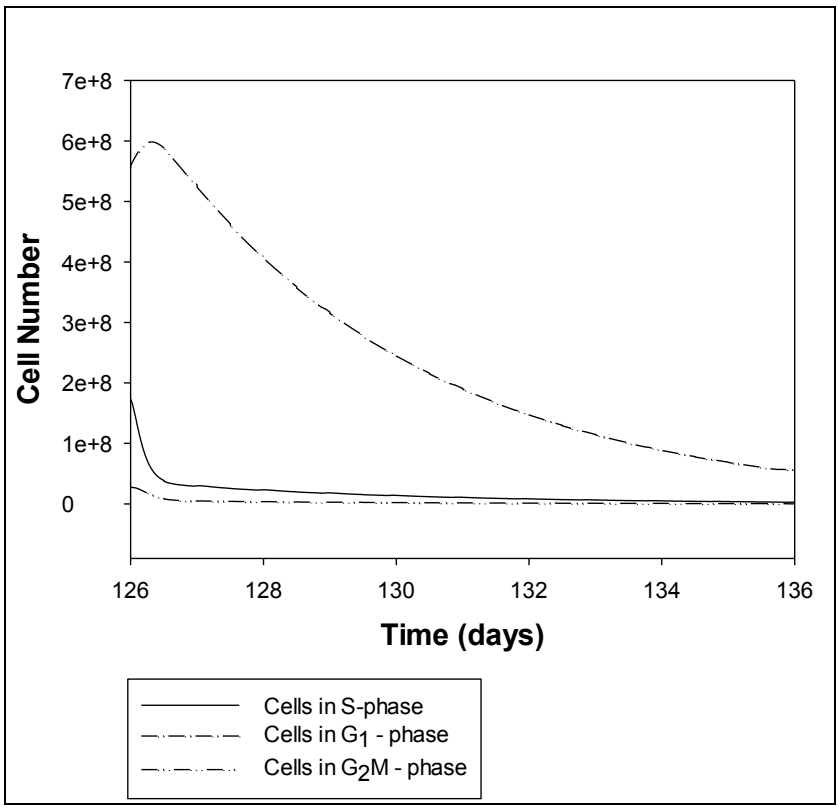

Figure A19: Patient H1 Cells in S-phase, G1-phase and G2M-phase over the 4th cycle of the LDAC optimisation protocol

A6: Patient H1 under optimisation of DA protocol

Table A6: Cells in S-phase, G_1-phase and G_2M-phase of Patient H1 under optimisation of DA protocol

	Cells in S-phase	Cells in G_1-phase	Cells in G_2M - phase
Beginning of 1st Cycle	4.12E+10	1.34E+11	6.50E+09
End of 1st Cycle	813636.7	6.63E+07	90931.73
Beginning of 2nd Cycle	6.60E+08	4.87E+08	2.36E+07
End of 2nd Cycle	243661.14	240380.83	329.75244
Beginning of 3rd Cycle	542857.1	1771428.6	85714.29
End of 3rd Cycle	10.729266	874.11456	1.1991037
Beginning of 4th Cycle	1978.9404	6457.595	312.4643
End of 4th Cycle	0.03832092	3.1918411	0.004544233

*The initial population of cells in the separate phases is calculated by the multiplication of the leukemic population at the beginning of each cycle times the percentage of cell population in each phase for each cycle (equations 3.15-3.17 section 3.3.1).

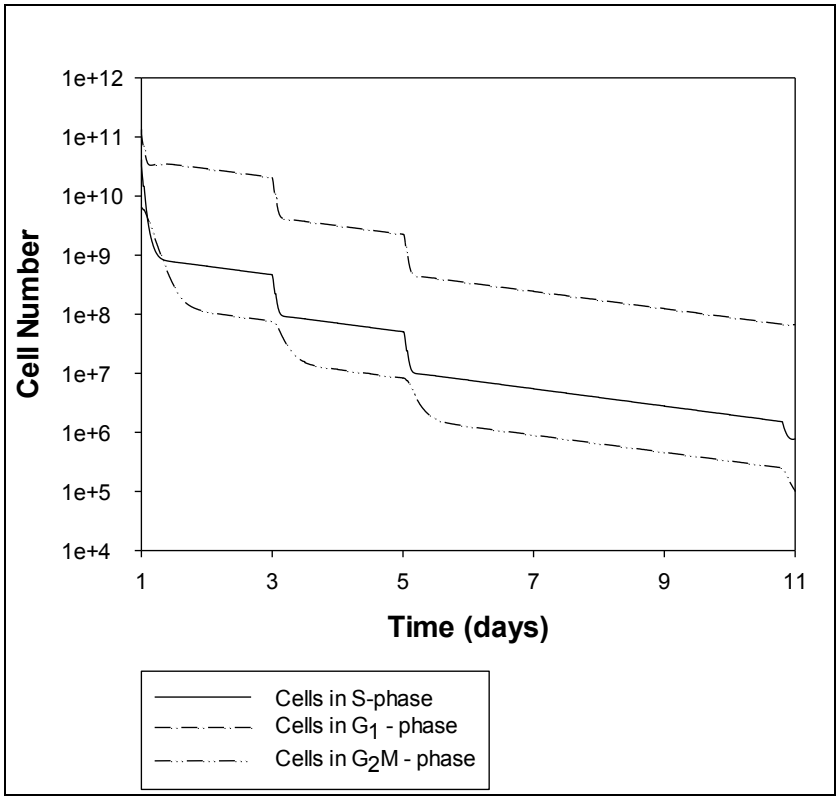

Figure A21: Patient H1 Cells in S-phase, G1-phase and G2M-phase over the 1st cycle of the DA optimisation protocol

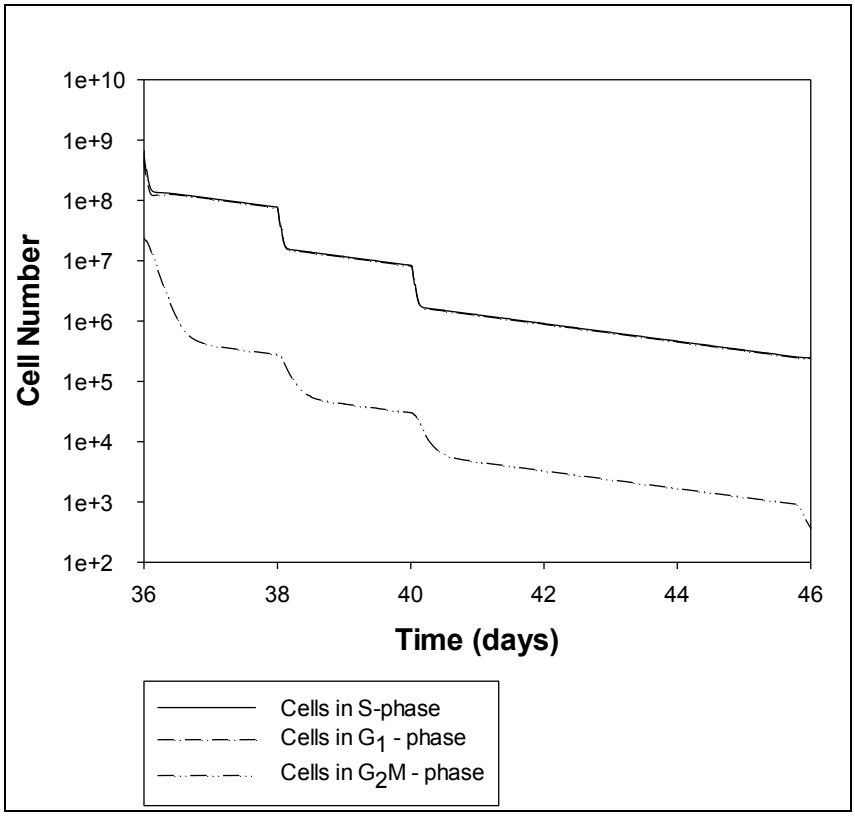

Figure A22: Patient H1 Cells in S-phase, G1-phase and G2M-phase over the 2nd cycle of the DA optimisation protocol

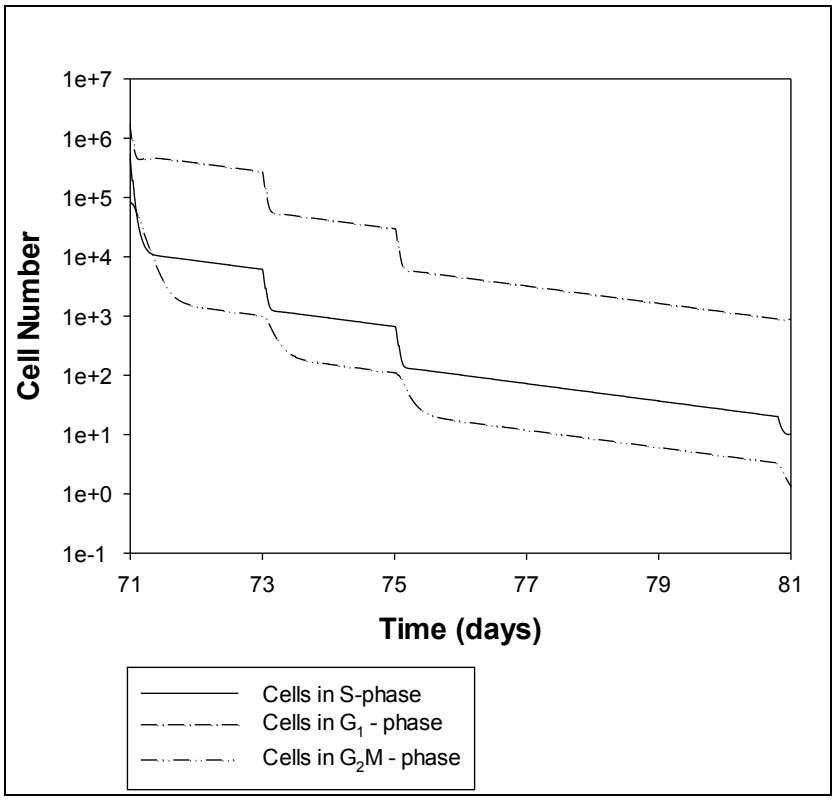

Figure A23: Patient H1 Cells in S-phase, G1-phase and G2M-phase over the 3rd cycle of the DA optimisation protocol

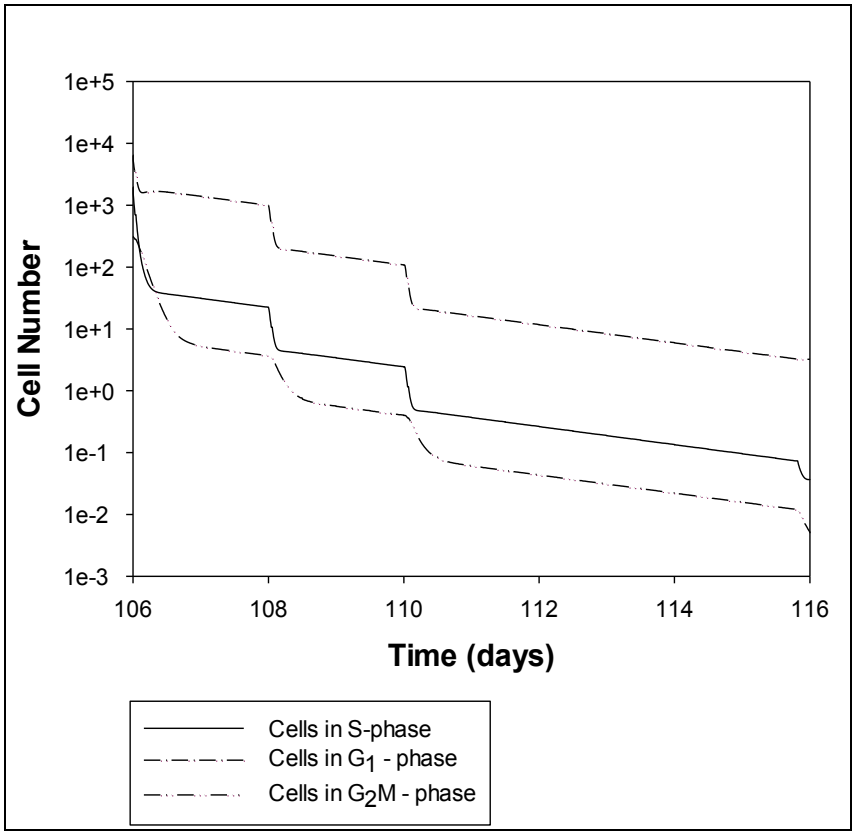

Figure A24: Patient H1 Cells in S-phase, G1-phase and G2M-phase over the 4th cycle of the DA optimisation protocol

A7: Patient H2 under optimisation of LDAC protocol

Table A7: Cells in S-phase, G_1-phase and G_2M-phase of Patient H2 under the optimisation of LDAC protocol

	Cells in S-phase	Cells in G_1-phase	Cells in G_2M - phase
Beginning of 1st Cycle	4.93E+10	5.60E+10	6.72E+09
End of 1st Cycle	1.97E+07	1.99E+08	1774969.5
Beginning of 2nd Cycle	1.06E+09	1.21E+09	1.45E+08
End of 2nd Cycle	424974.2	4308155.5	38352.02
Beginning of 3rd Cycle	2.30E+07	2.62E+07	3138000
End of 3rd Cycle	9184.359	93106.01	828.84735
Beginning of 4th Cycle	504000	624000	72000
End of 4th Cycle	289.5426	3035.9255	26.171131

*The initial population of cells in the separate phases is calculated by the multiplication of the leukemic population at the beginning of each cycle times the percentage of cell population in each phase for each cycle (equations 3.15-3.17 section 3.3.1).

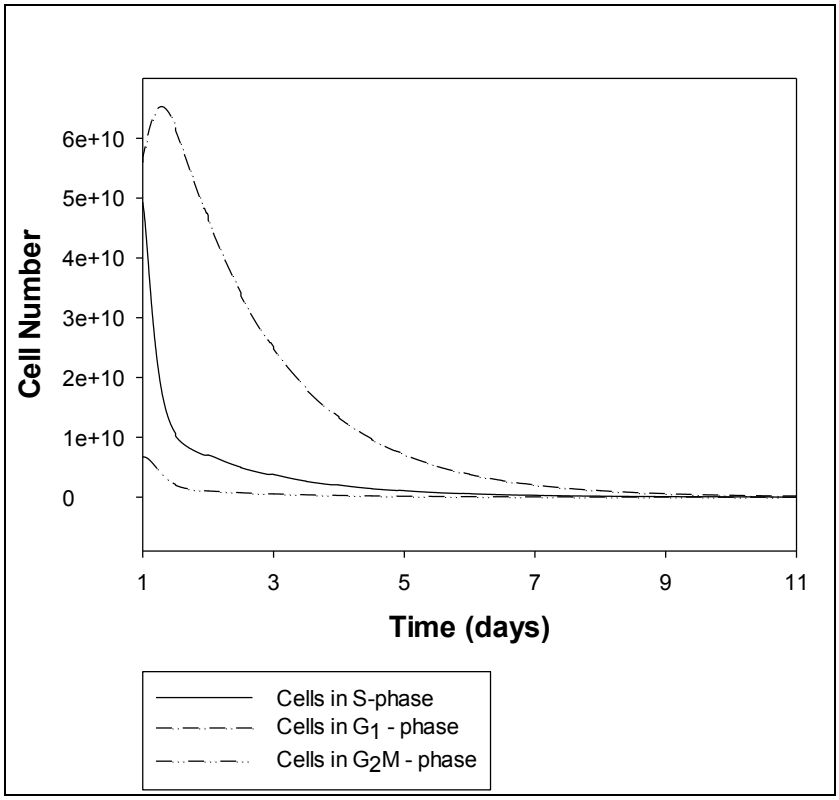

Figure A25: Patient H2 Cells in S-phase, G1-phase and G2M-phase over the 1st cycle of the LDAC optimisation protocol

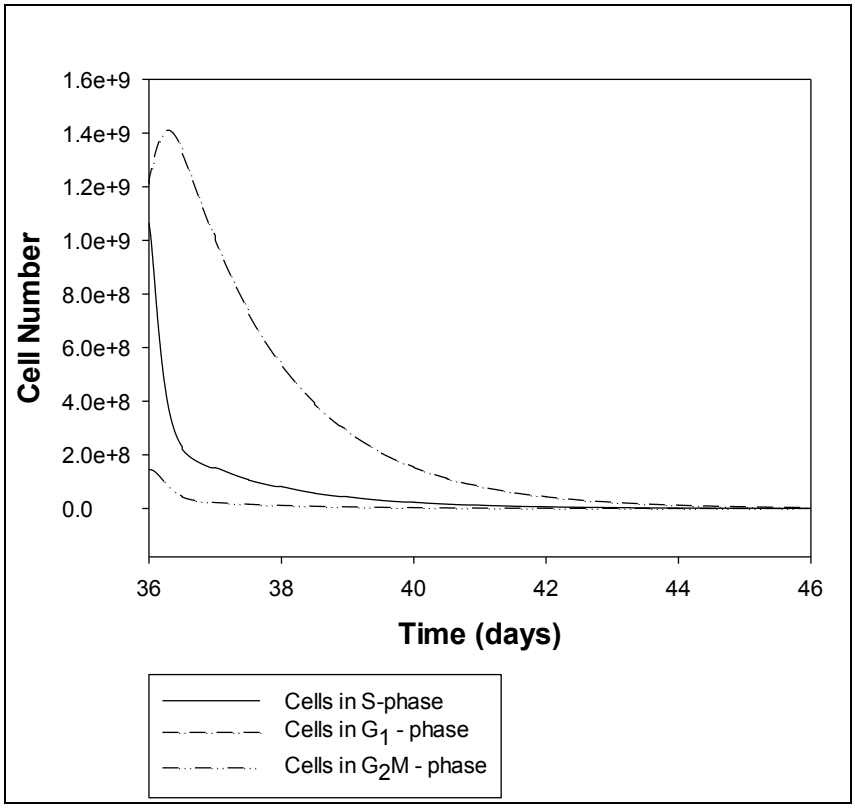

Figure A26: Patient H2 Cells in S-phase, G1-phase and G2M-phase over the 2nd cycle of the LDAC optimisation protocol

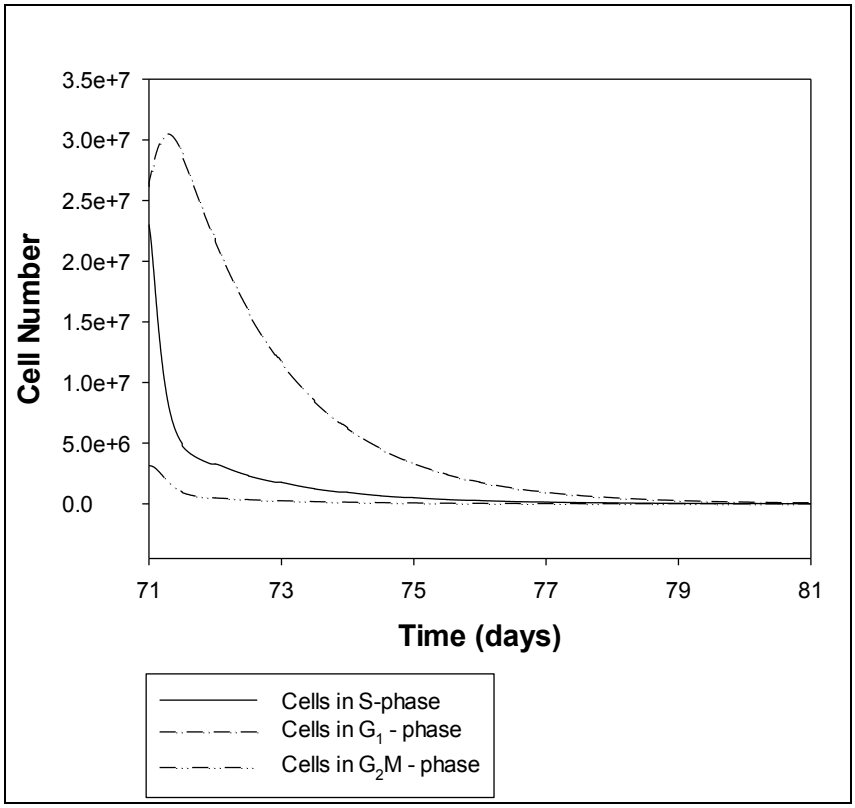

Figure A27: Patient H2 Cells in S-phase, G1-phase and G2M-phase over the 3rd cycle of the LDAC optimisation protocol

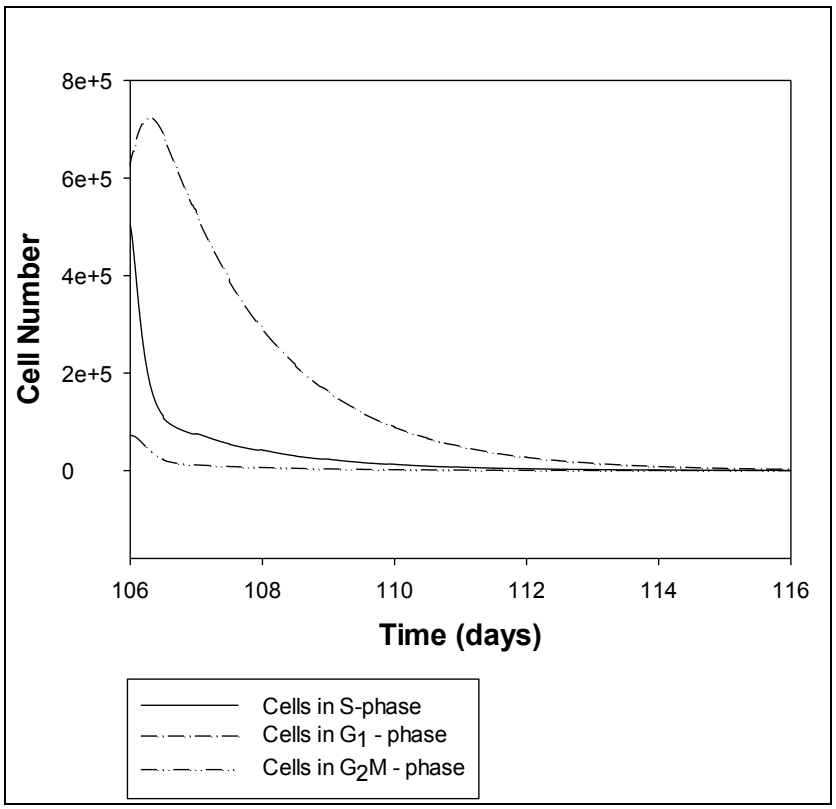

Figure A28: Patient H2 Cells in S-phase, G1-phase and G2M-phase over the 4th cycle of the LDAC optimisation protocol

A8: Patient H2 under optimisation of DA protocol

Table A8: Cells in S-phase, G_1-phase and G_2M-phase of Patient H2 under the optimisation of DA protocol

	Cells in S-phase	Cells in G_1-phase	Cells in G_2M - phase
Beginning of 1st Cycle	4.93E+10	5.60E+10	6.72E+09
End of 1st Cycle	20083.977	347152.5	3051.4778
Beginning of 2nd Cycle	1500000	1600000	200000
End of 2nd Cycle	0.09313364	0.6952326	0.018685918

*The initial population of cells in the separate phases is calculated by the multiplication of the leukemic population at the beginning of each cycle times the percentage of cell population in each phase for each cycle (equations 3.15-3.17 section 3.3.1).

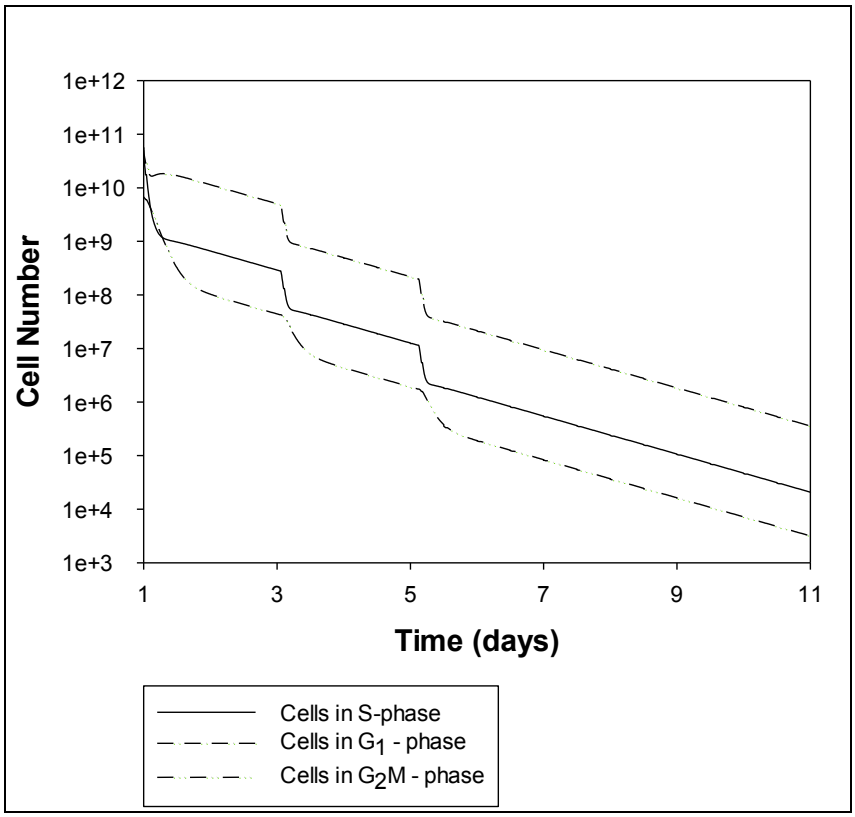

Figure A29: Patient H2 Cells in S-phase, G1-phase and G2M-phase over the 1st cycle of the DA optimisation protocol

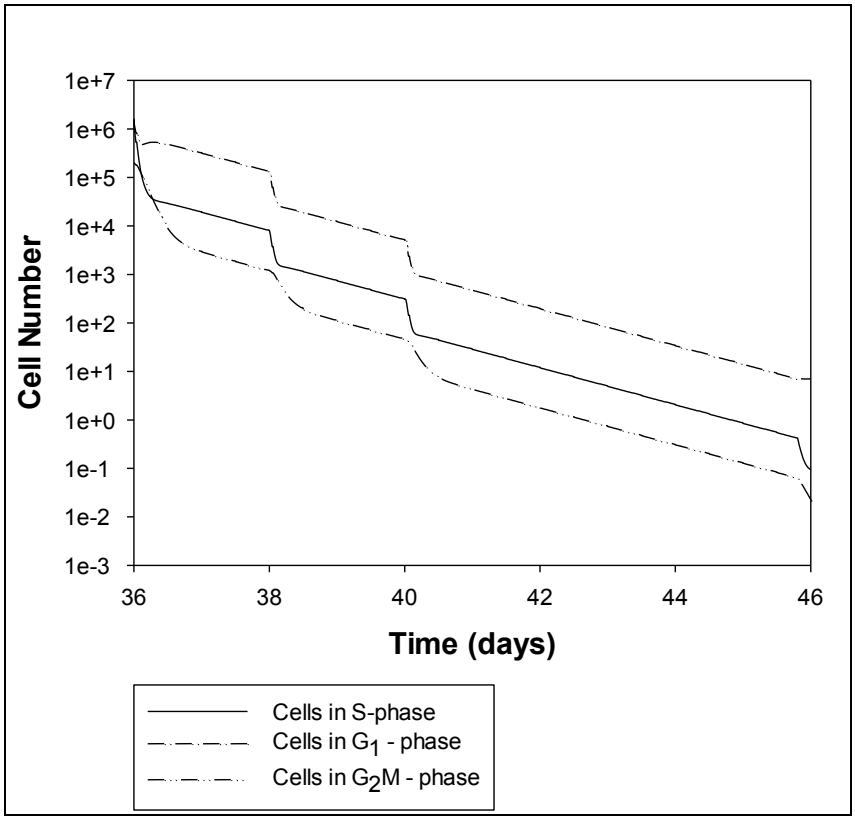

Figure A30: Patient H2 Cells in S-phase, G1-phase and G2M-phase over the 2nd cycle of the DA optimisation protocol

Appendix B:
Patient Protocols

Patient number: 001

Disease status: Secondary

Patient Characteristics:

Age: 75 years Sex: F Height: 152 cm

Body Weight: 56 Kg BSA: 1.54 m^2

I. Baseline Characteristics:

Pre-treatment Data	
Bone Marrow Aspirate	
%Blasts in BM aspirate	21 %
Prognostic category	Intermediate
Full Blood Count	**Date: 12/03/2010**
WBC (x10^9L)	8.7

II. Chemotherapy Treatment Schedule

Cycle	Date	Drugs	Doses	Dose Reduction	Route	Number of days and schedule given
1	Day 1	Ara-C	20 mg		SC	10 days, twice a day every 12 hrs
2	Day 37	Ara-C	20 mg		SC	10 days, twice a day every 12 hrs
3	Day 69	Ara-C	20 mg		SC	10 days, twice a day every 12 hrs
4	Day 105	Ara-C	20 mg		SC	10 days, twice a day every 12 hrs

III. Response to Treatment

Completion of Course	Cycle 1	Repeat marrow	Cycle 2	Repeat marrow	Cycle 3	Repeat marrow	Cycle 4	Repeat marrow
Date	Day 36		Day 70		Day 91		Day 146	
Cellularity (1= hypo, 2=normo, 3= hyper)	3		3		2		3	
Blasts (%)	14		4		5		15	
Marrow Response	PR		CR		CR		Relapse	

Patient number: 002

Disease status: Secondary

Patient Characteristics:
Age: 72 years Sex: F Height: 150 cm

Body Weight: 47 Kg BSA: 1.4 m^2

I. Baseline Characteristics:

Pre-treatment Data	
BM Aspirate	
%Blasts in BM aspirate	83 %
Prognostic category	Intermediate
Full Blood Count	**Date: 06/02/2008**
WBC (x10^9L)	46.5

II. Chemotherapy Treatment Schedule

Cycle	Date	Drugs	Doses	Dose Reduction	Route	Number of days and schedule given
1	Day 1	Ara-C	20 mg		SC	10 days, twice a day every 12 hrs
2						
3						
4						

III. Response to Treatment
Marrow examinations

Completion of Course	Cycle 1	Repeat marrow	Cycle 2	Repeat marrow	Cycle 3	Repeat marrow	Cycle 4	Repeat marrow
Date	Day 48							
Cellularity (1= hypo, 2=normo, 3= hyper)	3							
Blasts (%)	4							
Marrow Response	CR							

Patient number: 006

Disease status: De Novo

Patient Characteristics:
Age: 71 years Sex: F Height: 160 cm

Body Weight: 57 Kg BSA: 1.59 m^2

I. Baseline Characteristics:

Pre-treatment Data	
BM Aspirate	
%Blasts in BM aspirate	36 %
Prognostic category	-
Full Blood Count	**Date: 06/02/2008**
WBC (x10^9L)	1.6

II. Chemotherapy Treatment Schedule

Cycle	Date	Drugs	Doses	Dose Reduction	Route	Number of days and schedule given
1	Day 1	Ara-C	20 mg		SC	10 days, twice a day every 12 hrs
2	Day 42	Ara-C	20 mg		SC	10 days, twice a day every 12 hrs
3	Day 74	Ara-C	20 mg		SC	10 days, twice a day every 12 hrs
4	Day 109	Ara-C	20 mg		SC	10 days, twice a day every 12 hrs

III. Response to Treatment
Marrow examinations

Completion of Course	Cycle 1	Repeat marrow	Cycle 2	Repeat marrow	Cycle 3	Repeat marrow	Cycle 4	Repeat marrow
Date	Day 42		Day 70		Day 110		Day 145	
Cellularity (1= hypo, 2=normo, 3= hyper)	1		1		3		1	
Blasts (%)	3		2		2		0	
Marrow Response	CR		CR		CR		CR	

Patient number: 011

Disease status: Secondary

Patient Characteristics:
Age: 24 years Sex: M Height: 170 cm

Body Weight: 59.5 Kg BSA: 1.68 m^2

I. Baseline Characteristics:

Pre-treatment Data	
BM Aspirate	
%Blasts in BM aspirate	56 %
Prognostic category	-
Full Blood Count	**Date: 18/10/2011**
WBC (x10^9L)	0.9

II. Chemotherapy Treatment Schedule

Cycle	Date	Drugs	Doses	Dose Reduction	Route	Number of days and schedule given
1	Day 1	Ara-C	168 mg		IV	10 days, twice a day every 12 hrs
		DNR	100 mg		IV	1-hour dose on days 1,3,5
2						
3						
4						

III. Response to Treatment
Marrow examinations

Completion of Course	Cycle 1	Repeat marrow	Cycle 2	Repeat marrow	Cycle 3	Repeat marrow	Cycle 4	Repeat marrow
Date	Day 48							
Cellularity (1= hypo, 2=normo, 3= hyper)	1							
Blasts (%)	3							
Marrow Response	CR							

Patient number: 016

Disease status: Secondary

Patient Characteristics:
Age: 80 years Sex: M Height: 167.5 cm

Body Weight: 79.3 Kg BSA: 1.92 m^2

I. Baseline Characteristics:

Pre-treatment Data	
BM Aspirate	
%Blasts in BM aspirate	90 %
Prognostic category	-
Full Blood Count	**Date: 30/06/2010**
WBC (x10^9L)	3.3

II. Chemotherapy Treatment Schedule

Cycle	Date	Drugs	Doses	Dose Reduction	Route	Number of days and schedule given
1	Day 1	DNR	95 mg		IV	1-hour dose on days 1,3,5
		Ara-C	190 mg		IV	10 days, twice a day every 12 hrs
2	Day 66	Ara-C	20		SC	10 days, twice a day every 12 hrs
3						

III. Response to Treatment
Marrow examinations

Completion of Course	Cycle 1	Repeat marrow	Cycle 2	Repeat marrow	Cycle 3	Repeat marrow	Cycle 4	Repeat marrow
Date	Day 45		Day 101					
Cellularity (1= hypo, 2=normo, 3= hyper)	3		2					
Blasts (%)	1		1					
Marrow Response	CR		CR					

Patient number: 026

Disease status: De novo
Patient Characteristics:
Age: 45 years Sex: F Height: 169.3 cm

Body Weight: 94.8 Kg BSA: 2.11 m^2

I. Baseline Characteristics:

Pre-treatment Data	
BM Aspirate	
%Blasts in BM aspirate	71 %
Prognostic category	-
Full Blood Count	**Date: 26/05/2011**
WBC (x10^9L)	1.2

II. Chemotherapy Treatment Schedule

Cycle	Date	Drugs	Doses	Dose Reduction	Route	Number of days and schedule given
1	Day 1	DNR	150 mg		IV	1-hour dose on days 1,3,5
		Ara-C	170 mg		IV	10 days, twice a day every 12 hrs
2	Day 56	DNR	85 mg		IV	1-hour dose on days 1,3,5
		Ara-C	170 mg		IV	8 days, twice a day every 12 hrs
3						

III. Response to Treatment
Marrow examinations

Completion of Course	Cycle 1	Repeat marrow	Cycle 2	Repeat marrow	Cycle 3	Repeat marrow	Cycle 4	Repeat marrow
Date	Day 48		Day 116					
Cellularity (1= hypo, 2=normo, 3= hyper)	2		2					
Blasts (%)	0		0					
Marrow Response	CR		CR					

Appendix C:

Treatment outcome is highly dependent on the duration of the S-phase (Ts) and the total cycle duration (Tc). For this reason in this Appendix the dynamics of the leukemic cell population in the particular cell phases are presented for the six patients studied and analysed in Part II.

C1: Patient P001 under simulation of LDAC protocol

Table C1: Cells in S-phase, G_1-phase and G_2M-phase of patient P001 under the simulation of LDAC protocol

	Cells in S-phase	Cells in G_1-phase	Cells in G_2M - phase
Beginning of 1st Cycle	5.82E+10	1.28E+11	1.33E+10
End of 1st Cycle	1.65E+09	8.08E+09	2.77E+08
Beginning of 2nd Cycle	6.03E+10	7.57E+10	1.10E+10
End of 2nd Cycle	9.95E+08	2.65E+09	1.38E+08
Beginning of 3rd Cycle	9.24E+09	2.67E+10	2.57E+09
End of 3rd Cycle	9.39E+08	5.05E+09	1.87E+08
Beginning of 4th Cycle	2.42E+10	5.88E+10	4.03E+09
End of 4th Cycle	9.25E+08	5.72E+09	1.15E+08

*The initial population of cells in the separate phases is calculated by the multiplication of the leukemic population at the beginning of each cycle times the percentage of cell population in each phase for each cycle (equations 3.15-3.17 section 3.3.1).

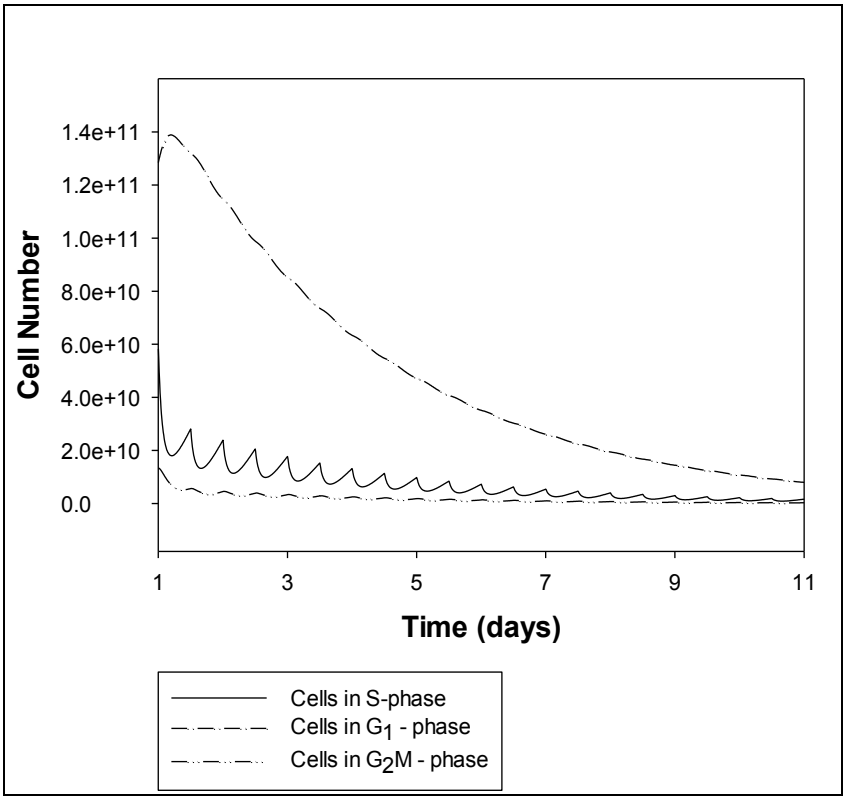

Figure C1: Patient P001 Cells in S-phase, G1-phase and G2M-phase over the 1st cycle of the LDAC simulation protocol

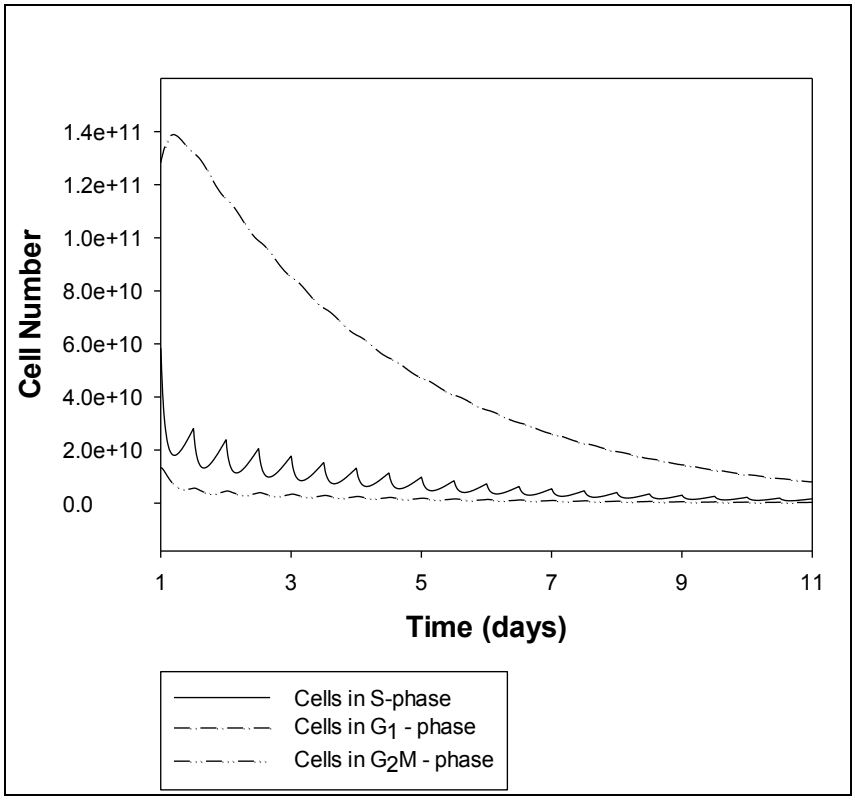

Figure C2: Patient P001 Cells in S-phase, G1-phase and G2M-phase over the 2nd cycle of the LDAC simulation protocol

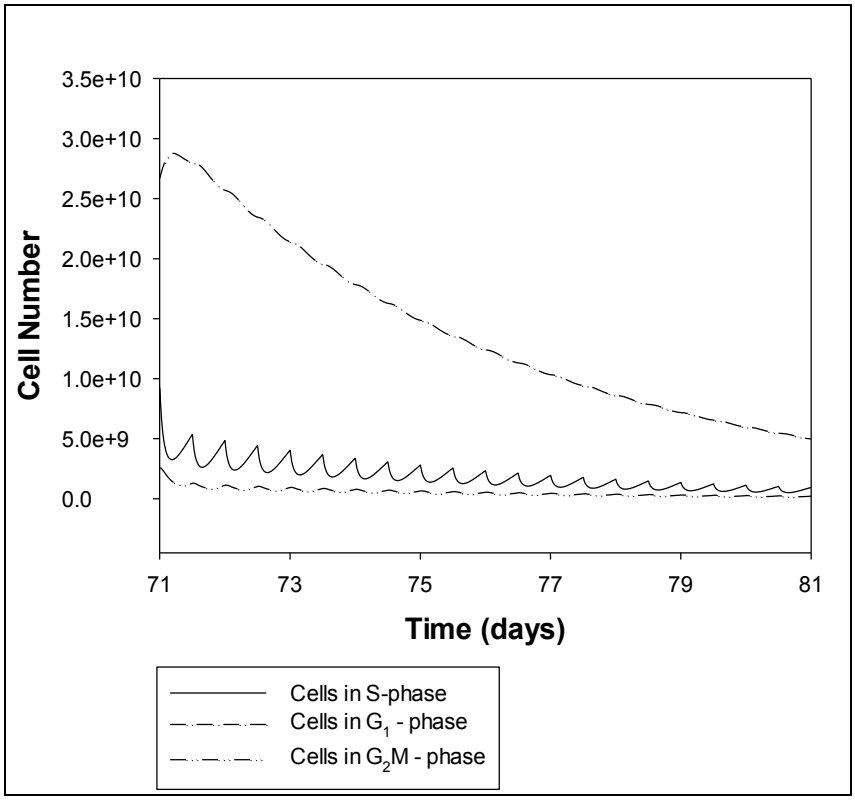

Figure C3: Patient P001 Cells in S-phase, G1-phase and G2M-phase over the 3rd cycle of the LDAC simulation protocol

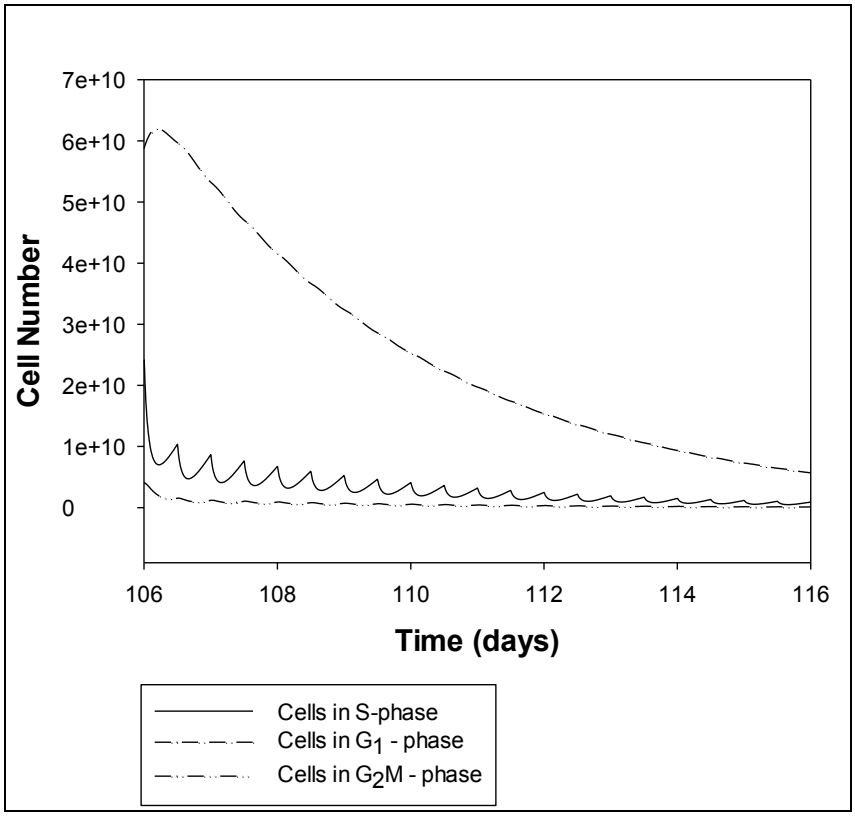

Figure C4: Patient P001 Cells in S-phase, G1-phase and G2M-phase over the 4th cycle of the LDAC simulation protocol

C2: Patient P002 under simulation of LDAC protocol

Table C2: Cells in S-phase, G_1-phase and G_2M-phase of patient P002 under the simulation of LDAC protocol

	Cells in S-phase	Cells in G_1-phase	Cells in G_2M - phase
Beginning of 1st Cycle	3.71E+11	3.66E+11	5.30E+10
End of 1st Cycle	1.87E+08	6.55E+08	2.15E+07

*The initial population of cells in the separate phases is calculated by the multiplication of the leukemic population at the beginning of each cycle times the percentage of cell population in each phase for each cycle (equations 3.15-3.17 section 3.3.1).

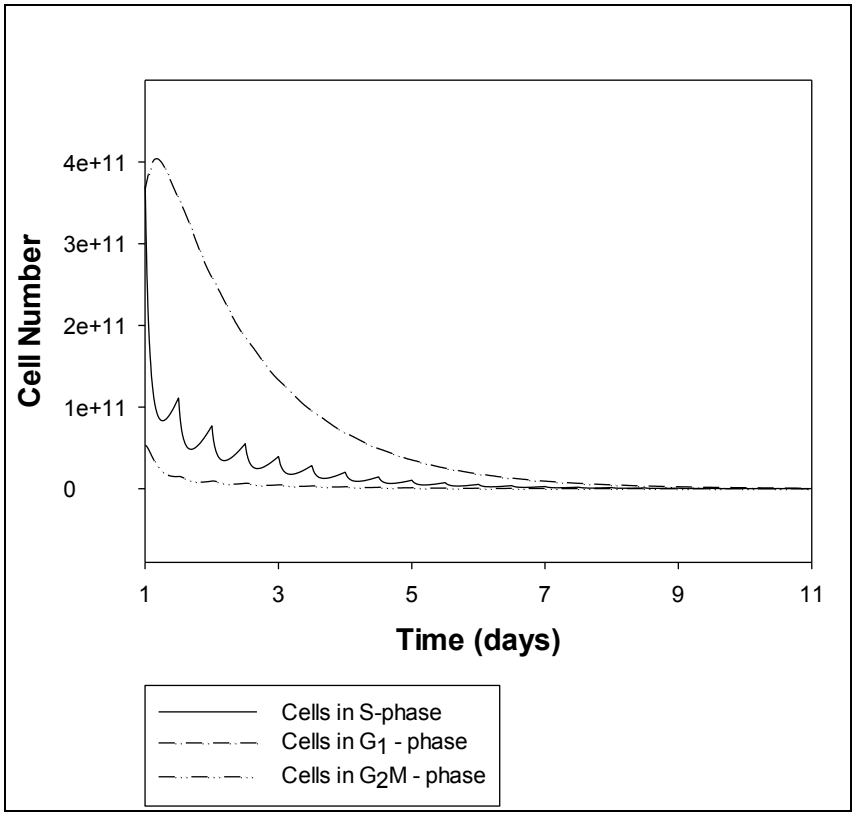

Figure C5: Patient P002 Cells in S-phase, G1-phase and G2M-phase over the 1st cycle of the LDAC simulation protocol

C3: Patient P006 under simulation of LDAC protocol

Table C3: Cells in S-phase, G_1-phase and G_2M-phase of patient P006 under the simulation of LDAC protocol

	Cells in S-phase	Cells in G_1-phase	Cells in G_2M - phase
Beginning of 1st Cycle	1.98E+11	1.12E+11	2.97E+10
End of 1st Cycle	8.87E+07	1.18E+08	1.07E+07
Beginning of 2nd Cycle	1.85E+09	3.86E+09	3.96E+08
End of 2nd Cycle	1.23E+08	5.02E+08	1.94E+07
Beginning of 3rd Cycle	1.19E+09	4.42E+09	2.59E+08
End of 3rd Cycle	1.75E+08	1.27E+09	2.74E+07
Beginning of 4th Cycle	9.69E+09	7.80E+09	1.42E+09
End of 4th Cycle	1.86E+07	4.71E+07	2282685

*The initial population of cells in the separate phases is calculated by the multiplication of the leukemic population at the beginning of each cycle times the percentage of cell population in each phase for each cycle (equations 3.15-3.17 section 3.3.1).

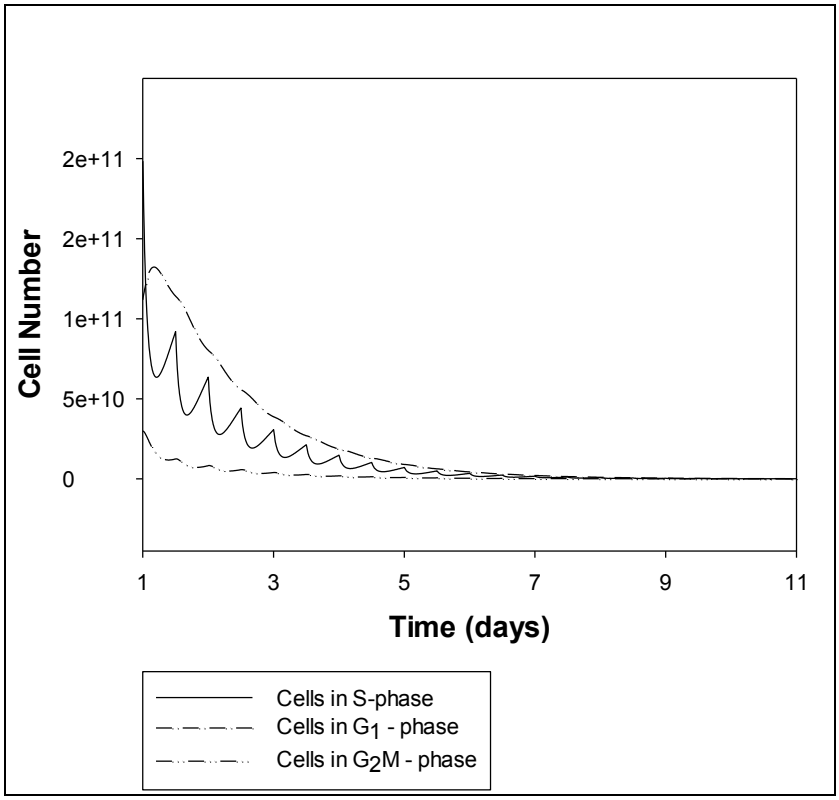

Figure C6: Patient P006 Cells in S-phase, G1-phase and G2M-phase over the 1st cycle of the LDAC simulation protocol

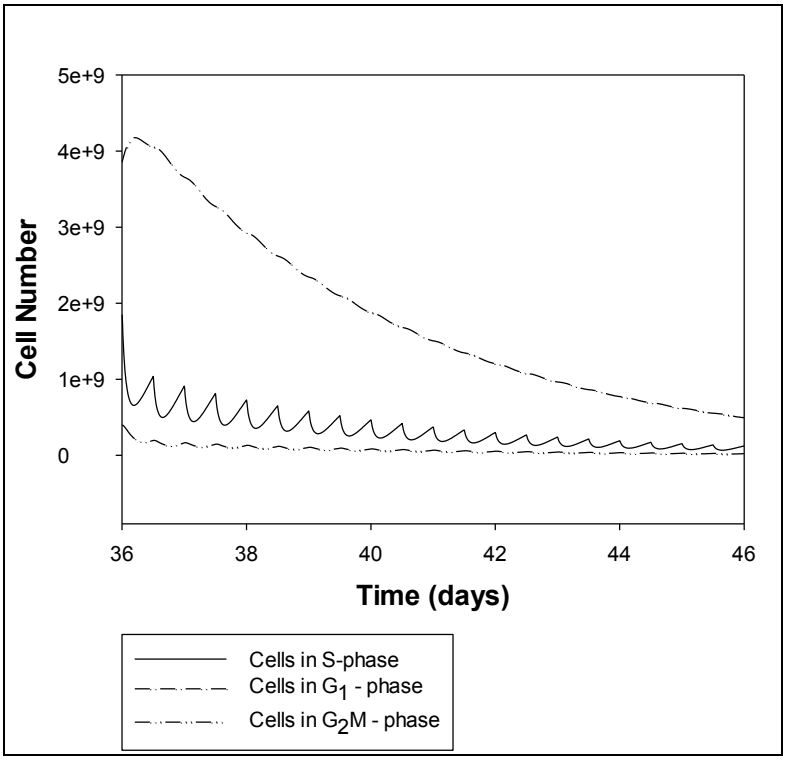

Figure C7: Patient P006 Cells in S-phase, G1-phase and G2M-phase over the 2nd cycle of the LDAC simulation protocol

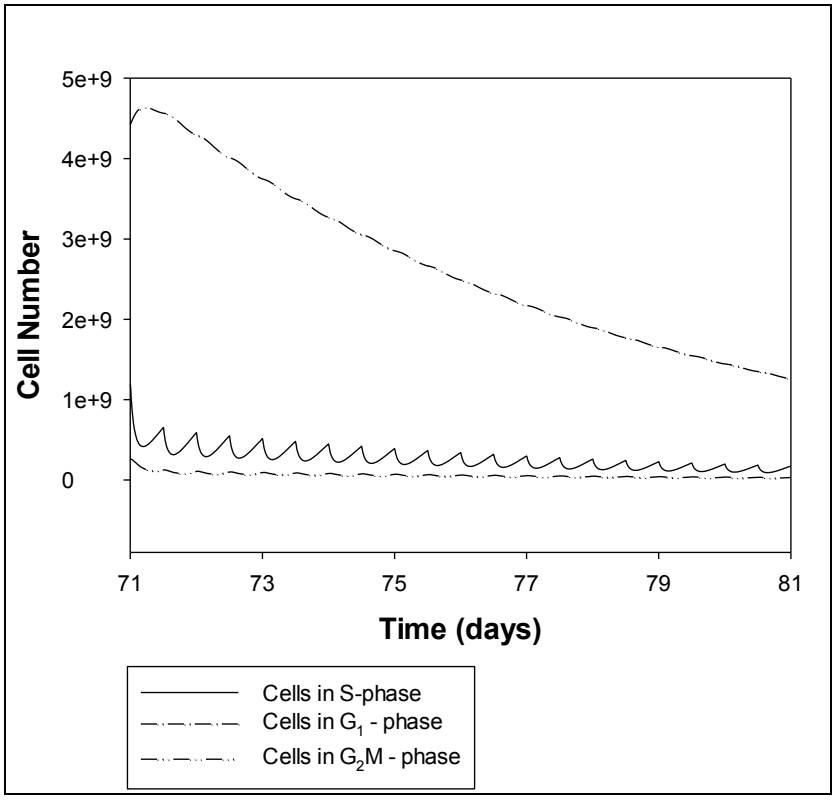

Figure C8: Patient P006 Cells in S-phase, G1-phase and G2M-phase over the 3rd cycle of the LDAC simulation protocol

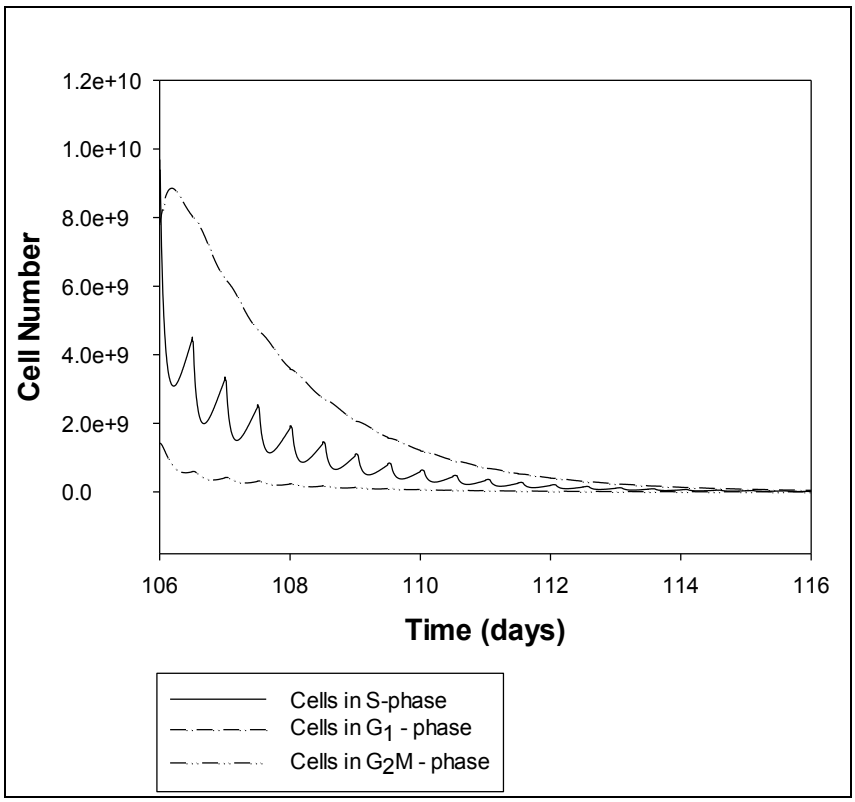

Figure C9: Patient P006 Cells in S-phase, G1-phase and G2M-phase over the 4th cycle of the LDAC simulation protocol

C4: Patient P011 under simulation of DA protocol

Table C4: Cells in S-phase, G_1-phase and G_2M-phase of patient P011 under the simulation of LDAC protocol

	Cells in S-phase	Cells in G_1-phase	Cells in G_2M - phase
Beginning of 1st Cycle	9.03E+10	4.12E+11	3.01E+10
End of 1st Cycle	7289276	1.54E+08	2120402.8

*The initial population of cells in the separate phases is calculated by the multiplication of the leukemic population at the beginning of each cycle times the percentage of cell population in each phase for each cycle (equations 3.15-3.17 section 3.3.1).

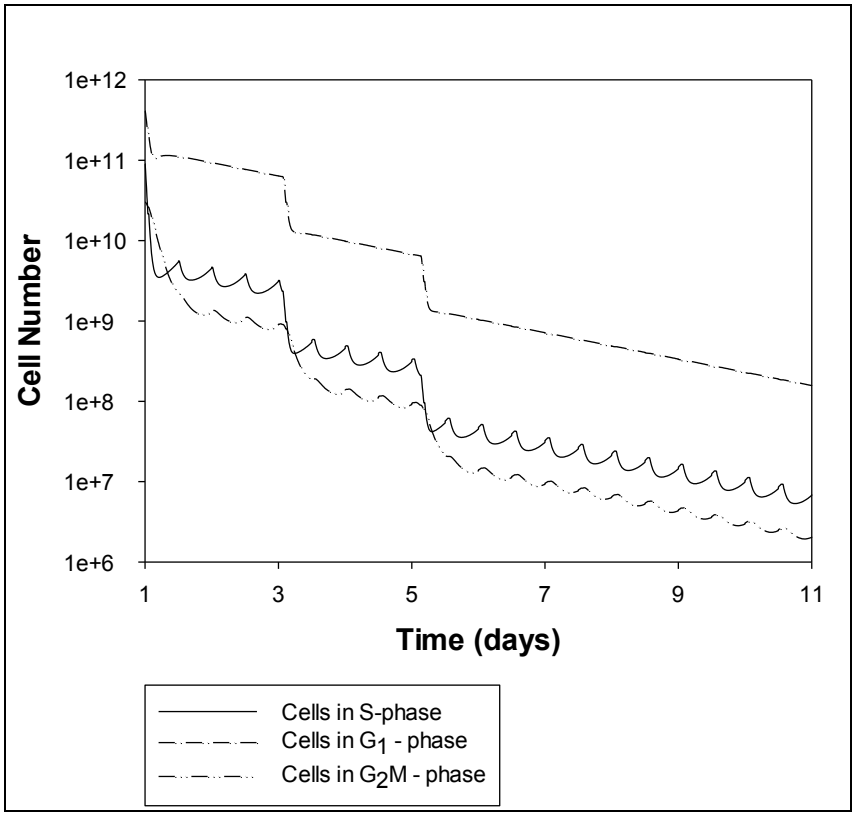

Figure C10: Patient P011 Cells in S-phase, G1-phase and G2M-phase over the 1st cycle of the DA simulation protocol

C5: Patient P016 under simulation of DA / LDAC protocol

Table C5: Cells in S-phase, G_1-phase and G_2M-phase of patient P016 under the simulation of DA / LDAC protocol

	Cells in S-phase	Cells in G_1-phase	Cells in G_2M - phase
Beginning of 1st Cycle	1.52E+11	6.55E+11	4.75E+10
End of 1st Cycle	1.63E+07	3.11E+08	4353955
Beginning of 2nd Cycle	2.35E+10	4.76E+10	5.08E+09
End of 2nd Cycle	3.93E+07	3.48E+08	7081176

*The initial population of cells in the separate phases is calculated by the multiplication of the leukemic population at the beginning of each cycle times the percentage of cell population in each phase for each cycle (equations 3.15-3.17 section 3.3.1).

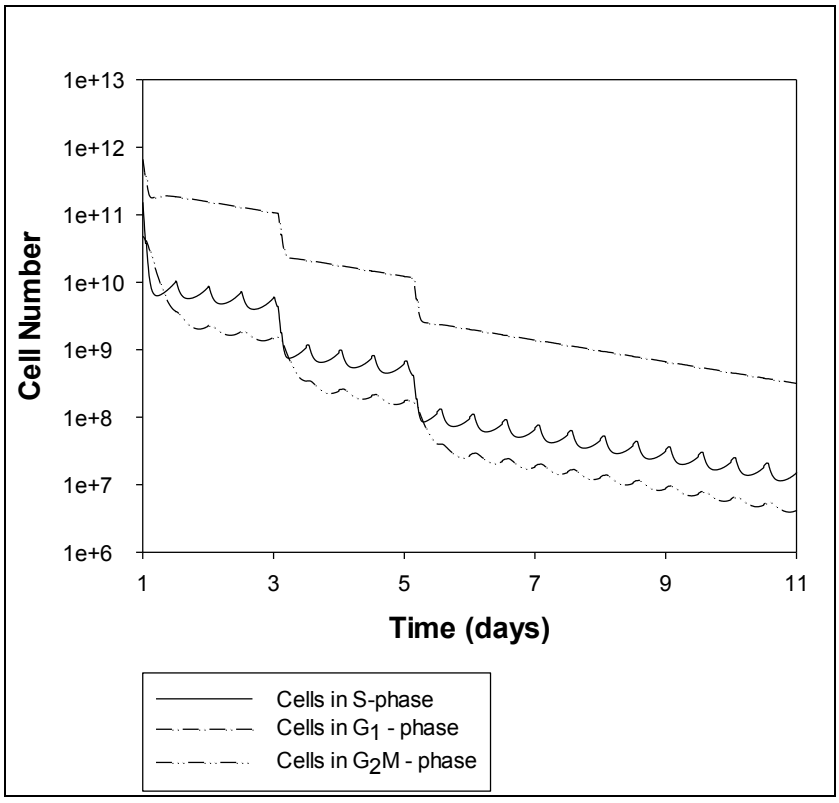

Figure C11: Patient P016 Cells in S-phase, G1-phase and G2M-phase over the 1st cycle of the DA simulation protocol

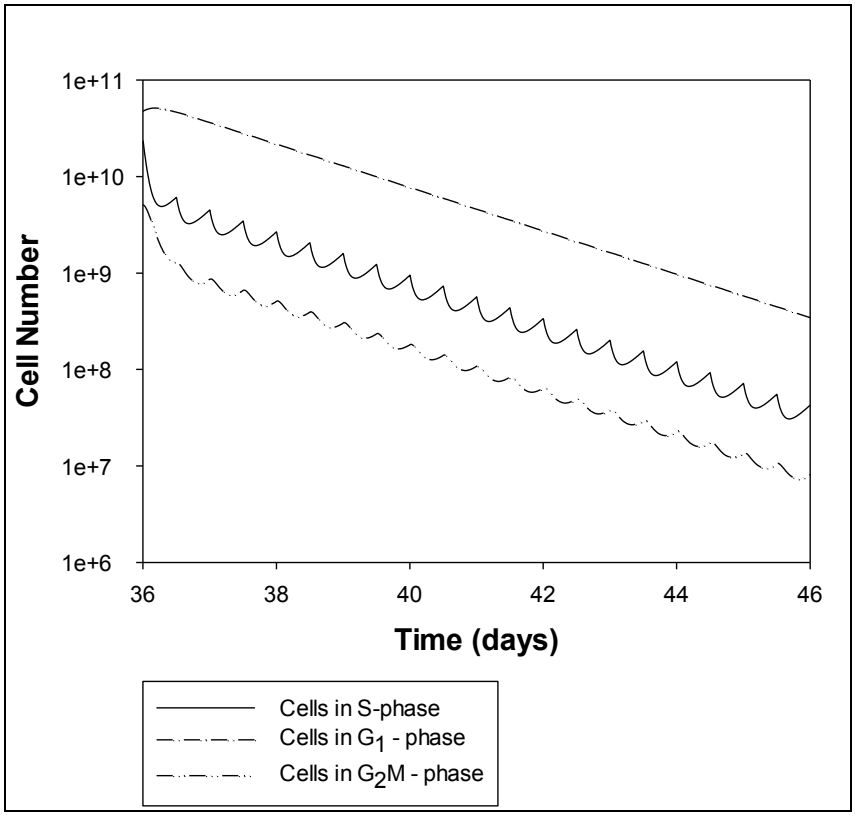

Figure C12: Patient P016 Cells in S-phase, G1-phase and G2M-phase over the 2nd cycle of the LDAC simulation protocol

C6: Patient P026 under simulation of DA protocol

Table C6: Cells in S-phase, G_1-phase and G_2M-phase of patient P026 under the simulation of DA protocol

	Cells in S-phase	Cells in G_1-phase	Cells in G_2M - phase
Beginning of 1st Cycle	2.15E+11	4.16E+11	4.31E+10
End of 1st Cycle	966444.7	1.15E+07	164596.27
Beginning of 2nd Cycle	3.94E+08	5.78E+08	7.88E+07
End of 2nd Cycle	3646.3252	34955.99	652.36597

*The initial population of cells in the separate phases is calculated by the multiplication of the leukemic population at the beginning of each cycle times the percentage of cell population in each phase for each cycle (equations 3.15-3.17 section 3.3.1).

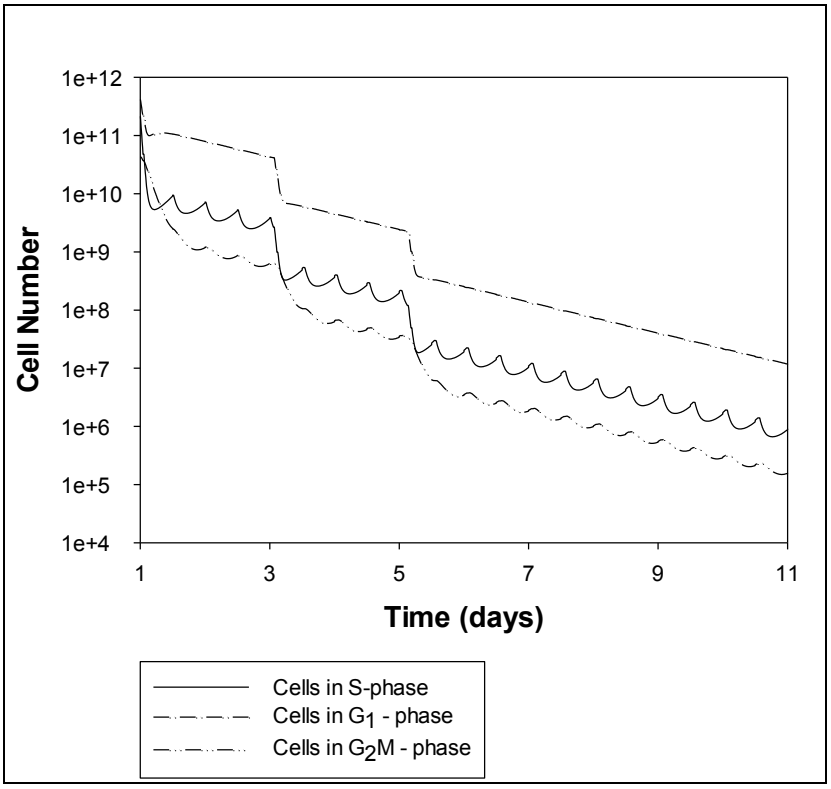

Figure C12: Patient P026 Cells in S-phase, G1-phase and G2M-phase over the 1st cycle of the DA simulation protocol

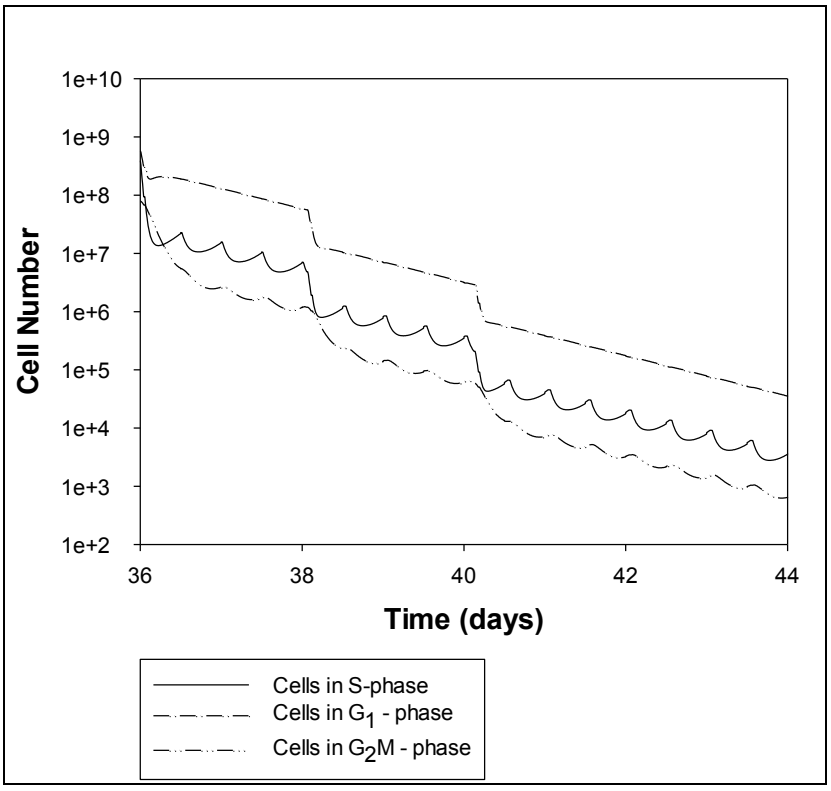

Figure C13: Patient P026 Cells in S-phase, G1-phase and G2M-phase over the 2nd cycle of the DA simulation protocol

C7: Patient P001 under optimisation of LDAC protocol

Table C7: Cells in S-phase, G_1-phase and G_2M-phase of patient P001 under the optimisation of LDAC protocol

	Cells in S-phase	Cells in G_1-phase	Cells in G_2M - phase
Beginning of 1st Cycle	5.82E+10	1.28E+11	1.33E+10
End of 1st Cycle	2.77E+08	3.37E+09	2.71E+07
Beginning of 2nd Cycle	1.99E+10	2.50E+10	3.64E+09
End of 2nd Cycle	8660943	8.11E+07	860415.2
Beginning of 3rd Cycle	2.06E+08	5.96E+08	5.73E+07
End of 3rd Cycle	2544783	3.36E+07	256695.48
Beginning of 4th Cycle	1.21E+08	2.94E+08	2.01E+07
End of 4th Cycle	955109.8	1.40E+07	79868.37

*The initial population of cells in the separate phases is calculated by the multiplication of the leukemic population at the beginning of each cycle times the percentage of cell population in each phase for each cycle (equations 3.15-3.17 section 3.3.1).

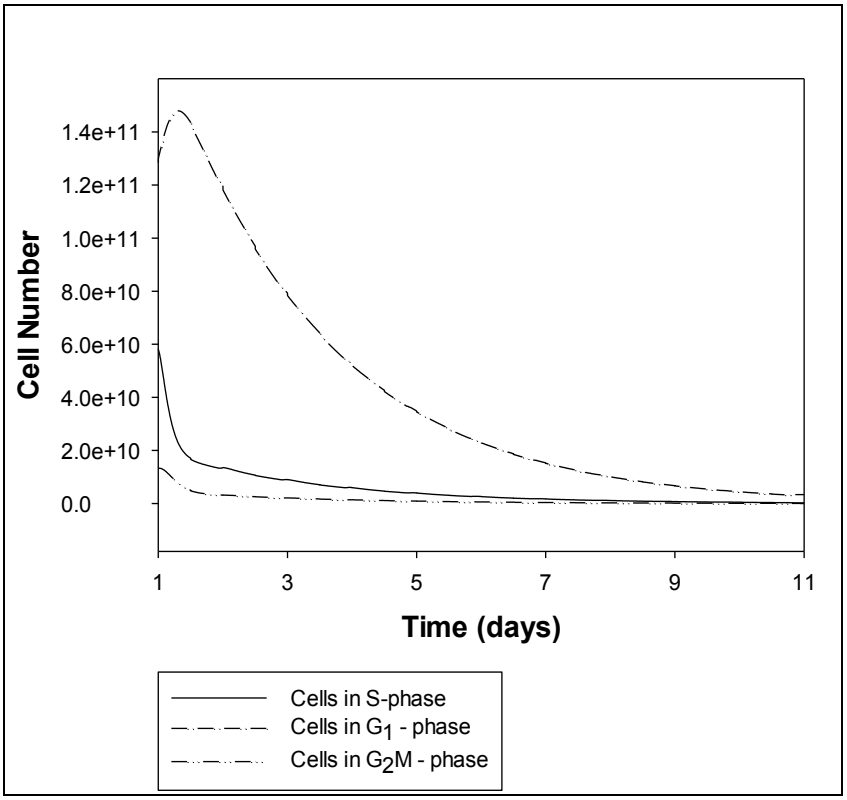

Figure C14: Patient P001 Cells in S-phase, G1-phase and G2M-phase over the 1st cycle of the LDAC optimisation protocol

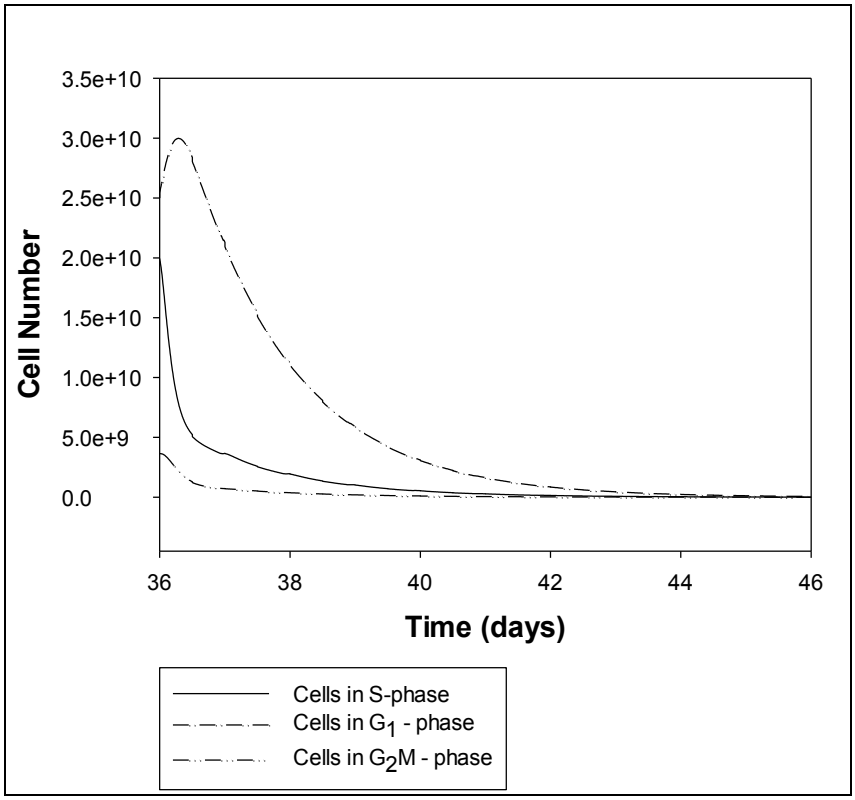

Figure C15: Patient P001 Cells in S-phase, G1-phase and G2M-phase over the 2nd cycle of the LDAC optimisation protocol

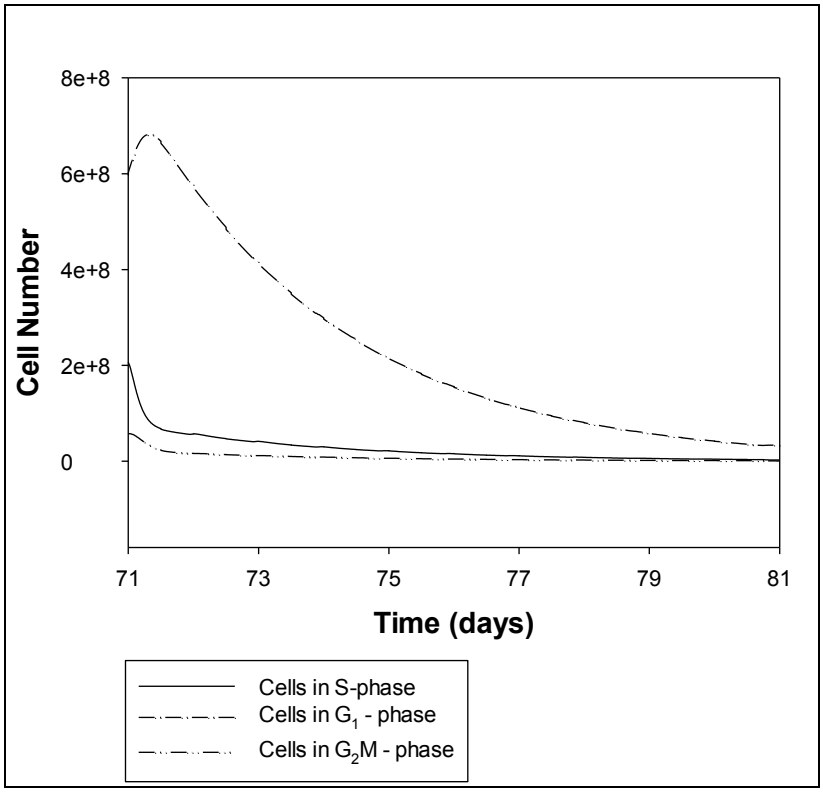

Figure C16: Patient P001 Cells in S-phase, G1-phase and G2M-phase over the 3rd cycle of the LDAC optimisation protocol

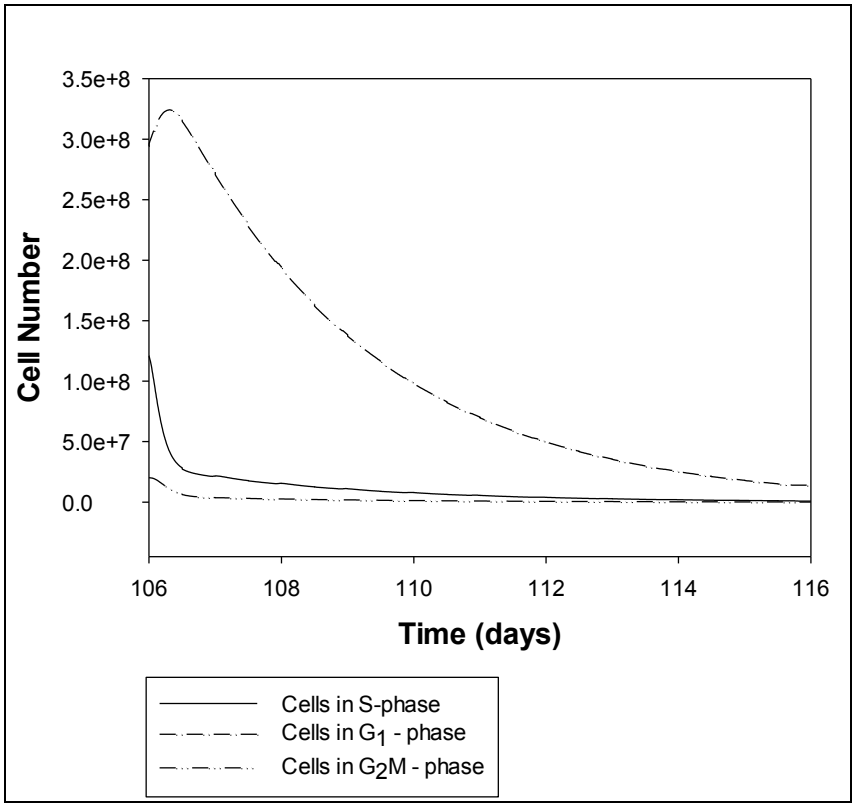

Figure C17: Patient P001 Cells in S-phase, G1-phase and G2M-phase over the 4th cycle of the LDAC optimisation protocol

C8: Patient P002 under optimisation of LDAC protocol

Table C8: Cells in S-phase, G_1-phase and G_2M-phase of patient P002 under the optimisation of LDAC protocol

	Cells in S-phase	Cells in G_1-phase	Cells in G_2M - phase
Beginning of 1st Cycle	3.71E+11	3.66E+11	5.30E+10
End of 1st Cycle	3739450.2	2.49E+07	591878.75

*The initial population of cells in the separate phases is calculated by the multiplication of the leukemic population at the beginning of each cycle times the percentage of cell population in each phase for each cycle (equations 3.15-3.17 section 3.3.1).

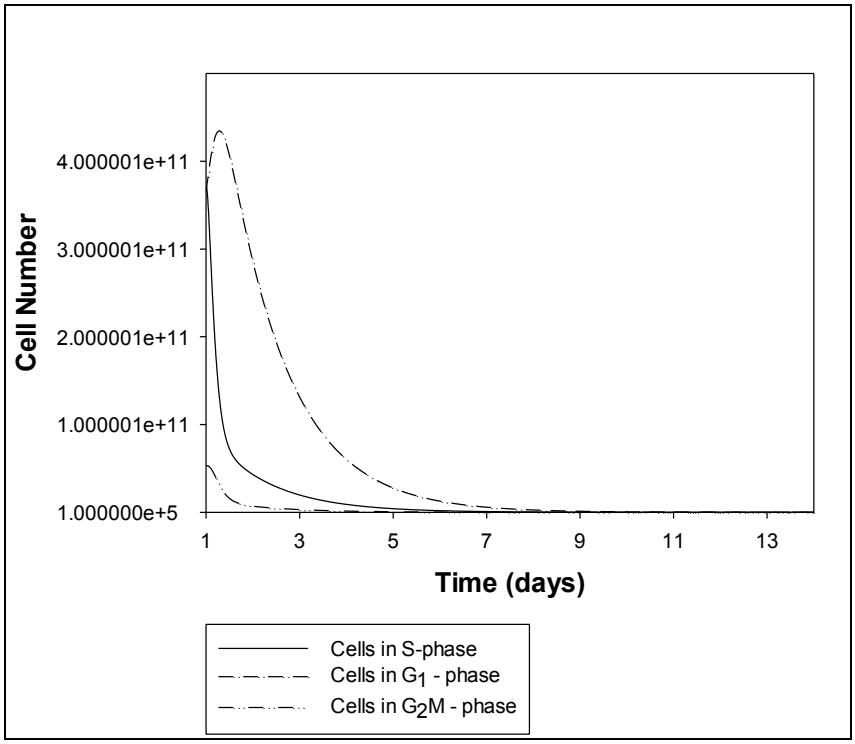

Figure C18: Patient P002 Cells in S-phase, G1-phase and G2M-phase over the 1st cycle of the LDAC optimisation protocol

C9: Patient P006 under optimisation of LDAC protocol

Table C9: Cells in S-phase, G_1-phase and G_2M-phase of patient P006 under the optimisation of LDAC protocol

	Cells in S-phase	Cells in G_1-phase	Cells in G_2M - phase
Beginning of 1st Cycle	1.98E+11	1.12E+11	2.97E+10
End of 1st Cycle	1104074.8	5432401.5	110485.08
Beginning of 2nd Cycle	4.70E+07	9.80E+07	1.01E+07
End of 2nd Cycle	266451.8	2849935.5	24962.537
Beginning of 3rd Cycle	5195294	1.93E+07	1129411.8
End of 3rd Cycle	160901.05	2365376.5	13430.869
Beginning of 4th Cycle	1.54E+07	1.24E+07	2250000
End of 4th Cycle	1089.6929	7181.63	103.36292

*The initial population of cells in the separate phases is calculated by the multiplication of the leukemic population at the beginning of each cycle times the percentage of cell population in each phase for each cycle (equations 3.15-3.17 section 3.3.1).

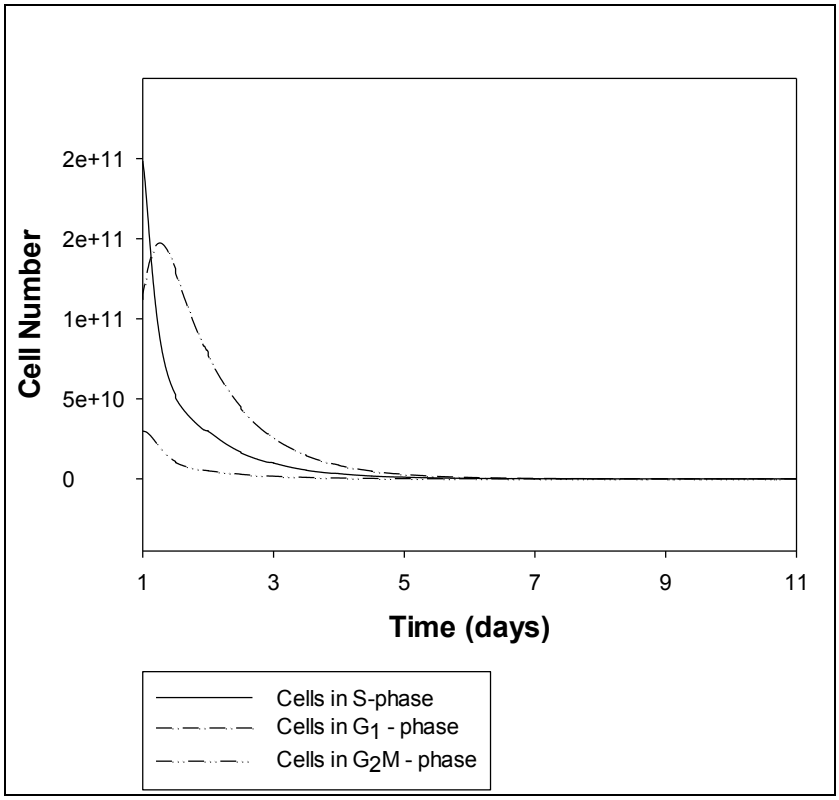

Figure C19: Patient P006 Cells in S-phase, G1-phase and G2M-phase over the 1st cycle of the LDAC optimisation protocol

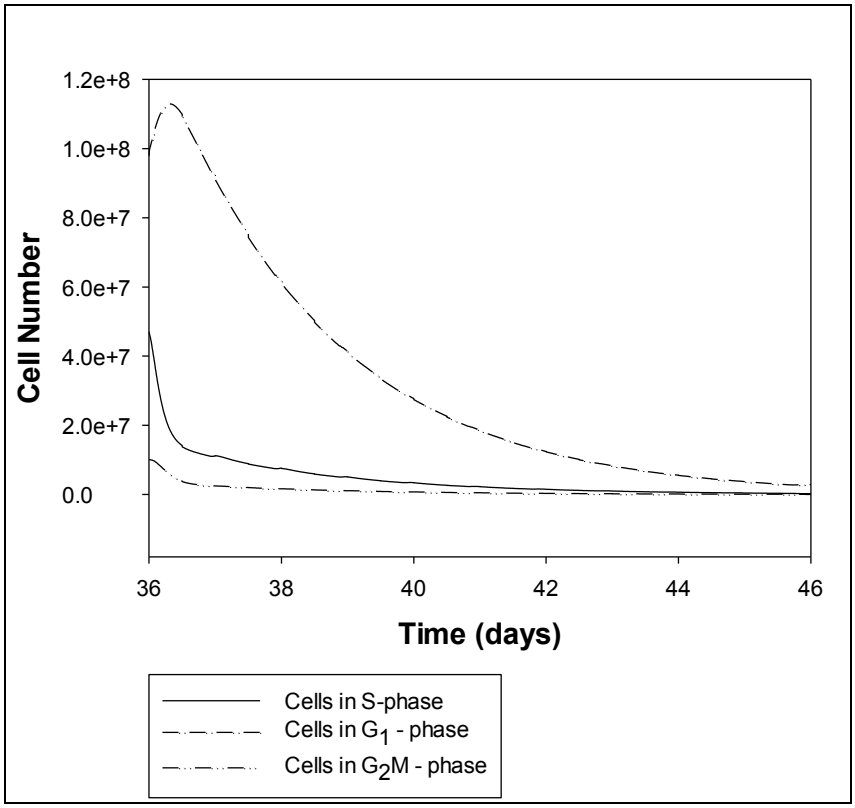

Figure C20: Patient P006 Cells in S-phase, G1-phase and G2M-phase over the 2nd cycle of the LDAC optimisation protocol

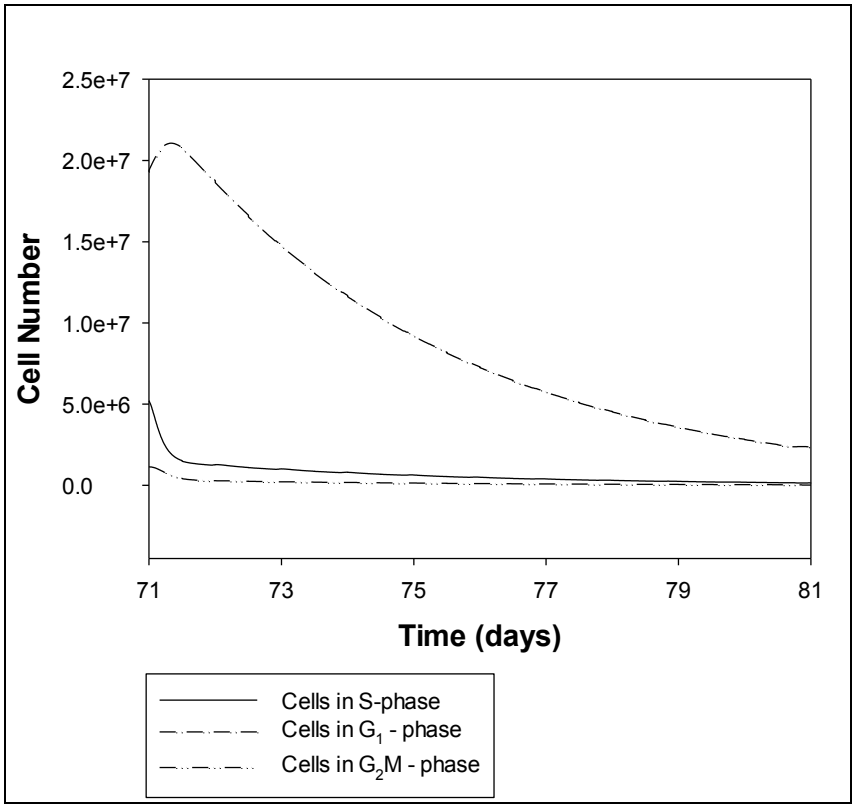

Figure C21: Patient P006 Cells in S-phase, G1-phase and G2M-phase over the 3rd cycle of the LDAC optimisation protocol

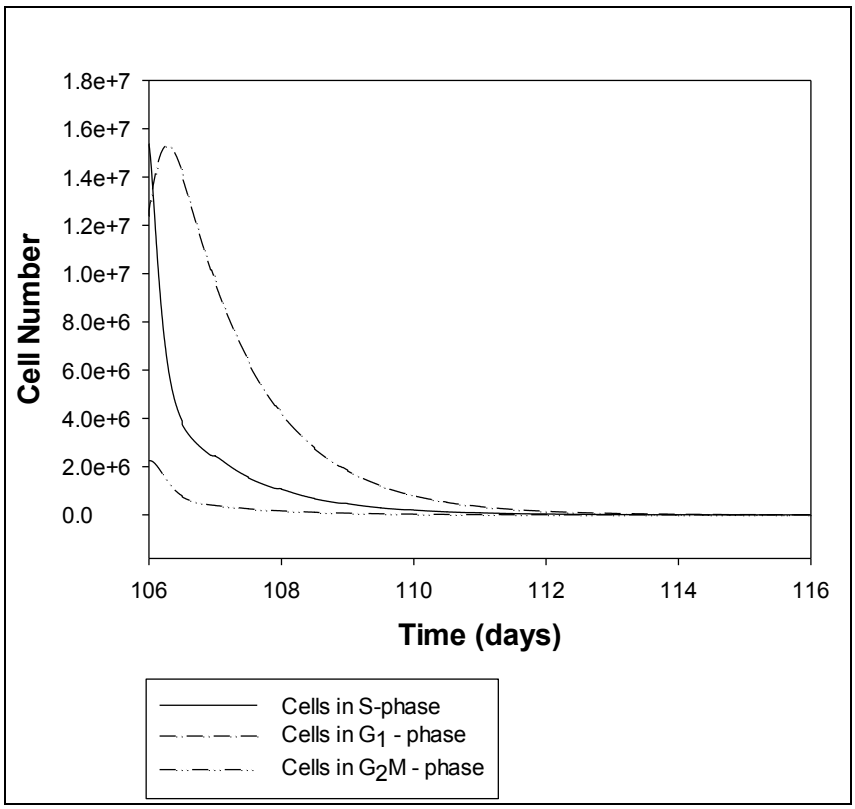

Figure C22: Patient P006 Cells in S-phase, G1-phase and G2M-phase over the 4th cycle of the LDAC optimisation protocol

C10: Patient P011 under optimisation of DA protocol

Table C10: Cells in S-phase, G_1-phase and G_2M-phase of patient P011 under the optimisation of DA protocol

	Cells in S-phase	Cells in G_1-phase	Cells in G_2M - phase
Beginning of 1st Cycle	9.03E+10	4.12E+11	3.01E+10
End of 1st Cycle	1805735.2	5.93E+07	634875.94

*The initial population of cells in the separate phases is calculated by the multiplication of the leukemic population at the beginning of each cycle times the percentage of cell population in each phase for each cycle (equations 3.15-3.17 section 3.3.1).

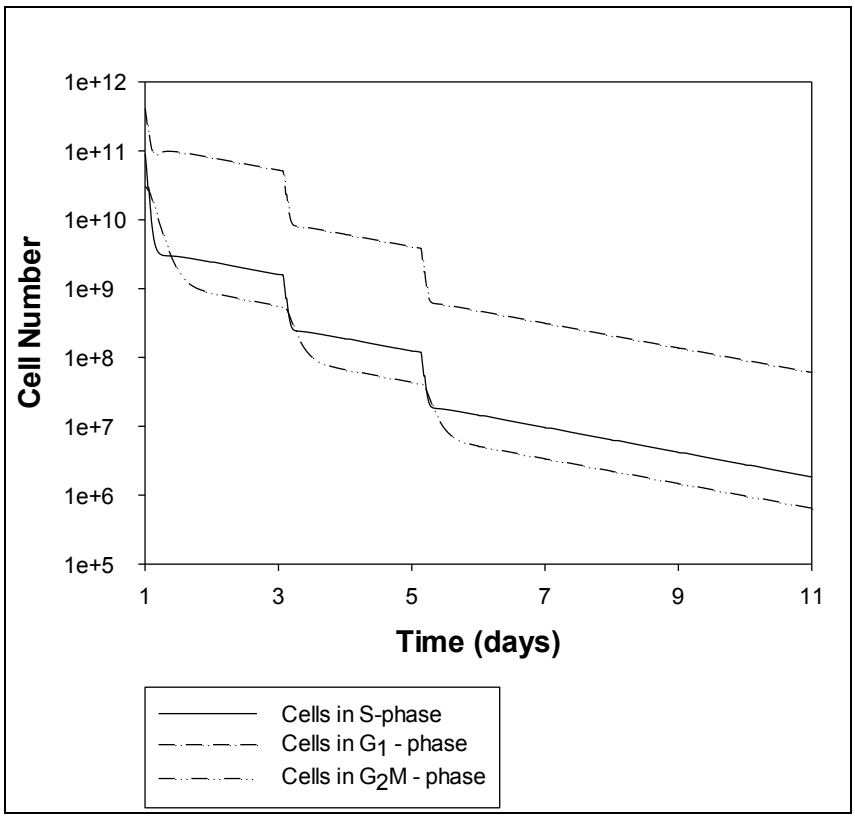

Figure C23: Patient P011 Cells in S-phase, G1-phase and G2M-phase over the 1st cycle of the DA optimisation protocol

C11: Patient P016 under optimisation of DA / LDAC protocol

Table C11: Cells in S-phase, G_1-phase and G_2M-phase of patient P016 under the optimisation of DA / LDAC protocol

	Cells in S-phase	Cells in G_1-phase	Cells in G_2M - phase
Beginning of 1st Cycle	1.52E+11	6.55E+11	4.75E+10
End of 1st Cycle	1085740.9	8.32E+07	221250.19
Beginning of 2nd Cycle	5.64E+09	1.14E+10	1.21E+09
End of 2nd Cycle	2350522.5	6.90E+07	293168.84

*The initial population of cells in the separate phases is calculated by the multiplication of the leukemic population at the beginning of each cycle times the percentage of cell population in each phase for each cycle (equations 3.15-3.17 section 3.3.1).

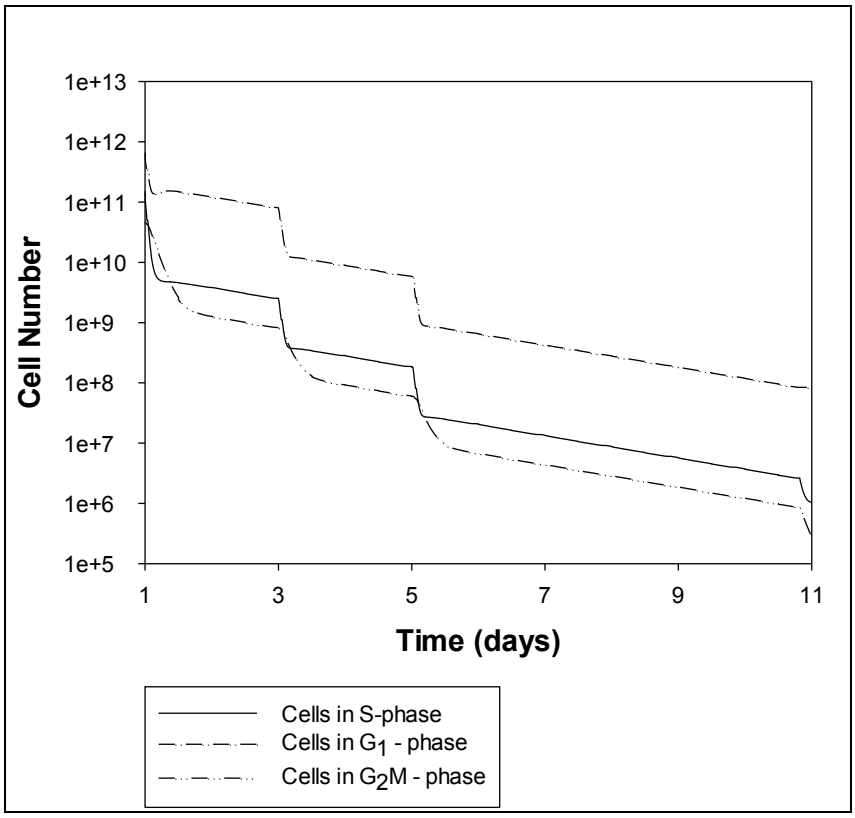

Figure C24: Patient P016 Cells in S-phase, G1-phase and G2M-phase over the 1st cycle of the DA optimisation protocol

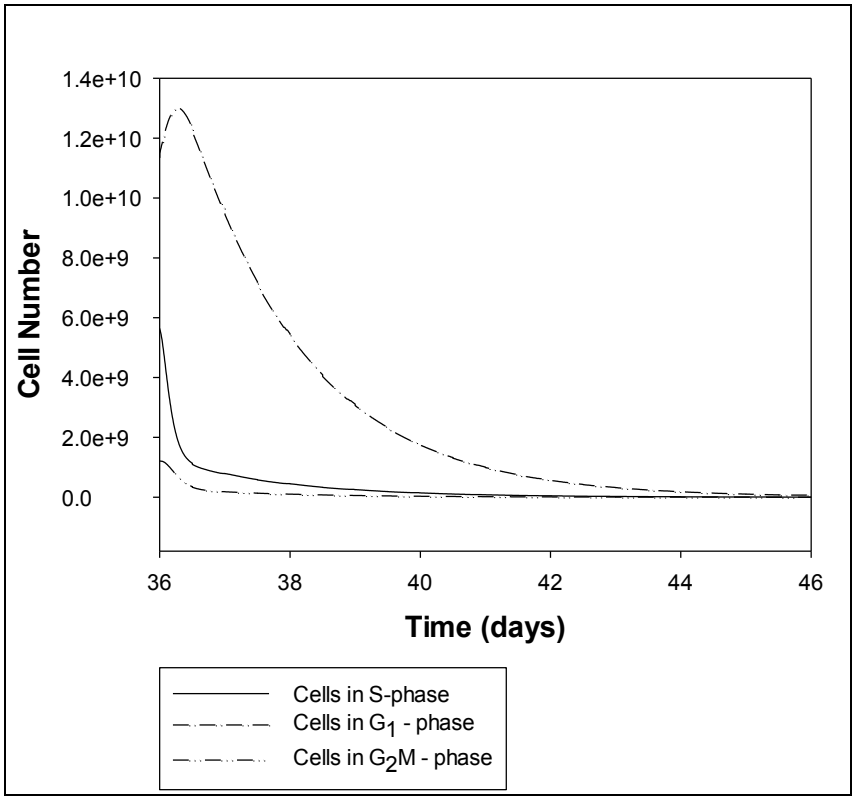

Figure C25: Patient P016 Cells in S-phase, G1-phase and G2M-phase over the 2nd cycle of the DA optimisation protocol

C12: Patient P026 under optimisation of DA / LDAC protocol

Table C12: Cells in S-phase, G_1-phase and G_2M-phase of patient P026 under the optimisation of DA protocol

	Cells in S-phase	Cells in G_1-phase	Cells in G_2M - phase
Beginning of 1st Cycle	2.15E+11	4.16E+11	4.31E+10
End of 1st Cycle	100510.36	7562396	21018.395
Beginning of 2nd Cycle	9.98E+07	1.46E+08	2.00E+07
End of 2nd Cycle	97.1664	5616.5044	34.06412

*The initial population of cells in the separate phases is calculated by the multiplication of the leukemic population at the beginning of each cycle times the percentage of cell population in each phase for each cycle (equations 3.15-3.17 section 3.3.1).

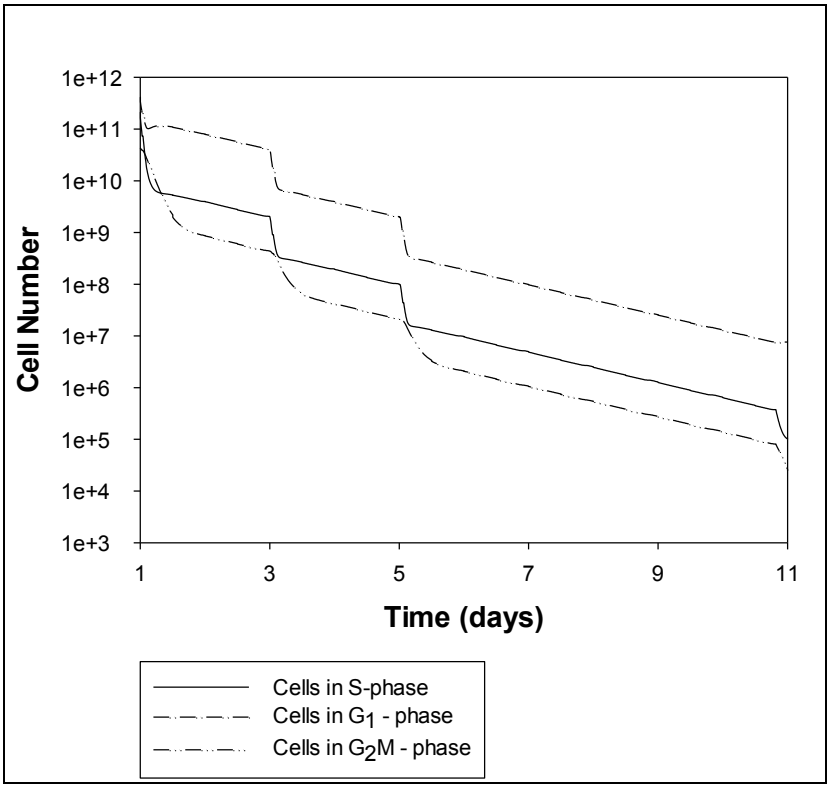

Figure C26: Patient P026 Cells in S-phase, G1-phase and G2M-phase over the 1st cycle of the DA optimisation protocol

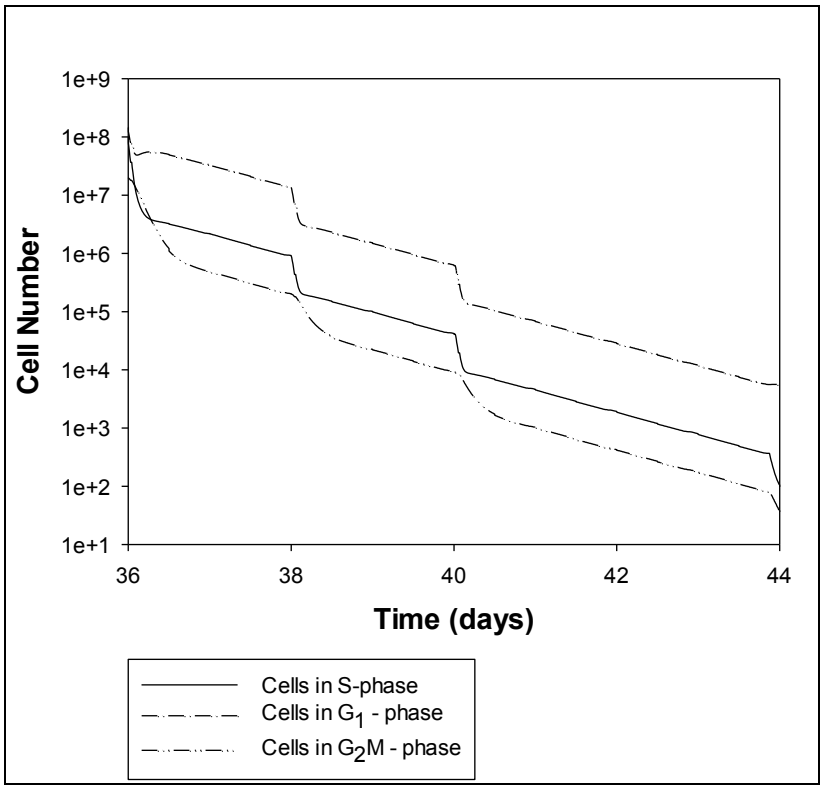

Figure C27: Patient P026 Cells in S-phase, G1-phase and G2M-phase over the 2nd cycle of the DA optimisation protocol